

**Virus-like particles as a novel platform for delivery of protective
Burkholderia antigens**

Submitted by Marc Ashley Bayliss to the University of Exeter
as a thesis for the degree of
Doctor of Philosophy in Biological Sciences
In September 2016

This thesis is available for Library use on the understanding that it is copyright material and that no quotation from the thesis may be published without proper acknowledgement.

I certify that all material in this thesis which is not my own work has been identified and that no material has previously been submitted and approved for the award of a degree by this or any other University.

©Crown copyright 2016. Published with the permission of the Defence Science and Technology Laboratory.

DSTL/PUB097268

DSTL/PUB097468

Table of Contents

List of Tables	9
List of Figures.....	10
Abstract.....	18
Acknowledgments.....	20
List of abbreviations	21
Chapter 1: General Introduction	25
1.1 <i>Burkholderia</i>	25
1.2 <i>Burkholderia pseudomallei</i> and melioidosis	25
1.2.1 Diagnosis and treatment.....	27
1.2.2 <i>Burkholderia pseudomallei</i> intracellular infection and mechanisms of virulence	28
1.3 <i>Burkholderia mallei</i> and glanders.....	30
1.4 <i>Burkholderia cepacia</i>	31
1.5 <i>Burkholderia thailandensis</i>	31
1.6 Bacterial polysaccharides	32
1.6.1 <i>B. pseudomallei</i> and <i>B. mallei</i> capsular polysaccharide	32
1.7 Vaccines.....	38
1.7.1 Barriers to vaccine development.....	39
1.7.2 Economics of vaccine development.....	41
1.7.3 Biodefense vaccines.....	42
1.7.4 Animal models	43
1.7.5 Live attenuated vaccines	44
1.7.6 Inactivated vaccines	45
1.7.7 Subunit vaccines and toxoids	46
1.8 Vaccine immunology	55
1.8.1 Th1/Th2 response.....	56
1.8.2 Immune response to polysaccharides	56

1.8.3	Immune response to proteins (MHC-I and MHC-II)	58
1.8.4	Immune response to <i>B. pseudomallei</i> infection	59
1.9	Correlates of protection	60
1.10	Vaccine adjuvants and delivery systems	61
1.10.1	Adjuvants.....	61
1.10.2	Virus-like particles.....	62
1.11	Project aims	66
Chapter 2: Materials and methods		67
2.1	Preparation of antibiotics	67
2.2	Preparation of reagents and buffers	67
2.2.1	ABTS buffer pH 4.37 (Citric acid/phosphate buffer).....	67
2.3	Preparation of growth media	67
2.3.1	Luria Bertani (LB) broth	68
2.3.2	LB agar	68
2.3.3	Enhanced phytone peptone broth.....	68
2.3.4	M9 minimal media.....	68
2.3.5	Tryptone peptone broth	69
2.3.6	Brain Heart Infusion broth.....	69
2.3.7	Brain Heart Infusion agar.....	69
2.4	Microbiology techniques	70
2.4.1	Bacterial strains and plasmids	70
2.4.2	Growth and manipulation of bacteria	70
2.5	Extraction of CPS from <i>B. pseudomallei</i> K96243 and <i>B. thailandensis</i> E555	71
2.5.1	Growth of <i>Burkholderia</i> spp. on solid media	71
2.5.2	Growth of <i>Burkholderia</i> spp. in liquid cultures.....	71
2.5.3	Extraction of CPS from <i>Burkholderia</i> spp. by ethanol precipitation.....	72

2.5.4	Phenol extraction of CPS from <i>Burkholderia spp.</i> utilising an LPS extraction method	72
2.5.5	Associate Professor Paul Brett's CPS extraction method.....	73
2.5.6	Monosaccharide analysis of CPS	74
2.6	Development of a quantitative CPS ELISA	74
2.6.1	Dot-blot analysis	74
2.6.2	ELISA utilising plate bound CPS.....	75
2.6.3	Generation of biotinylated monoclonal antibody DSTL189	75
2.6.4	ELISA method for biotin interference	76
2.6.5	Development of ELISA purified CPS standard curve	77
2.6.6	<i>B. pseudomallei</i> 1026b and <i>B. thailandensis</i> E555 :: <i>wbil</i> (Km ^r) purified CPS recognition with DSTL189.....	78
2.6.7	Measurement of <i>B. thailandensis</i> E555 :: <i>wbil</i> (Km ^r) CPS culture concentration	78
2.6.8	Final ELISA method for determination of <i>B. thailandensis</i> E555 :: <i>wbil</i> (Km ^r) culture CPS content	78
2.6.9	Determination of ELISA LOD utilising <i>B. thailandensis</i> CDC2721121	79
2.6.10	Determination of ELISA purified CPS limit of detection (LOD).....	79
2.6.11	Determination of ELISA purified CPS limit of quantification (LOQ)80	
2.7	CPS expression optimisation – growth.....	80
2.7.1	Measurement of CPS expression from a <i>B. thailandensis</i> E555 :: <i>wbil</i> (Km ^r) culture inoculated from a glycerol stock	80
2.7.2	Measurement of CPS expression from a <i>B. thailandensis</i> E555 :: <i>wbil</i> (Km ^r) culture inoculated from a subbed culture	80
2.7.3	Measurement of CPS expression from a <i>B. thailandensis</i> E555 :: <i>wbil</i> (Km ^r) culture inoculated into different growth medias	81
2.7.4	Measurement of CPS expression from a <i>B. thailandensis</i> E555 :: <i>wbil</i> (Km ^r) culture inoculated into baffled flasks	82

2.7.5	Measurement of CPS expression from a <i>B. thailandensis</i> E555 :: <i>wbil</i> (Km ^r) culture inoculated with iron sulfate	82
2.7.6	Measurement of CPS expression from a reduced volume <i>B. thailandensis</i> E555 :: <i>wbil</i> (Km ^r) culture.....	83
2.7.7	Measurement of CPS expression from a <i>B. thailandensis</i> E555 :: <i>wbil</i> (Km ^r) culture inoculated with mannose.....	83
2.8	CPS expression optimisation – extraction.....	84
2.8.1	Determination of CPS from <i>B. thailandensis</i> E555 :: <i>wbil</i> (Km ^r) supernatant and pellet fractions.....	84
2.8.2	Determination of CPS concentration (µg/mL) from <i>B. thailandensis</i> E555 :: <i>wbil</i> (Km ^r) live and frozen culture fractions	85
2.9	<i>Burkholderia</i> CPS immunogenic epitope.....	85
2.9.1	Recognition of purified CPS and deacetylated CPS with the <i>B. pseudomallei</i> K96243 anti-CPS monoclonal antibody DSTL189.....	85
2.9.2	Recognition of purified CPS and deacetylated CPS with four <i>B. pseudomallei</i> K96243 anti-CPS monoclonal antibodies	86
2.9.3	Heavy and light chain variable region sequencing of four <i>B. pseudomallei</i> K96243 anti-CPS monoclonal antibodies	86
2.10	Importance of the CPS acetyl group.....	89
2.10.1	CPS and deacetylated CPS-specific IgG and IgM serum antibody analysis of CPS and deacetylated CPS vaccinated mice	89
2.11	Expression of Tandem CoreTM with peptide inserts.....	90
2.11.1	Determination of LoIC expression in VLP-LoIC fusion constructs by ELISA from the baculovirus expression system.....	90
2.12	VLP expression systems	91
2.12.1	Expression and purification of VLPs in <i>E.coli</i>	91
2.12.2	Expression and purification of VLPs from <i>baculovirus</i>	91
2.12.3	Expression of Tandem Core TM constructs in <i>Nicotiana benthamiana</i>	92
2.12.4	Expression of tandem core constructs in <i>Pichia pastoris</i>	93

2.12.5	Expression of monomeric VLP construct	94
2.13	Production and analysis of conjugate vaccines	95
2.13.1	Conjugation of CPS antigen to selected protein or rVLP	95
2.13.2	Phenol sulfuric acid analysis of CPS conjugate vaccines	95
2.13.3	BCA analysis of CPS conjugate vaccines.....	96
2.14	Vaccine efficacy studies	96
2.14.1	Preparation of vaccines prior to administration	96
2.14.2	Animal Husbandry	97
2.14.3	Immunisation and challenge schedule.....	97
2.14.4	Intraperitoneal exposure of <i>B. pseudomallei</i> K96243	98
2.14.5	Statistical analysis	98
2.14.6	Enumeration of bacterial loads	98
2.14.7	Determination of sera IgG and IgM antibody levels to antigen	99
2.14.8	IFN- γ Enzyme Linked Immuno-spot assay (ELISPOT)	100
Chapter 3:	<i>Burkholderia</i> capsular polysaccharide	101
3.1	Introduction	101
3.2	Extraction of CPS from <i>B. pseudomallei</i> K96243 and <i>B. thailandensis</i> E555	103
3.3	Development of a quantitative CPS ELISA	107
3.4	CPS expression optimisation – growth.....	119
3.5	CPS expression optimisation – extraction.....	130
3.6	<i>Burkholderia</i> CPS immunogenic epitope.....	132
3.6.1	Antibody recognition to deacetylated CPS.....	132
3.6.2	Comparison of CPS antibody sequences	134
3.7	Importance of the CPS acetyl group.....	137
3.8	Discussion	139
Chapter 4:	Immunogenic <i>Burkholderia</i> proteins	145
4.1	Introduction	145

4.2	Immunogenic <i>Burkholderia</i> protein selection	147
4.3	Expression of Tandem Core™ with peptide inserts.....	149
4.3.1	Prediction of <i>Burkholderia</i> protein membrane spanning domains	152
4.3.2	In-silico <i>Burkholderia</i> protein MHC-I and MHC-II epitope predictions	153
4.4	Discussion	164
4.5	Supplementary information.....	166
4.5.1	Expression of Tandem Core™ with peptide inserts	166
4.5.2	Prediction of <i>Burkholderia</i> protein membrane spanning domains	167
4.5.3	In-silico <i>Burkholderia</i> protein MHC-I and MHC-II epitope predictions	173
4.5.4	Programs for transmembrane helices prediction and MHC-I/MHC-II epitope predictions.....	179
Chapter 5: Immunogenicity and efficacy of candidate vaccines		183
5.1	Introduction	183
5.2	VLP expression systems	187
5.3	Production and analysis of conjugate vaccines	188
5.4	Initial vaccine efficacy study of candidates in mice using IP challenge with <i>B. pseudomallei</i>.....	188
5.4.1	Efficacy testing of conjugates in mice with a high challenge dose of <i>B. pseudomallei</i>	196
5.4.2	<i>Burkholderia</i> protein and VLP expression system efficacy assessment.....	204
5.4.3	Animal efficacy study – formulation	215
5.5	Discussion	224
5.6	Supplementary information.....	235
5.6.1	VLP expression systems	235
5.6.2	Expression of tandem core constructs in <i>Pichia pastoris</i>	237

Chapter 6: Discussion	238
6.1 Introduction	238
6.2 Summary of results.....	238
6.2.1 CPS extraction and optimisation.....	238
6.2.2 CPS immunogenicity	240
6.2.3 VLP fusion constructs	241
6.2.4 CPS conjugate vaccine efficacy.....	242
6.3 Challenges encountered in this work.....	242
6.4 Implications for <i>Burkholderia</i> vaccine development	245
6.5 Future work.....	247
6.6 Conclusion.....	249
Chapter 7: Bibliography.....	251

List of Tables

Table 1 Bacterial strains used in this thesis and reference information	70
Table 2 Biotinylated antibody molar coupling ratios and the volume of reconstituted label required to achieve them.....	76
Table 3 Calculation of CPS ELISA limit of detection from purified CPS mean OD values.....	117
Table 4 Summary of purified <i>B. thailandensis</i> E555 :: <i>wbil</i> (Km ^r) CPS concentration data used to calculate ELISA upper and lower limits of quantification (ULOQ / LLOQ).	119
Table 5 Measurement of <i>B. thailandensis</i> E555 :: <i>wbil</i> (Km ^r) bacterial culture CPS concentration (µg/mL), OD _{590 nm} and CFU/mL, 17-72 hours after inoculation of LB media from a glycerol stock.	120
Table 6 Average CPS concentration (µg/mL) and CFU/mL of three <i>B. thailandensis</i> E555 :: <i>wbil</i> (Km ^r) bacterial cultures, 17-72 hours after inoculation of LB media from a starter culture.	121
Table 7 Identified <i>Burkholderia</i> proteins from the literature that could be used as antigens in a <i>Burkholderia</i> vaccine.....	148
Table 8 Experimental plan for initial efficacy study detailing vaccine candidates, number of mice and adjuvant.	189
Table 9 Experimental plan for full efficacy study detailing vaccine candidates, number of mice and adjuvant.	197
Table 10 Experimental plan for assessment of <i>Burkholderia</i> protein and VLP expression system efficacy, detailing vaccine candidates, number of mice and adjuvant.....	206
Table 11 Median survival of Crm197-CPS conjugate vaccine co-mixed with the <i>Burkholderia</i> proteins PotF, OppA, Hcp6 and LolC.	209
Table 12 Experimental plan for Adjuvant selection study detailing vaccine candidates, number of mice, adjuvant and immunisation route.....	217
Table 13 Median survival of mice following vaccination with Crm197-CPS + LolC adjuvantised with either Alhydrogel®, Poly (I:C) + Alhydrogel®, AddaVax™ or AS04.	220

List of Figures

Figure 1 Intracellular lifecycle of <i>B. pseudomallei</i> adapted from Willcocks <i>et al.</i> , 2016.	30
Figure 2 CPS (2-O-acetyl-6-deoxy-D-manno-heptopyranose) monosaccharide (1) and the CPS homopolymer (2).....	33
Figure 3 Genetic organisation of the CPS gene cluster in <i>B. pseudomallei</i> K96243.....	35
Figure 4 Model of <i>B. pseudomallei</i> CPS biosynthesis	36
Figure 5 Polysaccharides expressed by <i>B. pseudomallei</i>	38
Figure 6 Common carrier proteins used in conjugate vaccines.	51
Figure 7 Hepatitis B core protein and Tandem Core™ VLPs.	65
Figure 8 Vaccine efficacy study schedule.....	97
Figure 9 NMR spectra of CPS isolated from <i>B. thailandensis</i> E555 :: <i>wbil</i> (Km ^r) (Bottom) with reference to purified CPS from <i>B. pseudomallei</i> 1026b (Top)..	105
Figure 10 Monosaccharide analysis of fully hydrolysed <i>B. thailandensis</i> E555 :: <i>wbil</i> (Km ^r) CPS polysaccharide	105
Figure 11 NMR spectra of phenol extract from heat-killed <i>B. thailandensis</i> E555 :: <i>wbil</i> (Km ^r) sample (Bottom) with reference to purified CPS from <i>B. pseudomallei</i> 1026b (Top).	106
Figure 12 Stacked NMR spectra for CPS obtained from <i>B. pseudomallei</i> 1026b (Top), <i>B. thailandensis</i> E555 :: <i>wbil</i> (Km ^r) cultured in LB media (Middle) and <i>B. thailandensis</i> E555 :: <i>wbil</i> (Kmr) cultured in BHI media (Bottom).....	107
Figure 13 Dot-blot for detection of purified CPS with the anti-CPS monoclonal antibody DSTL189.....	108
Figure 14 Detection of purified CPS by ELISA.	109
Figure 15 ELISA to assess recognition of purified CPS with biotinylated DSTL189 monoclonal antibody at different molar coupling ratios.....	110
Figure 16 OD values from CPS capture ELISA with purified <i>B. pseudomallei</i> 1026b.	111
Figure 17 Purified <i>B. pseudomallei</i> 1026b CPS ELISA standard curve generated from OD values in Figure 15 and plotted against log-transformed CPS concentration.	112
Figure 18 Comparison of antibody recognition to CPS extracted from <i>B. pseudomallei</i> and <i>B. thailandensis</i>	113

Figure 19 ELISA results of <i>B. thailandensis</i> E555 :: <i>wbil</i> (Km ^r) culture CPS concentration.....	114
Figure 20 ELISA to determine suitability of <i>B. thailandensis</i> CDC2721121 as the negative control for CPS ELISA development.	115
Figure 21 Calculation of CPS ELISA limit of detection: generation of negative control value.....	116
Figure 22 Typical standard curve generated from ELISA results of CPS purified from <i>B. thailandensis</i> E555 :: <i>wbil</i> (Km ^r).....	118
Figure 23 Comparison of glycerol stock to starter culture inoculate on <i>B. thailandensis</i> E555 :: <i>wbil</i> (Km ^r) culture CPS concentration	122
Figure 24 Effect of different microbiological growth media on <i>B. thailandensis</i> E555 :: <i>wbil</i> (Km ^r) growth and CPS expression.....	123
Figure 25 Effect of baffled Erlenmeyer flasks on <i>B. thailandensis</i> E555 :: <i>wbil</i> (Km ^r) growth and CPS expression inoculated into LB media.	124
Figure 26 Effect of baffled Erlenmeyer flasks on <i>B. thailandensis</i> E555 :: <i>wbil</i> (Km ^r) growth and CPS expression inoculated into enhanced phytone peptone broth.	125
Figure 27 Effect of iron sulfate on <i>B. thailandensis</i> E555 :: <i>wbil</i> (Km ^r) growth and CPS expression.....	126
Figure 28 Effect of reducing culture volume on <i>B. thailandensis</i> E555 :: <i>wbil</i> (Km ^r) growth and CPS expression	127
Figure 29 Effect of mannose on <i>B. thailandensis</i> E555 :: <i>wbil</i> (Km ^r) growth and CPS expression.....	128
Figure 30 Increase in <i>B. thailandensis</i> E555 :: <i>wbil</i> (Km ^r) CPS expression from the use of starter cultures, enhanced phytone peptone broth, baffled flasks, and a 27 hour incubation period.	129
Figure 31 Stacked NMR spectra for CPS obtained from <i>B. thailandensis</i> E555 :: <i>wbil</i> (Km ^r) cultured in enhanced phytone peptone media (Top) and <i>B. thailandensis</i> E555 :: <i>wbil</i> (Km ^r) cultured in LB media (Bottom).....	130
Figure 32 CPS concentration of <i>B. thailandensis</i> E555 :: <i>wbil</i> (Km ^r) culture, supernatant and pellet fractions.	131
Figure 33 CPS concentration of <i>B. thailandensis</i> E555 :: <i>wbil</i> (Km ^r) culture, supernatant and pellet fractions following overnight storage at -20°C.....	132
Figure 34 Lack of DSTL189 antibody recognition to deacetylated CPS.	133

Figure 35 Detection of acetylated and deacetylated <i>B. thailandensis</i> E555 :: <i>wbil</i> (Km ^r) CPS with four anti-CPS monoclonal antibodies.....	134
Figure 36 Amino acid sequence of variable light (VL) and heavy (VH) chain framework regions (FR1-4) and complementarity determining regions (CDR1-3) of four Dstl anti-CPS antibodies (DSTL189, DSTL187, DSTL188 and DSTL190).	138
Figure 37 Amino acid sequence of variable light (VL) chain framework regions (VLFR1-4) and complementarity determining regions (VLCDR1-3) of DSTL189; Dstl's anti-CPS antibody, an anti-pneumococcal C-polysaccharide backbone antibody (CAQ76891) and an anti- <i>F. tularensis</i> O-antigen antibody (4OTX_L).	136
Figure 38 Amino acid sequence of variable heavy (VH) chain framework regions (VHFR1-4) and complementarity determining regions (VHCDR1-3) of DSTL189; Dstl's anti-CPS antibody, an anti- <i>B. pseudomallei</i> antibody (ACZ650301) and anti- <i>S. flexneri</i> LPS antibody (1M71B).	137
Figure 39 Survival of BALB/c mice vaccinated with CPS-TetHc (acetylated and non-acetylated CPS), TetHc and alum followed by challenge with 1.17 x 10 ⁵ CFU via the IP route of <i>B. pseudomallei</i> K96243 (approximately 157 x median lethal doses (MLDs)).	138
Figure 40 ELISA analysis of acetylated and deacetylated CPS-specific IgG and IgM immune responses following vaccination with CPS conjugate vaccines. 138	
Figure 41 Transmission Electron Microscopy (TEM) analysis of <i>E. coli</i> expressed Tandem Core™ VLPs containing LolC fusion protein.....	149
Figure 42 Recognition of purified VLP and VLP-LolC antigen by ELISA with sera from mice immunised with adenovirus expressing LolC.....	150
Figure 43 Recognition of purified VLP and VLP-LolC antigen by ELISA with sera from mice immunised with LolC.....	150
Figure 44 Recognition of purified VLP and VLP-LolC recognition by ELISA with sera from mice immunised with purified LolC.....	151
Figure 45 TMHMM calculated probabilities for transmembrane domains within the <i>Burkholderia</i> protein LolC [BPSL2277].....	152
Figure 46 Overlay of TMHMM transmembrane helices prediction onto the amino acid sequence of LolC.	153
Figure 47 A flow diagram for generation of MHC-I epitope predictions.	154

Figure 48 The top 10 highest scoring LoIC protein H2-Kd (MHC-I) nonamer epitope predictions from Syfpeithi, Immuneepitope and Propred.	155
Figure 49 The top 10 highest scoring LoIC protein H2-Kd (MHC-I) decamer epitope predictions from Syfpeithi, Immuneepitope and NetMHC3.2.	156
Figure 50 The top 10 highest scoring LoIC protein H2-Dd (MHC-I) epitope predictions from NetMHC3.2, Immuneepitope and Propred.	157
Figure 51 The top 10 highest scoring LoIC protein H2-Ld (MHC-I) nonamer epitope predictions from Syfpeithi, Immuneepitope and Propred.	158
Figure 52 Predicted LoIC MHC-I epitopes collated from shortlists generated for each H2-d allele.	159
Figure 53 LoIC amino acid sequence highlighting transmembrane helices and MHC-I epitope predictions.	160
Figure 54 The top 10 highest scoring LoIC protein H2 I-Ad (MHC-II) epitope predictions from Syfpeithi, Immuneepitope and NetMHCII.	161
Figure 55 The top 10 highest scoring LoIC protein H2 I-Ed (MHC-II) epitope predictions from Syfpeithi and Immuneepitope.	162
Figure 56 MHC-II collated LoIC sequences from both alleles of the H2-d region.	163
Figure 57 LoIC amino acid sequence highlighting transmembrane helices and MHC-II epitope predictions.	163
Figure 58 LoIC amino acid sequence highlighting transmembrane helices, MHC-I and MHC-II epitope predictions.	164
Figure 59 Negative stain TEM images of plant expressed VLP-ExLoIC in clarified lysate, after filtration and sucrose density gradient purification.	167
Figure 60 TMHMM calculated probabilities for transmembrane domains within the <i>Burkholderia</i> protein PotF [BPSL1555].	168
Figure 61 Amino acid sequence of PotF. No membrane spanning domains are predicted.	168
Figure 62 TMHMM calculated probabilities for transmembrane domains within the <i>Burkholderia</i> protein OppA [BPSS2141].	169
Figure 63 Amino acid sequences of OppA highlighting transmembrane helices predictions.	169
Figure 64 TMHMM calculated probabilities for transmembrane domains within the <i>Burkholderia</i> protein Omp85 [BPSL2151].	170

Figure 65 Amino acid sequence of Omp85. No membrane spanning domains are predicted.	170
Figure 66 TMHMM calculated probabilities for transmembrane domains within the <i>Burkholderia</i> protein Hcp2 [BPSS0518]	171
Figure 67 Amino acid sequence of Hcp2. No membrane spanning domains are predicted.....	171
Figure 68 TMHMM calculated probabilities for transmembrane domains within the <i>Burkholderia</i> protein Hcp6 [BPSL3105].....	172
Figure 69 Amino acid sequence of Hcp6. No membrane spanning domains are predicted.....	172
Figure 70 MHC-I collated PotF amino acid sequences from all H2-d alleles.	173
Figure 71 MHC-II collated PotF sequences from both alleles of the H2-d region.	174
Figure 72 MHC-I collated OppA amino acid sequences from all H2-d alleles.	174
Figure 73 MHC-II collated OppA sequences from both alleles of the H2-d region.	175
Figure 74 MHC-I collated Omp85 amino acid sequences from all H2-d alleles.	176
Figure 75 MHC-II collated Omp85 sequences from both alleles of the H2-d region.	177
Figure 76 MHC-I collated Hcp2 amino acid sequences from all H2-d alleles.	178
Figure 77 MHC-II collated Hcp2 sequences from both alleles of the H2-d region.	179
Figure 78 Animal study schedule and justification	187
Figure 79 Efficacy of antigens against 103 and 240 x MLD <i>B. pseudomallei</i> K96243 challenge.....	191
Figure 80 ELISA analysis of the CPS specific IgG and IgM antibody response from mouse sera obtained from the 103 and 240 x MLD challenge study.....	192
Figure 81 Initial vaccine efficacy study – bacterial burden.....	193
Figure 82 Bodyweight data of VLP-CPS vaccinated groups from the initial efficacy study up to 35 days after challenge with 103 or 240 x MLD of <i>B. pseudomallei</i> K96243.	194

Figure 83 Bodyweight data of Crm197-CPS vaccinated groups from the initial efficacy up to 35 days after challenge with 103 and 240 x MLD of <i>B. pseudomallei</i> K96243.	195
Figure 84 Efficacy of control antigens against 489 x MLD <i>B. pseudomallei</i> K96243 challenge.....	198
Figure 85 Efficacy of conjugate vaccines against 489 x MLD <i>B. pseudomallei</i> K96243 challenge.....	200
Figure 86 Effect of LoIC on VLP-CPS conjugate efficacy against 489 x MLD <i>B. pseudomallei</i> K96243 challenge.	200
Figure 87 Effect of VLP on LoIC-CPS conjugate efficacy against 489 x MLD <i>B. pseudomallei</i> K96243 challenge.	201
Figure 88 Efficacy comparison of plant purified VLPs conjugated to CPS, with and without addition of LoIC, to Crm197-CPS against 489 x MLD <i>B. pseudomallei</i> K96243 challenge.	201
Figure 89 ELISA analysis of the CPS specific IgG antibody response from mouse sera obtained from the 489 x MLD challenge study.....	202
Figure 90 ELISA analysis of the CPS specific IgM antibody response from mouse sera obtained from the 489 x MLD challenge study.....	202
Figure 91 ELISA analysis of the LoIC specific IgG antibody response from mouse sera obtained from the 489 x MLD challenge study.....	203
Figure 92 ELISA analysis of the LoIC specific IgM antibody response from mouse sera obtained from the 489 x MLD challenge study.....	203
Figure 93 Efficacy comparison of vaccine antigens to 103, 240 and 489 x MLD <i>B. pseudomallei</i> K96243 challenge.	204
Figure 94 Efficacy comparison of Crm197-CPS conjugate vaccines with and without <i>Burkholderia</i> proteins added as co-antigens against 399 x MLD <i>B. pseudomallei</i> K96243 challenge.	208
Figure 95 Efficacy comparison of <i>Burkholderia</i> protein antigens against 399 x MLD <i>B. pseudomallei</i> K96243 challenge.....	209
Figure 96 ELISA analysis of the <i>Burkholderia</i> protein specific IgG antibody response from mouse sera obtained from the 399 x MLD challenge study....	210
Figure 97 Efficacy comparison of plant-expressed VLPs conjugated to CPS vs Crm197-CPS against 399 x <i>B. pseudomallei</i> K96243 challenge.....	210

Figure 98 Efficacy comparison of plant-expressed VLPs conjugated to CPS vs yeast expressed VLPs conjugated to CPS against 399 x <i>B. pseudomallei</i> K96243 challenge.....	211
Figure 99 Efficacy comparison of yeast-expressed VLPs conjugated to CPS with and without Hcp6 against 399 x <i>B. pseudomallei</i> K96243 challenge.....	211
Figure 100 ELISA analysis of the VLP specific IgG antibody response from mouse sera obtained from the 399 x MLD challenge study.....	212
Figure 101 ELISA analysis of the CPS specific IgG antibody response from mouse sera obtained from the 399 x MLD challenge study.....	213
Figure 102 Liver, Spleen and Lung bacterial burden from the 399 x MLD challenge study.	214
Figure 103 Efficacy comparison of Crm197-CPS conjugate with different adjuvants against a 750 x MLD <i>B. pseudomallei</i> K96243 challenge.	220
Figure 104 Vaccinated mice splenocyte IFN- γ recall response to Crm197 determined by ELISpot.....	221
Figure 105 ELISA analysis of the Crm197 specific IgG antibody response from mouse sera obtained after each vaccination from the adjuvant selection study.	222
Figure 106 ELISA analysis of the LolC specific IgG antibody response from mouse sera obtained after each vaccination from the adjuvant selection study.	222
Figure 107 Effect of vaccination route on Crm197-CPS vaccine efficacy against a 750 x MLD <i>B. pseudomallei</i> K96243 challenge.....	223
Figure 108 Efficacy comparison of Tandem Core TM and monomeric core VLPs conjugated to CPS against a 450 x MLD <i>B. pseudomallei</i> K96243 challenge.....	223
Figure 109 ELISA analysis of the VLP specific IgG antibody response from mouse sera obtained after each vaccination from the adjuvant selection study.	224
Figure 110 Efficacy of Crm197-CPS conjugate vaccines with different CPS-protein ratios against 103, 240, 399 and 489 x MLD <i>B. pseudomallei</i> K96243 challenge.....	233
Figure 111 Efficacy of VLP-CPS conjugate vaccines with different CPS-protein ratios against 399, 450 and 489 x MLD <i>B. pseudomallei</i> K96243 challenge..	234
Figure 112 TEM analysis of <i>E. coli</i> expressed tandem core VLPs.	235
Figure 113 Electron micrograph of VLP from <i>Baculovirus</i>	236

Figure 114 SDS PAGE (a) western blot (b), and negative stain TEM analysis of purified VLP. 1. Protein standards, 2. Purified VLPs (neat), 3 Purified VLPs (1:10 diluted). 237

Abstract

A thesis by Marc Ashley Bayliss entitled 'Virus-like particles as a novel platform for delivery of protective *Burkholderia* antigens' and submitted to the University of Exeter for the degree of Doctor of Philosophy.

There is currently no licensed vaccine available for the global tropical pathogen *Burkholderia pseudomallei* which is the causative agent of melioidosis and a potential bio-threat agent.

The capsule polysaccharide (CPS) expressed by *B. pseudomallei* has been shown to offer some protection against bacterial challenge. Polysaccharide immunogenicity can be enhanced by conjugation to a carrier protein and several licensed vaccines utilise this technology.

Virus-like particles (VLPs) are non-infectious, non-replicating, viral proteins that self-assemble into viral structures and are in several licensed vaccines as primary antigens. VLPs are also effective delivery platforms for foreign antigens by genetic insertion or chemical conjugation.

iQur, a collaborator on this project, has developed Tandem Core™ that consists of two genetically linked hepatitis B core proteins that allow insertion of large proteins into each core whilst remaining assembly competent.

The aim of this thesis was to assess the protective efficacy of Tandem Core™ VLPs chemically conjugated to CPS and Tandem Core™ *Burkholderia* protein fusion constructs. This involved three objectives; reduce the cost of CPS extraction; identify immunogenic *Burkholderia* proteins; and test candidate vaccine efficacy in an animal model of acute melioidosis against *B. pseudomallei* challenge.

To reduce the cost of extraction, CPS was purified from *B. thailandensis* strain E555 and bacterial culture CPS concentration optimised which first required development of a quantitative ELISA.

Immunogenic *Burkholderia* proteins were identified from the literature but Tandem Core™ fusion constructs containing these proteins were not assembly competent. The *Burkholderia* proteins were added as co-antigens to the VLP-CPS conjugate vaccine but did not improve efficacy.

Tandem Core™ VLPs conjugated to CPS were protective against *B. pseudomallei* challenge and were compared to CPS conjugated to Crm197: a commercially available carrier protein used in several licensed vaccines. At lower challenge doses, survival was greater in mice vaccinated with the VLP-CPS conjugate although at higher doses, Crm197-CPS efficacy was greater.

Acknowledgments

I would like to thank my supervisors, Associate professor Jo Prior and Dr Nicholas Harmer for their advice and support over these last 4 years. Thank you to all the collaborators on this project; Prof. Rob Field, Dr Sergey Nepogodiev and Dr Giulia Pergolizzi at the John Innes Centre and Mark Davies and Dr Lucy Beales at Mologic.

I would also like to thank all of my colleagues at Dstl for the technical expertise and advice they have provided me.

This work was funded by the US Defense Threat Reduction Agency under contract HDTRA1-12-D-0003-0002.

List of abbreviations

ABTS	2,2'-azino-bis(ethylbenzthiazoline-6-sulphonic acid)
ADCP	Advisory Committee on Dangerous Pathogens
ADH	adipic acid dihydrazide
AEX	Anion exchange chromatography
Alum	Aluminium Hydroxide
ANN	Artificial neural networks
APC	Antigen presenting cells
BARDA	Biomedical Advanced Research and Development Authority
BCA	Bicinchoninic Acid Protein Assay
Bcc	<i>B. cepacia</i> complex
BCG	Bacillus Calmette-Guérin
BCIP/NBT	5-bromo-4-chloro-3'-indolyphosphate / nitro-blue tetrazolium
BHI	Brain Heart Infusion broth
Bps	<i>Burkholderia pseudomallei</i>
BSA	Bovine serum albumin
Bt	<i>Burkholderia thailandensis</i>
CDAP	1-cyano-4-dimethylaminopyridinium tetrafluoroborate
CDR	Complementarity determining regions
CDS	Coding sequences
CFU	Colony-forming units
CIES	Carrier induced epitopic suppression
CL3	Containment level 3
CLR	C-type lectin-like receptors
CNBr	Cyanyogen bromine
CPS	Capsule polysaccharide
CT	Cholera toxin
DAB	3-3'-Diaminobenzidine
DARPA	Defense Advanced Research Projects Agency
DMF	Dimethylformamide
DNA	Deoxyribonucleic acid
DT	Diphtheria toxoid
DTRA	Defense Threat Reduction Agency
EDTA	Ethylenediaminetetraacetic acid

EEE	Eastern equine encephalitis
ELISA	Enzyme-linked immunosorbent assay
EPS	exopolysaccharide
ER	Endoplasmic reticulum
FBU	FastBac Ultra
FDA	Food and Drug Administration
FR	Framework Region
GFP	Green fluorescent protein
HBcAg	Hepatitis B core antigen
HBV	Hepatitis B virus
HEPA	High efficiency particulate absorption
Hib	<i>H. influenza</i> type b
HIV	Human immunodeficiency virus
HLA	Human leukocyte antigen
HMM	Hidden Markov model
HPLC	High performance liquid chromatography
HPV	Human papilloma virus
HRP	Horse radish peroxidase
IFN- γ	Gamma interferon
IM	Intra-muscular
IP	Intra-peritoneal
IPTG	Isopropyl β -D-1-thiogalactopyranoside
JIC	John Innes Centre
Km ^r	Kanamycin resistance
KPL	Tetramethylbenzidine
LB	Luria-Bertani
LLOQ	Lower Limit of Quantification
LOD	Limit of Detection
LOQ	Limit of Quantification
LPS	Lipopolysaccharide
LSHTM	London School of Hygiene and Tropical Medicine
MCR	Molar Coupling Ratio
MenC	Meningococcal group C
MIR	Major insertion regions
MHC	Major histocompatibility complex

MLD	Median lethal dose
MLST	Multilocus sequence typing
MNGC	Multi-nucleated giant host cell
MPL	monophosphoryl lipid A
MRC	Medical Research Council
MTTD	Mean time to death
NaIO ₄	Sodium periodate
NK	Natural killer cells
NLR	NOD-like receptors
NMR	Nuclear magnetic resonance
NOD	Nucleotide oligomerization domain
OD	Optical density
ORF	Open reading frame
PAMP	Pathogen associated molecular patterns
PBS	Phosphate buffered saline
PCR	Polymerase chain reaction
PEG	Polyethylene glycol
Poly (I:C)	polyinosinic-polycytidylic acid
PRR	Pattern-recognition receptors
RIG	Retinoic acid-inducible gene
SC	Subcutaneous
SD	Standard deviation
SDS PAGE	Sodium dodecyl sulfate polyacrylamide gel electrophoresis
SMM	Stabilized matrix method
SP	Streptavidin peroxidase
SWR	Standard working reagent
T3SS	Type III secretion system
T6SS	Type VI secretion system
TAP	Transporter associated with antigen processing
TD	T-cell dependent
TEM	Transmission electron microscopy
TetHc	Tetanus toxoid Hc fragment
TFA	Trifluoroacetic acid
TI	T-cell independent
TLR	Toll-like receptors

TM	Trade mark
TMB	Tetramethylbenzidine
TNF	Tumor necrosis factor
Tni	Insect cell line used by Oxford expression technologies
TRS	Technical Series of Reports
ULOQ	Upper Limit of Quantification
VEE	Venezuelan equine encephalitis
VLP	Virus-Like Particles
WEE	Western equine encephalitis
WHO	The World Health Organisation
YPDS	Yeast Extract Peptone Dextrose Sorbitol

Chapter 1: General Introduction

1.1 *Burkholderia*

The genus *Burkholderia* was first defined in 1992 and originally consisted of only seven species which has expanded to consist of nearly 100 species of Gram-negative, motile, aerobic bacilli. These were previously considered part of the genus *Pseudomonas* (Daligault *et al.*, 2014; Eberl and Vandamme, 2016). These bacteria are found in soils and groundwater worldwide and colonise a diverse range of hosts as a result of considerable genetic versatility (Coenye and Vandamme, 2003). The environmental lifestyle of *Burkholderia* species benefit scientific and industrial use and several species are used in nitrogen fixation, biological control of plant diseases, and water management (Coenye and Mahenthiralingam, 2014). However, several species are animal, human and plant pathogens capable of causing life-threatening infections (Coenye and Vandamme, 2003).

Prominent pathogenic members of the *Burkholderia* genus include the human pathogens *B. pseudomallei*, the causative agent of melioidosis, *B. mallei* which causes glanders, and 20 related species of *Burkholderia* termed the *B. cepacia* complex, which are responsible for opportunistic infections (Whitmore 1913, Redfearn *et al.*, 1966, Chou *et al.*, 2013, Silva and Dow, 2013, Pradenas *et al.*, 2016). An interesting *Burkholderia* species is *B. thailandensis* strain E555, which, although essentially avirulent, produces the same polysaccharide capsule as *B. pseudomallei* and *B. mallei*, and is used in the study of *B. pseudomallei* infection (Sim *et al.*, 2010).

1.2 *Burkholderia pseudomallei* and melioidosis

B. pseudomallei is the causative agent of melioidosis, a potentially lethal human and animal disease, found in soil and water and is a resilient organism capable of survival in hostile environments (Wuthiekanun *et al.*, 1995, Pumpuang *et al.*, 2011, Baker *et al.*, 2015). *B. pseudomallei* is classified as a Tier 1 bio-threat

agent by the US Centers for Disease Control and Prevention (CDC) which regulates the possession, use and transfer of biological agent (Rotz *et al.*, 2002, Peacock *et al.*, 2008). The criteria for Tier 1 agents include; the ability to cause mass casualties or economic devastation; communicability or dispersibility; low infectious dose; and intent of weaponisation (Wagar 2016). Concerns about *B. pseudomallei* use as a potential bioweapon stem primarily from a relatively high mortality rate, infectivity via the inhalational route, lack of a vaccine and intrinsic resistance to frontline antibiotics (Silva *et al.*, 2013). For these reasons, development of a *B. pseudomallei* vaccine is a priority.

Several *B. pseudomallei* genomes have been sequenced (Galyov *et al.*, 2010) but the reference strain of *B. pseudomallei* is considered to be strain K96243, isolated in 1996 from a female diabetic patient in Thailand (Holden *et al.*, 2004). The genome of *B. pseudomallei* K96243 consists of two chromosomes of 4.07 Mb and 3.17 Mb in size and is large in comparison to typical prokaryotes (Holden *et al.*, 2004). Chromosome 1 (4.07 Mb) contains coding sequences (CDSs) involved in core functions such as amino acid metabolism, nucleotide and protein synthesis, chemotaxis and motility (Holden *et al.*, 2004). Chromosome 2 contains more CDSs for accessory functions such as osmotic protection and iron acquisition secondary metabolism (Holden *et al.*, 2004). *B. pseudomallei* evolution seems largely driven by horizontal gene transfer (Holden *et al.*, 2004).

Melioidosis was first described as a glanders-like disease among morphine addicts in Burma by Whitmore in 1912 but is now recognised as a worldwide tropical pathogen and a major cause of pneumonia and sepsis across Asia and Northern Australia (Whitmore 1913, Currie and Kaestli, 2016). It is estimated that the annual number of deaths resulting from melioidosis (89,000) is comparable to that of measles (Limmathurotsakul *et al.*, 2016). Clinical presentation of melioidosis is broad and ranges from asymptomatic seroconversion to acute septicaemia and pneumonia (Choh *et al.*, 2013). Melioidosis is fatal in up to 50 % of cases depending on geographical region (Wiersinga *et al.*, 2012), although acute septicaemia is associated with the worst prognosis with a mortality rate of approximately 95 % without antibiotic therapy (Cheng *et al.*, 2007, Currie *et al.*, 2000). Infected patients do not

develop protective immunity to re-infection as relapse does occur regardless of high antibody titres and some individuals will develop chronic, subclinical infections (Silva *et al.*, 2013, Choh *et al.*, 2013). Due to its ability to evade the immune system and manipulate host immune responses *B. pseudomallei* may also cause a latent infection with delayed symptoms up to 62 years after infection (Ngauy *et al.*, 2005, Vellasamy *et al.*, 2016). At one time this was considered a serious potential health risk for US personnel returning from the Vietnam War and was dubbed 'the Vietnamese time bomb' (Sanford 1978).

The main routes of infection with *B. pseudomallei* are thought to be direct inoculation through cuts and abrasions in the skin or via the gastrointestinal and inhalational routes (Cheng and Currie, 2005, West *et al.*, 2010). The route of infection correlates to disease severity with inhalational infection associated with severe infection (Silva *et al.*, 2013). Risk factors associated with melioidosis infection include diabetes mellitus, pulmonary disease, chronic renal impairment, alcoholism, and a suppressed immune system (Foong *et al.*, 2014). In locations with access to laboratory diagnostics and treatment for sepsis, patients that die from melioidosis are almost always those with identified risk factors (Currie 2015).

Melioidosis is known to be endemic in 48 countries across Southeast Asia, the Middle East, Africa, Latin America, the Caribbean and the Pacific, although recent modelling suggests that melioidosis is probably endemic in another 34 countries (Limmathurotsakul *et al.*, 2016). The lack of accurate epidemiology data is thought to result from the lack of diagnosis capability in these countries and the non-specific symptoms associated with infection (Currie and Kaestli, 2016).

1.2.1 Diagnosis and treatment

Culture identification from clinical samples is still the 'gold standard' of *B. pseudomallei* diagnosis but can take up to 7 days (Currie 2015, Lau *et al.*, 2015). *B. pseudomallei* is easily cultured on readily available, commercial media but misidentification is common due to the relatively nondescript colony

morphology (Wikraiphath *et al.*, 2015). Identification is improved with selective media such as Ashdown's agar, which contains gentamycin, but colony morphology from clinical samples demonstrates considerable variability (Chantratita *et al.*, 2007, Currie 2015).

Methods to reduce diagnostic time have been developed including indirect hemagglutination or ELISA, but are inadequate because of high background seroconversion of people living in endemic areas (Currie 2015). Other techniques include real-time PCR, and lateral flow immunoassays, which are rapid but less sensitive than blood culture; and rapid immunofluorescence microscopy, although the lack of facilities limits availability in some areas. In Thailand, identification is also performed by the latex agglutination test which is sensitive and specific but this is not widely available (Cheng and Currie, 2005, Currie 2015).

Treatment of melioidosis is based on a series of clinical trials conducted in Thailand over the past 25 years and is separated into the acute and eradication phase (Dance 2014). Current guidelines suggest intravenous ceftazidime or a carbapenem for 10 to 14 days (acute phase) – to stop patients dying of sepsis - followed by oral trimethoprim-sulfamethoxazole, doxycycline or amoxicillin-clavulanate for 3 to 6 months in the eradication phase to prevent relapse (Pitman *et al.*, 2015, Dance 2014). Despite this regime, relapse occurs in between 5.7 % to 9.3 % of surviving patients and is thought to result from the intracellular lifestyle of *B. pseudomallei* (Limmathurotsakul *et al.*, 2006, Allwood *et al.*, 2011, Sarovich *et al.*, 2014).

1.2.2 *Burkholderia pseudomallei* intracellular infection and mechanisms of virulence

B. pseudomallei can invade and multiply in both phagocytic and non-phagocytic cells (Jones *et al.*, 1996). *B. pseudomallei* is believed to invade cells by first adhering to the cell surface by expression of type IV pili and the adhesion proteins BoaA and BoaB, as mutation of the *pilA*, *boaA* and *boaB* genes reduces adherence to epithelial cells (Essex-Lopresti *et al.*, 2005, Balder *et al.*, 2010). Invasion of non-phagocytic cells relies on the type III secretion system

(T3SS) components; BipD, BopE and BsaQ (Stevens *et al.*, 2003, Muangsombut *et al.*, 2008). The T3SS comprises approximately 20 proteins that form a syringe-like structure that span the inner and outer membrane and enable *B. pseudomallei* to secrete and inject effector molecules into host cells (Allwood *et al.*, 2011). The T3SS is also important in escape of *B. pseudomallei* from the phagosome by the effector protein BopA (Gong *et al.*, 2011). In addition, mutations of other T3SS proteins results in delayed phagosomal escape (Allwood *et al.*, 2011). In the cytoplasm, *B. pseudomallei* polymerises actin which allows for cell-to-cell spread and evasion of host immunity and autophagy (Choh *et al.*, 2013, Kespichayawattana *et al.*, 2000). The BimA protein has been shown to interact directly with actin and a *bimA* *B. pseudomallei* mutant does not polymerise actin (Lazar Adler *et al.*, 2009).

B. pseudomallei has six type VI secretion systems (T6SS), of which T6SS-1 has also been shown to be critical for intracellular spread in both phagocytic and non-phagocytic cells by inducing plasma membrane fusion resulting in formation of multinucleated giant cells (Burtnick *et al.*, 2011, Hopf *et al.*, 2014). The intracellular lifecycle of *B. pseudomallei*, adapted from Willcocks *et al.* (2016) is shown in Figure 1.

The basis of *B. pseudomallei* pathogenicity is not fully understood but cytotoxicity involves cellular caspase-1 activation, T3SS effector proteins, flagellar hook-associated protein and induction of apoptosis-related genes and proteins (Sun *et al.*, 2005, Bachert *et al.*, 2015, Gourlay *et al.*, 2015, Hseu *et al.*, 2013).

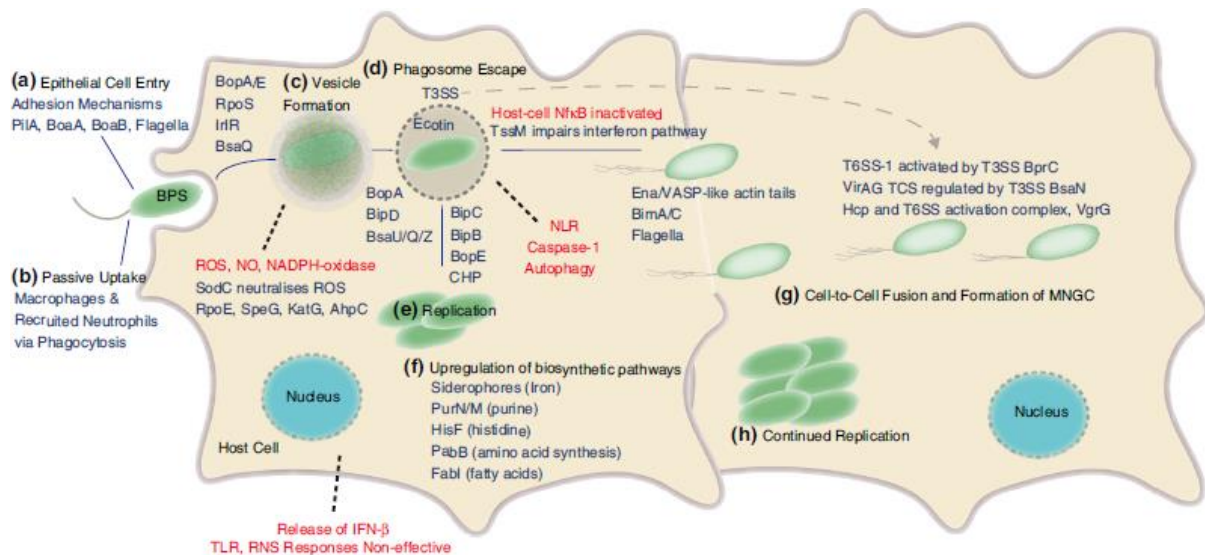


Figure 1 Intracellular lifecycle of *B. pseudomallei* adapted from Willcocks *et al.*, 2016.

B. pseudomallei gains access to cells by macrophage/neutrophil uptake or invasion of non-phagocytic cells by the use of flagella and adhesion factors (a, b). When inside the host cell, *B. pseudomallei* is enveloped in an endocytic vesicle or phagosome where T3SS is required for escape (c, d). *B. pseudomallei* replicates intracellularly (e) and upregulates biosynthetic pathways (f). Host actin is utilised for polymerisation of Ena/VASP-like tails which, alongside T6SS-1, results in successful dissemination to surrounding cells with formation of multinucleated giant host cells (MNGC's) (g) and continued replication (h). Black text describes intracellular processes. Blue text lists genes important for intracellular survival. Some of the host responses are shown in red and the dashed-arrow indicates the connection between T3SS and T6SS. Actin tails are not structurally accurate.

1.3 *Burkholderia mallei* and glanders

B. mallei is the causative agent of glanders, a disease of solipeds, and cannot survive outside of a host (Redfean *et al.*, 1966). Glanders was eradicated in many countries in the early 20th century but sporadic cases still occur in South America, Asia, Africa and the Middle East (Ulrich *et al.*, 2005). Human infection typically occurs as a consequence of occupational exposure and is almost always fatal without antibiotic therapy (DeShazer *et al.*, 2001). The transmission routes and symptoms are similar to *B. pseudomallei* with the septicaemic form associated with a mortality rate of greater than 95 % without treatment (Zandt *et al.*, 2013). *B. mallei* is highly infectious by the aerosol route and was allegedly used as a biological weapon during World Wars I and II (Choh *et al.*, 2013). Although glanders was recognised centuries before melioidosis, whole genome

sequencing and multilocus sequence typing (MLST) has actually shown *B. mallei* to be a clonal derivative of *B. pseudomallei* (Currie 2015).

As for melioidosis, definitive diagnosis of glanders is by culture identification. Because of the rarity of human glanders cases, there is limited information on antibiotic therapy but recommendations mirror the treatment regime of melioidosis (Zandt *et al.*, 2013).

1.4 *Burkholderia cepacia*

B. cepacia complex (Bcc) bacteria, traditionally plant pathogens, were first described in 1950 following observation of onion bulb disease (Burkholder 1950). From recent reporting this complex consists of 20 species (Pradenas *et al.*, 2016). Respiratory disease is a major cause of morbidity and mortality in patients with cystic fibrosis and Bcc bacteria are recognised as opportunistic pathogens in these patients which can cause a rapid deterioration in respiratory function, pneumonia and sepsis (Horsley *et al.*, 2016). Treatment of Bcc infection in cystic fibrosis patients is difficult due to antibiotic resistance and the lack of an optimal antibiotic regime (Horsley *et al.*, 2016). In contrast to *B. pseudomallei*, patient-to-patient transmission of Bcc bacteria has been shown (Manno *et al.*, 2004).

1.5 *Burkholderia thailandensis*

B. thailandensis is an organism closely related to *B. pseudomallei* and *B. mallei* but with a $> 10^5$ -fold reduction in virulence in an animal model of acute melioidosis (Brett *et al.*, 1998). As *B. thailandensis* can be handled at lower levels of containment, has an intracellular lifecycle and is very similar genetically to *B. pseudomallei*, it is often used as a substitute in melioidosis research (Haraga *et al.*, 2008, Brett *et al.*, 2011, French *et al.*, 2011, Choh *et al.*, 2013). The lack of *B. thailandensis* virulence is often attributed to the presence of an arabinose biosynthesis operon, which is not present in *B. pseudomallei*, differences in fimbrial gene clusters and the lack of a type III

secretion system (Sirisinha *et al.*, 1998, Rainbow *et al.*, 2002, Moore *et al.*, 2004, Yu *et al.*, 2006).

1.6 Bacterial polysaccharides

Bacteria express a diverse range of polysaccharides which are often an essential component of bacterial membranes and may function as structural components or virulence factors (Cooper *et al.*, 2015).

Capsular polysaccharides are a structurally diverse set of carbohydrates that form a major component of bacterial cell envelopes. They generally consist of long chains of repeating oligosaccharide sequences which tend to be anionic in nature and may contain as many as seven or eight sugar residues (Liebert *et al.*, 2000). The repeat units can be either linear or branched and contain non-carbohydrate substituents such as O-acetyl, glycerol phosphate, or pyruvate ketals. Capsular polysaccharides are fundamental to pathogenesis of many bacteria including *Neisseria meningitidis* (Fiebig *et al.*, 2014), and both *B. pseudomallei* and *B. mallei* (Reckseidler *et al.*, 2001, Deshazer *et al.*, 2001). They can exhibit a variety of functions including resistance to environmental insult including salts, heavy metals and antimicrobial peptides and can also actively inhibit the human immune system (Whitfield 2006, Llobet *et al.*, 2008). A variety of mechanisms for this action are known, including reduction of the amount of bound complement (Cuccui *et al.*, 2012), inhibition of the complement cascade (Reckseidler-Zenteno, *et al.*, 2005), or interference with recognition by phagocytic receptors on immune cells (Cartee *et al.*, 2005).

1.6.1 *B. pseudomallei* and *B. mallei* capsular polysaccharide

In 1995, research into vaccine candidates for melioidosis identified an O-antigenic polysaccharide produced by *B. pseudomallei*. This polysaccharide, originally termed OPS-I, was identified as an unbranched homopolymer of -3-)-2-O-acetyl-6-deoxy- β -D-manno-heptopyranose-(-1 (Perry *et al.*, 1995). Further work determined this polysaccharide as a capsular polysaccharide (CPS) on the basis of high molecular mass; importance to virulence; and, most importantly,

genetic homology of OPS-I genes to other bacterial genes responsible for CPS biosynthesis (Reckseidler *et al.*, 2001). In 2012 it was demonstrated that CPS is produced by both *B. pseudomallei* and *B. mallei* and suggested that this antigen could be used in a vaccine against both melioidosis and glanders (Heiss *et al.*, 2012).

The molecular weight of CPS is estimated to be around 200 kDa and contains approximately 1000 monosaccharide units (Scott *et al.*, 2013). A representation of the CPS monosaccharide and homopolymer is shown in Figure 2.

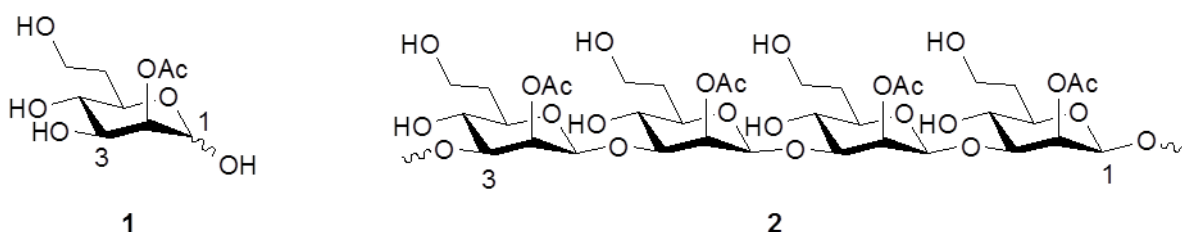


Figure 2 CPS (2-O-acetyl-6-deoxy-D-manno-heptopyranose) monosaccharide (1) and the CPS homopolymer (2)

The determination of CPS as a virulence determinant of both *B. pseudomallei* and *B. mallei* was demonstrated with CPS mutants. Loss of capsule expression resulted in attenuation in median lethal dose (MLD) from <10 colony forming units (CFU) to greater than 10^5 CFU in mouse models of disease (Reckseidler *et al.*, 2001, Deshazer *et al.*, 2001). CPS has been shown to be anti-phagocytic and inhibits complement deposition and clearance which may explain its role in virulence (Reckseidler *et al.*, 2005).

In addition to a virulence factor, CPS is also a protective immunogen. Vaccination with CPS in an experimental mouse model has been shown to give a degree of protection to *B. pseudomallei* challenge (Nelson *et al.*, 2004), as does the passive transfer of antibodies raised against CPS (Jones *et al.*, 2002). Antibodies to CPS have also been detected in convalescent patient sera (Parthasarathy *et al.*, 2006), which together suggest that CPS could be a good vaccine candidate. This may be explained by its expression on the surface of the bacterium, thus maximising exposure to the immune system upon infection (Reckseidler *et al.*, 2001). CPS could make a useful component of a subunit

vaccine as successful polysaccharide vaccines are already in use for a range of other pathogenic bacteria (Jones 2005). Despite recent advances in methods for CPS purification from pathogenic *Burkholderia* (Heiss *et al.*, 2012), the yields are low, and require cultivation of unacceptably large quantities of select agent.

Most strains of *B. thailandensis* do not produce the 6-deoxy heptan capsular polysaccharide with the exception of strain E555 and CDC3015869 which were identified by Sim *et al.* in 2010. The capsular polysaccharide produced by strain E555 was shown to cross-react with an antibody raised against *B. pseudomallei* CPS, although the structure of this CPS was not solved (Sim *et al.*, 2010). Genome sequencing by Sim did confirm the presence of a gene cluster within *B. thailandensis* with 94.4 % sequence homology to the CPS gene cluster within *B. pseudomallei* (Sim *et al.*, 2010).

1.6.1.1 The *B. pseudomallei* CPS operon

The 34.5 kb gene cluster encoding CPS in *B. pseudomallei* is located on chromosome 1 and is shown in Figure 3 which illustrates the genetic organisation and direction of transcription (Reckseidler *et al.*, 2001, Cuccui *et al.*, 2012).

A study in 2007 by Cuccui *et al.* (2007) investigated the effect on CPS expression by transposon mutagenesis of CPS genes. The results confirmed previous work that disruption of *wcbB*, which encodes a glycosyltransferase, resulted in loss of CPS expression (Cuccui *et al.*, 2007, Reckseidler *et al.*, 2001, Atkins *et al.*, 2002). In addition, disruption of *wcbN* and *wcbC* attenuated *B. pseudomallei* in mice whilst retaining the immuno-reactive epitope of CPS (Cuccui *et al.*, 2007).

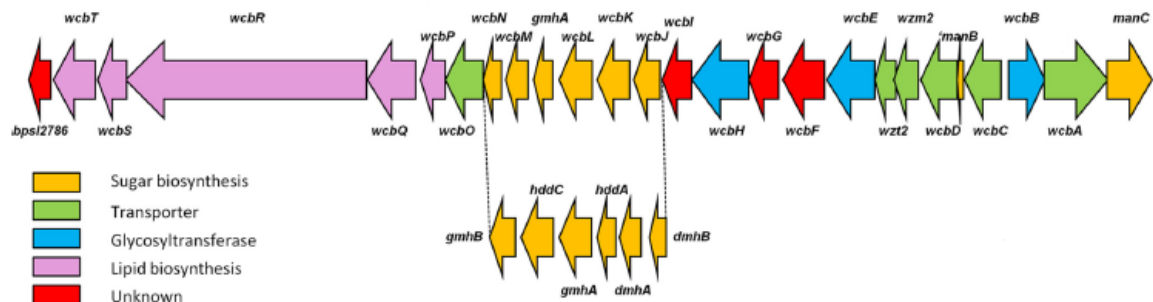


Figure 3 Genetic organisation of the CPS gene cluster in *B. pseudomallei* K96243. Broken lines indicate a cassette of genes orthologous to *Y. pseudotuberculosis* H897/87 involved in biosynthesis of GDP-6-deoxy-D-manno-heptose Adapted from Cuccui *et al.* (2012).

In 2012, a comprehensive study of individual open reading frames (ORFs) within the CPS coding region of *B. pseudomallei* generated a model of CPS biosynthesis and export from inactivation of 18 of the CPS genes. The effect on phenotype was assessed by Western blot, immunofluorescence microscopy and *B. pseudomallei* virulence in an animal model. The gene cluster was reported to contain a central sugar biosynthesis cassette, with six of the proteins orthologous to proteins involved in the biosynthesis of GDP-6-deoxy-D-manno-heptose in *Yersinia pseudotuberculosis*. Glycosyltransferases encoded by WcbB, WcbE, and WcbH are proposed responsible for transfer of the sugar residues to the polysaccharide chain which is attached to a phospholipid by WcbA/WcbO. Movement of CPS across the inner membrane occurs by the action of Wzt2/Wzm2 and movement to the outer membrane by WcbC/WcbD (Cuccui *et al.*, 2012). The model proposed by Cuccui *et al.* (2012) is shown in (Figure 4).

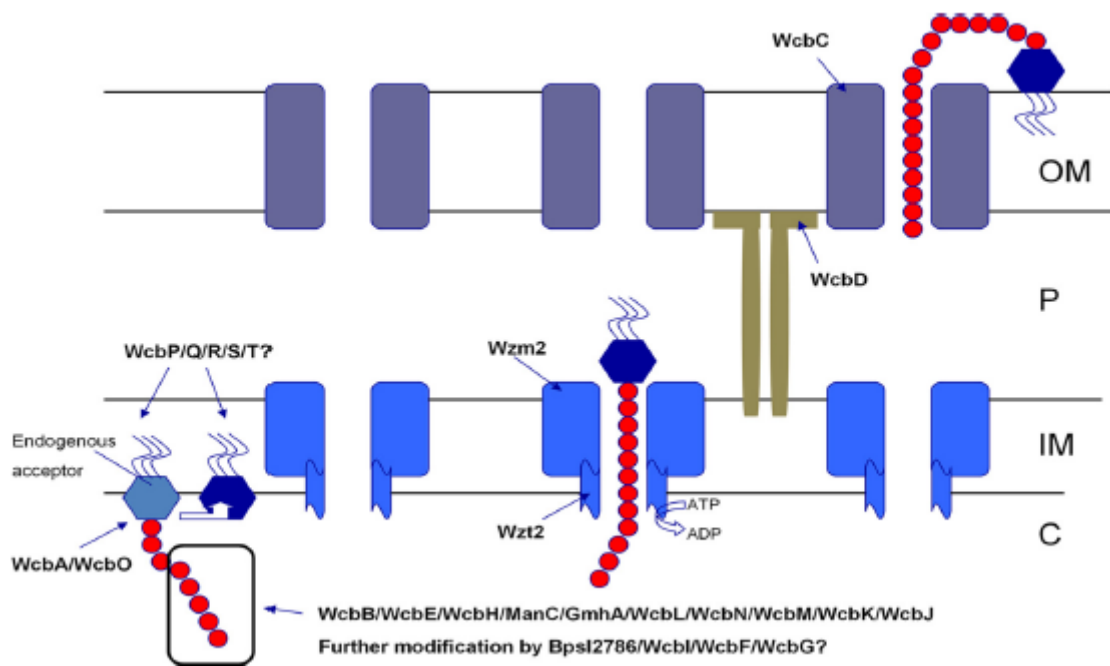


Figure 4 Model of *B. pseudomallei* CPS biosynthesis. WcbA and WcbO coordinate the glycosyltransferases to initiate and synthesise the CPS chain on a lipid anchor. GmhA, WcbL, WcbN, WcbM, WcbK, and WcbJ synthesise CPS, which is acetylated by an undetermined enzyme, assembled on a priming sugar encoded by ManC, and polymerised by the action of glycosyltransferases WcbB, WcbE, and WcbH. The polysaccharide is moved from the cytoplasm into the periplasm via a complex composed of Wzm2 and Wzt2. The polysaccharide is presented on the bacterial surface by WcbD and WcbC. C, cytoplasm; IM, inner membrane; P, periplasm; OM, outer membrane. Taken from Cuccui *et al.* (2012).

1.6.1.2 Other *B. pseudomallei* and *B. mallei* polysaccharides

Another well described polysaccharide is lipopolysaccharide (LPS), formerly known as type II O-PS, and is an unbranched heteropolymer of repeating D-glucose and L-talose units with the structure -3- β -D-glucopyranose-(1-3)-6-deoxy- α -L-talopyranose-(1- (Knirel *et al.*, 1992, Perry *et al.*, 1995). LPS has been shown to be a protective antigen against *B. pseudomallei* challenge and virulence determinant (Nelson *et al.*, 2004, DeShazer *et al.*, 1998). LPS has four distinct genotypes; A, B, B2, and rough. It has been reported that serotype A is found in the majority of strains and B2 is a variant of genotype B (Tuanyok *et al.*, 2012). In addition, *B. pseudomallei* LPS is produced in two forms on the basis of L-talose 2-O-methyl, 4-O-acetyl and 2-O-acetyl substituents. This

raises the possibility that an LPS-based melioidosis vaccine may not be protective across all strains.

In 2004, two additional gene clusters were identified which were predicted to be responsible for CPS biosynthesis and export (Holden *et al.*, 2004). In 2010, these were designated, along with a further operon, as CPS II, CPS III and CPS IV (Reckseidler *et al.*, 2010). It was demonstrated in this same study that CPS III does not contribute to *B. pseudomallei* virulence. The impact of CPS II and IV was not investigated but it was shown that all three capsules are present in *B. pseudomallei* and *B. thailandensis*, but not *B. mallei* so it was suggested that they may play a role in environmental survival (Reckseidler *et al.*, 2010). The chemical structure of each of these CPSs is currently unknown but CPS III was reported by Reckseidler *et al.* (2010) to contain galactose, glucose, mannose, xylose and rhamnose.

Other work has identified a branched 1,4-linked glucan polymer, and an unbranched polymer of tetrasaccharide units with the structure -3)-2-O-acetyl- β -D-Galp-(1-4)- α -D-Galp-(1-3)- β -D-Galp(1-5)- β -D-KDOp-(2-. These were described as CP-1a and exopolysaccharide (EPS) respectively (Masoud *et al.*, 1997, Nimitz *et al.*, 1997, Kawahara *et al.*, 1998). It is possible that both of these structures are the CPS II and IV referred to by Reckseidler *et al.* (2010).

The known *B. pseudomallei* polysaccharides are represented in Figure 5 from George 2013.

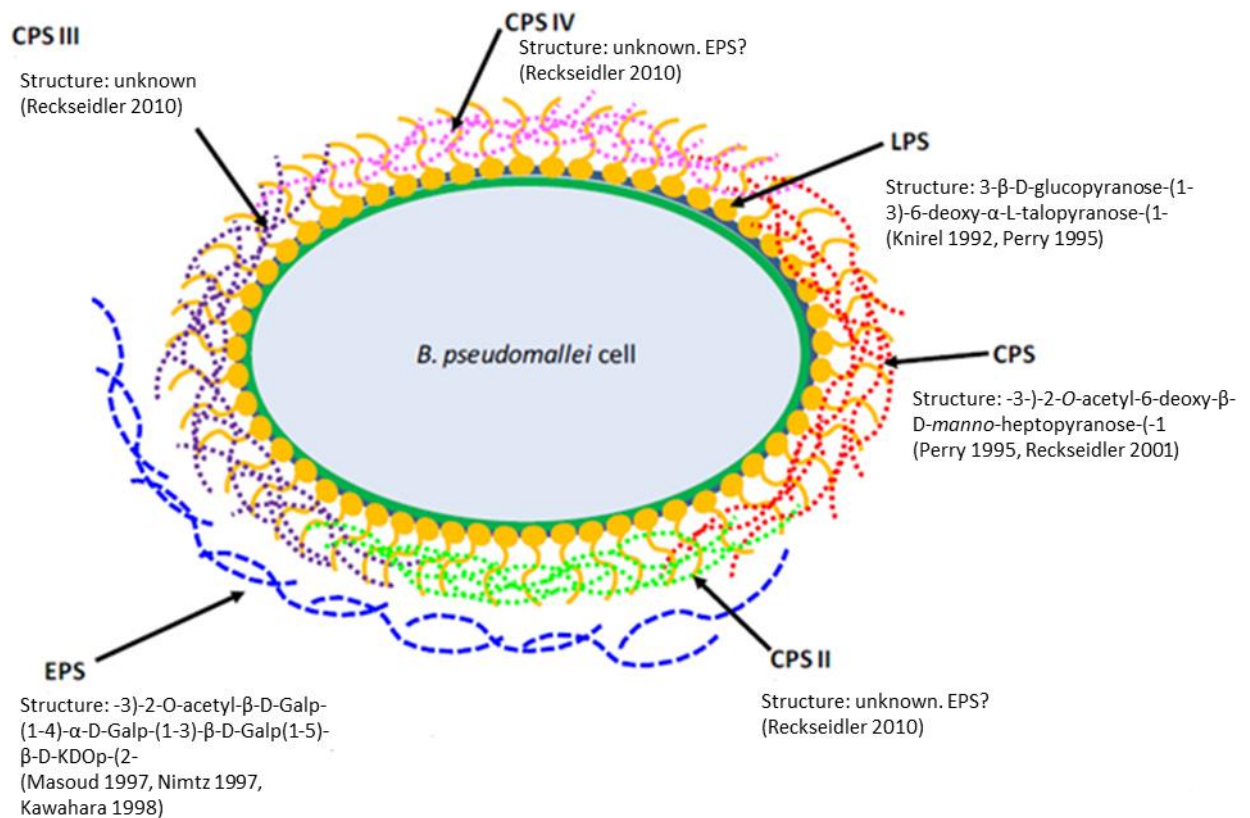


Figure 5 Polysaccharides expressed by *B. pseudomallei*. Amended from George 2013

1.7 Vaccines

In the history of human medicine, no discovery has reduced mortality as much as vaccines which are estimated to have saved hundreds of millions of lives (Plotkin *et al.*, 2013).

The first known vaccination was recorded in England 1774 when Benjamin Jesty, a cattle breeder, inoculated his wife and children with cowpox to protect them against a smallpox outbreak (Plotkin *et al.*, 2013). It was not until 1796, when the first scientific studies into vaccination were performed by Edward Jenner, that cowpox inoculation was demonstrated to protect against smallpox infection (Kaper *et al.*, 2013). The next major advance in vaccinology occurred in the late 1870s when Louis Pasteur developed a vaccine to chicken cholera, and later rabies and anthrax, with laboratory-attenuated cultures of the bacteria (Hussein *et al.*, 2015). Following this work, the 1870s and 1880s saw the development of killed vaccines for typhoid, plague and cholera (Plotkin *et al.*, 2013) and the use of inactivated bacterial toxins in the late 1890s (Hussein *et al.*, 2015).

Since this early work, immunisation programs have led to the elimination and/or control of several different infectious diseases, including smallpox, polio, measles, mumps, rubella, *Haemophilus influenzae* type B disease, pertussis, tetanus, and diphtheria (Rosenthal 2005). These vaccines were developed with either killed-organism, vaccination with a serologically related virus, or attenuation of the organism to produce live vaccines with substantially reduced virulence (Rosenthal 2005). Targets for current vaccine development include some of the more difficult infectious agents, such as human immunodeficiency virus (HIV), *Mycobacterium tuberculosis*; and parasitic diseases, such as malaria (Kaper *et al.*, 2013).

A vaccine is required for melioidosis as treatment of *B. pseudomallei* infection is difficult due to resistance to many front-line antibiotics including aminoglycosides, quinolones, polymyxins and B-lactams (Currie 2015). The environmental lifestyle of *B. pseudomallei* increases the chances of native populations or visitors in endemic areas coming into contact with *B. pseudomallei* as indicated by the high levels of seroconversion seen in Thailand (Wuthiekanun *et al.*, 2006). As *Burkholderia* spp. are highly adaptable, deliberate release into non-endemic areas will be difficult to remove and may result in initial high mortality in populations with no prior exposure to the organism, therefore a melioidosis vaccine that provides sterilising immunity or extends the therapeutic window for antibiotic therapy can be of significant clinical benefit (Choh *et al.*, 2013).

Despite the advances shown by vaccines, vaccine development currently takes approximately 20 years and costs approximately \$500 million. Unfortunately, it is not the only barrier for development (Barrett and Beasley, 2009).

1.7.1 Barriers to vaccine development

1.7.1.1 Legal obstacles

Like all medicines, vaccines can elicit unpredictable immune responses in some population groups. However, as vaccines are prophylactic there is little

tolerance from regulatory bodies and the public for side effects (Rosenthal 2005). The fear of litigation on the part of the public inhibits vaccine development and significantly increases costs (Kaper *et al.*, 2013). Several controversies have resulted in significant litigation which includes the supposed link to autism by the use of Thiomersal and the MMR vaccine (Baker 2008).

1.7.1.2 Technical barriers / Vaccine licensure

There are many technical challenges that remain in vaccine development and an in-depth discussion is out of the scope of this thesis, however, main themes revolve around the lack of licensed adjuvants, correlates of protection, animal models and knowledge of mucosal immunity for development of oral and nasal vaccine delivery systems (Kaper *et al.*, 2013). For viral haemorrhagic fevers and the alpha viruses; Venezuelan equine encephalitis (VEE); Western equine encephalitis (WEE); and Eastern equine encephalitis (EEE), vaccine candidates have been identified but progress is delayed by development and validation of appropriate animal models and correlates of protection (Wolfe *et al.*, 2013).

For melioidosis, as for other diseases endemic in economically developing countries, the lack of clinical trials facilities can hinder vaccine development (Kaper *et al.*, 2013). The recruitment of volunteers for efficacy testing, can be difficult if the disease is rare or if the vaccine is designed to protect against inhalational exposure, cases of which can be very rare. Therefore, clinical trials, if possible, may not achieve statistical power to demonstrate efficacy (Barrett 2009). For bio-threat agents, human efficacy trials cannot be conducted for these same reasons and that disease severity is too great (Wolfe *et al.*, 2013).

For this reason, the US Food and Drug Administration (FDA) introduced the animal rule, which allows for substitution of animal studies for human studies to demonstrate vaccine efficacy, where efficacy studies in human populations is difficult or unethical (Barrett 2009). Protective efficacy must be demonstrated in an animal model in which both the mechanism of disease pathogenesis is established and the protective immune response is relevant to human disease, but defining correlates of protection in animals is difficult (Barrett 2009, Kaper *et*

al., 2013). In addition, some pathogens do not infect non-human species and in those that do, disease pathogenesis may not be identical (Kaper *et al.*, 2013).

1.7.1.3 Economic barriers

It can be difficult to justify development of a vaccine that has uncertain monetary value because due to the prophylactic nature of the technology, health authorities and the public are reluctant to pay high prices when the benefit is not immediately realised. This leads to low profit margins and jeopardises innovation. With the exception of HIV and biowarfare agents, little public funding is available in the US for vaccine development (Kaper *et al.*, 2013).

1.7.2 Economics of vaccine development

Economic evaluation is an important aspect of any vaccine development, which in turn is based on demand, shelf-life and price (Barrett 2009). These factors can be insufficient to support commercial vaccine development, as for bio-threat agents, but global travel; high mortality from bio-threat agents; and the lack of alternative therapies means that these criteria alone should not dictate vaccine development.

There are few incentives for pharmaceutical companies to develop vaccines for biodefence given that the return on investment is uncertain (Kaper *et al.*, 2013). Vaccines for defence purposes are, however, developed for stockpiling that can act as an incentive for vaccine funding. Government funding decisions may also include the cost-saving of disease prevention and environmental decontamination therefore the return on investment will be higher than for a pharmaceutical company (Barrett 2009).

1.7.2.1 Funding bodies

The US National Institutes of Health is the primary funding source for both academic and industrial vaccine development programmes (Rosenthal 2005). Other major funding bodies include the Bill and Melinda Gates foundation, the Wellcome Trust, the UK Vaccine Network, and the Medical Research Council (MRC).

Other US agencies include the FDA; Biomedical Advanced Research and Development Authority (BARDA); Defense Advanced Research Projects Agency (DARPA); and the Defense Threat Reduction Agency (DTRA).

DTRA, who has funded this thesis, ensures the US military can operate in the face of a chemical or biological threat (Wolfe *et al.*, 2013).

1.7.3 Biodefense vaccines

Vaccine development is considered a deterrent to the use of specific bio-threat agents because it reduces the potential for effectiveness and decreases utility as a battlefield weapon (Rosenthal 2005).

Currently, there are only two vaccines available against bio-threat agents; anthrax and smallpox, but these are associated with safety concerns based on reactogenicity and do not meet current safety standards (Poland *et al.*, 2009, Chitlaru *et al.*, 2016).

The development of biodefence vaccines depends on the threat which has changed from state-run weapons programmes to terrorism. Vaccine candidates for filoviruses, alphaviruses, ricin and anthrax are undergoing preclinical testing but investment in new antigen expression systems and flexible manufacturing facilities is considered crucial (Wolfe *et al.*, 2013).

1.7.4 Animal models

Selection of an appropriate animal model is critical for biodefence vaccines given that licensure will ultimately require approval via the animal rule (Wolfe *et al.*, 2013).

The animal models used extensively for *B. pseudomallei* investigation include rodent models of the inbred mice strains BALB/c and C57BL/6 (Scott *et al.*, 2013, Scott *et al.*, 2014, Breitbart *et al.*, 2006). The Syrian golden hamster is highly susceptible to *B. pseudomallei* infection and has been used in virulence studies, but use of this model is limited because of the sensitivity to infection which does not mimic human disease (Brett *et al.*, 1997, Bondi and Goldberg, 2008).

A hallmark of human acute melioidosis is release of proinflammatory cytokines which correlates with disease severity (Lauw *et al.*, 1999, Wiersinga and Van der Poll, 2009). The releases of proinflammatory cytokines has been observed in BALB/c mice, peaking between 24-48 hours after infection with inefficient clearance of *B. pseudomallei* as a result of poor recruitment of lymphocytes and macrophages to the infection site (Lazar Adler *et al.*, 2009). It is on this basis that the BALB/c mouse resembles acute human melioidosis and is used as the standard animal model to study acute *B. pseudomallei* infection (Norris *et al.*, 2011, Judy *et al.*, 2012, Barnes *et al.*, 2013).

In contrast, C57BL/6 mice release lower levels of proinflammatory cytokines which peak between 48-72 hours after infection with efficient *B. pseudomallei* clearance mediated by increased neutrophil and macrophage infiltration to the infection site (Lazar Adler *et al.*, 2009). This indicates that C57BL/6 mice are inherently more resistant to *B. pseudomallei* infection than BALB/c mice, and on this basis is an appropriate model for the study of chronic melioidosis (Tan *et al.*, 2008, Conejero *et al.*, 2011).

A shortcoming of both the BALB/c and C57BL/6 mice is that neither model displays long-term latency which is an important feature of human melioidosis. Therefore, an animal model to study this stage of *B. pseudomallei* infection is

still required (Choh *et al.*, 2013). It has been suggested that an outbred strain of mice which are highly resistant to *B. pseudomallei* infection could be used as a model of latent *B. pseudomallei* infection (Titball *et al.*, 2008).

When using mouse models of *B. pseudomallei* infection it is important to not over extrapolate findings. *B. pseudomallei* infection exhibits organotropism for the spleen (Hoppe *et al.*, 1999). However, the mouse spleen exhibits a different structure of the white pulp to human spleen. In addition, B1 cells, which are not common in humans, can contribute significantly to the polysaccharide immune response in mice (Salehen and Stover, 2008).

1.7.5 Live attenuated vaccines

Live attenuated vaccines were among the first vaccines developed which included smallpox, rabies and tuberculosis (Plotkin *et al.*, 2013). Live attenuated vaccines stimulate strong humoral and cell-mediated immune responses and can provide protection after a single dose. However, they have the potential for reversion to virulence and replication can be problematic for some populations and are therefore unlikely to reach licensure today (Strugnell *et al.*, 2011, Silva and Dow, 2013).

1.7.5.1 Live attenuated vaccines against *B. pseudomallei*

The most effective melioidosis vaccines to date have utilised attenuated *B. pseudomallei* strains (Silva and Dow, 2013).

Disruption of the *ilvI* gene of *B. pseudomallei* 576 by transposon mutagenesis generated a mutant (2D2) auxotrophic for branched chain amino acids (leucine, isoleucine and valine) and highly attenuated in mice by both the intraperitoneal and intranasal route. Clearance of *B. pseudomallei* 2D2 infection from the lung and spleen was reported one week after administration (Atkins *et al.*, 2002, Easton *et al.*, 2011). Furthermore, immunisation with 2D2 was efficacious against challenge with virulent *B. pseudomallei* (Atkins *et al.*, 2002a, Haque *et al.*, 2006, Easton *et al.*, 2011) which was reported to be mediated by IFN- γ

release from CD4+ T-cells (Haque *et al.*, 2006). Other *B. pseudomallei* transposon mutants in purine biosynthesis pathways have been evaluated including *purN*, *purM*, *hisF*, and *pabB* which were efficacious against acute melioidosis but not against chronic infection (Pilatz *et al.*, 2006, Breitbach *et al.*, 2008).

Other approaches include the use of a T3SS *bipD* mutant, which was partly efficacious against virulent *B. pseudomallei* challenge (Stevens *et al.*, 2004) and an acapsular *B. pseudomallei* mutant (1E10) which was not protective (Atkins *et al.*, 2002b). In a novel approach, BALB/c mice vaccinated with *B. thailandensis* E555 by Scott *et al.* were significantly protected against *B. pseudomallei* challenge compared to controls. In addition, sterilising immunity was achieved in the lung; liver; and spleen by day 3 post-challenge (Scott *et al.*, 2013).

1.7.6 Inactivated vaccines

Organisms inactivated by heat or chemical means have been shown to be effective vaccines for a range of diseases including polio, hepatitis A and cholera (Plotkin *et al.*, 2013). They are less complicated to produce and safer than attenuated vaccines, although local reactions at injection sites are a potential problem and they usually require adjuvants due to reduced immunogenicity (Strugnell *et al.*, 2011, Silva and Dow, 2013).

1.7.6.1 Inactivated vaccines against *B. pseudomallei*

Immunisation of mice by the intraperitoneal (IP) route with heat-killed *B. pseudomallei*, *B. thailandensis* or *B. mallei* has been reported to give significant protection against IP *B. pseudomallei* challenge. This was hypothesised to be a result of CD4+ dependent antibody responses to CPS and LPS (Sarkar-Tyson *et al.*, 2009). In the same study, the same vaccines were administered by the IP route but animals were challenged with an inhalation exposure of *B. pseudomallei*. Protective efficacy of each vaccine was much lower but still protective (Sarkar-Tyson *et al.*, 2009).

1.7.7 Subunit vaccines and toxoids

Subunit vaccines are less reactogenic than whole cell vaccines (Zepp 2010). However, it is known that vaccines consisting of pure or recombinant antigens can be less immunogenic than whole-cell alternatives and usually require an adjuvant to increase immunogenicity (Mohan *et al.*, 2013).

1.7.7.1 Polysaccharide subunit vaccines

The first attempts to utilise capsular polysaccharides as vaccine candidates were in the late 1940s but the introduction of antibiotics delayed development of this field until the 1960s (Jones 2005).

Polysaccharide-based vaccines have an advantage over protein based vaccines in that the expression of carbohydrates is not under direct genetic control, therefore genetic variation in a pathogen does not result in a change of the cell surface oligosaccharides (Hecht *et al.*, 2009). The main disadvantage of polysaccharide vaccines is lack of a protective immune response in young children (Ada and Isaacs, 2003).

The CPS and LPS of many bacteria have been shown to be protective against challenge and several polysaccharide vaccines have been licensed including *Neisseria meningitidis*, *Salmonella enterica* and *S. pneumoniae* (Jones 2005).

In contrast to *B. pseudomallei*, where the deoxy-manno-heptose CPS is the most clinically relevant, pneumococcal disease is caused by ninety different serotypes and meningococcal disease is principally by Groups B and C, although Groups W135 and Y are important in human disease. Therefore, most polysaccharide-based vaccines must contain multiple CPSs to provide adequate disease coverage (Jones 2005).

1.7.7.2 Polysaccharide subunit vaccines for *B. pseudomallei*

Both the CPS and LPS of *B. pseudomallei* have been investigated as polysaccharide vaccines. Nelson *et al.* (2004) showed that vaccination of BALB/c mice with either CPS or LPS increased mean time to death (MTTD) following challenge compared to controls.

Another study has demonstrated that the LPS O-antigen of *B. thailandensis* provides similar levels of efficacy in comparison to vaccination with *B. pseudomallei* LPS O-antigen to *B. pseudomallei* challenge (Ngugi *et al.*, 2010).

1.7.7.3 Protein subunit vaccines

The use of protein vaccine candidates is advantageous as they are immunogenic in infants and the elderly because of their T-cell dependent nature (Plotkin *et al.*, 2013). If the proteins are well conserved, they have the potential to protect against all pathogenic serotypes of an organism (Ginsburg *et al.*, 2012).

1.7.7.4 Protein subunit vaccines for *B. pseudomallei* and *B. mallei*

Several recombinant protein candidates have been shown to protect against *B. pseudomallei* infection. The most investigated is LolC, an outer membrane protein of *B. pseudomallei* associated with an ATP-binding cassette system (Harland *et al.*, 2007a). This was efficacious against a ~50 x MLD *B. pseudomallei* challenge by the IP route. Other subunits investigated by Harland *et al.* include the periplasmic binding protein PotF; and oligopeptide binding protein OppA, with survival of 50 and 22 % respectively 42 days after challenge (Harland *et al.*, 2007a).

Burntack *et al.* (2011) identified six Hcp proteins (Hcp 1-6) which are components of the T6SS as potential vaccine candidates. Protective efficacy

was similar to that reported for LolC by Harland *et al.* (2007a). Mice vaccinated with Hcp2 had the greatest survival rate of 80 %, 42 days after challenge. However, sterilising immunity was only seen in the mice vaccinated with Hcp1 and Hcp6 (Burtnick *et al.*, 2011).

Other subunit vaccine candidates included the outer membrane proteins; Omp3; Omp7; and Omp85, and plasmid DNA encoding flagellin, which were protective against *B. pseudomallei* challenge in vaccinated mice (Hara *et al.*, 2009, Su *et al.*, 2010, Chen *et al.*, 2006). A further outer membrane protein; OmpW was also shown to significantly improve survival in both BALB/c and C57BL/6 mice to *B. pseudomallei* challenge which was attributed to IgG1 and IgG2a antibody generation (Casey *et al.*, 2016).

In an approach shown effective for *M. tuberculosis* infection, four proteins expressed by *B. pseudomallei* in the chronic stage of infection were shown to be protective in BALB/c mice. Interestingly, these proteins were significantly more efficacious than CPS or LolC (Champion *et al.*, 2016). One of the proteins tested (BPSL2765) has been shown to give 10-fold higher antibody levels in patients who had suffered only one episode of melioidosis rather than patients with recurrent melioidosis (Suwannasaen *et al.*, 2011).

Other subunit antigens investigated which did not give statistically greater protection to *B. pseudomallei* challenge than controls were peptide mimotopes of exopolysaccharide (Legutki *et al.*, 2007) and the T3SS proteins BipB, BipC and BipD (Druar *et al.*, 2008).

1.7.7.5 Polysaccharide conjugate vaccines

There is no other example where introduction of a new approach to vaccine development has had such a rapid and positive effect in preventing infections by human pathogens as the development of conjugate vaccines (Plotkin *et al.*, 2013). The first conjugate vaccine was introduced in the 1990s for *H. influenza* type b (Hib) and consisted of polysaccharide conjugated to a non-toxic mutant of diphtheria toxin, Crm197 (Lai and Schreiber 2009). The Hib vaccine arose

from work in the 1980s and involved reductive amination of periodate activated oligosaccharides to a carrier protein with the resultant conjugate approximately 90 kDa and contained an average of six glycan chains per carrier protein (Anderson *et al.*, 1985).

Since then, conjugate vaccines have been developed for *S. pneumoniae*, and *N. meningitidis* serogroup C which has significantly reduced the burden of childhood disease and mortality from these pathogens (Pobre *et al.*, 2014).

1.7.7.6 Polysaccharide conjugate vaccines for *B. pseudomallei*

The first polysaccharide conjugate vaccine developed against *B. pseudomallei* was LPS O-antigen conjugated to flagellin protein which elicited IgG responses to both flagellin and LPS and protected diabetic rats against *B. pseudomallei* challenge (Brett *et al.*, 1996).

Other work has focussed on LPS O-antigen and CPS chemically conjugated to either bovine serum albumin (BSA) or tetanus toxin H_c (TetH_c). Mice vaccinated with these conjugates are significantly protected against *B. pseudomallei* challenge compared to controls, but sterilising immunity is not always achieved (Burtnick *et al.*, 2012, Scott *et al.*, 2014a, Scott *et al.*, 2014b).

A novel conjugate vaccine containing *B. pseudomallei* O polysaccharide (type III OPS) conjugated to glycoprotein AcrA in *E. coli* has been produced and shown to be partially protective against *B. pseudomallei* intranasal challenge (Quintanilla *et al.*, 2014).

An additional novel concept was the use of a synthetic hexasaccharide CPS conjugated to TetH_c. Mice immunised with this conjugate developed antibodies that recognised native CPS and were protected against *B. pseudomallei* infection (Scott *et al.*, 2016).

1.7.7.7 Carrier proteins

The three most commonly used carrier proteins for use in conjugate vaccines are Tetanus Toxoid (TT), diphtheria toxoid (DT) and Crm197, although others include *N. meningitidis* outer membrane protein and non-typeable *H. influenzae* derived protein D (Pobre *et al.*, 2014). A summary of each carrier protein is given in Figure 6. However, clear differences have yet to be established between them with regards to vaccine potency because of the large group sizes needed in clinical trials and inconsistent immunogenicity data which can make the choice of carrier protein for conjugate vaccine development difficult (Knuf *et al.*, 2011).

The earliest and most widely used carrier proteins were the tetanus and diphtheria toxoids and these were used in licensed vaccines for Hib and *N. meningitidis* (Broker *et al.*, 2011). Tetanus toxoid is derived from *Clostridium tetani*. Diphtheria toxoid is formaldehyde inactivated toxin from *Corynebacterium diphtheria* which itself is a product of the diphtheria toxin gene carried by corynebacteriophages. Integration of the bacteriophage into *C. diphtheria* converts it into a virulent strain (Broker *et al.*, 2011).

Crm197 is a mutated form of DT with an amino acid substitution from a glycine to a glutamic acid residue in the 'fragment A' region at amino acid position 52 which removes enzymatic activity and hence toxicity (Giannini *et al.*, 1984). The first Crm197 conjugate vaccine developed was against Hib related disease (Shinefield 2010). Like DT, Crm197 is a single polypeptide chain of 535 amino acids (Malito *et al.*, 2012) but does not require chemical inactivation which makes conjugate vaccines less difficult to characterise and control (Knuf *et al.*, 2011). In addition, Crm197 T-cell epitopes are reported to be better preserved than the epitopes of DT, as are potential binding sites which consist of 39 lysine residues available for chemical conjugation (Jones 2005). This may result from the absence of formaldehyde inactivation. This in turn may explain the superiority of Crm197 as a carrier protein (Dagan *et al.*, 2010, Knuf *et al.*, 2011). It is thought that the conformation of Crm197 differs from DT, leading to lower B-cell responses (Dagan *et al.*, 2010).

Carrier proteins are considered safe as inferred from their use in several licensed vaccines. A study of Hib conjugates showed that after three doses, redness, pain and swelling were less frequent in children receiving DT and Crm197 than OMP and TT. In a comparative study of meningococcal Crm197 and DT vaccines, mild pain was the most common adverse effect. It is difficult to differentiate between carrier proteins with regards to safety as adverse effects are mild but hypersensitivity may be more common with Hib-OMP and Hib-TT conjugate vaccines (Knuf *et al.*, 2011).

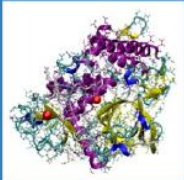


Tetanus Toxoid (TT)	Diphtheria Toxoid (DT)	Cross-Reactive Material 197 (CRM ₁₉₇)	<i>N. meningitidis</i> Outer Membrane Protein (OMP)	Non-Typeable <i>H. influenzae</i> Derived Protein D (PD)
				
<ul style="list-style-type: none"> Derived from <i>Clostridium tetani</i> Inactivated with formalin Purified with ammonium sulfate and filter sterilized prior to conjugation process 	<ul style="list-style-type: none"> Derived from <i>Corynebacterium diphtheriae</i> Detoxified with formaldehyde Purified by ammonium sulfate fractionation and diafiltration 	<ul style="list-style-type: none"> Enzymatically inactive, nontoxic mutant of diphtheria toxin Requires no formaldehyde detoxification Obtained at near 100% purity 	<ul style="list-style-type: none"> Outer membrane protein complex derived from <i>N. meningitidis</i> serogroup B strain 11 Purified by detergent extraction, ultracentrifugation, diafiltration, and sterile filtration 	<ul style="list-style-type: none"> Antigenically conserved surface lipoprotein found in all <i>H. influenzae</i> Used in a nonacylated, antigenically active form
• 140 kD	• 63 kD	• 63 kD	• 37 kD	• 42 kD

Figure 6 Common carrier proteins used in conjugate vaccines. Image taken from Knuf (2011)

1.7.7.8 Conjugation chemistry

Polysaccharides require activation before attachment to the carrier protein and sometimes it is necessary to activate the carrier protein as well (Jones 2005). Classically, activation has been performed by two primary methods; periodate oxidation and cyanlation. Sodium periodate reacts with vicinal hydroxyl groups to form reactive aldehydes. These reactive aldehyde groups are then conjugated to lysine residues on the carrier protein by reductive amination,

usually in the presence of sodium cyanoborohydride, that forms a stable secondary amine. Any remaining aldehyde groups are quenched with sodium borohydride which reduces them back into hydroxyls (Frasch 2009).

Cyanylation initially used cyanogen bromide (CNBr) to create random reactive cyanoester groups on the polysaccharide and was used in the first Hib conjugate but has now been replaced with the superior cyanylating agent CDAP (1-cyano-4-dimethylaminopyridinium tetrafluoroborate). CDAP does not require the use of reactive linkers such as adipic acid dihydrazide (ADH) which were used to compensate for the low efficiency of CNBr. The cyanoesters formed react with the epsilon amines of lysine to form a stable O-alkyl-isourea linkage. The reaction is then quenched with glycine (Frasch 2009).

In all the current conjugate vaccines, polysaccharide is conjugated to either lysine residues or the amino group at the N-terminus of the carrier protein. Different conjugation chemistries are likely to have different specificities for available amines, depending on differences in pKa and steric accessibility (Jones 2005).

1.7.7.9 Novel conjugation methodologies

A novel method was developed for *N. meningitidis* group Y CPS conjugation to TT. Polyethylene glycol (PEG) was reacted with cyanylated CPS to introduce a maleimide group which lead to higher conjugation efficiency. This PEG spacer had the additional benefits of potentially decreasing the shielding effect of the polysaccharide on the carrier protein and vice-versa which may enhance vaccine bioavailability (Huang *et al.*, 2013).

1.7.7.10 Analysis of polysaccharide conjugate vaccines

NMR spectroscopy is the dominant method to identify CPS and determine purity (Jones 2005). An estimation of the average size of activated polysaccharide can also be achieved by NMR or size exclusion chromatography with light scattering or anion exchange chromatography. It has been reported for other conjugate

vaccines that NMR spectroscopy can be performed on the final product to ensure the degree of O-acetylation and absence of degradation of the polysaccharide (Jones 2005).

1.7.7.11 Considerations for the use of conjugate vaccines

A major consideration with the use of conjugate vaccines is carrier priming, which is enhancement of the immune response to the polysaccharide of a conjugate in individuals previously vaccinated with the same carrier protein (Pobre *et al.*, 2014). The main carrier proteins used in conjugate vaccines are TT, DT or Crm197. Therefore, carrier priming may occur following previous administration with a number of vaccines given in childhood including meningococcal and Hib (Tontini *et al.*, 2013, Pichichero 2013). It is thought to occur as a result of an increase in the number of carrier protein-specific T-cells which stimulate expansion of B-cells specific to the polysaccharide (Pobre *et al.*, 2014).

In some cases, carrier priming can suppress the immune response to the polysaccharide of a conjugate vaccine by a mechanism known as carrier induced epitopic suppression (CIES), which particularly occurs when the conjugate vaccine has a low polysaccharide to protein ratio (Pobre *et al.*, 2014). This is thought to occur primarily from either a reduced carrier protein immune response – possibly by carrier-specific regulatory T-cells or competition for limited numbers of carrier-specific T-cells which generate an antibody response primarily to the carrier protein (Dagan *et al.*, 2010, Knuf *et al.*, 2011, Pobre *et al.*, 2014). Alternative suggestions include pre-existing carrier-specific antibodies shielding the polysaccharide from polysaccharide-specific B-cells, or dominant carrier-specific B-cells outcompeting polysaccharide-specific B-cells for T-cell help (Dagan *et al.*, 2010). Because of this, it has been suggested that an ideal carrier protein is one unable to induce a significant antibody response to itself (Pobre *et al.*, 2014). It has been reported that the interference mechanisms between carrier proteins can consist of B-cell or T-cell dominant mechanisms (Dagan *et al.*, 2010). This suggests that CIES is not simply a

matter of carrier protein immunogenicity but also the dominance of B- and T-cell relevant epitopes.

Other major considerations revolve around the development and manufacture of conjugate vaccines of which perhaps the most important is the amount of free polysaccharide, which has been shown to suppress pneumococcal conjugate vaccine immunogenicity when higher than 10 % (Rodriguez *et al.*, 1998). It has been reported that publications frequently overlook the possible presence of free polysaccharide by mistakenly assuming that all polysaccharide used in the conjugation reaction is bound (Suarez *et al.*, 2008). The Hib conjugate vaccine was the first for which a maximum limit of free polysaccharide was described (deSouza *et al.*, 2013). The World Health Organization (WHO) has published recommended limits of free protein and polysaccharide for meningococcal and pneumococcal conjugate vaccines (Frasch 2009). The Technical Series of Reports (TRS) from the WHO also detail other quality control measures which include control of polysaccharide size, both before and after activation, monitoring of polysaccharide structure, purity and O-acetyl content (WHO TRS 924, TRS 927, TRS 962).

A problem reported for Crm197 is that there is a lack of clinical data of conjugate efficacy in immunocompromised patients. It has been reported that in HIV-positive African children, the failure rate of *Haemophilus b* oligosaccharide conjugate vaccine is approximately 35-fold higher than negative-HIV children. A partial loss of memory response was observed in those administered with the pneumococcal vaccine PCV7 (Shinefield 2010).

1.7.7.12 DNA vaccines

DNA vaccines work on the principle that a small amount of host cells will express the gene products of injected genetic material. These can generate effective humoral and cellular immune responses to protein antigens, although they are reported to induce weaker immune responses in humans than mice (Liu 2011, Choh *et al.*, 2013).

1.7.7.13 DNA vaccines for *B. pseudomallei* and *B. mallei*

The only research carried out to date on DNA vaccines for *B. pseudomallei* was in 2006 when Chen *et al.* immunised mice with plasmid DNA encoding the *fliC* flagellar subunit. In comparison to vaccination with recombinant FliC protein, survival was greater in mice that received the DNA vaccine and addition of a CpG adjuvant further improved survival (Chen *et al.*, 2006).

1.8 Vaccine immunology

Vaccine efficacy against disease is primarily mediated by antigen-specific antibodies and long-term protection requires maintenance of these antibodies and/or generation of memory cells capable of reacting to subsequent bacterial exposure (Plotkin *et al.*, 2013).

Antibodies are produced by B lymphocytes and antibody mediated protection is termed humoral immunity. Antibodies are produced by binding of antigen to B-cell receptors which initially results in the production of IgM antibodies. The transition from naïve B-cells to plasma cells secreting high affinity IgG antibody requires T-cell help (Nishat and Andreana, 2016).

T-cell mediated protection is another important mechanism of protection and is termed cellular immunity. There are two main subsets of T lymphocytes differentiated by surface molecules known as CD8 and CD4 which are expressed by cytotoxic T-cells and T-helper cells respectively (Roche and Cresswell, 2016).

CD4+ T-cells produce cytokines and support the generation of B-cells and CD8+ T-cells. They can be divided into T helper 1 (T_h1), T_h2, T_h17, T_h9, T_h22, T follicular-helper (T_{fh}) and T-regulatory (T_{reg}) subtypes on the basis of secreted cytokines (Hirahara and Nakayama, 2016).

1.8.1 Th1/Th2 response

Both antibody and cellular responses are produced as part of a T_h1-type response characterised by interleukin 12 (IL-12), gamma interferon (IFN- γ) and tumor necrosis factor (TNF) (Plotkin *et al.*, 2013). T_h1-type responses are necessary to control intracellular infections (Hirahara and Nakayama 2016). T_h2-type immune responses are directed by IL-4, IL-5, IL-9 and IL-13 cytokine expression resulting in predominantly IgG1 and IgE antibody isotype class switching and recruitment of inflammatory cells (Sahoo *et al.*, 2016). T_h2 responses are necessary to control extracellular infections (Oliphant *et al.*, 2011). While both T_h1 and T_h2-type immune responses can be raised at the same time, T_h1 and T_h2 responses are generally antagonistic and the cytokines necessary for either response will inhibit the other (Kaiko *et al.*, 2008).

1.8.2 Immune response to polysaccharides

Polysaccharides are poorly immunogenic. They raise antibody responses through crosslinking of approximately 15-20 receptors on a B-cell of appropriate specificity, and through pathogen associated molecular pattern receptors (PAMP) (Jones 2005, Nishat and Andreana, 2016). Polysaccharides are considered T-cell independent antigens (TI), but this is not strictly true as generation of anti-polysaccharide antibodies requires B7 ligand dependent co-stimulation of B-cells by T-cells. This interaction is short and T-cell receptor unspecific (Salehen and Stover, 2008). There are polysaccharides that are zwitterionic - both positive and negative electrical charges are present on the molecule - which are uniquely processed and presented by antigen presenting cells (Lai and Schreiber 2009).

Generated anti-polysaccharide antibodies are generally IgM and IgG2. These are not good activators of complement and fail to induce immune responses in infants below the age of 2 years (Jones 2005). This has been attributed to the immaturity of the infant immune system in the expression of B cell receptors, including complement receptor type 2 (CR2) (Perciani *et al.*, 2013). Antibodies generated to TI antigens exhibit less avidity, opsonophagocytic and bacteriolytic

activity than T-cell dependent (TD) antigens which is explained by the absence of somatic hypermutation (Salehen and Stover 2008). Repeat vaccination with polysaccharides does not boost antibody titres (Jones 2005). Previously, dogma dictated that polysaccharides were not able to stimulate a memory B-cell response; however, work has shown that IgM memory B-cells are generated independent of T-cell help in addition to persistent stimulation of B-cell receptors which can provide long lasting antibody levels (Salehen and Stover 2008).

The immediate polysaccharide immunoglobulin response is mainly generated by marginal zone B-cells concentrated in the spleen and lymph nodes (Salehen and Stover 2008). An immune response is initiated through binding of polysaccharide to B-cell receptors or by C3d deposition on the polysaccharide (Breukels *et al.*, 2005). Marginal zone B-cells are a non-activated B-cell subset, distinct from follicular B-cells of splenic germinal centers, but on activation migrate to the follicular zone where CD21 (CR2) is proteolytically cleaved and antigen transferred to follicular dendritic cells (Salehen and Stover 2008, Zandvoort and Timens 2002). There is no T-cell help, however, due to inefficient processing and presentation of polysaccharides, and the lack of co-stimulatory molecule upregulation via solely CR2 mediated B-cell triggering (Salehen and Stover 2008). As the immune response develops, germinal centers in the spleen develop, as for T-cell dependent antigens, but without T-cell help these are transient (Lentz and Manser 2001).

In 1931, Avery and Goebel discovered that the immunogenicity of polysaccharides could be increased by covalent attachment of the polysaccharide to a protein carrier to form a conjugate (Avery and Goebel 1931). The mechanism by which a polysaccharide is capable of inducing an immune response resembling that of a TD antigen following conjugation to a carrier protein is not completely understood. It is thought to involve delivery to APCs and B7-CD28 and CD40-CD40L interactions between B-cells specific for polysaccharide and T cells which is characterised by antibody isotype switching from IgM to IgG (Salehen and Stover 2008, Lai and Schreiber 2009).

There are two main theories of how this occurs. The first is that immunisation with a conjugate induces carrier-protein specific T-cells that provide cytokine help for expansion of B-cells specific to the polysaccharide, leading to IgG antibody formation and B-cell memory (Lai and Schreiber 2009, Huang *et al.*, 2013). However, the mere presence of carrier protein is not sufficient; conjugation to the polysaccharide is required which suggests close interaction upon antigen processing and recruitment of T-cells (Schneerson *et al.*, 1980). In addition, immunisation with a meningococcal polysaccharide conjugated to TT has been reported to induce polysaccharide-specific T-cells in mice (Muthukkumar and Stein, 2004).

An alternative proposed hypothesis is that polysaccharide is processed along with the carrier protein in the endosome and the resultant MHC-II bound carrier-peptide presents the polysaccharide to T-cells leading to clonal expansion of polysaccharide-specific B-cells. This has been shown to be the case for pneumococcal polysaccharide serotypes 14 and 19F, labelled with Alexa Fluor® 594 hydrazine, conjugated to Crm197 (Lai and Schreiber 2009). In addition, studies have shown T-cell responses specific to the carbohydrate portion of glycopeptides (Deck *et al.*, 1999, Purcell *et al.*, 2008). However, this theory is still incomplete as significantly different antibody responses and antigen processing efficiency was seen with seven different pneumococcal CPS serotypes conjugated to Crm197 (Leonard *et al.*, 2003). This suggests that an unknown characteristic of the polysaccharides affected endosomal processing of the carrier protein and resultant immunogenicity (Lai and Schreiber 2009).

1.8.3 Immune response to proteins (MHC-I and MHC-II)

Major histocompatibility complex class I and II molecules (MHC-I and MHC-II) are transmembrane glycoproteins that present short peptides generated by the cells that express MHC molecules (Roche and Cresswell 2016). MHC-II molecules are expressed on antigen presenting cells (APCs), which include dendritic cells (DCs) and B-cells, but expression can be induced on most cell types by IFN- γ , whereas MHC-I molecules are expressed by all nucleated cells (Roche and Cresswell 2016).

The processing of peptides and presentation to CD4+ and CD8+ T-cells is a critical step in the development of adaptive immune responses (Baumgartner and Malherbe 2011). MHC-II molecules present peptide antigens between 12 and 26 amino acids in length to CD4+ T-cells. This process starts with antigen uptake by APCs by the process of endocytosis; macropinocytosis; phagocytosis; or autophagy, followed by proteolysis in the endosome or lysosome. Following a series of degradation and binding steps, immunodominant MHC-II-peptide complexes, formed within the endosome, are moved to the plasma membrane (Baumgartner and Malherbe 2011, Roche and Cresswell 2016).

In contrast, MHC-I present peptides between 8 and 10 amino acids long to CD8+ T-cells from newly synthesised proteins in the cytosol which are degraded by the proteasome. The degraded peptides are transported by the transporter associated with antigen processing (TAP) into the endoplasmic reticulum (ER). Following a series of peptide editing steps, high-affinity peptides associate with MHC-I molecules and the complex is transported to the cell surface (Baumgartner and Malherbe 2011, Roche and Cresswell 2016).

1.8.4 Immune response to *B. pseudomallei* infection

Both clinical and experimental studies have shown that a fully functional innate immune system is critical to the control of initial *B. pseudomallei* infection, primarily by gamma interferon (IFN- γ), macrophages and neutrophils (Silva and Dow 2013). Deficiencies in innate immunity present in risk factors for melioidosis, such as diabetes, also suggest the importance of these mechanisms (Hodgson *et al.*, 2011).

The role of IFN- γ has been investigated in several studies; both IFN- γ depleted and knockout mice are highly susceptible to *B. pseudomallei* infection (Santanirand *et al.*, 1999, Haque *et al.*, 2006). The IFN- γ response has been shown to be rapidly generated by natural killer cells (NK), NK T-cells and conventional T-cells in an IL-12 and IL-18 dependent manner (Haque *et al.*,

2006, Koo and Gan, 2006). Neutrophils and macrophages have been shown to be crucial in controlling early stage infection following depletion in animal models of melioidosis, which in turn is facilitated by complement, opsonising antibodies and serum opsonins (Breitbach *et al.*, 2006, Easton *et al.*, 2007, Mulye *et al.*, 2014).

Other components necessary for protection against *B. pseudomallei* infection include, TNF- α and if chronic infection is established; CD4+ T-cells. TNF- α knockout mice exhibit increased susceptibility to *B. pseudomallei* infection with increased bacterial loads recovered from spleen and liver tissue (Barnes *et al.*, 2008). Although it has been demonstrated that T-cells were dispensable for initial control of *B. pseudomallei*, mice depleted of CD4+ T-cells were significantly more susceptible to infection (Haque *et al.*, 2006).

1.9 Correlates of protection

Most vaccines on the market today use antibody generation, or generation of innate immunity as correlates of protection against disease. For some of the major disease-causing encapsulated bacteria (Hib, pneumococci and meningococci), the correlates of protection are opsonophagocytic or bactericidal antibodies (Plotkin 1999 Barrett 2009 Plotkin 2010). With the partial exception of the Bacillus Calmette-Guérin (BCG) vaccine for tuberculosis, control of intracellular pathogens by vaccination has not been achieved (Plotkin 2010).

Humoral and cellular immunity have been reported critical for protection of either BALB/c or C57BL/6 mice against *B. pseudomallei* challenge in several studies, which includes monoclonal antibody induced protection by passive transfer (Jones *et al.*, 2002, Liu *et al.*, 2002, Healey *et al.*, 2005). In recent work, partial protection against intranasal *B. pseudomallei* challenge in mice was achieved following passive transfer of sera from mice immunised with a highly attenuated, select agent excluded, *purM* deletion mutant of *B. pseudomallei* (Bp82). Protection was associated with humoral immunity as B-cell deficient mice were not protected by immunisation, but were partially protected by

passive transfer of sera from Bp82 vaccinated wild-type mice (Silva and Dow, 2013).

1.10 Vaccine adjuvants and delivery systems

1.10.1 Adjuvants

The term adjuvant is derived from the Latin word *adjuvare*, meaning ‘to assist or help’ (Sivakumar *et al.*, 2011). Adjuvants are key components added to vaccines, especially subunit vaccines, to increase immunogenicity (Apostolico and Lunardelli, 2016). Adjuvants can also assist by reducing the amount of doses required for generation of immunity. Since most of the adjuvants currently licensed induce antibody responses, there exists a need for adjuvants that stimulate cell-mediated immunity (Knudsen *et al.*, 2016).

Adjuvants are broadly classified into three types; delivery systems; immune potentiators; and mucosal adjuvants. Delivery systems are further subdivided into; mineral salts - such as aluminum salts; microparticles – such as non-enveloped virus like particles; and lipid particles - such as MF59. An example of immune potentiator adjuvants are polyinosinic-polycytidylic acid (Poly (I:C) and monophosphoryl lipid A (MPL) (Apostolico and Lunardelli 2016). These are both pathogen-associated molecular patterns (PAMPs), which are generic triggers for the innate immune system. An example of a mucosal adjuvant is cholera toxin (CT) (Lawson *et al.*, 2011).

This classification system of adjuvants is based on mechanism of action (Apostolico and Lunardelli 2016). Delivery systems act as antigen carriers and create local inflammatory responses for activation of innate immunity (Goto and Akama, 1982). Immune potentiators also stimulate innate immune responses but through activation of pattern-recognition receptors (PRRs) that result in the production of cytokines and chemokines (Olive 2012). PRRs are evolutionarily conserved, germ-line encoded molecules including; toll-like receptors (TLRs); retinoic acid-inducible gene (RIG)-I-like receptors; C-type lectin-like receptors (CLRs); and nucleotide oligomerization domain (NOD)-like receptors (NLRs)

and DNA sensors. A classic PAMP is lipopolysaccharide but others include flagellin, double-stranded RNA and unmethylated CpG motifs (Mahla *et al.*, 2013).

With exception of CT, the adjuvants named have been included in this thesis and further information can be found in Chapter 5; Immunogenicity and efficacy of candidate vaccines.

1.10.2 Virus-like particles

Virus-like particles (VLPs) are formed from viral structural proteins, typically capsid or envelopes, which have the property of self-assembly for formation of structures that mimic intact virus particles (Grgacic and Anderson, 2006). The size and morphology of VLPs depend on the viral proteins utilised. They are all non-infectious and non-replicating as they do not contain viral genetic material (Kushnir *et al.*, 2012). The size and particulate nature of VLPs leads to efficient uptake by DC's and are capable of presentation on both MHC-I and MHC-II molecules. Antigenic epitopes in a VLP construct are also displayed in a highly repetitive manner which leads to B-cell receptor crosslinking and with CD4+ and CD8+ T-cell stimulation induces both humoral and cellular immune responses (Grgacic and Anderson 2006, Ludwig and Wagner, 2007, Zabel *et al.*, 2013).

Prior to 1969, all anti-viral vaccines used either inactivated or attenuated strains. Following demonstration that cells infected with hepatitis B virus (HBV) produced empty 22 nm particles, the first VLP vaccines were developed in the 1980s from HBV core antigen (HBcAg) and surface antigen (HBsAg) proteins (Ludwig and Wagner 2007, Pushko *et al.*, 2013). Licensed VLP vaccines now include GlaxoSmithKline's Engerix-B® and Merck's Gardasil®, vaccines for HBV and human papilloma virus (HPV) respectively, which contain the appropriate viral core protein (Kushnir *et al.*, 2012, Ludwig and Wagner, 2007). VLPs can be formed from non-enveloped viruses, such as HBcAg, or enveloped, such as influenzae and Ebola virus, which contain a lipoprotein membrane derived from host cell membranes that surrounds a nucleocapsid (Pushko *et al.*, 2013).

In addition to candidate vaccines, VLPs are also considered to be effective antigen delivery platforms, which make them ideal for use in conjugate vaccine development (Grgacic and Anderson 2006, Noad and Roy, 2003, Scheerlinck and Greenwood, 2008, Vietheer *et al.*, 2007). VLPs can act as antigen delivery platforms by two approaches; genetic insertion of protein epitopes; or chemical conjugation to protein or polysaccharide antigens (Pushko *et al.*, 2013).

The crystal structure of HBcAg was solved in 1999 which showed a long α -helical hairpin and hydrophobic core. A dimer is formed by spontaneous association of two α -helical hairpins and capsid is formed by assembly of up to 120 dimers. The resulting four-helix bundle of each dimer protrudes as a spike from the capsid surface and is called the major immunodominant region (MIR) (Crowther *et al.*, 1994, Conway *et al.*, 1998, Wynne *et al.*, 1999, Whitacre *et al.*, 2009). The MIR of HBcAg contains dominant B-cell epitopes and is the favoured site for genetic insertion of foreign antigenic sequences resulting in strong immune responses to the insert (Schodel *et al.*, 1992, Whitacre *et al.*, 2009). Genetic insertion of antigens into HBcAg has been demonstrated for; malarial circumsporozoite protein; tuberculosis culture filtrate protein 10; anthrax protective antigen; and influenzae M2e peptide (Gregson *et al.*, 2008, Dhanasooraj *et al.*, 2013, Yin *et al.*, 2014, Tsybalova *et al.*, 2015). Genetic insertion in HBcAg is however limited to small, hydrophobic antigens due to steric hindrance at the MIR site which has limited HBcAg development as a vaccine platform (Peyret *et al.*, 2015).

iQur, a collaborator on this project, has developed Tandem CoreTM which consists of two HBcAg genetically linked via a flexible GGS₇ linker from amino acid 149 of the upstream core to the N-terminus of the downstream core. This dimer forms VLPs morphologically indistinguishable from native HBcAg dimers and allows for insertion of single large proteins in each MIR, as assembly of the 4 helix bundle is facilitated by covalent linkage (Peyret *et al.*, 2015). In addition to foreign protein insertion, a further advantage of Tandem CoreTM is the insert of lysine residues into the MIRs which can then be used for chemical conjugation to polysaccharide antigens, such as *Burkholderia* CPS, and thus facilitates presentation of both *Burkholderia* protein and CPS in a highly immunogenic context. Tandem CoreTM also differs from native HBcAg through

the use of truncated cores in order to remove or reduce the amount of host expression-system nucleic acid content, which may make licensure of an HBcAg based vaccine easier. In heterotandem core constructs, the upstream core protein is truncated at amino acid 149, which removes the nucleic acid binding domain, and the downstream copy is full length. In homotandem constructs both core proteins are truncated, although the utility of this approach is uncertain as it is known that the positively charged nucleic acid binding domain influences particle stability and VLP assembly (Peyret *et al.*, 2015). The formation of native HBcAg VLPs, the Tandem Core™ construct, insertion/conjugation of foreign antigens and formation of Tandem Core™ VLPs is illustrated in Figure 7.

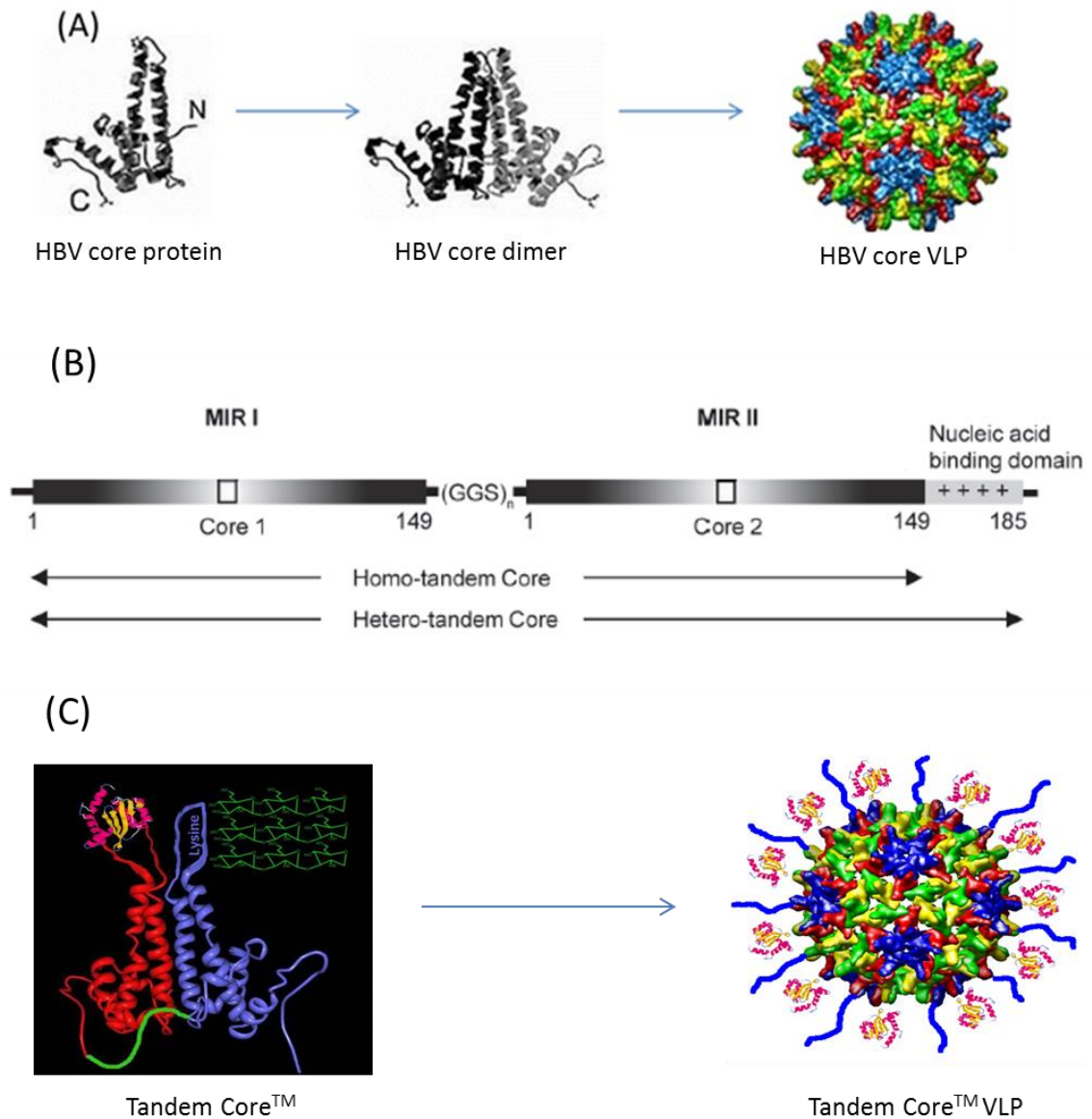


Figure 7 Hepatitis B core protein and Tandem Core™ VLPs. (A) VLP formation from native HBV core protein first occurs by spontaneous formation of an HBcAg dimer. 90-120 dimeric subunits then assemble a VLP. (B) Two Hepatitis B core protein sequences fused together via a repeating GGS linker to form the Tandem Core™ construct from either hetero-tandem (one full length, one truncated, core protein) or homo-tandem (both cores truncated) for removal of the nucleic acid binding domain(s). Illustrated are the major immunodominant regions (MIRs I and II) which can accommodate insertion of foreign proteins or lysine residues for polysaccharide conjugation. Adapted from Peyret *et al.*, 2015 (C) Tandem Core™ molecule expressing foreign protein (pink) in MIR I (red) and lysine residues in MIR II (blue) chemically conjugated to *Burkholderia* CPS. Assembly of this construct forms the Tandem Core™ VLP, expressing both foreign protein (pink) and CPS (blue) on the outside of the molecule. Images provided by Mologic.

1.11 Project aims

There is not a licensed vaccine available for the disease melioidosis. Despite reports on the ability of several *Burkholderia* vaccines to confer some protection, none of the vaccines have reached the clinical trial state and the ability to achieve sterilising immunity is inconsistent.

The aim of the project work reported in this thesis was to develop an efficacious vaccine against *B. pseudomallei* based on Tandem Core™ technology combined with capsular polysaccharide and protein antigens from *B. pseudomallei*.

The development of the conjugate vaccine first required optimisation of CPS production in order to reduce the cost of extraction. The *B. thailandensis* strain E555 was investigated following reports of an expressed polysaccharide that cross-reacts with an antibody generated against *B. pseudomallei*. The use of *B. pseudomallei* protein antigens required identification of candidates and identification of immunogenic regions for potential insertion into the Tandem Core™.

The second part of this study was to assess the protective efficacy of developed conjugate vaccine in an animal model of acute melioidosis and investigate the effect on efficacy of different adjuvants.

Chapter 2: Materials and methods

All chemicals and reagents were supplied by Sigma-Aldrich Company Ltd. (Poole, Dorset), unless otherwise stated.

Phosphate buffered saline (1x Dulbecco's PBS) and distilled water was supplied by Life Technologies unless otherwise stated.

2.1 Preparation of antibiotics

For addition of kanamycin to microbiological media for growth of *B. thailandensis* E555 :: *wbil* (Km^r), 200 µL of a stock concentration of kanamycin at 50 mg/mL was added to 199.8 mL of media to give a final concentration of 50 µg/mL.

2.2 Preparation of reagents and buffers

2.2.1 ABTS buffer pH 4.37 (Citric acid/phosphate buffer)

ABTS buffer was produced by a Dstl colleague (Scott Underwood).

Citric acid (11.76 g/L), and Na₂HPO₄ (12.49 g/L) were added to Milli-Q® water, pH adjusted to 4.37 (with either citric acid or disodium phosphate) and sterilised at 121°C for 15 minutes.

2.3 Preparation of growth media

All media was produced by a Dstl colleague (Scott Underwood). The media used in this this is detailed in Handbook of microbiological media, 2nd edition, Ronald M. Atlas, edited by Lawrence C. Parks, CRC. ISBN: 0-8493-2638-9.

2.3.1 Luria Bertani (LB) broth

Difco tryptone peptone (10 g), Difco Bacto yeast extract (5 g) and sodium chloride (5 g) were added to 1000 mL of Milli-Q® water, pH adjusted to 7.2 if necessary and sterilised at 121°C for 15 minutes.

2.3.2 LB agar

Difco tryptone peptone (10 g), Difco Bacto yeast extract (5 g), sodium chloride (5 g) and Difco Bacto agar (20 g) were added to 1000 mL of Milli-Q® water, pH adjusted to 7.2 if necessary and sterilised at 121°C for 15 minutes.

2.3.3 Enhanced phytone peptone broth

Two buffers were first prepared; phosphate buffer by addition of 12.5 g of K_2HPO_4 and 2.31 g of KH_2PO_4 in 100 mL of Milli-Q® water followed by sterilisation at 121°C for 15 minutes; and 1 M $MgSO_4 \cdot 7H_2O$; by addition of 24.65 g of $MgSO_4 \cdot 7H_2O$ in 100 mL of H_2O followed by 0.35 μm filter sterilisation.

Phytone peptone (24 g), yeast extract (72 g) and glycerol (25 g) were added to 900 mL of Milli-Q® water followed by sterilisation at 121°C for 15 minutes after which the phosphate buffer (100 mL) and 1 M $MgSO_4 \cdot 7H_2O$ (10 mL) was added.

2.3.4 M9 minimal media

The following solutions were prepared; 20 % (w/v) glucose (20.0 g/100 mL Milli-Q® water, sterilised at 121°C for 15 minutes); 1 M $MgSO_4 \cdot 7H_2O$: (246.5 g in 1 L of Milli-Q® water, sterilised at 121°C for 15 minutes); 0.1 % (w/v) thiamine-HCl (10 mg in 10 ml of Milli-Q® water, 0.35 μm filter sterilised); and 133 mM $CaCl_2$ (14.7 g in 1 L of Milli-Q® water, sterilised at 121°C for 15 minutes).

The following components were dissolved in Milli-Q® water with the final volume adjusted to 987 mL with Milli-Q® water; Na₂HPO₄ (6 g/L), KH₂PO₄ (3 g/L), NH₄Cl (0.5 g/L). This solution was pH adjusted to 7.0 and sterilised at 121°C for 15 minutes. Once cooled, 10 mL of 20 % (w/v) glucose solution; 1 mL of 1 M MgSO₄.7H₂O; 1 mL of 0.1 % (w/v) thiamine-HCl; and 1 mL of CaCl₂ were added aseptically.

2.3.5 Tryptone peptone broth

Oxoid tryptone soya broth (30 g/L) was added to 1 L of Milli-Q® water, adjusted to pH 7.3 and sterilised at 121°C for 15 minutes.

2.3.6 Brain Heart Infusion broth

Difco brain heart infusion broth (37 g/L) was added to 1 L of Milli-Q® water and sterilised at 121°C for 15 minutes.

2.3.7 Brain Heart Infusion agar

Difco brain heart infusion agar (52 g/L) was added to 1 L of Milli-Q® water and sterilised at 121°C for 15 minutes.

2.4 Microbiology techniques

2.4.1 Bacterial strains and plasmids

Strain or plasmid	Relevant information
<i>B. pseudomallei</i> K96243	Natural isolate (Holden <i>et al.</i> , 2004)
<i>B. pseudomallei</i> 1026b	Natural isolate (Hayden <i>et al.</i> , 2012)
<i>B. thailandensis</i> E555	Natural isolate (Sim <i>et al.</i> , 2010)
<i>B. thailandensis</i> CDC2721121	Natural isolate (Sim <i>et al.</i> , 2010)

Table 1 Bacterial strains used in this thesis and reference information

Master stocks of all *B. pseudomallei* and *B. thailandensis* strains were provided by Dr Andy Scott, Dstl, Porton Down. *B. thailandensis* E555 :: *wbil* (Km^r) was provided by Dr Andy Scott, Dstl, Porton Down. Briefly, this mutant was generated by insertional inactivation of the *wbil* gene using the pKnock-Km suicide vector (Alexeyev 1999). An internal fragment from the *wbil* gene in *B. thailandensis* E555 was amplified by polymerase chain reaction (PCR); ligated into pKnock-Km vector and cloned into *E. coli* S17-1 λ -pir. The resulting vector was transferred into *B. thailandensis* E555 by conjugation (Hamad *et al.*, 2009) and recombinants selected by supplementing growth media with kanamycin (750 μ g/mL) and gentamicin (50 μ g/mL). Loss of O-antigen synthesis was confirmed by A. Scott by Western hybridization following SDS PAGE using the O-antigen specific monoclonal CC6 (Jones *et al.*, 2002). Continued synthesis of CPS was confirmed by Western hybridization using the capsule-specific monoclonal DSTL189.

2.4.2 Growth and manipulation of bacteria

B. pseudomallei is classed as a hazard group 3 pathogen by The Advisory Committee on Dangerous Pathogens (ACDP). Therefore, all manipulation of *B. pseudomallei* was carried out within a Class III microbiological safety cabinet, located within a designated containment level 3 laboratory.

B. thailandensis is not classified as hazardous by the ACDP therefore all manipulation was carried out within a Class II microbiological safety cabinet, located within a designated containment level 2 laboratory.

2.5 Extraction of CPS from *B. pseudomallei* K96243 and *B. thailandensis* E555

2.5.1 Growth of *Burkholderia* spp. on solid media

B. pseudomallei K96243 was inoculated into 100 mL of LB broth. *B. thailandensis* E555 :: *wbil* (Km^r) was inoculated into 100 mL of LB broth with 50 µg/mL kanamycin. Both cultures were incubated overnight at 37°C, shaking at 180 rpm. Each culture was used to inoculate 32 large tissue culture flasks containing LB agar and incubated for 48 hours at 37°C. Cells were harvested in 4 mL of PBS with the use of glass beads. The cells were split into 10 mL aliquots and heat inactivated at 80°C for 4 hours. Each 10 mL aliquot was sterility checked by inoculation of fresh LB with 1 mL and incubated for seven days at 37°C followed by plating of 250 µL volumes onto LB plates and incubation for seven days at 37°C. Plates were inspected for absence of bacteria.

2.5.2 Growth of *Burkholderia* spp. in liquid cultures

Burkholderia K96243 was inoculated into 50 mL LB broth and *B. thailandensis* E555 :: *wbil* (Km^r) inoculated into 50 mL of LB broth with 50 µg/mL kanamycin. All cultures were incubated at 37°C overnight, shaking at 180 rpm. The cells were split into 10 mL aliquots and heat inactivated at 80°C for 4 hours. Each 10 mL aliquot was sterility checked by inoculation of fresh LB with 1 mL and incubated for seven days at 37°C followed by plating of 250 µL volumes onto LB plates and incubation for seven days at 37°C. Plates were inspected for absence of bacteria.

2.5.3 Extraction of CPS from *Burkholderia spp.* by ethanol precipitation

50 mL of the cell suspension from method 2.5.1 or 2.5.2 was centrifuged (30 minutes, 12,000 x g, 4°C), the supernatant removed and centrifuged again under the same conditions. The resulting supernatant was removed and precipitated with ice-cold absolute ethanol to a final concentration of 80 % vol/vol. This was then centrifuged (30 minutes, 5,000 x g, 4°C) and the pellet collected. The pellet was re-suspended in 100 mL 80% ethanol before centrifugation (30 minutes, 5,000 x g, 4°C). This wash stage was repeated and the pellet suspended in 10 mL PBS containing 1 mM CaCl₂ and 1 mM MgCl₂. 100 µg/mL each of RNase A, DNase I and lysozyme was added and the sample incubated for 2.5 hours at 37°C. Proteinase K was then added to final concentration of 100 µg/mL and the suspension incubated for a further 2.5 hours at 37°C. Samples were then centrifuged (30 minutes, 5,000 x g, 4°C), the supernatant removed and precipitated with ice-cold absolute ethanol to a final concentration of 80 % vol/vol. This was stored overnight at -20°C. Samples were centrifuged (30 minutes, 5,000 x g, 4°C) and the resulting pellet washed in 50 mL of 80 % ethanol for 30 minutes before further centrifugation (30 minutes, 5,000 x g, 4°C). The pellet was re-suspended in distilled water and heated to 37°C before dialysis overnight (10,000 Da molecular weight cut-off) against distilled water. The final sample was obtained by lyophilisation of the dialysed material with an Edwards Modulyo freeze dryer.

2.5.4 Phenol extraction of CPS from *Burkholderia spp.* utilising an LPS extraction method

Sterility checked bacteria generated from Method 2.5.1 or 2.5.2 was lyophilised. 5 g of bacteria was suspended in 50 mL of 50 mM sodium phosphate buffer (with 5mM EDTA, pH 7). Lysozyme (15,000 units per mg of bacteria) was added and the mixture stirred for 8 hours at room temperature, or for 16 hours at 4°C. The solution was then made up to 150 mL with 20 mM MgCl₂ with 20 µg/mL each of DNase and RNase added, and the solution stirred overnight at room temperature. The solution was made up to 90 % (vol/vol) phenol and stirred (10 mins, 60°C) before adding 50 µg/mL proteinase K. This solution was stirred for 6 hours at room temperature. The phenol and heat-killed cell mixture

was warmed to 70°C before adding an equal volume of 90 % (vol/vol) phenol to the cells and stirring by hand vigorously for 30 minutes while maintaining the temperature. The solution was then dialysed 3 times per day (10,000 Da molecular weight cut-off) against tap water to remove phenol (3-5 days) followed by lyophilisation. The lyophilised material was dissolved in 30 mg/mL of 10 mM Tris-HCl (pH 7) containing 1 mM CaCl₂, 1 mM MgCl₂ and DNase and RNase (20 µg/mL) and incubating for 2 hours at 37°C. Proteinase K was then added (50 µg/mL) and the solution incubated at 45°C for 4 hours before ultracentrifugation (100,000 x *g* for 3 hours). The gel-like pellets were solubilised in distilled water before dialysis against distilled water (10,000 Da molecular weight cut-off) and lyophilisation.

2.5.5 Associate Professor Paul Brett's CPS extraction method

This modified hot-phenol CPS extraction method was provided by Assoc. Prof. Brett and has been described previously (Perry *et al.* 1995, Heiss *et al.* 2012). A starter culture was set up by inoculation of 25 mL of growth media (typically LB + 50 µg/mL kanamycin) into a 250 mL Erlenmeyer flask and incubated overnight at 37°C. A 5 mL aliquot of this starter culture was then inoculated into 4 x 500 mL of growth media in 2 L Erlenmeyer flasks and incubated at 37°C, shaking at 180 rpm on an orbital shaker for 37 hours. The bacterial culture was centrifuged for 10 minutes at 8000 x *g* and the pellet re-suspended in distilled water. The re-suspended culture was then added in equal parts (vol/vol) to 90 % (w/v) phenol and heated to 80°C. The phenol was dialysed against distilled water using a Spectra/Por 6-8K MWCO dialysis membrane and the resulting cell debris removed by centrifugation (10 minutes at 11,900 x *g*). The samples were then enzymatically digested with 50 µg/mL DNase and RNase at 37°C for 2 hours and 50 µg/mL proteinase K at 60°C for 3 hours. The sample was then centrifuged at 11,900 x *g* for 40 minutes and the CPS isolated from the supernatant as precipitated gel following ultracentrifugation at 100,000 x *g* for 6 h. The gel pellet was re-suspended in ultrapure water and lyophilised to concentrate. Rough LPS contaminants were then removed by acid hydrolysis with 2 % (v/v) acetic acid at 100°C for 2 hours. The sample was centrifuged at 11,900 x *g* for 40 minutes and the supernatants lyophilised to concentrate. The samples were then reconstituted at 20 mg/mL in ultrapure water and loaded

onto a Sephadex G-50 column (40 cm x 2.6 cm). The purified CPS was eluted isocratically in ultrapure water at a rate of 4 mL/min. The fractions were analysed for carbohydrate using the phenol-sulphuric acid method (Masuko 2005) with the appropriate fractions combined and lyophilised.

2.5.6 Monosaccharide analysis of CPS

The polysaccharide sample (20 µL of a 3 mg/mL solution) was mixed with distilled water (150 µL) and neat TFA (30 µL, 12.8 M) and the reaction was heated to 100°C for 4 hours. TFA was removed by evaporation using a SpeedVac® evaporation centrifuge. The polysaccharide sample was reconstituted in distilled water (300 µL), vortexed for 30 seconds and then centrifuged for 5 minutes at 14,000 x *g*. 10 µL (2 µg) of the polysaccharide sample was injected onto the Dionex® ICS-5000® HPAE-PAD for analysis. This method was performed by collaborators at the John Innes Centre.

2.6 Development of a quantitative CPS ELISA

2.6.1 Dot-blot analysis

A nitrocellulose membrane was first prepared by rinsing in PBS and leaving to air-dry. Next, purified CPS samples were diluted, in PBS, from 1:10 down to 1:83886080 with a 1:2 dilution factor between samples. 5 µL of the samples were spotted on the nitrocellulose membrane and allowed to dry. The membrane was then incubated in Blotto (5 % (w/v) skimmed milk powder in PBS) overnight at 4°C. The primary antibody (DSTL189) was added at 1:1000 dilution in blocking reagent and incubated at room temperature, with shaking for 45 minutes. The membrane was then washed with washing buffer (0.1 % (v/v) Tween 20 in PBS). Triplicate washes are performed at room temperature for 5 minutes each. A goat anti-mouse-ALP conjugate (Biorad) was added to detect the DSTL189 as a 1:1000 dilution in 5 % (w/v) Blotto and incubated at room temperature for 45 minutes. The membrane was washed 3 times with washing buffer at room temperature, with shaking for 5 minutes per wash, removed from washing buffer and then soaked in SIGMAFAST™ 3-3'-Diaminobenzidine (DAB;

0.7 mg/mL, urea hydrogen peroxide; 0.67 mg/mL) and a colour change observed.

2.6.2 ELISA utilising plate bound CPS

Diluted samples of purified CPS, in PBS, from 1:10 down to 1:83886080 with a 1:2 dilution factor between samples were prepared and 100 μ L added to each well of a 96-well plate. The plate was incubated overnight at 4°C and washed 3 times with 300 μ L of PBS with 0.01 % (v/v) Tween 20. During all incubations, the microtiter plates were covered with BIS Ltd microplate sealers (7740005). The plate was blocked by addition of 100 μ L of 5 % (w/v) Blotto. The plate was then incubated at room temperature for 1 hour and washed 3 times with 300 μ L of PBS with 0.01 % (v/v) Tween 20. DSTL189 was diluted 1:1000 in Blotto and 100 μ L added to each well. The plate was then incubated at room temperature for 45 minutes and washed 3 times with 300 μ L of PBS with 0.01 % (v/v) Tween 20. Goat anti-mouse-HRP conjugate (Biorad) was diluted 1:1000 in blocking agent and 100 μ L added to each well. The plate was again incubated at room temperature for 45 minutes and washed 3 times with 300 μ L of PBS with 0.01 % (v/v) Tween 20. Bound antibody was detected with 100 μ L of enzyme substrate (50 mg of 2,2'-azino-bis(ethylbenzthiazoline-6-sulphonic acid) - ABTS added to 100 mL of ABTS buffer (Method 2.2.1) and 100 μ L of hydrogen peroxide solution (30 % w/w). The reaction was left to develop for 15 minutes at room temperature and absorbance read at 414_{nm} on a Labsystems, Multiskan Ascent spectrophotometer.

2.6.3 Generation of biotinylated monoclonal antibody DSTL189

DSTL189 antibody was diluted to 1 mg/mL in PBS. Using a syringe and needle, 1 mL of dimethylformamide (DMF) was introduced into a vial of hapten-NHS ester (Molecular Devices Corp.) and mixed until the label had completely dissolved. The dissolved label was removed using the syringe and introduced into a 1.5 mL Eppendorf tube and then placed in a foil wrapper to prevent UV degradation of the label. The required volume of label (Table 2) was then added to 1 mL of antibody solution and mixed thoroughly before incubating at room

temperature for 2 hours in the dark. During this incubation, a PD-10 column (GE Healthcare) was equilibrated with 25 mL of PBS. A further 1 to 2 mL of PBS was added to the column and the bottom of the column capped (to prevent the upper disc from drying out over the remainder of the incubation period). Once incubation was complete, the cap was removed from the PD-10 column for the PBS to drain through. The 1 mL reaction volume was added to the columns, allowed to drain through and 1.25 mL of PBS added to each column to stop the reaction. Using graduated Eppendorfs to collect fractions, 3 mL of PBS was added to the column. The first 0.75 mL was collected in the first Eppendorf, 1.5 mL in the second Eppendorf and the remaining 0.75 mL in the third Eppendorf. This was repeated for the remaining reactions. The absorbance of the fractions was measured on a UV-VIS spectrophotometer at 280 nm and 362 nm. The labelled antibodies were stored at -70°C until use.

Molar Coupling Ratio	Volume of biotin-NHS added (µL)
5	5.4
10	10.8
20	21.6
30	32.4

Table 2 Biotinylated antibody molar coupling ratios and the volume of reconstituted label required to achieve them.

2.6.4 ELISA method for biotin interference

A 96-well plate was coated with 100 µL/well of CPS (10 µg/mL) and incubated at 4°C overnight. During all incubations, the microtiter plates were covered with BIS Ltd microplate sealers (7740005). The plate was washed 3 times with PBS + 0.05 % (v/v) Tween 20, 200 µL of 1 % (w/v) Blotto added to every well and incubated at 37°C for 1 hour. The plate was then washed 3 times with PBS + 0.05 % (v/v) Tween 20. Each antibody aliquot was diluted (10 µg/mL) and 100 µL of 1 % (w/v) Blotto was pipetted into all wells except column 1. Into wells A1 and E1 of column 1 was added 200 µL of x5 (MCR) mAb, 200 µL of x10 (MCR) mAb into wells B1 and F1, 200 µL of x20 (MCR) mAb into wells C1 and G1 and 200 µL of x30 (MCR) mAb into wells D1 and H1. Each antibody was then diluted across the plate (100 µL) until Column 11. Column 12 contained only

100 μ L of Blotto (blank). The plate was then incubated for 1 hour at 37°C and washed 3 times with PBS + 0.05 % (v/v) Tween 20. Streptavidin peroxidase (SP) was diluted 1:1000 and 100 μ L added wells A1-D12. To control for the possibility of biotinylation having failed, 100 μ L of goat anti-mouse horse radish peroxidase (HRP, Biorad) – diluted 1:1000, was added to wells E1–H12. The plate was incubated for 1 hour at 37°C and washed 6 times with PBS + 0.05 % (v/v) Tween 20. Bound antibody was detected with 100 μ L of enzyme substrate (50 mg 2,2'-azino-bis(ethylbenzthiazoline-6-sulphonic acid) - ABTS, added to 100 mL of ABTS buffer (Method 2.2.1) and 100 μ L of hydrogen peroxide 30 % w/w). The reaction was left to develop for 15 minutes at room temperature and absorbance read at 414 nm on a Labsystems, Multiskan Ascent spectrophotometer.

2.6.5 Development of ELISA purified CPS standard curve

A 96-well microtiter plate was coated overnight at 4°C with 100 μ L/well of purified DSTL189 monoclonal antibody diluted to 5 μ g/mL in PBS. During all incubations, the microtiter plates were covered with BIS Ltd microplate sealers (7740005). Each well was washed three times with PBS supplemented with 0.05 % (v/v) Tween 20 and blocked with 200 μ L of PBS containing 2 % (w/v) Blotto for 1 hour at 37°C. A reference sample (purified CPS from *B. thailandensis* E555 ::*wbil* (KmR)) was diluted to initial concentrations of 10, 5 or 1.25 μ g/mL and serially diluted two-fold in 100 μ L aliquots on the plate. Following incubation for 1 hour at 37°C, each well was washed three times with PBS supplemented with 0.05 % (v/v) Tween 20 and 100 μ L/well of biotinylated DSTL189 antibody (diluted in 2 % (w/v) Blotto to 5 μ g/mL) was added. The plate was incubated for 1 hour at 37°C and each well then washed three times with PBS supplemented with 0.05 % (v/v) Tween 20. A 1:1000 dilution of streptavidin peroxidase in Blotto was then added and incubated at 37°C for 1 hour. Each well was washed six times with PBS supplemented with 0.05 % (v/v) Tween 20 and bound conjugate detected with 100 μ L of enzyme substrate (50 mg 2,2'-azino-bis(ethylbenzthiazoline-6-sulphonic acid) - ABTS, added to 100 mL of ABTS buffer (Method 2.2.1) and 100 μ L of hydrogen peroxide 30 % w/w). The reaction was left to develop for 15 minutes at room temperature and

absorbance read at 414 nm on a Labsystems, Multiskan Ascent spectrophotometer.

2.6.6 *B. pseudomallei* 1026b and *B. thailandensis* E555 :: *wbil* (Km^r) purified CPS recognition with DSTL189

The capture ELISA method detailed under Method 2.6.5 was followed with the exception that CPS from both *B. pseudomallei* K96243 and *B. thailandensis* E555 :: *wbil* (Km^r) was diluted in 2 % Blotto to an initial concentration of 10 µg/mL, then diluted 1:3 across the plate to a concentration of 0.007 µg/mL (in duplicate). The last row was left blank.

2.6.7 Measurement of *B. thailandensis* E555 :: *wbil* (Km^r) CPS culture concentration

The capture ELISA method detailed under Method 2.6.5 was followed with the exception that CPS from *B. thailandensis* E555 :: *wbil* (Km^r) was diluted in 2 % (w/v) Blotto to an initial concentration of 1.25 µg/mL. Neat cultures of *B. thailandensis* E555 :: *wbil* (Km^r) were also added and serially diluted in 2 % (w/v) Blotto, two-fold in 100 µL aliquots on the plate.

2.6.8 Final ELISA method for determination of *B. thailandensis* E555 :: *wbil* (Km^r) culture CPS content

A 96-well microtiter plate was coated overnight at 4°C with 100 µL/well of purified DSTL189 monoclonal antibody diluted to 5 µg/mL in PBS. During all incubations, the microtiter plates were covered with BIS Ltd microplate sealers (7740005). Each well was washed three times with PBS supplemented with 0.05 % (v/v) Tween 20 and blocked with 200 µL of PBS containing 2 % (w/v) Blotto for 1 hour at 37°C. A reference sample (purified CPS from *B. thailandensis* E555 :: *wbil* (Km^r)) was diluted to an initial concentration of 100 ng/mL and test samples diluted 1:512 in Blotto and serially diluted two-fold in 100 µL aliquots on the plate. Following incubation for 1 hour at 37°C, each well was washed three times with PBS supplemented with 0.05 % (v/v) Tween

20 and 100 µL/well of biotinylated DSTL189 antibody (diluted in 2 % (w/v) Blotto to 5 µg/mL) was added. The plate was incubated for 1 hour at 37°C and each well then washed three times with PBS-Tween 20. A 1:1000 dilution of streptavidin peroxidase in 2 % (w/v) Blotto was then added and incubated at 37°C for 1 hour. Each well was washed six times with PBS supplemented with 0.05 % (v/v) Tween 20 and bound conjugate detected with 100 µL/well of enzyme substrate (50 mg 2,2'-azino-bis(ethylbenzthiazoline-6-sulphonic acid)) - ABTS, added to 100 mL of ABTS buffer (Method 2.2.1) and 100 µL of hydrogen peroxide 30 % w/w). The reaction was left to develop for 20 minutes at room temperature and absorbance read at 414 nm on a Labsystems, Multiskan Ascent spectrophotometer.

2.6.9 Determination of ELISA LOD utilising *B. thailandensis* CDC2721121

10 mL of LB media was inoculated with a loop of *B. thailandensis* CDC2721121 from a glycerol stock and incubated overnight at 37°C with shaking (180 rpm). The capture ELISA method detailed under Method 2.6.8 was followed with the exception that 100 µL of the test samples, in this case *B. thailandensis* CDC2721121 culture, was added at a neat concentration and diluted 1:2 across the plate in 2 % (w/v) Blotto. *B. thailandensis* E555 :: *wbil* (Km^r) was also added to the plate as a control.

2.6.10 Determination of ELISA purified CPS limit of detection (LOD)

The capture ELISA method detailed under Method 2.6.5 was followed with the exception that CPS from *B. thailandensis* E555 :: *wbil* (Km^r) was diluted in 2 % (w/v) Blotto to an initial concentration of 100 ng/mL and diluted 1:2, in 2 % (w/v) Blotto, across the plate to a final concentration of 98 pg/mL. These were the test samples. A purified CPS standard curve was not added. Neat cultures of *B. thailandensis* CDC2721121 were added as a negative control.

2.6.11 Determination of ELISA purified CPS limit of quantification (LOQ)

The capture ELISA method detailed under Method 2.6.5 was followed with the exception that a reference sample of purified CPS from *B. thailandensis* E555 :: *wbil* (Km^r) was diluted in 2 % (w/v) Blotto to an initial concentration of 100 ng/mL and diluted 1:2, in 2 % (w/v) Blotto, across the plate. Test samples (purified CPS, were diluted in 2 % (w/v) Blotto to an initial concentration of 100 ng/mL and diluted 1:2, in 2 % (w/v) Blotto, to 98 pg/mL across the plate. Neat cultures of *B. thailandensis* CDC2721121 were added as a negative control.

2.7 CPS expression optimisation – growth

2.7.1 Measurement of CPS expression from a *B. thailandensis* E555 :: *wbil* (Km^r) culture inoculated from a glycerol stock

25 mL of LB with 50 µg/mL kanamycin was inoculated with a loop of *B. thailandensis* E555 :: *wbil* (Km^r) from a glycerol stock and incubated at 37°C, shaking at 180 rpm in an orbital incubator. In addition, 10 mL of LB growth media was inoculated with *B. thailandensis* CDC2721121 with a loop from a glycerol stock and incubated overnight at 37°C, shaking at 180 rpm to act as the negative control.

At 17, 18, 19, 20, 21, 22, 23, 24, 25, 26, 27, 42, 48, 66 and 72 hours after inoculation, 1 mL culture samples were serially diluted 1:10 and plated onto LB media and incubated for up to 48 hours to count the number of colony-forming units. Additional culture samples (1.5 mL) were taken and frozen at -20°C.

The capture ELISA method detailed under Method 2.6.8 was followed.

2.7.2 Measurement of CPS expression from a *B. thailandensis* E555 :: *wbil* (Km^r) culture inoculated from a subbed culture

25 mL of LB with 50 µg/mL kanamycin was inoculated with a loop of *B. thailandensis* E555 :: *wbil* (Km^r) from a glycerol stock and incubated at 37°C, shaking at 180 rpm in an orbital incubator. This was termed the starter culture. 50 mL of growth media with 50 µg/mL kanamycin was inoculated with 500 µL of

the starter culture and incubated at 37°C, shaking at 180 rpm in an orbital incubator. In addition, 10 mL of LB growth media was inoculated with *B. thailandensis* CDC2721121 with a loop from a glycerol stock and incubated overnight at 37°C, shaking at 180 rpm to act as the negative control.

At 17, 18, 19, 20, 21, 22, 23, 24, 25, 26, 27, 42 and 48 hours after inoculation, 1 mL culture samples were serially diluted 1:10, plated onto LB media and incubated for up to 48 hours to count the number of colony-forming units (CFU). Additional culture samples (1.5 mL) were taken and frozen at -20°C.

The capture ELISA method detailed under Method 2.6.8 was followed.

2.7.3 Measurement of CPS expression from a *B. thailandensis* E555 :: *wbil* (Km^r) culture inoculated into different growth medias

25 mL of growth media (LB, M9 minimal media, tryptone soya broth and enhanced phytone peptone) with 50 µg/mL kanamycin was inoculated with a loop of *B. thailandensis* E555 :: *wbil* (Km^r) from a glycerol stock and incubated at 37°C, shaking at 180 rpm on an orbital incubator. This was termed the starter culture. 50 mL of growth media (LB, M9 minimal media, tryptone soya broth and enhanced phytone peptone) with 50 µg/mL kanamycin was inoculated with 500 µL of the starter culture and incubated at 37°C, shaking at 180 rpm in an orbital incubator. In addition, 10 mL of LB growth media was inoculated with *B. thailandensis* CDC2721121 with a loop from a glycerol stock and incubated overnight at 37°C, shaking at 180 rpm to act as the negative control.

At 20, 24 and 27 hours after inoculation, 1 mL culture samples were serially diluted 1:10, plated onto LB media and incubated for up to 48 hours to count the number of colony-forming units (CFU). Additional culture samples (1.5 mL) were taken and frozen at -20°C.

The capture ELISA method detailed under Method 2.6.8 was followed with the exception that the M9 minimal media test samples were diluted 1:16 rather than 1:512 to allow for interpolation from the standard curve of the lower expected CPS concentration.

2.7.4 Measurement of CPS expression from a *B. thailandensis* E555 :: *wbil* (Km^r) culture inoculated into baffled flasks

25 mL of LB with 50 µg/mL kanamycin was inoculated with a loop of *B. thailandensis* E555 :: *wbil* (Km^r) from a glycerol stock and incubated at 37°C, shaking at 180 rpm in an orbital incubator. This is the starter culture. Two aliquots of 50 mL LB media with 50 µg/mL kanamycin, one in a flat bottomed flask and one in a baffled flask, was inoculated with 500 µL of the starter culture and incubated at 37°C, shaking at 180 rpm in an orbital incubator. In addition, 10 mL of LB growth media was inoculated with *B. thailandensis* CDC2721121 with a loop from a glycerol stock and incubated overnight at 37°C, shaking at 180 rpm to act as the negative control.

At 20, 24 and 27 hours after inoculation, 1 mL culture samples were serially diluted 1:10 and plated onto LB media and incubated for up to 48 hours to count the number of colony-forming units. Additional culture samples (1.5 mL) were taken and frozen at -20°C.

The capture ELISA method detailed under Method 2.6.8 was followed.

2.7.5 Measurement of CPS expression from a *B. thailandensis* E555 :: *wbil* (Km^r) culture inoculated with iron sulfate

25 mL of LB with 50 µg/mL kanamycin was inoculated with a loop of *B. thailandensis* E555 :: *wbil* (Km^r) from a glycerol stock and incubated at 37°C, shaking at 180 rpm in an orbital incubator. This is the starter culture. Four aliquots of 50 mL LB media with 50 µg/mL kanamycin with an iron sulfate concentration of 0 mM, 50 µM, 0.5 mM and 5 mM, were inoculated with 500 µL of the starter culture and incubated at 37°C, shaking at 180 rpm in an orbital incubator. In addition, 10 mL of LB growth media was inoculated with *B. thailandensis* CDC2721121 with a loop from a glycerol stock and incubated overnight at 37°C, shaking at 180 rpm to act as the negative control.

At 20, 24 and 27 hours after inoculation, 1 mL culture samples were serially diluted 1:10 and plated onto LB media and incubated for up to 48 hours to count the number of colony-forming units. Additional culture samples (1.5 mL) were taken and frozen at -20°C.

The capture ELISA method detailed under Method 2.6.8 was followed.

2.7.6 Measurement of CPS expression from a reduced volume *B. thailandensis* E555 :: *wbil* (Km^r) culture

25 mL of LB with 50 µg/mL kanamycin was inoculated with a loop of *B. thailandensis* E555 :: *wbil* (Km^r) from a glycerol stock and incubated at 37°C, shaking at 180 rpm in an orbital incubator. This is the starter culture. An aliquot of 50 mL LB media with 50 µg/mL kanamycin was inoculated with 500 µL of the starter culture and incubated at 37°C, shaking at 180 rpm in an orbital incubator. An aliquot 25 mL LB media with 50 µg/mL kanamycin was inoculated with 250 µL of the starter culture and incubated at 37°C, shaking at 180 rpm in an orbital incubator. In addition, 10 mL of LB growth media was inoculated with *B. thailandensis* CDC2721121 with a loop from a glycerol stock and incubated overnight at 37°C, shaking at 180 rpm to act as the negative control.

At 20, 24 and 27 hours after inoculation, 1 mL culture samples were serially diluted 1:10 and plated onto LB media and incubated for up to 48 hours to count the number of colony-forming units. Additional culture samples (1.5 mL) were taken and frozen at -20°C.

The capture ELISA method detailed under Method 2.6.8 was followed.

2.7.7 Measurement of CPS expression from a *B. thailandensis* E555 :: *wbil* (Km^r) culture inoculated with mannose

25 mL of LB with 50 µg/mL kanamycin and 2.5 g/L mannose was inoculated with a loop of *B. thailandensis* E555 :: *wbil* (Km^r) from a glycerol stock and incubated at 37°C, shaking at 180 rpm in an orbital incubator. This is the starter culture. An aliquot of 50 mL LB media with 50 µg/mL kanamycin with a mannose concentration of 2.5 g/L was inoculated with 500 µL of the starter culture and incubated at 37°C, shaking at 180 rpm in an orbital incubator. In addition, 10 mL of LB growth media was inoculated with *B. thailandensis* CDC2721121 with a loop from a glycerol stock and incubated overnight at 37°C, shaking at 180 rpm to act as the negative control.

At 20, 24 and 27 hours after inoculation, 1 mL culture samples were serially diluted 1:10 and plated onto LB media and incubated for up to 48 hours to count the number of colony-forming units. Additional culture samples (1.5 mL) were taken and frozen at -20°C.

The capture ELISA method detailed under Method 2.6.8 was followed.

2.8 CPS expression optimisation – extraction

2.8.1 Determination of CPS from *B. thailandensis* E555 :: *wbil* (Km^r) supernatant and pellet fractions

25 mL of LB with 50 µg/mL kanamycin was inoculated with a loop of *B. thailandensis* E555 :: *wbil* (Km^r) from a glycerol stock and incubated at 37°C, shaking at 180 rpm in an orbital incubator for 24 hours. This was the starter culture. 50 mL of growth media with 50 µg/mL kanamycin was inoculated with 500 µL of the starter culture and incubated at 37°C, shaking at 180 rpm in an orbital incubator for 27 hours. In addition, 10 mL of LB growth media was inoculated with *B. thailandensis* CDC2721121 with a loop from a glycerol stock and incubated for 27 hours after inoculation at 37°C, shaking at 180 rpm to act as the negative control. At 27 hours after inoculation a 1 mL culture sample was taken for analysis. A further 1 mL culture sample was taken, centrifuged at 10,000 x *g* for 10 minutes and the supernatant removed for ELISA analysis. The resultant pellet was re-suspended in 1 mL of 2 % (w/v) Blotto and also analysed.

The capture ELISA method detailed under Method 2.6.8 was followed with the exception that the supernatant and pellet fractions were initially diluted 1:64 rather than 1:512 to allow for interpolation from the standard curve of the lower expected CPS concentrations.

2.8.2 Determination of CPS concentration ($\mu\text{g/mL}$) from *B. thailandensis* E555 :: *wbil* (Km^r) live and frozen culture fractions

The procedure detailed in method 2.8.1 was repeated to obtain live culture, supernatant and pellet fractions for immediate analysis by ELISA. Half of each fraction was frozen at -20°C overnight for analysis by ELISA the following day. For all samples the capture ELISA method detailed under Method 2.6.8 was followed.

2.9 *Burkholderia* CPS immunogenic epitope

2.9.1 Recognition of purified CPS and deacetylated CPS with the *B. pseudomallei* K96243 anti-CPS monoclonal antibody DSTL189

A 96-well microtiter plate was coated overnight at 4°C with $100\ \mu\text{L/well}$ of *B. thailandensis* E555 :: *wbil* (Km^r) purified CPS and de-acetylated CPS (gift from Prof. Rob Field, John Innes Centre) at $10\ \mu\text{g/mL}$ in PBS. During all incubations, the microtiter plates were covered with BIS Ltd microplate sealers (7740005). Each well was washed three times with PBS supplemented with $0.05\ \%$ (v/v) Tween 20 (PBS-Tween 20) and blocked with $200\ \mu\text{L}$ of PBS containing $2\ \%$ (w/v) Blotto for 1 hour at 37°C . The primary antibody; DSTL189 was diluted to $5\ \mu\text{g/mL}$ in $2\ \%$ (w/v) Blotto and $100\ \mu\text{L}$ was added to the plate in duplicate. The plate was then incubated for 1 hour at 37°C and each well washed three times with PBS-Tween 20. Goat anti-mouse IgG-HRP conjugate was diluted 1:2000 in $2\ \%$ (w/v) Blotto, $100\ \mu\text{L}$ added to each well and the plate incubated at 37°C for 1 hour. Each well was washed six times with PBS-Tween 20 and bound conjugate detected with $100\ \mu\text{L/well}$ of enzyme substrate (50 mg 2,2'-azino-bis(ethylbenzthiazoline-6-sulphonic acid) - ABTS, added to 100 mL of ABTS buffer (Method 2.2.1) and $100\ \mu\text{L}$ of hydrogen peroxide $30\ \%$ w/w). The reaction was left to develop for 20 minutes at room temperature and absorbance read at $414\ \text{nm}$ on a Labsystems, Multiskan Ascent spectrophotometer.

2.9.2 Recognition of purified CPS and deacetylated CPS with four *B. pseudomallei* K96243 anti-CPS monoclonal antibodies

A 96-well microtiter plate was coated overnight at 4°C with 100 µL/well of *B. thailandensis* E555 :: *wbil* (Km^r) purified CPS and de-acetylated CPS (gift from Prof. Rob Field) at 10, 5, 2.5 or 1.25 µg/m in PBS. During all incubations, the microtiter plates were covered with BIS Ltd microplate sealers (7740005). Each well was washed three times with PBS supplemented with 0.05 % (v/v) Tween 20 (PBS-Tween 20) and blocked with 200 µL of PBS containing 2 % (w/v) Blotto for 1 hour at 37°C. Primary antibodies (DSTL189, 4V8IIA11, 3VIE5, 4VA5) were diluted to 5 µg/mL in 2 % (w/v) Blotto and 100 µL was added to the plate in duplicate. The plate was then incubated for 1 hour at 37°C and each well washed three times with PBS-Tween 20. Goat anti-mouse IgG-HRP conjugate was diluted 1:2000 in 2 % (w/v) Blotto, 100 µL added to each well and the plate incubated at 37°C for 1 hour. Each well was washed six times with PBS-Tween 20 and bound conjugate detected with 100 µL/well of enzyme substrate (50 mg 2,2'-azino-bis(ethylbenzthiazoline-6-sulphonic acid)) - ABTS, added to 100 mL of ABTS buffer (Method 2.2.1) and 100 µL of hydrogen peroxide 30 % w/w). The reaction was left to develop for 20 minutes at room temperature and absorbance read at 414 nm on a Labsystems, Multiskan Ascent spectrophotometer.

2.9.3 Heavy and light chain variable region sequencing of four *B. pseudomallei* K96243 anti-CPS monoclonal antibodies

A 2-step cDNA synthesis and PCR protocol was used (Burmester, J., Pluckthun, A., 2001). Construction of scFv Fragments from Hybridoma or Spleen cells by PCR assembly. Antibody engineering, 1st edition, pp. 19-40. Edited by S. Dubel. Heidelberg: Springer). The full method is given below but in brief, RNA was extracted from hybridoma cell lines with TRIzol® (Invitrogen, Life Technologies), followed by synthesis of cDNA and subsequently PCR amplification of the variable light and variable heavy domains (ThermoScript™ RT-PCR system, Invitrogen, Life Technologies). Resultant PCR products were then cloned into the pCR™2.1 Vector and transformed into *E. coli* XL1 blue.

The plasmids harboring the variable fragments were purified by miniprep, the presence of insert checked by restriction digest, and sequenced.

2.9.3.1 Preparation of RNA

Cells from each antibody producing hybridoma cell line were grown by BBI detection and supplied in T75 tissue culture flasks.

The cells were lysed by addition of 2 mL of TRIzol® to each tissue culture flask followed by brief mixing by pipette. The homogenised samples were then incubated at room temperature for 5 minutes and 0.4 mL of chloroform added to each sample. The samples were shaken by hand and incubated for a further 3 minutes at room temperature. The samples were then centrifuged at 10,000 x *g* for 15 minutes at 4°C. The resultant aqueous phase was transferred to a fresh tube and RNA precipitated by addition of 1 mL of isopropyl alcohol. Samples were then incubated for 10 minutes at room temperature followed by centrifugation at 10,000 x *g* for 10 minutes at 4°C. The resultant supernatant was discarded and the RNA pellet was washed by addition of 2 mL of 75 % ethanol in DEPC-water, vortex mixed and centrifuged at 7000 x *g* for 5 minutes at 4°C. The resultant supernatant was discarded and the RNA pellet allowed to air dry for 5 minutes. RNA was then dissolved in 50 µL RNase-free water and RNA concentration was measured by nanodrop ready for cDNA synthesis and stored at -80°C until use.

2.9.3.2 First strand cDNA synthesis

cDNA synthesis was performed with Thermoscript™ RT-PCR system (product number 11146024, Invitrogen, Life Technologies) according to the manufacturer's instructions. In a reaction volume of 20 µL for each RNA sample the following reaction mixture was prepared; 8 µL of master reaction mix; 1 µL random hexamer primers (50 ng/µL); < 500 ng template RNA, 2 µL dNTPs (10mM) and 8 µL DEPC-water. The reaction mixtures were transferred to a thermal cycler and incubated at 25°C for 10 minutes, followed by 30 minutes at 50°C. The reaction was terminated by incubation at 85°C for 5 minutes. 1 µL of

RNase H was added to each reaction and incubated at 20 minutes at 37°C. cDNA was stored at -20°C until ready for use.

2.9.3.3 PCR amplification of antibody variable gene fragments

The PCR primers used in this reaction were a mixture formulated to cover all of the V-gene segments of the heavy and light chain of the mouse according to Burmester, J., Pluckthun, A., 2001. Construction of scFV Fragments from Hybridoma or Spleen cells by PCR assembly. Antibody engineering, 1st edition, pp. 19-40. Edited by S. Dubel. Heidelberg: Springer.

PCR of the variable regions was performed with Platinum® *Taq* DNA polymerase according to manufacturer's instructions (Invitrogen, Life Technologies). 2 µL of cDNA was added to 48 µL of master mix containing 10X High Fidelity PCR buffer, 50 mM MgSO₄, 10 mM dNTPs and 10 µM of each primer. The PCR reaction conditions were an initial PCR activation step of 94°C for 2 minutes followed by 30 cycles of 94°C for 30 seconds (denaturation), 55°C for 30 seconds (annealing), 72°C for 60 seconds. A final cycle of 94°C for 30 seconds (denaturation), 55°C for 30 seconds (annealing) and 72°C for 10 minutes (extension) was then performed to ensure full extension of all PCR amplicons. Reactions were performed using an Eppendorf mastercycler gradient cycler.

2.9.3.4 Cloning and sequencing

PCR products from 2.9.3.3 were cloned directly into a TA Cloning® Kit, with pCR™2.1 Vector and One Shot® TOP10 Chemically Competent *E. coli* (Product number K203040, Life Technologies) as per manufacturer's instructions.

In brief, a 10 µL ligation reaction was setup with 1 µL of fresh PCR product and incubated at room temperature for 30 minutes, transformed into One Shot® TOP10 Chemically Competent *E. coli* and plated onto LB agar plates containing 100 µg/mL of ampicillin and spread with X-Gal (40 µL of 40 mg/mL, Promega).

The plates were incubated overnight at 37°C and transferred to 4°C for 2 hours to allow for proper colour development.

Following incubation, four white colonies for each antibody were grown overnight in 5 mL of LB broth containing 100 µg/mL of ampicillin. The plasmid was isolated by miniprep according to manufacturer's instructions (Promega Wizard® Plus SV minipreps DNA purification system, A1460) and the presence of insert checked by restriction digest with *EcoRI*. Each insert was then sequenced with M13 uni 21 and M13 rev 29 primers by Eurofins.

2.10 Importance of the CPS acetyl group

2.10.1 CPS and deacetylated CPS-specific IgG and IgM serum antibody analysis of CPS and deacetylated CPS vaccinated mice

ELISAs were performed on sera collected 2 weeks post-vaccination. 96 well plates were coated with either purified CPS, or deacetylated CPS at 10 µg/mL in PBS and incubated overnight at 4°C. During all incubations, the microtiter plates were covered with BIS Ltd microplate sealers (7740005). Each well was washed three times with PBS supplemented with 0.05 % (v/v) Tween 20. The wells were then blocked with 2 % (w/v) Blotto and incubated at 37°C for 1 hour. Following three further washes with PBS-Tween 20, two-fold dilutions of the mouse serum samples in PBS supplemented with 2 % (w/v) Blotto were made across the plate. To act as a standard curve, one row of wells was coated with 5 µg/mL anti-F_{ab} antibody (AbD Serotec), incubated and washed as described above. Appropriate isotype standards were diluted two-fold across the plate. Also included into separate wells were serum from PBS and TetHc vaccinated control mice as negative controls. The plate was incubated for a further 1 hour at 37°C and washed three times in PBS-Tween. A 1:2000 dilution of isotype specific goat anti-mouse horseradish peroxidase conjugate (Biorad) in 2 % (w/v) Blotto was added to each well and the plate incubated at 37°C for 1 hour. Following six washes in PBS-Tween 20, 100 µl of Tetramethylbenzidine (KPL) substrate was added to each well according to the manufacturer's instructions

and incubated at room temperature for 20 minutes prior to measuring the absorbance at 620_{nm} with a Labsystems, Multiskan Ascent spectrophotometer.

2.11 Expression of Tandem Core™ with peptide inserts

All Tandem Core™ expression was performed by collaborators at Mologic and John Innes Centre.

2.11.1 Determination of LolC expression in VLP-LolC fusion constructs by ELISA from the baculovirus expression system

A 96-well microtiter plate was coated for 24 hours at 4°C with 100 µL/well of purified LolC (standard, 2-0.03 µg/mL), VLPs (negative control, 30-0.2 µg/mL) or VLP-LolC (test sample, 30-0.2 µg/mL). All samples were serially diluted two-fold in PBS. During all incubations, the microtiter plates were covered with BIS Ltd microplate sealers (7740005). Each well was washed three times with PBS-0.05% Tween 20 (PBS-Tween 20), and blocked with 200 µL of PBS containing 5 % (w/v) Blotto for 1 hour at 37°C. Each well was then washed three times with PBS-0.05% Tween 20 and a 1:1000 dilution of sera from mice vaccinated with either; a DNA vaccine expressing LolC; *E. coli* expressed LolC; or endotoxin-free LolC protein (Lionex) was added (100 µL/well) and the plate incubated for 1 hour at 37°C. Following three washes in PBS-Tween 20, a 1:2000 dilution of IgG goat anti-mouse horseradish peroxidase conjugate (AbD Serotec) in 2 % (w/v) Blotto was added to each well (100 µL) and incubated for 1 hour at 37°C. Each well was washed a further six times in PBS-Tween 20 and bound conjugate detected with 100 µL/well of enzyme substrate (50 mg 2,2'-azino-bis(ethylbenzthiazoline-6-sulphonic acid) - ABTS, added to 100 mL of ABTS buffer (Method 2.2.1) and 100 µL of hydrogen peroxide 30 % w/w). The reaction was left to develop for 20 minutes at room temperature and absorbance read at 414_{nm} on a Labsystems, Multiskan Ascent spectrophotometer.

2.12 VLP expression systems

2.12.1 Expression and purification of VLPs in *E.coli*

ClearColi™ BL21 (DE3) cells were selected for expression of Tandem Core™ due to the low level of endotoxicity associated with this cell line. Electrocompetent cells were transformed with plasmids according to manufacturer's guidelines. For expression, a starter culture from one selected colony using 15 mL of LB broth containing 50 µg/ml kanamycin was incubated at 37°C and 320 rpm overnight. A 500 mL culture of LB broth in a baffled 2 L flask was inoculated with 3 mL of the overnight starter culture. Expression cultures were grown to an OD_{600 nm} of ~0.6 and induced with 1 mM IPTG at 12°C for 16.5-17 hours. After induction, cells were harvested by centrifugation at 3000 x g for 5-10 minutes. Cell pellets were stored at -20°C. To generate purified VLPs, approximately 6 g cells were re-suspended in 80 mL lysis buffer (20 mM Tris-HCl pH 8, 5 mM EDTA, 2 mM AEBSF, 5 mM DTT, 250 U Benzonase) lysed by 2 passes of pressure homogenisation at 1,200 bar (~17,400 psi). Soluble core was extracted from crude lysate with 0.05 % (v/v) Tween 20 in PBS for 1 hour and then centrifuged at 20,000 x g for 30 minutes at 4°C. The supernatant (80 mL) was diluted with 500 mL 20 mM Tris-HCl pH 8, 5 mM EDTA and vacuum filtered through 0.8 µm, 0.45 µm and 0.22 µm membrane filters. The final filtrate was washed on a 1 MDa Pellicon® crossflow filter, reducing the volume to 25 mL and further filtered through a 0.2 µm syringe filter. The cleaned lysate was then further purified on a Sepharose CL4B column (XK26/92) and eluted into 20 mM Tris-HCl pH 8.4, 5 mM EDTA. The VLPs are captured in the void volume (40 mL).

2.12.2 Expression and purification of VLPs from *baculovirus*

Baculovirus was prepared by Oxford Expression Technologies under a sub-contract. The construct was cloned by iQur into their proprietary OET1 plasmid. Tni cells (standard insect cell line used by Oxford Expression Technologies) were infected with *baculovirus* carrying the above plasmid and then tissue culture supernatant analysed for VLP expression using the following protocol;

Tni FastBac Ultra (FBU) pellet was thawed and re-suspended in PBS to a total volume of 20 mL. 5 mL aliquots were spun (2000 x g, 15 minutes) and the supernatant decanted. The pellet was re-suspended in 8 mL lysis buffer (20 mM Tris-HCl pH 8.4, 1 mM EDTA, 0.1 % (v/v) Triton X-100, 2 mM DTT, 2 mM AEBSF) and sonicated at 50 % power for 3 x 10 sec. The sample was then subjected to 5 freeze / thaw cycles (methanol-dry ice/ 37°C water bath) before further sonication (50 % power 3 x 10 sec). Lysis was monitored by 100 % trypan blue. The lysate was centrifuged at 13,000 x g for 15 minutes and pellets re-suspended to original volume in lysis buffer. The samples were purified with a CL4B column and purity of the fractions assessed by silver staining and western blotting.

2.12.3 Expression of Tandem Core™ constructs in *Nicotiana benthamiana*

All expression constructs were transformed into *Agrobacterium tumefaciens* LBA4404 by electroporation and propagated at 28°C in LB media containing 50 µg/mL kanamycin and 50 µg/mL rifampicin. Transient expression was carried out by agroinfiltration of 3 - 4 week old *Nicotiana benthamiana* leaves. *Agrobacterium tumefaciens* strains were sub-cultured and grown overnight, pelleted and re-suspended to OD_{600 nm} = 0.4 in MMA (10 mM MES-NaOH, pH 5.6; 10 mM MgCl₂; 100 mM acetosyringone) and then infiltrated into leaf intercellular spaces using a blunt-ended syringe. Plants were grown in a greenhouse maintained at 23 - 25°C and infiltrated 3 - 4 weeks after the seedlings were pricked out. The first four mature leaves of each plant were selected for infiltration. Plant tissue was harvested 6 days post infiltration.

The fresh plant material was weighed (100 g leaves harvested from 60 plants) and added to phosphate buffer [100 mM sodium phosphate; Roche complete protease inhibitor tablet (EDTA free) as per manufacturer's instructions] (3 mL per gram of plant material) and homogenised in a blender. Large debris was removed by centrifugation at 15,000 x g for 14 minutes and the supernatant filtered through a 0.45 µm syringe filter. The volume of the clarified lysate was then reduced from 380 mL to 180 ml on a rotavapor at 15°C. The supernatant was purified using a 2 step sucrose cushion with 75 % and 25 % sucrose layers in ultracentrifuge tubes. The gradients were centrifuged at 240,000 x g for 2.5 hours at 4°C. The sucrose layers were collected and dialyzed against PBS and

analyzed by western blot. The VLP containing fractions were combined and extensively dialyzed (5 x 1 L) against ammonium bicarbonate (20 mM, pH 7.4). The fractions from the 75 % and 75-25 % interface of the sucrose gradient, containing most of the VLPs, were subjected to further purification on a sephacryl S500 column over 5 runs. The first chromatography run was eluted into PBS and all subsequent runs were eluted into 20 mM ammonium bicarbonate buffer pH 7.4. Samples were analysed using SDS-PAGE, western blot and TEM.

2.12.4 Expression of tandem core constructs in *Pichia pastoris*

For transformation, 40 mL overnight cultures of *Pichia pastoris* strain X33 or KM71H at an early-mid phase of exponential growth were pelleted by centrifugation at 3,000 rpm using rotor JA (Beckmann) and re-suspended in 1 ml YPDS-HEPES (YPDS [1 % (w/v) yeast extract, 2 % (w/v) peptone, 2 % (w/v) dextrose (D-glucose), 0.5 M sorbitol] + 20 mM HEPES-NaOH). The resulting cell suspension was transferred to a 1.5 mL microtube and 35 μ L 1 M DTT added with gentle swirling or inversion to mix. The cells were incubated at room temperature for 30 minutes and harvested by pulse centrifugation at 13,000 rpm. The resulting cell pellet was washed 6 times in 750 μ L 1 M sorbitol and re-suspended in a 'pellet volume' of 1 M sorbitol (80 - 200 μ L). For each transformation, 40 μ L of the cell suspension was mixed gently with 100 - 600 ng linearised plasmid DNA and incubated at room temperature for 15 minutes prior to electroporation using pre-chilled 2 mm gap electro-cuvettes at 2.0 kV in a Biorad *E. coli* Pulser electroporator. Immediately after electroporation, 1 mL YPDS was added, the cells transferred to clean 1.5 mL microtube and incubated for 1 hour at room temperature. The transformed cells (200 μ L) were spread onto YPDS + zeocin (100 μ g/mL) selective agar plates. A spread plate of 40 μ L untransformed cells was prepared as a selection control.

After 3 days incubation at 25°C, colonies were selected and re-streaked onto YPD + zeocin plates and incubated at 25°C for 3 days. Colonies were then picked for inoculation into 10 mL YPD medium in McCartney bottles which was termed the starter culture.

A 200 μ L aliquot of the starter culture was used to inoculate 200 mL BMGY (1 % (w/v) yeast extract, 2 % (w/v) peptone, 100 mM potassium phosphate, pH

6.0, 0.2 % (w/v) YNB, 4×10^{-5} % (w/v) biotin, 1 % (v/v) glycerol) in 500 mL conical flasks. Cultures were incubated in an orbital shaker at 180 rpm at 25°C for 3 days prior to harvesting of cells by centrifugation at 2000 x g for 4 minutes and transfer to 125 mL induction media (succinate/YNB). The cells were returned to a 500 mL conical flask, induced with 1 mL methanol and incubated with shaking as above. Cultures were supplemented with a further 1 mL methanol after 24 and 48 hr incubation.

After 72 hour induction, the cells were harvested by centrifugation as above. Supernatants were removed and the cells re-suspended in water and centrifuged at 2,000 x g for 3 minutes. The supernatant was discarded and cells re-suspended to a total of 11 mL in iQur lysis buffer (20 mM Tris-HCl pH 8.0, 5 mM EDTA, 5 mM DTT with protease inhibitor cocktail). Tubes were then vortex mixed at high speed for 30 min, rested on ice for 5 minutes and vortex mixed a further 30 minutes. Cell debris was removed by centrifugation at 2,000 x g for 3 minutes and the supernatant retained.

To remove small, non-assembled contaminants, the clarified supernatant was sequentially filtered through 0.45 µm and 0.2 µm disc filters prior to applying to a distilled water flushed Pellicon XL Ultrafiltration Module, Biomax 1,000 kDa device. The sample was initially concentrated to 10 mL, diluted with 40 mL 20 mM Tris-HCl pH 8.0 and re-concentrated to 10 mL. The crossflow filtered sample was then purified further by anion exchange chromatography.

2.12.5 Expression of monomeric VLP construct

Conjucore is a full length HBV core protein produced by collaborators at Mologic that was engineered to introduce 3 lysine residues in the antigenic loop. The insert was charge neutralised by 3 alternate aspartic acid residues (DKDKDK).

Conjucore was expressed in *P. pastoris* as previously described and initially purified by size exclusion chromatography after filtration. The elution profile was similar to that seen for equivalent Tandem CoreTM constructs. Negative stain TEM revealed the presence of correctly assembled VLPs. SDS PAGE and western blot analyses of purified, pooled fractions of VLPs confirm the identity of the purified protein and show reproducibly high levels of purity.

2.13 Production and analysis of conjugate vaccines

All conjugate vaccine production and analysis was performed by collaborators at John Innes Centre.

2.13.1 Conjugation of CPS antigen to selected protein or rVLP

CPS was oxidised according to Prof. Brett's procedure. Purified CPS was dissolved in 1 x PBS buffer at 5 mg/mL concentration and sodium periodate (NaIO_4) was added to give a final 28 mM concentration. The reaction mixture was vortexed until dissolution of NaIO_4 and then gently shaken for 3 hours at room temperature. To remove the excess NaIO_4 , the reaction mixture was dialysed against MilliQ water in a dialysis tube with a molecular weight cut-off of 6-8 KDa and lyophilised.

CPS was conjugated to proteins by reductive amination according to Assoc. Prof. Brett's procedure. Oxidised CPS and the chosen carrier protein were dissolved in 1 x PBS buffer to give a final concentration ranging from 0.2 to 6 mg/mL. Then, 10 μL of 1 M NaCNBH_3 solution in 10 mM NaOH was added for each mL of the reaction mixture, which was gently shaken at room temperature for 10 days. Afterwards, the reaction mixture was quenched by adding 10 μL of 1 M NaBH_4 solution in 10 mM NaOH for each mL of the reaction mixture with shaking at room temperature for 3 hours. The reaction mixture was dialysed against Milli-Q water in a dialysis tube with a molecular weight cut-off of 6-8 KDa and lyophilised. The products were analysed by gel electrophoresis, immunoblot and TEM, if applicable. Quantification of total heptose was carried out by phenol-sulphuric acid assay (Masuko 2005, Section 2.13.2). Total protein quantification was carried out by BCA assay (Section 2.13.3).

2.13.2 Phenol sulfuric acid analysis of CPS conjugate vaccines

150 μL of concentrated sulphuric acid was rapidly added to 50 μL of sample to cause maximum mixing. Immediately, 30 μL of 5 % (v/v) phenol in water was added and the plate incubated at 90°C for 5 minutes in a static water bath. The

plate was then allowed to cool to room temperature, wiped dry and absorbance measured at 490 nm (Masuko 2005).

2.13.3 BCA analysis of CPS conjugate vaccines

This method was performed by collaborators at the John Innes centre.

The BCA assay consists of two reagents. Reagent A was made of sodium bicinchoninate (0.1 g), $\text{Na}_2\text{CO}_3 \cdot \text{H}_2\text{O}$ (2.0 g), sodium tartrate (dihydrate) (0.16 g), NaOH (0.4 g) and NaHCO_3 (0.95 g), made up to 100 mL in water and pH adjusted to 11.25 with NaHCO_3 or NaOH. Reagent B was made of $\text{CuSO}_4 \cdot 5\text{H}_2\text{O}$ (0.4 g) in 10 mL of water. Standard working reagent (SWR) was then made by addition of 100 volumes of reagent A with 2 volumes of reagent B.

For analysis of protein content, 25 μL of each standard or unknown sample was pipetted into a microplate well. SWR was added to each well (200 μL) and mixed thoroughly on a plate shaker for 30 seconds. The plate was then covered and incubated at 37°C for 30 minutes. The plate was allowed to cool to room temperature and absorbance at 562 nm was measured.

2.14 Vaccine efficacy studies

2.14.1 Preparation of vaccines prior to administration

Vaccines for all studies were prepared on the morning of administration. The antigens were diluted to the required concentration in PBS and the adjuvant added as the final component and allowed to mix for at least 30 minutes prior at administration. The appropriate vaccines contained the following adjuvant amounts; Alhydrogel® - 15-18 %; Poly (I:C) - 30 μg per dose; AS04 - MPL 10 μg per dose, 18 % Alhydrogel®; and MF59 - 1:1 ratio to antigen volume.

2.14.2 Animal Husbandry

All animal investigations were performed in accordance with the Animal (Scientific Procedures) Act 1986.

Female BALB/c mice of approximately 6 weeks of age were caged together with free access to food and water and subjected to a 12 hour light/dark cycle. After challenge, all animals were handled under containment level III conditions within an isolator (BS5726).

2.14.3 Immunisation and challenge schedule

All animals were immunised via the intra-muscular or sub-cutaneous route according to the individual plans for each study with the exception of naïve controls where indicated. Animals were challenged intraperitoneally on day 63 with *B. pseudomallei* K96243 at a dose specified within the results chapter and monitored for signs of disease for 35 days and culled at pre-determined humane end-points. An illustration of the schedule for the vaccine efficacy studies is shown in Figure 8.

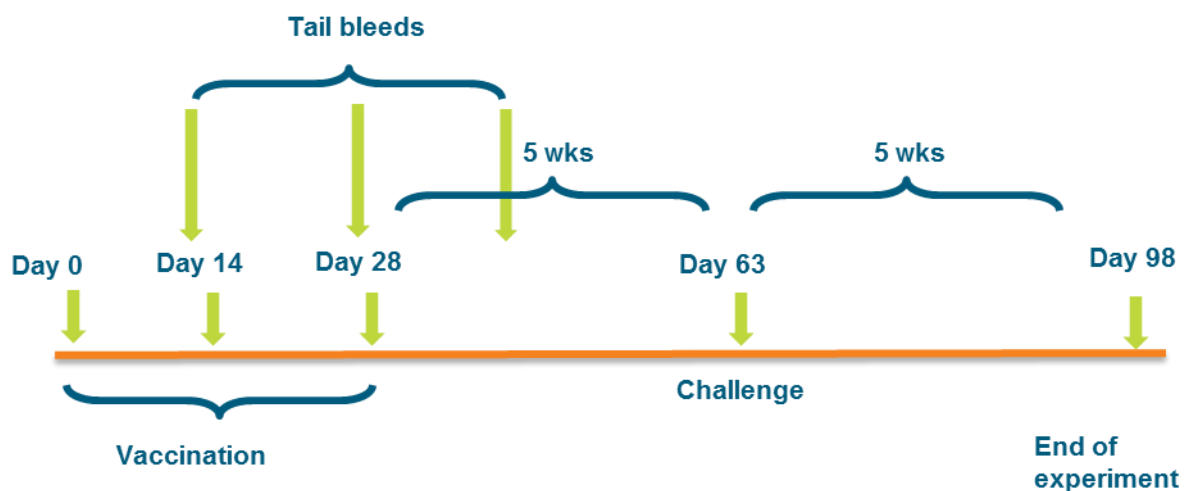


Figure 8 Vaccine efficacy study schedule

2.14.4 Intraperitoneal exposure of *B. pseudomallei* K96243

24 hours prior to use, 100 mL of LB broth (at room temperature) was inoculated with a loop of *B. pseudomallei* K96243 working stock in a 250 mL Erlenmeyer flask. This was incubated at 37°C, shaking at 180 rpm, for 24 hours. On the day of challenge, the *B. pseudomallei* culture was adjusted with LB media to OD_{590 nm} 0.4. The OD adjusted culture was diluted 1:10 to 10⁻⁷ in LB. The culture was vortexed between each dilution to ensure efficient mixing. The 10⁻⁵, 10⁻⁶ and 10⁻⁷ dilutions were plated onto 4 LB plates (250 µL per plate) and incubated at 37°C. The appropriate dilution was then diluted further with LB to get the required MLD challenge dose. For example; a target challenge dose of 300 x MLD = 2.23 x 10⁵ CFU per mouse. 1 MLD is approximately 744 CFU of *B. pseudomallei* K96243 (Dstl data). A bacterial culture with OD_{590 nm} 0.4 contains approximately 4 x 10⁸ CFU/mL. A 1:10 dilution of the 0.4 culture contains approximately 4 x 10⁷ CFU/mL. A further dilution of 1:17.9 would contain approximately 2.23 x 10⁶ CFU/mL. Each challenge dose (0.1 mL) would contain the target dose of 2.23 x 10⁵ CFU.

2.14.5 Statistical analysis

The statistical analysis used throughout the results chapters were performed using GraphPad Prism version 6.0.2 for Windows software (GraphPad Software, San Diego, USA).

The Mantel-Cox (Log rank) test was used to assess the significance of vaccine efficacy at the 95% confidence level.

2.14.6 Enumeration of bacterial loads

Mice surviving to day 35 post-challenge were humanely culled and the spleens, livers and lungs removed aseptically into 2 mL PBS. The organs were homogenised into 900 µL PBS using a sterile 40 µm disposable cell sieve and the barrel of a sterile syringe. A dilution series (10⁻¹ to 10⁻⁷) was prepared in 24 well-tissue culture plates (900 µL PBS per well with the addition of 100 µL of

sample) and 250 µL from each dilution (neat to 10⁻⁶) were plated onto LB agar. Plates were incubated for 48 hours at 37°C and the number of bacterial CFU was determined.

2.14.7 Determination of sera IgG and IgM antibody levels to antigen

2.14.7.1 Dose ranging ELISA of mouse sera (in order to determine dilution factors for sera samples)

ELISA plates were coated with purified antigen (10 µg/mL CPS or 5 µg/mL protein antigens) in PBS and incubated at 4°C overnight. During all incubations, the microtiter plates were covered with BIS Ltd microplate sealers (7740005). The plates were washed 3 times with 300 µL of PBS + 0.05 % (v/v) Tween 20 on a plate washer. The plate was blocked with 2 % (w/v) Blotto (200 µL/well), incubated at 37°C for 1 hour and washed 3 times with PBS + 0.05 % (v/v) Tween 20. Mouse sera (neat concentration) was added to the plate (100 µL/well) and diluted 1:2 across the plate in 2 % (w/v) Blotto. IgG or IgM standards were diluted in 2 % Blotto to a starting concentration of 100 ng/mL, added to the plate at 100 µL/well and diluted 1:2 across the plate. The plate was incubated for 1 hour at 37°C and washed 3 times with 300 µL of PBS + 0.05 % (v/v) Tween 20. Goat anti-mouse IgG-HRP or IgM-HRP conjugate was diluted 1:2000 in 2 % (w/v) Blotto and 100 µL added to each well. The plate was incubated for 1 hour at 37°C and washed 6 times with 300 µL of PBS + 0.05 % (v/v) Tween 20. 100 µL of TMB (3,3',5,5'-tetramethylbenzidine) was then added at all wells and the colour developed. Absorbance was read at 620 nm on a Labsystems, Multiskan Ascent spectrophotometer. The dilution factor which gave an OD value closest to 1 was used in the analysis of the samples.

2.14.7.2 ELISA IgG and IgM analysis of mouse sera samples

Plates were coated with purified antigen (10 µg/mL CPS or 5 µg/mL protein antigens) in PBS and incubated at 4°C overnight. During all incubations, the microtiter plates were covered with BIS Ltd microplate sealers (7740005).

The plates were washed 3 times with 300 μ L of PBS + 0.05 % (v/v) Tween 20 on a plate washer. The plate was blocked with 200 μ L/well of 2 % (w/v) Blotto, incubated at 37°C for 1 hour, then washed 3 times with PBS + 0.05 % (v/v) Tween 20. Mouse sera was diluted in 2 % (w/v) Blotto at the dilution indicated from the dose ranging ELISA. IgG or IgM standards were diluted in 2 % (w/v) Blotto to a starting concentration of 100 ng/mL. These standards and sera samples were added to the plate, in duplicate, at 100 μ L per well and diluted 1:2 across the plate. The plate was then incubated for 1 hour at 37°C and washed 3 times with 300 μ L of PBS + 0.05 % Tween 20 (v/v). Goat anti-mouse IgG-HRP or IgM-HRP conjugate was diluted 1:2000 in 2 % (w/v) Blotto and 100 μ L added to each well. The plate was then incubated for 1 hour at 37°C and washed 6 times with 300 μ L of PBS + 0.05 % Tween 20. 100 μ L of TMB (3,3',5,5'-tetramethylbenzidine) was then added at all wells and the colour developed. Absorbance was read at 620 nm on a Labsystems, Multiskan Ascent spectrophotometer.

2.14.8 IFN- γ Enzyme Linked Immuno-spot assay (ELISPOT)

Splenocytes were isolated by maceration of individual spleens in 5 mL of RPMI1640 medium (Life Technologies) supplemented with 10 % (v/v) Foetal Bovine Serum, non-essential amino acids - final concentration of 100 μ M glycine, L-alanine, L-asparagine, L-aspartic acid, L-glutamic acid, L-proline and L-serine (Life Technologies), 50 μ M final concentration 2-mercaptoethanol (Life Technologies), 100 U/mL penicillin and 100 mg/mL streptomycin sulphate (Life Technologies) and passage through a 40 μ m cell sieve. The isolated splenocytes were diluted to 2.5×10^6 cells/mL in supplemented RPMI1640 medium. These were incubated in the presence of medium alone, antigen or mitogen (Concanavalin-A) at 37°C in a 5 % CO₂ atmosphere using 96-well PVDF ELISPOT plates pre-coated with an IFN- γ capture antibody (Mabtech). Following a 20 hour incubation period, development of IFN- γ spots was performed using a commercially available murine IFN- γ ELISPOT kit (Mabtech). Spot enumeration was performed using an AID automated reader.

Chapter 3: *Burkholderia capsular polysaccharide*

3.1 Introduction

An important factor in the development of a vaccine is cost of production (Kaper *et al.*, 2013). One of the technical challenges in developing a *B. pseudomallei* vaccine is the cost of extracting *B. pseudomallei* CPS in containment level 3 laboratories. This requires the use of specialised facilities and the handling of agent within class III microbiological cabinets and is laborious and time consuming in comparison to working at lower levels of containment. Local procedures may also be in place which limit the amount of organism grown in a single culture or restrict the use of certain techniques such as freeze-drying to reduce risk in case of an accident. Depending on efficacy and protective duration, this may make a vaccine prohibitively expensive, especially for civilian use in the areas of the world where melioidosis is endemic (Peacock *et al.*, 2012).

The aim of this chapter is to address the issue of cost with three objectives. The first was to determine the structural similarity of CPS extracted from *B. thailandensis* E555 to that from *B. pseudomallei*. This built on previous work from Sim *et al.* 2010 where *B. thailandensis* E555 CPS was shown to cross-react with an anti *B. pseudomallei* CPS monoclonal antibody. As *B. thailandensis* can be handled in lower levels of containment, extraction of the CPS would be quicker, safer and cheaper.

The second objective was to optimise purified CPS extraction by improving yield or reducing the time taken to extract CPS. This chapter focussed on improving yield by increasing the amount of CPS in the bacterial culture and therefore the amount available for extraction. This was investigated by altering growth conditions which included aeration and the use of different media with the hypothesis that improved growth would improve CPS expression. It is known that different carbon sources can effect polysaccharide expression (Yuksekdag and Aslim 2008, Audy *et al.*, 2010), and so the addition of mannose to the microbiological growth media was assessed. The addition of iron sulfate was also assessed following demonstration of improved *B. pseudomallei* growth

(Wang-Ngarm *et al.*, 2014). This work, however, required the development of a method to quantify changes in CPS concentration. Reducing the time taken to extract CPS focussed on quantification of CPS in culture supernatant as it is known that bacteria shed their CPS into the environment (Joiner 1988). Identification of sufficient quantities of CPS in the supernatant may reduce the number of purification steps required and therefore time and may also increase purity of the starting material due to the absence of bacterial cells and proteins.

The use of CPS is not without disadvantages. These include the inability to generate known chain-lengths. This is known to affect conjugate vaccine efficacy, and so is an important variable to control in polysaccharide conjugate vaccine development (Carmenate *et al.*, 2004, Rana *et al.*, 2015). The use of native-length chains of CPS may also make difficult the separation of free polysaccharide from conjugated polysaccharide. This is also known to affect vaccine efficacy (Rodriguez *et al.*, 1998) and should be within limits shown to be clinically safe and efficacious according to the World Health Organisation recommendations for production and control of pneumococcal and meningococcal conjugate vaccines (WHO TRS 927 2005, 924 2004). One solution to these problems would be chemical synthesis of the polysaccharide, which may also lower cost of production. However, this is technically challenging due to the position of the acetyl group on the CPS molecule.

The final objective of this chapter was to investigate further the work by Marchetti *et al.* (2015), which suggests the importance of this acetyl group to antibody recognition, and confirm the importance of the acetyl moiety on CPS immunogenicity and protective efficacy. The focus of this work started with sequencing of the variable regions of the heavy and light chain of four Dstl anti-CPS antibodies in order to determine major amino acid differences. The binding of these antibodies against deacetylated CPS was then assessed. Finally, antibody cross-reactivity to CPS and de-acetylated CPS from mice immunized with a CPS conjugate and de-acetylated CPS conjugate was assessed as part of a vaccine efficacy study performed by a Dstl colleague.

3.2 Extraction of CPS from *B. pseudomallei* K96243 and *B. thailandensis* E555

The isolation of native *Burkholderia* CPS was a challenging process with the purity and yield of material lower than expected compared to reports of 10-15 mg of CPS per litre of bacterial culture (Burtnick *et al.*, 2012).

Initial attempts at CPS extraction were performed on *B. pseudomallei* strain K96243 and *B. thailandensis* strain E555 by the ethanol precipitation method with cells grown on solid media (Chapter 2, Method 2.5.3). The *B. thailandensis* E555 strain used in this study, provided by Andy Scott, Dstl, was previously modified by the insertion of a kanamycin resistance marker cassette (Km^r) into gene *wbil*; this genetic modification results in a loss of production of the lipopolysaccharide (LPS) O-antigen (*B. thailandensis* E555 :: *wbil* (Km^r)).

The cells were grown on solid media and an ethanol extraction method used previously described for *B. pseudomallei* CPS by George, 2013. Ethanol precipitation is also used in the production of several polysaccharide vaccines (Plotkin *et al.*, 2013). CPS extracts from *B. thailandensis* E555 :: *wbil* (Km^r) and *B. pseudomallei* strain K96243 were analysed by NMR by collaborators at the John Innes Centre (JIC) and shown to be of insufficient purity for VLP conjugation as the characteristic CPS spectra could not be identified.

A phenol-based extraction method on liquid cultures for isolation of *B. pseudomallei* CPS has been reported (Perry *et al.*, 1995, Heiss *et al.*, 2012). Dstl use a phenol-based method to extract lipopolysaccharide. Therefore this method was employed for extraction of CPS utilising *B. thailandensis* E555 :: *wbil* (Km^r) cultured using both liquid and solid media and *B. pseudomallei* K96243 cultured using solid media only (Chapter 2, Method 2.5.4). NMR analysis failed to confirm the presence of CPS in extracted material with a number of unidentified contaminants. The NMR analysis was negative for CPS from *B. pseudomallei* extracts. Therefore, it was concluded that the problem lay with the extraction method, rather than that *B. thailandensis* E555 did not produce CPS.

Subsequently, and via discussion with Assoc. Prof. Brett, two differences between the Dstl methodology and the published methodology from Assoc. Prof. Brett's lab (Heiss *et al.*, 2012) were identified:

1. Live cells were used for extractions in Brett's method whereas in Dstl's method, cells were first heat-killed at 80°C for 4 hours.
2. The phenol and culture mixture was maintained at 80°C in Brett's method rather than 60°C at Dstl.

Whilst changes were made to risk assessments at Dstl in order to carry out the extraction with these different conditions, a stock of *B. thailandensis* E555 :: *wbil* (Km^r) was sent to Matt Donaldson, (JIC) who could perform the modified hot-phenol extraction immediately, with a small amount of CPS purified from *B. pseudomallei* strain 1026b for use as a comparison in NMR analysis supplied from Assoc. Prof. Brett (Chapter 2, Method 2.5.5).

NMR analysis of the extracted material at the JIC from live *B. thailandensis* grown in liquid media confirmed the presence of CPS in comparison to the reference *B. pseudomallei* 1026b CPS. In conjunction with monosaccharide analysis performed at JIC (Chapter 2, Method 2.5.6), these results confirm that *B. thailandensis* CPS is structurally identical to that of CPS from *B. pseudomallei* strain 1026b (Figure 9 and Figure 10). This permits the use of *B. thailandensis* E555 as a source of CPS in future studies.

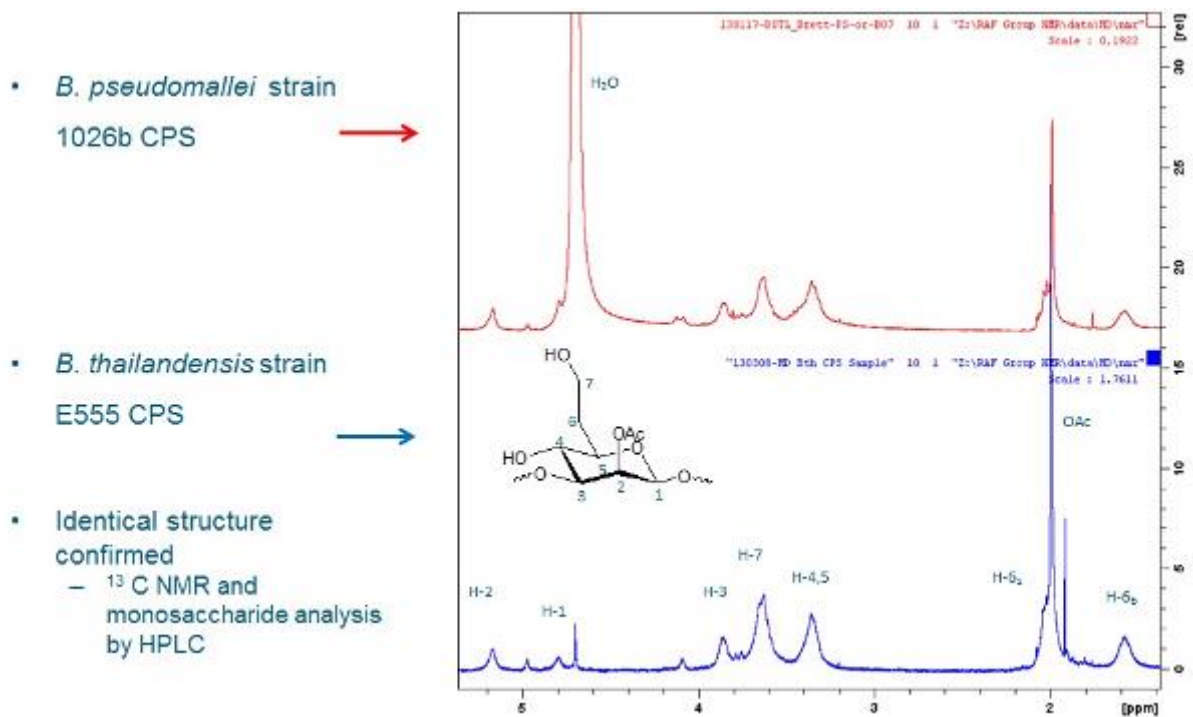


Figure 9 NMR spectra of CPS isolated from *B. thailandensis* E555 :: *wbil* (Km^r) (Bottom) with reference to purified CPS from *B. pseudomallei* 1026b (Top). The structure of CPS is illustrated with proton positions.

(Water is present in the sample from *B. pseudomallei* because the proton NMR was run without NOESY)

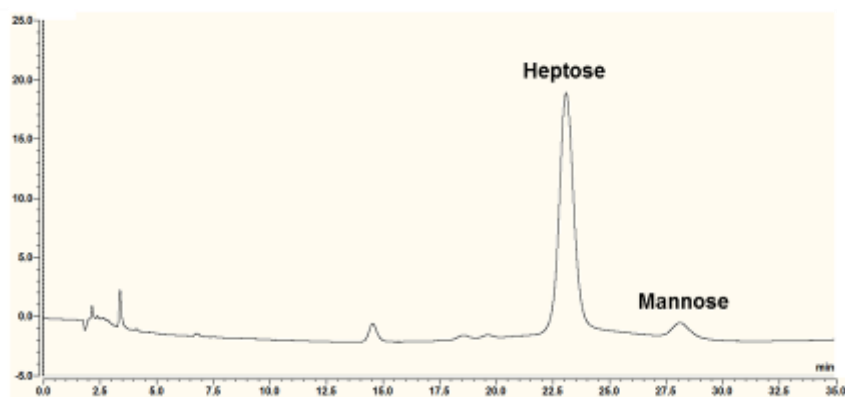


Figure 10 Monosaccharide analysis of fully hydrolysed *B. thailandensis* E555 :: *wbil* (Km^r) CPS polysaccharide

This result was also confirmed with subsequent NMR analysis of CPS extracted from *B. thailandensis* E555 :: *wbil* (Km^r) grown in liquid media at Dstl. In addition, the modified phenol method was employed on killed *B. thailandensis* E555 :: *wbil* (Km^r) grown on solid media, killed *B. pseudomallei* K96243 grown on solid media and killed *B. pseudomallei* 1026b grown in liquid media. Both of

the *B. pseudomallei* samples and the sample from solid media grown *B. thailandensis* E555 :: *wbil* (Km^r) were determined to be of insufficient purity by NMR (Figure 11). This demonstrates that use of live bacterial cultures grown in liquid media and maintaining the phenol extraction at 80°C is essential for extraction of CPS.

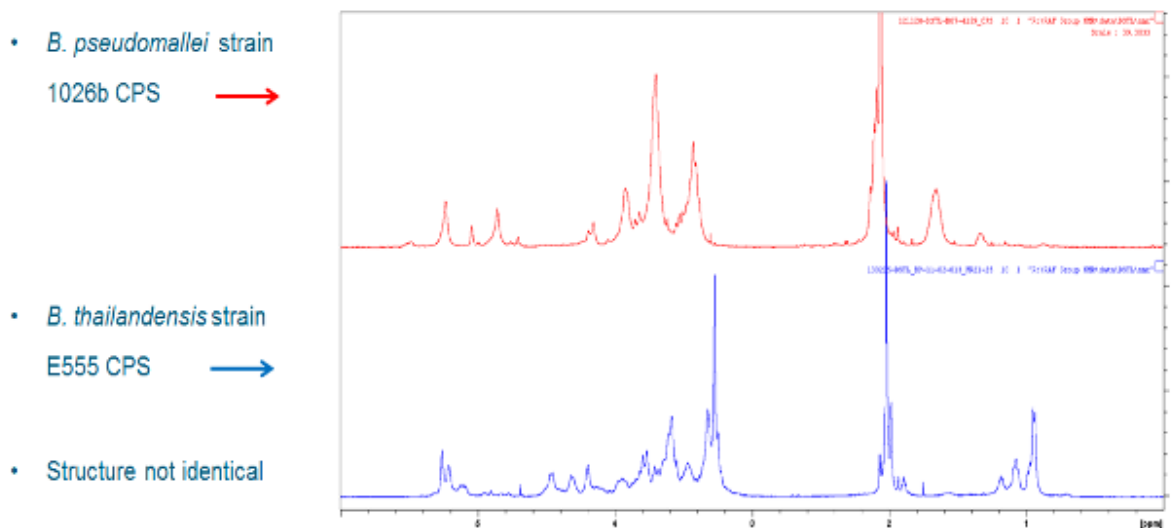


Figure 11 NMR spectra of phenol extract from heat-killed *B. thailandensis* E555 :: *wbil* (Km^r) sample (Bottom) with reference to purified CPS from *B. pseudomallei* 1026b (Top).

Following successful extraction of CPS from *B. thailandensis* E555, an acceptance criteria was adopted for use of this material which stated that the CPS be detectable by NMR and that spectra are in agreement with the reference sample (*B. pseudomallei* 1026b CPS from Assoc. Prof. Brett).

Several CPS extractions have been completed employing Assoc. Prof. Brett's phenol method with *B. thailandensis* E555 :: *wbil* (Km^r) cultured in LB broth. While purity of the CPS final product has remained consistently around 85 percent, yields have varied from 0.5 mg to 18 mg per litre of bacterial culture. Yield differences are considered a result of biological variation in bacterial growth, and therefore CPS expression, and batch-to-batch variation in extraction efficiency.

While the second objective of this work was to optimise CPS expression, previous studies have determined that CPS production by *B. pseudomallei* was increased if grown on Brain Heart Infusion media (BHI) containing 5 % (v/v)

glycerol (Kawahara *et al.*, 1998). To produce a stock of CPS for use in conjugation reactions, an extraction was performed from *B. thailandensis* E555 :: *wbil* (Km^r) cultured in 2 L Brain Heart Infusion (BHI) broth with a resultant yield of 19.9 mg. NMR analysis at JIC showed the presence of an unidentified contaminant (Figure 12) which has not been detected in CPS extracted from LB media cultures. Therefore, the use of BHI broth for culture of *B. thailandensis* E555 :: *wbil* (Km^r) prior to CPS extraction was discontinued.

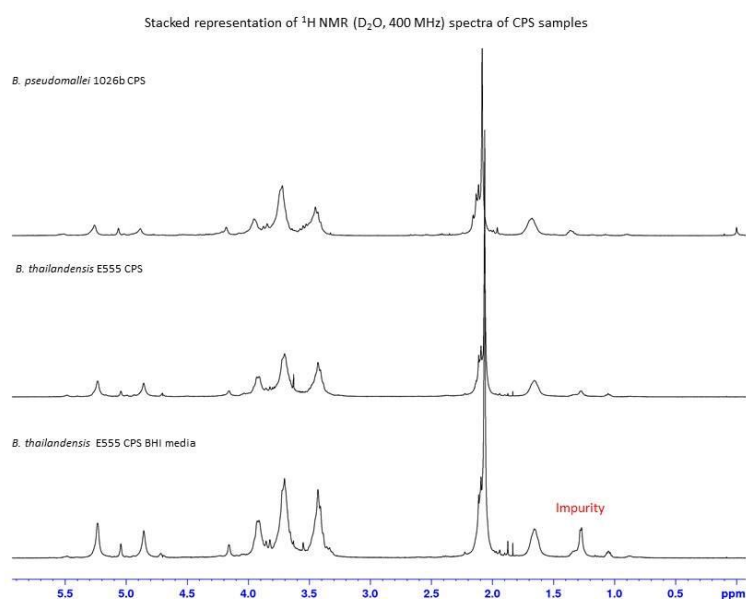


Figure 12 Stacked NMR spectra for CPS obtained from *B. pseudomallei* 1026b (Top), *B. thailandensis* E555 :: *wbil* (Km^r) cultured in LB media (Middle) and *B. thailandensis* E555 :: *wbil* (Kmr) cultured in BHI media (Bottom).

3.3 Development of a quantitative CPS ELISA

In order to optimise CPS production in *B. thailandensis* E555 :: *wbil* (Km^r) cultures, a method to rapidly quantitate capsular polysaccharide concentration in live cultures was developed as phenol extraction of CPS requires approximately 5 weeks to complete. It was considered that an antibody-based method would be suitable. Therefore a dot blot method was compared to an ELISA to assess detection of purified CPS bound directly to the membrane or

microtiter plate (Chapter 2, Method 2.6.1 and 2.6.2). Starting at a *B. pseudomallei* 1026b CPS concentration of 100 µg/mL, it was determined that the detection limits of both the dot blot and ELISA were acceptable. The provisional limit of detection was calculated to be approximately 780 ng/mL and 48 pg/mL for the dot blot and ELISA respectively (Figure 13 and Figure 14). Due to the increased sensitivity and advantages in reproducibility and quantification, the ELISA method was employed in all further optimisation experiments.

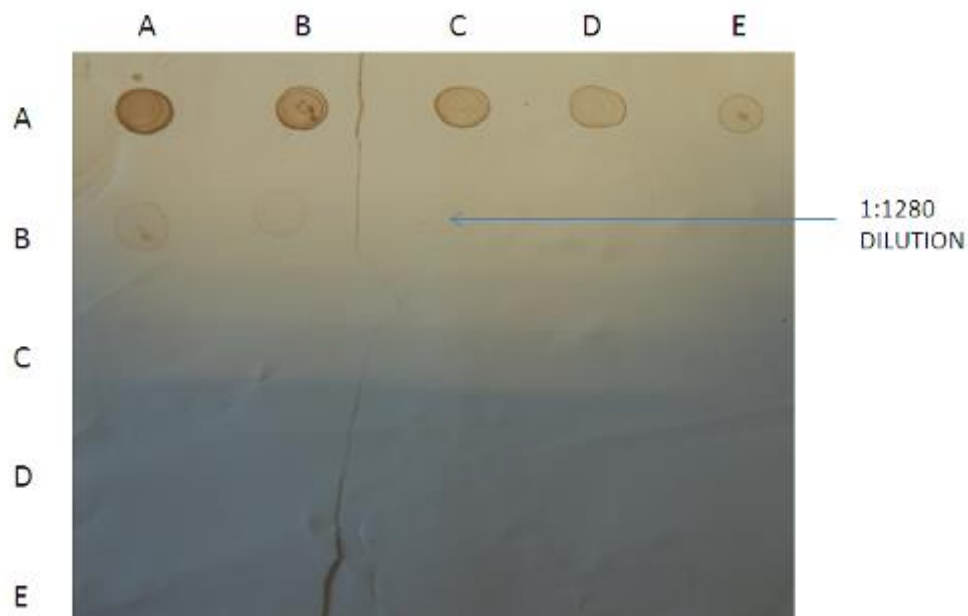


Figure 13 Dot-blot for detection of purified CPS with the anti-CPS monoclonal antibody **DSTL189**. CPS at a concentration of 100 µg/mL was serially diluted 1:2 and blotted onto the membrane, probed with antibody DSTL189 and detected with goat anti-mouse IgG-Alkaline phosphatase (ALP). The limit of detection (LOD) is determined at the last concentration with a visible blot, 781.3 ng/mL (1:1280 dilution).

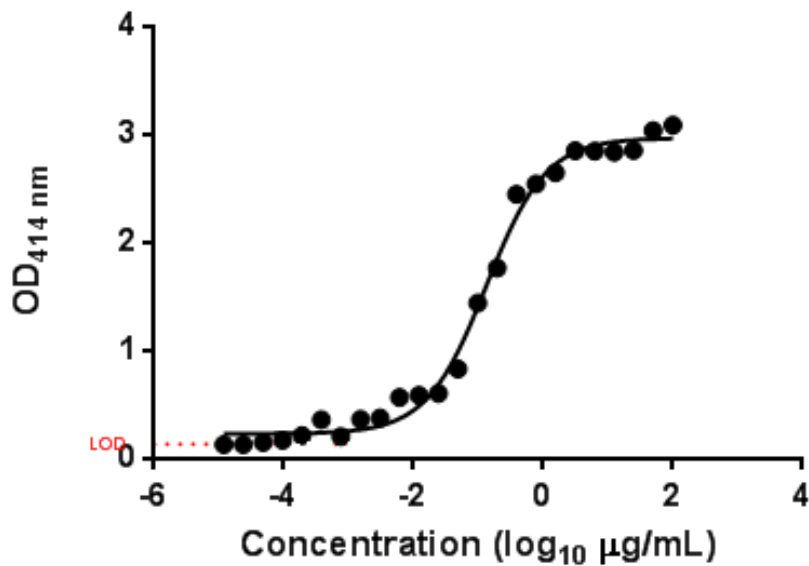


Figure 14 Detection of purified CPS by ELISA. CPS was diluted 1:2 from a starting concentration of 100 µg/mL (single value for each concentration). Detection is with the anti-CPS monoclonal DSTL189 and goat anti-mouse IgG-horse radish peroxidase (HRP). The limit of detection (LOD) illustrated is calculated from the mean OD plus 3 SD of four replicates of a blank. The limit of detection is calculated to be 48 pg/mL.

To further develop the ELISA for CPS quantification, a capture ELISA was produced. Capture ELISA's are considered to have greater specificity and sensitivity due to the reduced variability in binding of antigen to a capture antibody in comparison to binding of antigen to a microtitre plate surface. Dstl has an anti-CPS monoclonal antibody (DSTL189), which was used for both capture and detection purposes. This required biotinylation of the DSTL189 detection antibody as an anti-species monoclonal could not be used for detection when an antibody derived from the target animal spp. is used for detection and capture (Chapter 2 Method 2.6.3). Before a sandwich ELISA could be developed, the binding of biotinylated DSTL189 with streptavidin peroxidase to CPS bound directly to the microtiter plate was assessed. In the same study, different molar coupling ratios of biotin to DSTL189 were compared to determine whether biotin impaired the ability of DSTL189 to recognise CPS (Chapter 2, Method 2.6.4). The results demonstrated that biotinylation was suitable for use with the detection antibody (Figure 15). The OD readings from all molar coupling ratios were acceptable. While the OD readings for MCR of x20 and x30 were slightly higher than x10 across all antibody concentrations, non-linear regression analysis showed that the dose-response curve at x10

MCR had a greater R squared value (0.9996) than x20 or x30 MCR (0.9993 and 0.9986 respectively).

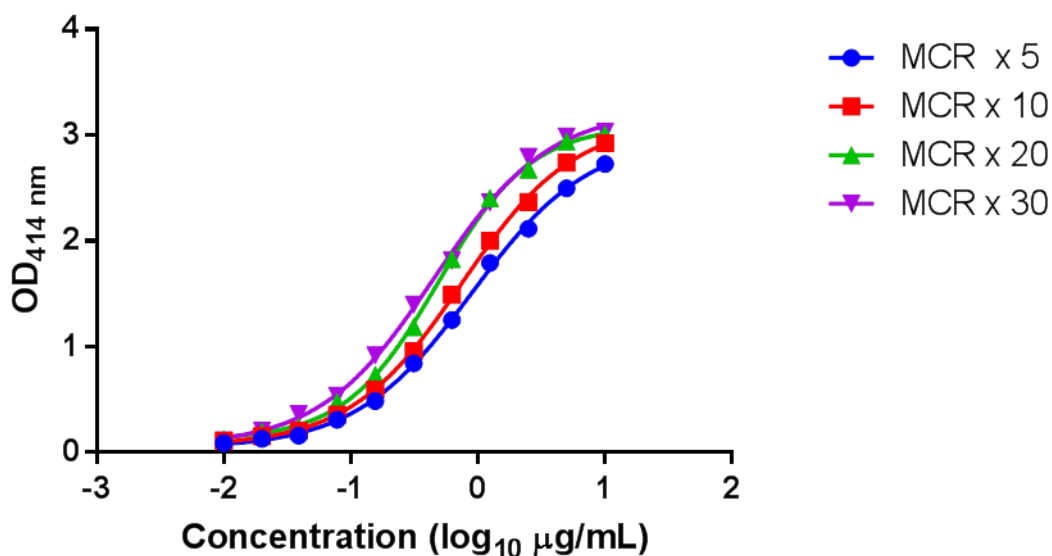


Figure 15 ELISA to assess recognition of purified CPS with biotinylated DSTL189 monoclonal antibody at different molar coupling ratios. A microtiter plate was coated with CPS (10 µg/mL). Biotinylated DSTL189 antibody was added at molar coupling ratios of x5, x10, x20 or x30 of biotin and diluted 1:2 across the plate followed by streptavidin peroxidase (1:1000 dilution).

To generate and optimise a standard curve for the capture ELISA, purified CPS, from *B. pseudomallei* 1026b, supplied by Prof. Paul Brett at Alabama University, with a stated purity of 95% was used. The purpose of this experiment (Chapter 2, Method 2.6.5) was to assess the assay with a lower concentration of capture and detection antibody of 5 µg/mL rather than 10 µg/mL, as with the biotinylation comparison; to assess CPS concentrations to generate the standard curve across the top 2 rows of a microtiter plate; and finally to assess OD variability across microtiter plates. A starting CPS concentration of 10, 5 and 1.25 µg/mL was diluted 1:2, in duplicate, with the resultant OD values (Figure 16) plotted as a single curve against log-transformed concentration and analysed by non-linear regression (Figure 17) The OD values were variable across microtiter plates, as demonstrated by the standard deviation, but showed the lower antibody concentration suitable and a maximum starting concentration of 1.25 mg/mL CPS. The variability in OD values was also shown by a decrease in the R square value to 0.8704 for the collated data curve, whereas a curve generated from the first microtiter plate (data not shown) had an R square value of 0.9923.

Measurement count: 1 Filter: 414											Blank	
	1	2	3	4	5	6	7	8	9	10	11	12
A	1.68	1.55	1.424	1.36	1.246	0.927	0.858	0.757	0.574	0.477	0.064	0.065
B	1.49	1.514	1.322	1.297	1.253	1.076	0.852	0.756	0.511	0.427	0.062	0.064
C	0.48	0.331	0.217	0.169	0.127	0.097	0.082	0.086	0.077	0.073	0.063	0.067
D	0.438	0.314	0.221	0.164	0.123	0.095	0.086	0.079	0.074	0.072	0.063	0.063
Starting CPS concentration of 10µg/mL												
Measurement count: 1 Filter: 414											Blank	
	1	2	3	4	5	6	7	8	9	10	11	12
A	1.222	1.273	1.324	1.158	1.076	1.076	0.861	0.738	0.598	0.51	0.499	0.074
B	1.214	1.188	1.278	1.058	1.025	0.971	0.91	0.777	0.576	0.503	0.422	0.073
Starting CPS concentration of 5ug/mL												
Measurement count: 1 Filter: 414											Blank	
	1	2	3	4	5	6	7	8	9	10	11	12
A	1.517	1.536	1.384	1.196	1.363	1.154	1.038	0.837	0.688	0.481	0.416	0.075
B	1.422	1.377	1.311	1.165	1.288	1.188	0.958	0.762	0.713	0.494	0.354	0.08
Starting CPS concentration of 5ug/mL												
Measurement count: 1 Filter: 414											Blank	
	1	2	3	4	5	6	7	8	9	10	11	12
A	1.537	1.868	1.811	1.611	1.439	1.3	1.039	0.774	0.588	0.394	0.34	0.13
B	1.461	1.662	1.799	1.451	1.413	1.189	0.917	0.707	0.538	0.392	0.29	0.129
Starting CPS concentration of 1.25ug/mL												
Measurement count: 1 Filter: 414											Blank	
	1	2	3	4	5	6	7	8	9	10	11	12
A	1.57	1.439	1.387	1.049	0.747	0.471	0.322	0.197	0.136	0.098	0.087	0.074
B	1.551	1.452	1.352	0.96	0.79	0.485	0.287	0.176	0.129	0.097	0.085	0.076
Starting CPS concentration of 1.25ug/mL												
Measurement count: 1 Filter: 414											Blank	
	1	2	3	4	5	6	7	8	9	10	11	12
A	1.043	1.679	1.593	1.355	1.282	1.261	1.216	0.997	0.835	0.642	0.48	0.077
B	1.005	1.457	1.358	1.22	0.971	1.117	1.138	1.01	0.833	0.643	0.462	0.072
C	0.305	0.237	0.152	0.112	0.09							0.073
D	0.279	0.214	0.141	0.108	0.093							0.074
Starting CPS concentration of 5ug/mL												
Measurement count: 1 Filter: 414											Blank	
	1	2	3	4	5	6	7	8	9	10	11	12
A	0.979	1.493	1.327	1.176	1.005	1.115	0.974	0.921	0.809	0.673	0.535	0.075
B	0.992	1.35	1.243	1.003	1.022	0.93	0.747	0.75	0.623	0.611	0.501	0.074
C	0.363	0.243	0.165	0.123	0.106							0.082
D	0.371	0.277	0.171	0.128	0.102							0.074
Starting CPS concentration of 5ug/mL												
Measurement count: 1 Filter: 414											Blank	
	1	2	3	4	5	6	7	8	9	10	11	12
A	1.686	1.673	1.599	1.495	1.561	1.208	1.1	0.937	0.868	0.64	0.475	0.073
B	1.598	1.628	1.522	1.419	1.466	1.078	1.036	0.926	0.736	0.642	0.59	0.073
C	0.403	0.264	0.179	0.133	0.105							0.079
D	0.41	0.323	0.179	0.143	0.106							0.072
Starting CPS concentration of 5ug/mL												
Purified CPS standard curve												
Negative control												

Figure 16 OD values from CPS capture ELISA with purified *B. pseudomallei* 1026b. Eight microtiter plates were coated with DSTL189 antibody at 5 µg/mL, CPS added to wells A1 and B1 at 10, 5 or 1.25 µg/mL and diluted 1:2 across each plate. For plates with rows A-D, diluted sample from well A10 and B10 was diluted 1:2 into wells C1 and D1 and further diluted across the plate. Biotinylated DSTL189 antibody was added at 5 µg/mL followed by streptavidin at 1:1000 dilution and ABTS.

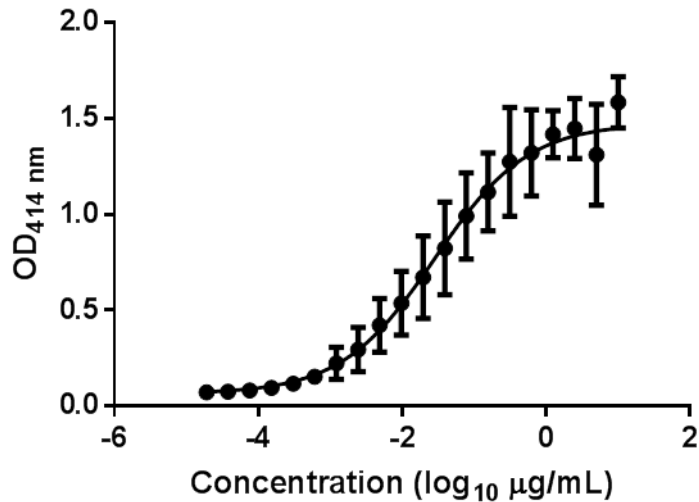


Figure 17 Purified *B. pseudomallei* 1026b CPS ELISA standard curve generated from OD values in Figure 16 and plotted against log-transformed CPS concentration. Data represent the mean +SD of two independent experiments at 10 µg/mL, 10 independent experiments at 5 and 2.5 µg/mL, and 16 independent experiments for all other concentrations.

As stated, CPS purified from *B. pseudomallei* 1026b (CPS supplied by Prof. Paul Brett at Alabama University) was used to generate standard curves. Once the structure of the CPS produced from *B. thailandensis* E555 :: *wbil* (Km^r) was confirmed by NMR to be identical to that produced by *B. pseudomallei* the source of material was changed. The *B. pseudomallei* derived anti-CPS monoclonal antibody (DSTL189) was used to compare the two CPS molecules (Chapter 2, Method 2.6.6). These data suggested that the two CPS molecules were immunologically indistinguishable (Figure 18).

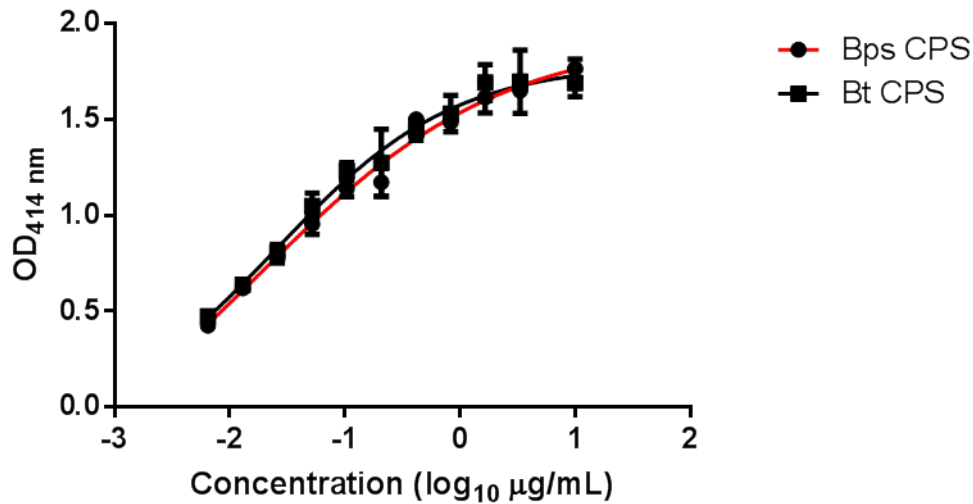


Figure 18 Comparison of antibody recognition to CPS extracted from *B. pseudomallei* and *B. thailandensis*. ELISA plates were coated with DSTL189 monoclonal antibody and purified *B. pseudomallei* (Bps CPS) and *B. thailandensis* E555 :: *wbil* (Km^r) CPS (Bt CPS) over a concentration range of 10 µg/ml to 0.007 µg/mL. There is no significant difference between the data sets (P 0.3434, Extra sum of squares F test). Data represent the mean +SD of 2 independent experiments.

To further develop the standard curve with purified CPS from *B. thailandensis* E555 :: *wbil* (Km^r), a further batch of biotinylated DSTL189 monoclonal antibody was produced. This provided sufficient quantities to determine a limit of detection (LOD), upper and lower limit of quantification (ULOQ, LLOQ) and for all future CPS optimisation work.

Before a LOD, ULOQ and LLOQ were determined, the suitability of the ELISA to measure *B. thailandensis* E555 :: *wbil* (Km^r) culture CPS concentration was investigated (Chapter 2, Method 2.6.7). *B. thailandensis* E555 :: *wbil* (Km^r) was cultured overnight at 37°C, a sample added in duplicate at 5.4 x 10⁸ CFU/mL and diluted 1:2 across the plate. Purified CPS was added to the plate to further develop the standard curve. This showed that the maximum CPS concentration could be reduced and that the ELISA could detect changes in *B. thailandensis* E555 :: *wbil* (Km^r), although only from a dilution of approximately 1:128 (Figure 19).

Measurement count: 1 Filter: 414		1	2	3	4	5	6	7	8	9	10	11	Blank	12
No changes in OD values between these concentrations	A	1.537	1.868	1.811	1.611	1.439	1.3	1.039	0.774	0.588	0.394	0.34	0.13	
	B	1.461	1.662	1.799	1.451	1.413	1.189	0.917	0.707	0.538	0.392	0.29	0.129	
	C	2.484	2.771	2.886	2.841	2.825	2.86	2.707	2.387	2.211	1.718	1.241	0.13	
	D	2.68	2.662	2.754	2.88	2.745	2.686	2.716	2.309	2.144	1.674	1.021	0.128	
	E	0.758	0.444	0.324	0.241	0.189	0.163	0.157	0.197	0.149	0.155	0.145	0.13	
	F	0.754	0.46	0.286	0.213	0.177	0.166	0.163	0.189	0.159	0.15	0.145	0.129	
	G	0.142	0.137	0.136	0.134	0.14	0.136	0.137	0.138	0.137	0.133	0.134	0.127	
	H	0.148	0.138	0.125	0.137	0.135	0.14	0.136	0.136	0.13	0.133	0.133	0.119	
		Purified CPS standard curve												
		Bt E555 :: <i>wbil</i>												
		Negative control												

Figure 19 ELISA results of *B. thailandensis* E555 :: *wbil* (Km^r) culture CPS concentration.

A microtiter plate coated with anti-CPS antibody DSTL189 was incubated with *B. thailandensis* E555 :: *wbil* (Km^r) at an initial culture concentration of 5.4×10^8 CFU/mL in wells C1 and D1 and diluted 1:2 across the plate. Samples from column 11 were diluted 1:2 into E1 and F1 and the dilution continued across the plate. Purified CPS was added to rows A and B for standard curve development starting at a concentration of 1.25 µg/mL and diluted 1:2 across the plate.

While assessment of the ELISA utilised *B. thailandensis* E555 :: *wbil* (Km^r), as the O-antigen mutant of *B. thailandensis* was to be used for CPS extraction, the same experiment was also performed with wild-type *B. thailandensis* E555 and the results were similar (data not shown).

Determination of the LOD required OD values of a negative to be obtained. It was decided that the CPS-negative *B. thailandensis* CDC2721121 (Sim *et al.*, 2010) would be appropriate. *B. thailandensis* CDC2721121 was incubated overnight at 37°C, a neat culture sample added in duplicate to the plate and diluted 1:2 across the plate. *B. thailandensis* E555 :: *wbil* (Km^r) was also added to the plate as a positive control, purified CPS added for development of the standard curve and 2 % milk powder in PBS added as the negative control (Chapter 2, Method 2.6.8). The mean OD values of both the negative control and the *B. thailandensis* CDC2721121 culture were 0.068 confirming that *B. thailandensis* CDC2721121 is CPS negative and suitable for use as the negative control in the CPS ELISA (Figure 20). In combination with the previous experiment, it also confirmed that the starting concentration of the purified CPS be reduced to approximately 100 ng/mL.

Measurement count: 1 Filter: 414												
	1	2	3	4	5	6	7	8	9	10	11	12
A	1.823	1.648	1.465	0.992	0.617	0.414	0.252	0.158	0.118	0.101	0.088	0.067
B	1.904	1.793	1.542	1.057	0.774	0.433	0.235	0.14	0.108	0.084	0.077	0.069
C	2.916	2.457	1.585	1.005	0.451	0.282	0.209	0.136	0.105	0.088	0.082	0.07
D	2.777	2.226	1.582	0.919	0.514	0.361	0.211	0.129	0.106	0.089	0.085	0.069
E	0.076	0.072	0.071	0.066	0.067	0.069	0.064	0.068	0.07	0.067	0.069	0.067
F	0.081	0.072	0.074	0.076	0.075	0.068	0.066	0.065	0.068	0.066	0.065	0.067
G	0.073	0.066	0.068	0.088	0.065	0.066	0.068	0.069	0.067	0.077	0.067	0.066
H	0.071	0.063	0.066	0.07	0.067	0.073	0.07	0.067	0.071	0.067	0.064	0.068
	Purified CPS											
	<i>B. t</i> E555 :: <i>wbil</i>											
	<i>B. t</i> CDC2721121											
	Blank											

B. thailandensis
 CDC2721121 is CPS
 negative

Figure 20 ELISA to determine suitability of *B. thailandensis* CDC2721121 as the negative control for CPS ELISA development. A microtiter plate coated with anti-CPS antibody DSTL189 was incubated with *B. thailandensis* CDC2721121 neat culture in wells E7 and F7 and diluted 1:2 across the plate. Samples from wells E11 and F11 were diluted 1:2 into wells G1 and H1 and further diluted across the plate to column 12. A neat culture sample of *B. thailandensis* E555 :: *wbil* (Km^r) was added as the positive control in wells C1 and D1 and diluted 1:2 across the plate. Samples from column 11 were diluted 1:2 into E1 and F1 and the dilution continued across the plate to wells E6 and F6. Purified CPS was added to rows A and B for standard curve development starting at a concentration of 1 $\mu\text{g/mL}$ and diluted 1:2 across the plate. 2 % milk powder in PBS was added to wells in column 12 as the blank.

As a back-up for *B. thailandensis* CDC2721121 as the negative control, *B. thailandensis* E264 was also analysed and was shown to have the same mean OD values as the negative control (data not shown).

To calculate a limit of detection (LOD) for the ELISA, 134 individual samples of CPS-negative *B. thailandensis* strain CDC2721121 were analysed, initially over a concentration range of approximately 10^8 CFU/mL to 1 CFU/mL with later samples at 10^8 CFU/mL to 10^5 CFU/mL (Chapter 2, Method 2.6.8). The OD values ($n=1492$) were collated into a single dataset (Figure 21) and a mean optical density ($OD_{414 \text{ nm}}$) plus three standard deviations was calculated to be 0.127.

With an OD value of 0.127 obtained from the *B. thailandensis* CDC2721121 negative control, the next step in determining the LOD of the CPS ELISA was to generate OD values with purified CPS. 144 samples of purified CPS were analysed over a concentration range of 100 ng/mL to 98 pg/mL (Chapter 2, Method 2.6.10). The mean OD value of 0.127 from the negative control was compared against the mean OD of each CPS concentration. The LOD was determined as the lowest CPS concentration with an OD value greater than the negative value (Table 3). From this a LOD of 391 pg/mL was calculated.

	CPS conc (µg/mL)	Mean	%CV	n
	0.1	1.348913	18.78763	144
	0.05	1.234948	18.83721	144
	0.025	1.01401	21.47754	144
	0.0125	0.776406	22.2718	144
	0.00625	0.562427	21.88934	144
	0.003125	0.38984	20.84562	144
	0.001371742	0.274576	17.75797	144
	0.00078125	0.197681	16.37003	144
LOD	0.000390625	0.14967	13.67689	144
	0.000195313	0.120135	12.00453	144
	9.76563E-05	0.102836	11.09981	143

Table 3 Calculation of CPS ELISA limit of detection from purified CPS mean OD values. 144 samples of *B. thailandensis* E555 :: *wbil* (Km^r) purified CPS at a concentration of 100 ng/mL to 98 pg/mL were analysed by ELISA. (Individual values not shown). A LOD of 391 pg/mL was calculated as the lowest CPS concentration with a mean OD value greater than 0.127 (the mean OD value from the negative control *B. thailandensis* CDC2721121). % coefficient of variance was calculated to measure deviation from the mean.

To calculate upper and lower limits of quantification (ULOQ/LLOQ), 30 replicates of purified *B. thailandensis* E555 :: *wbil* (Km^r) CPS were analysed over a concentration range of 100 ng/mL to 98 pg/mL (Chapter 2, Method 2.6.11). Limits of quantification were determined as the CPS concentrations where the accuracy of the mean reported concentrations from the standard curve was within 20 % of the known concentration and the coefficient of variance (% CV) was less than 20. This gave upper and lower limits of 25 ng/mL and 0.4 ng/mL respectively. Figure 22 illustrates the LOD and LOQs calculated and a typical standard curve generated by this ELISA following optimisation.

Table 4 is a summary of the data used to calculate the limits of quantification.

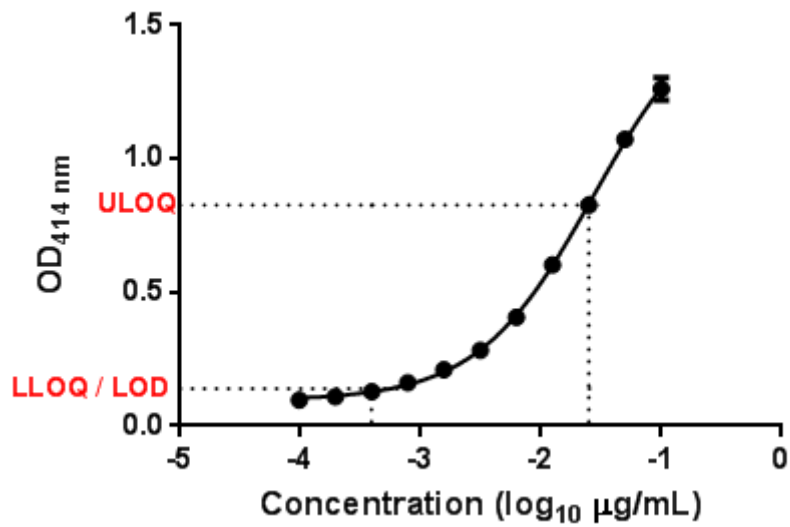


Figure 22 Typical standard curve generated from ELISA results of CPS purified from *B. thailandensis* E555 :: *wbil* (Km^r). Illustrated is the Upper Limit of Quantification (ULOQ) and Lower limit of quantification (LLOQ) determined from analysis of 28 samples of purified CPS where the calculated concentrations were accurate to within 20 % of the known concentration and the % CV was less than or equal to 20. Error bars = SD. n=2 at each concentration.

Expected concentration (ng/mL)	Mean calculated concentration (ng/mL)	% Coefficient of Variance	% accuracy	n
100	88.18	34	88	30
50	54.33	48	109	30
25	23.65	20	95	30
12.5	12.15	15	97	30
6.25	6.32	13	101	30
3.13	3.21	13	103	30
1.56	1.82	15	116	30
0.78	0.90	11	115	30
0.39	0.42	13	107	30
0.20	0.19	47	98	29
0.10	0.06	56	66	21

Table 4 Summary of purified *B. thailandensis* E555 :: *wbil* (Km^r) CPS concentration data used to calculate ELISA upper and lower limits of quantification (ULIQ / LLOQ). Known concentrations of CPS were analysed by ELISA with the OD values interpolated from the standard curve (data not shown) to give the mean calculated concentration. The %CV was calculated from all reported concentrations and the accuracy to the expected concentration (% accuracy) calculated from the mean calculated concentrations. Highlighted in red are the data that fall within the criteria of % CV ≤20 and % accuracy within 80-120 %, giving an upper limit of quantification of 25 ng/mL and a lower limit of 0.39 ng/mL

Following development of this ELISA, it was now possible to achieve quantification of CPS production from crude cultures grown over 24-48 hrs in contrast to requiring samples from a full CPS extraction process which takes several weeks.

3.4 CPS expression optimisation – growth

With a final method to quantify changes in CPS concentration available (Chapter 2, Method 2.7), optimisation of CPS expression was attempted by increasing the growth of *B. thailandensis* E555 :: *wbil* (Km^r) in culture.

Utilising set incubation conditions of 37°C and a shaking speed of 180 rpm, the amount of CPS produced ($\mu\text{g/mL}$), colony forming units (CFU/mL) and optical density ($\text{OD}_{590 \text{ nm}}$) during growth of the bacteria from 17 – 72 hours after inoculation with a glycerol stock was measured (Chapter 2, Method 2.7). A maximum CPS concentration of 34.6 $\mu\text{g/mL}$ was measured 72 hours after inoculation (Table 5). Measurement of CPS concentration at 0, 3, and 6 hours after inoculation were measured in a previous experiment and shown to be negligible (data not shown).

Incubation time after inoculation (Hrs)	$\text{OD}_{590 \text{ nm}}$	CFU/mL	Bacterial culture CPS concentration ($\mu\text{g/mL}$)
17	1.67	1.64E+09	7.6
18	1.76	1.94E+09	8.3
19	1.81	2.24E+09	9.0
20	1.93	2.54E+09	10.5
21	1.93	3.09E+09	14.6
22	2.00	3.52E+09	16.2
23	>2.00	3.40E+09	14.4
24	>2.00	4.38E+09	15.3
25	>2.00	4.03E+09	15.1
26	>2.00	4.33E+09	15.7
27	>2.00	4.56E+09	14.4
42	>2.00	2.09E+10	26.8
48	>2.00	2.21E+10	32.5
66	>2.00	2.95E+10	32.4
72	>2.00	3.56E+10	34.6

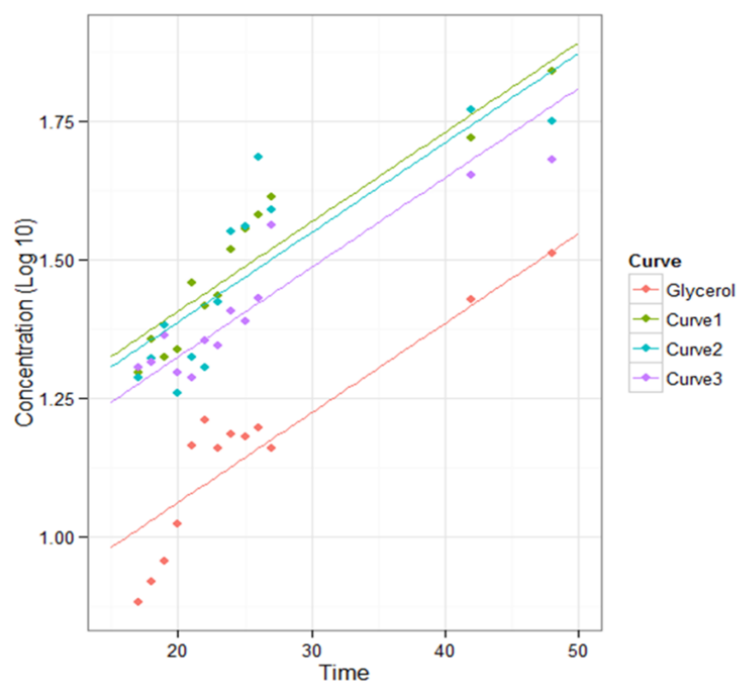
Table 5 Measurement of *B. thailandensis* E555 :: *wbil* (Km^r) bacterial culture CPS concentration ($\mu\text{g/mL}$), $\text{OD}_{590 \text{ nm}}$ and CFU/mL, 17-72 hours after inoculation of LB media from a glycerol stock.

To boost CPS concentration, the experiment was repeated but with three cultures that were inoculated with a *B. thailandensis* E555 :: *wbil* (Km^r) starter culture rather than glycerol stock. The starter culture was inoculated with a glycerol stock of *B. thailandensis* E555 :: *wbil* (Km^r) and incubated for 24 hours at 37°C, shaking at 180 rpm. A 500 μL aliquot of this culture was then

inoculated into 50 mL of LB media and incubated for 48 hours at 37°C, shaking at 180 rpm. CPS concentration and colony forming units were measured hourly from 17 – 27 hours, and at 42 and 48 hours after inoculation (Chapter 2, Method 2.7.2). Mean CPS concentration was at a maximum 48 hours after inoculation (57.7 µg/mL Table 6). At maximum CPS concentration for both test conditions, cultures were in stationary phase with CFU greater than 1 x 10¹⁰/mL. Figure 23 illustrates the measured CPS concentration (µg/mL) for the culture inoculated with the glycerol stock and the three bacterial cultures inoculated with a starter culture. Due to time constraints while optimisation work is being performed and to give the greatest chance of detecting differences in CPS concentration, future samples were taken at 20, 24 and 27 hours after inoculation. For all future optimisation work, a subbed culture will be also be used.

Incubation time after inoculation (Hrs)	Average CFU/mL	Average bacterial culture CPS concentration (µg/mL)
17	6.25E+09	19.8
18	6.55E+09	21.4
19	7.73E+09	22.8
20	8.21E+09	19.9
21	9.32E+09	23.0
22	9.31E+09	23.0
23	1.00E+10	25.3
24	1.00E+10	31.3
25	1.24E+10	32.2
26	1.44E+10	37.8
27	1.61E+10	38.8
42	2.03E+10	52.0
48	2.04E+10	57.7

Table 6 Average CPS concentration (µg/mL) and CFU/mL of three *B. thailandensis* E555 :: *wbiI* (Km^r) bacterial cultures, 17-72 hours after inoculation of LB media from a starter culture.



	Estimate	2.50%	97.50%	Std. Error	t value	Pr(> t)	
(Intercept)	0.738	0.667	0.809	0.036	20.419	< 2e-16	***
Time	0.016	0.014	0.018	0.001	13.922	< 2e-16	***
Curve1	0.345	0.288	0.402	0.029	11.829	1.08E-15	***
Curve2	0.326	0.269	0.383	0.029	11.175	7.87E-15	***
Curve3	0.263	0.205	0.320	0.029	9.006	8.38E-12	***

Figure 23 Comparison of glycerol stock to starter culture inoculate on *B. thailandensis* E555 :: *wbil* (Km^r) culture CPS concentration LB microbiological growth media was inoculated with a glycerol stock or starter culture of *B. thailandensis* E555 :: *wbil* (Km^r) and incubated for 50 hours at 37°C, shaking at 180 rpm. *** p ≤ 0.001

Following determination of incubation time following inoculation and the use of a subbed culture, CPS concentration and CFU/mL by *B. thailandensis* E555 :: *wbil* (Km^r) was then assessed in triplicate in four different microbiological growth medias; LB, M9 minimal media, Tryptone soya broth and Enhanced phytone peptone at 20, 24 and 27 hours after inoculation at 37°C, shaking at 180 rpm (Chapter 2, Method 2.7.3). LB is the standard media for CPS extraction. M9 media is a defined media with the potential to provide CPS with increased purity. Tryptone soya broth and enhanced phytone peptone media are complex media with the potential to significantly increase bacterial growth.

Changing growth media results in a statistically significant difference in culture CPS concentration compared to LB (Figure 24A). CPS concentration was lowest in M9 minimal media (3.7 µg/mL at 27 hr) and highest in enhanced

phytone peptone broth (58.7 $\mu\text{g/mL}$ at 27 hr). The increase in CPS with enhanced phytone peptone broth when compared to LB broth results from increased expression per CFU rather than an increase in bacterial biomass (Figure 24B&C). The enhanced phytone peptone broth will be used for future CPS production with LB broth used as a comparator.

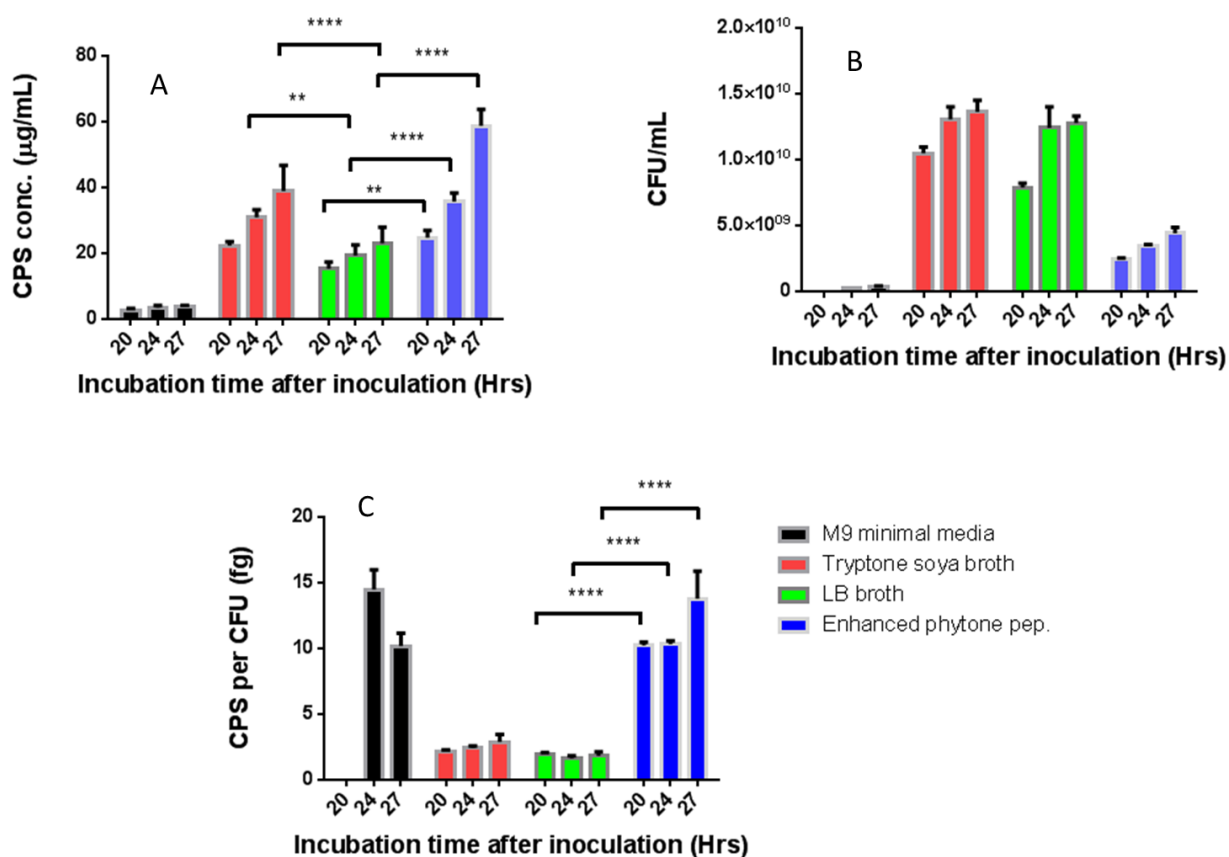


Figure 24 Effect of different microbiological growth media on *B. thailandensis* E555 :: *wbil* (Km^r) growth and CPS expression. An aliquot of a *B. thailandensis* E555 :: *wbil* (Km^r) starter culture was inoculated into four different microbiological media and culture samples analysed at 20, 24 and 27 hours after inoculation for CPS expression (A), CFU/mL (B), and CPS per CFU (C) Each value represents the mean +SD of three independent experiments. ** $p \leq 0.01$ **** $p \leq 0.0001$.

To investigate the impact of increased aeration on *B. thailandensis* E555 :: *wbil* (Km^r) culture CPS concentration, baffled Erlenmeyer flasks were used compared to non-baffled Erlenmeyer flasks (Chapter 2, Method 2.7.4). Utilising LB media, culture CPS concentration and CFU/mL were measured at 20, 24 and 27 hours after inoculation. As illustrated in Figure 25, baffled flasks did significantly increase culture CPS concentration from an average of 29.1 to 40.7 $\mu\text{g/mL}$ 27 hrs after inoculation (Figure 25A). This is explained by the significant

increase in CFU/mL rather than increased expression of CPS per CFU (Figure 25B and C).

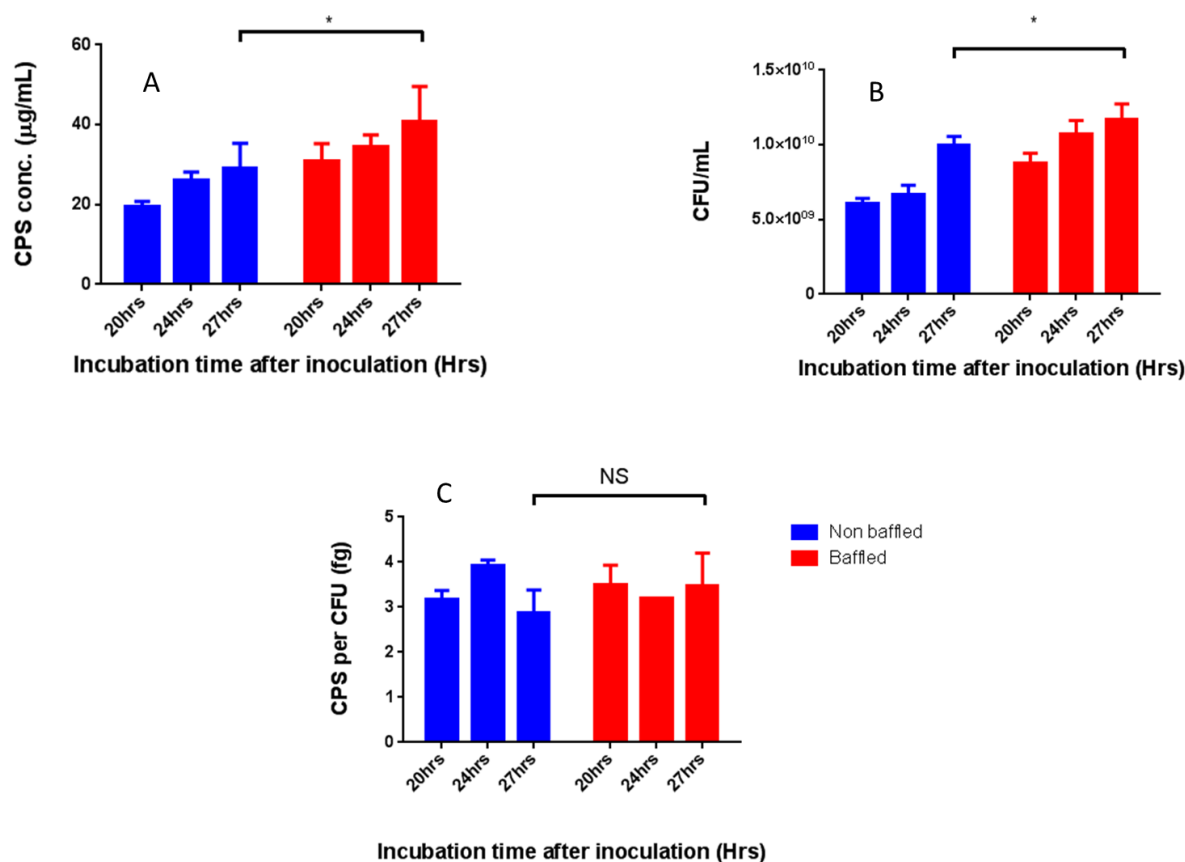


Figure 25 Effect of baffled Erlenmeyer flasks on *B. thailandensis* E555 :: *wbil* (Km^r) growth and CPS expression inoculated into LB media. An aliquot of a *B. thailandensis* E555 :: *wbil* (Km^r) starter culture was inoculated into baffled and non-baffled Erlenmeyer flasks containing LB media and culture samples analysed at 20, 24 and 27 hours after inoculation for CPS expression (A), CFU/mL (B), and CPS per CFU (C) Each value represents the mean +SD of three independent experiments. * $p \leq 0.05$, NS = no statistical significance (two-way RM ANOVA).

The effect of baffled Erlenmeyer flasks with enhanced phytone peptone broth on *B. thailandensis* E555 :: *wbil* (Km^r) culture CPS concentration was compared to non-baffled Erlenmeyer flasks. Culture CPS concentration (µg/mL) and CFU/mL were measured at 20, 24 and 27 hours after inoculation. CPS concentration was significantly increased at 24 and 27 hours ($p \leq 0.001$ and $p \leq 0.0001$ respectively) when compared to non-baffled flasks (Figure 26A). This was a result of a significant increase in both CFU/mL and the amount of CPS per CFU produced (Figure 26B and C).

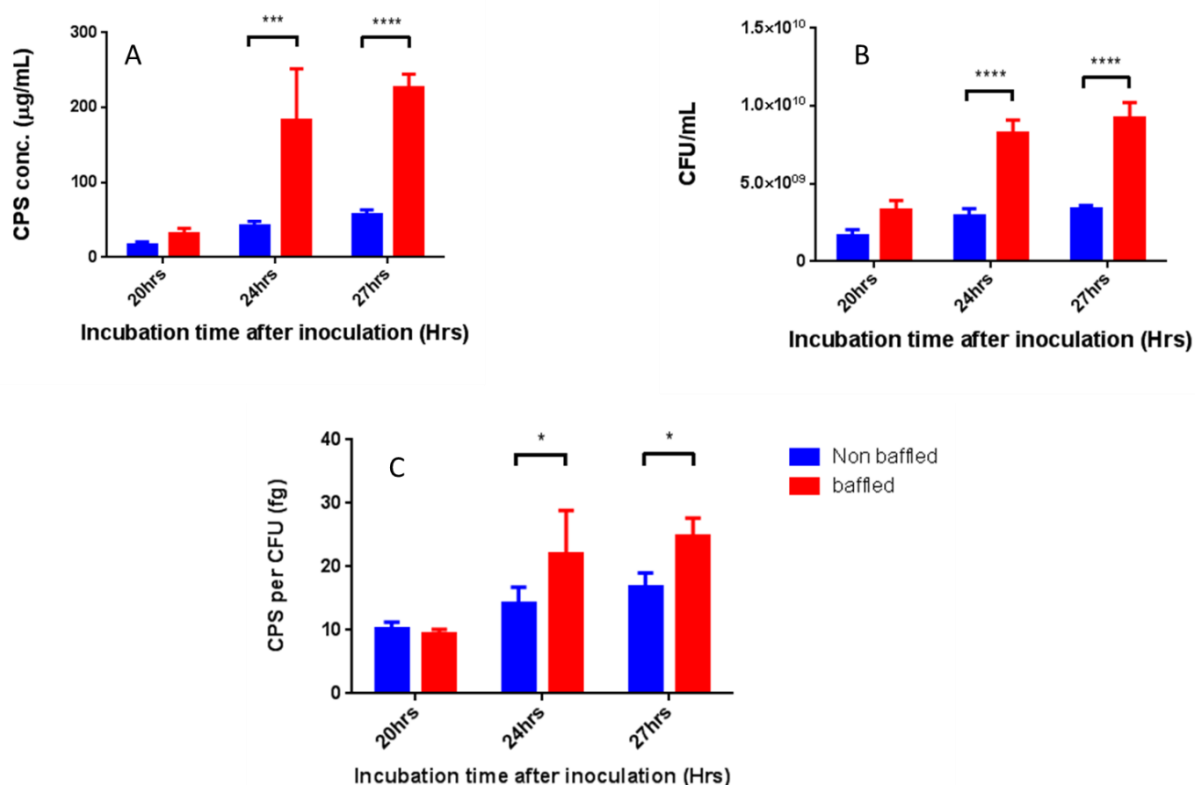


Figure 26 Effect of baffled Erlenmeyer flasks on *B. thailandensis* E555 :: *wbiI* (Km^r) growth and CPS expression inoculated into enhanced phytone peptone broth. An aliquot of a *B. thailandensis* E555 :: *wbiI* (Km^r) starter culture was inoculated into baffled and non-baffled Erlenmeyer flasks containing enhanced phytone peptone broth and culture samples analysed at 20, 24 and 27 hours after inoculation for CPS expression (A), CFU/mL (B), and CPS per CFU (C) Each value represents the mean +SD of three independent experiments. * $p \leq 0.05$, *** $p \leq 0.001$, **** $p \leq 0.0001$ (two-way RM ANOVA)

B. pseudomallei growth is significantly enhanced by increasing iron concentration (Wang-Ngarm *et al.*, 2014). The addition of 50 µM, 0.5 mM and 5 mM iron sulfate to enhanced phytone peptone broth (Chapter 2, Method 2.7.5) did not significantly increase CPS culture concentration ($p=0.3066$, Figure 27A). However, a significant increase in colony forming units (CFU/mL) was seen with 5 mM iron sulfate at 24 and 27 hours ($p \leq 0.05$, Figure 27B). There was a corresponding decrease in the amount of CPS per CFU with 5 mM at iron sulfate at 24 and 27 hours, but this was not statistically significant ($p=0.0762$, Figure 27C).

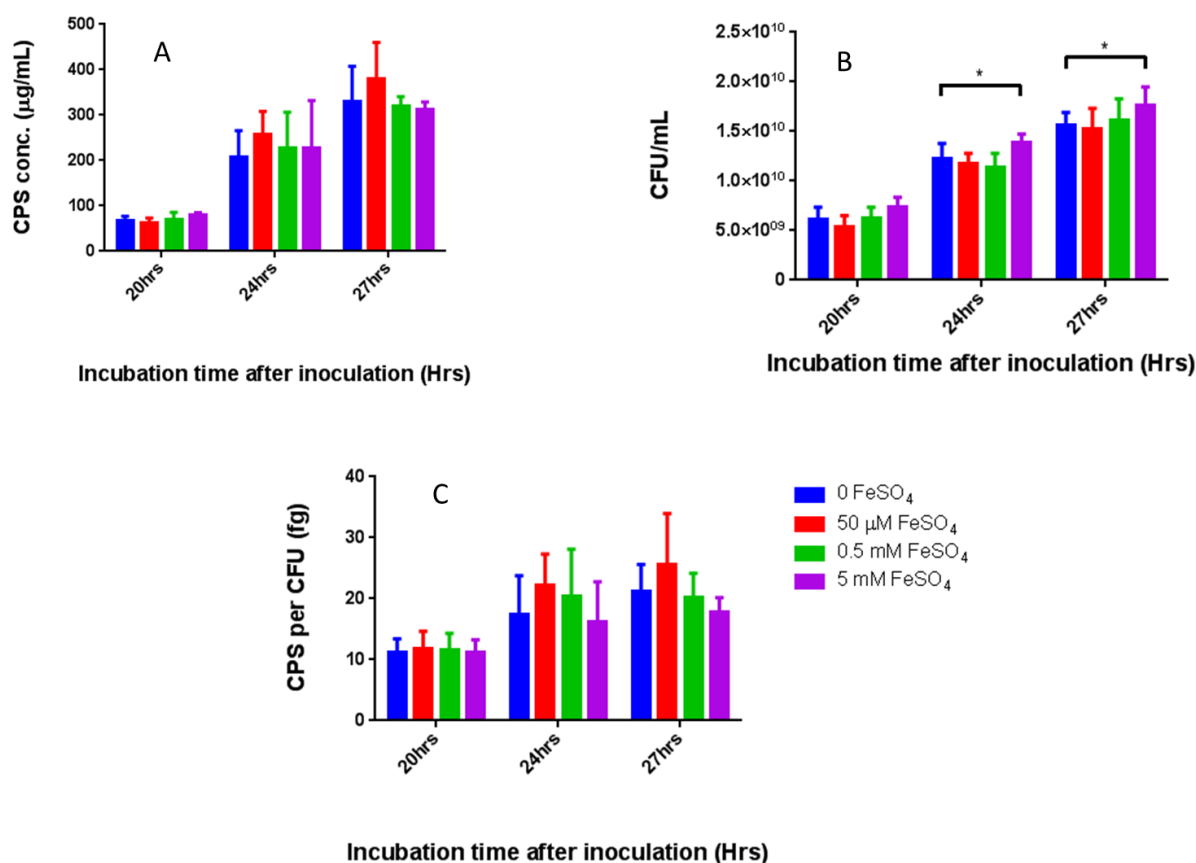


Figure 27 Effect of iron sulfate on *B. thailandensis* E555 :: *wbil* (Km^r) growth and CPS expression. An aliquot of a *B. thailandensis* E555 :: *wbil* (Km^r) starter culture was inoculated into enhanced phytone peptone broth with 50 μM, 0.5 mM or 5 mM FeSO₄ and culture samples analysed at 20, 24 and 27 hours after inoculation for CPS expression (A), CFU/mL (B), and CPS per CFU (C). Each value represents the mean +SD of three independent experiments. * p<0.05 (two-way RM ANOVA).

Other procedures assessed for effect on CPS culture concentration included decreasing the volume of culture media in the 250 mL flask from 50 mL to 25 mL in order to further improve aeration (Chapter 2, Method 2.7.6) and the addition of 2.5 g/L mannose to the culture media to act as an additional carbon source (Chapter 2, Method 2.7.7). Reducing the volume of media did not result in a significant increase in CPS culture concentration, CFU/mL and subsequently CPS per CFU; (Figure 28A, B and C).

The addition of mannose to LB media appeared to slightly decrease the amount of culture CPS concentration but statistically significance was not achieved

(Figure 29A). No statistically significant effects were seen on CFU/mL or CPS per CFU (Figure 29B and C).

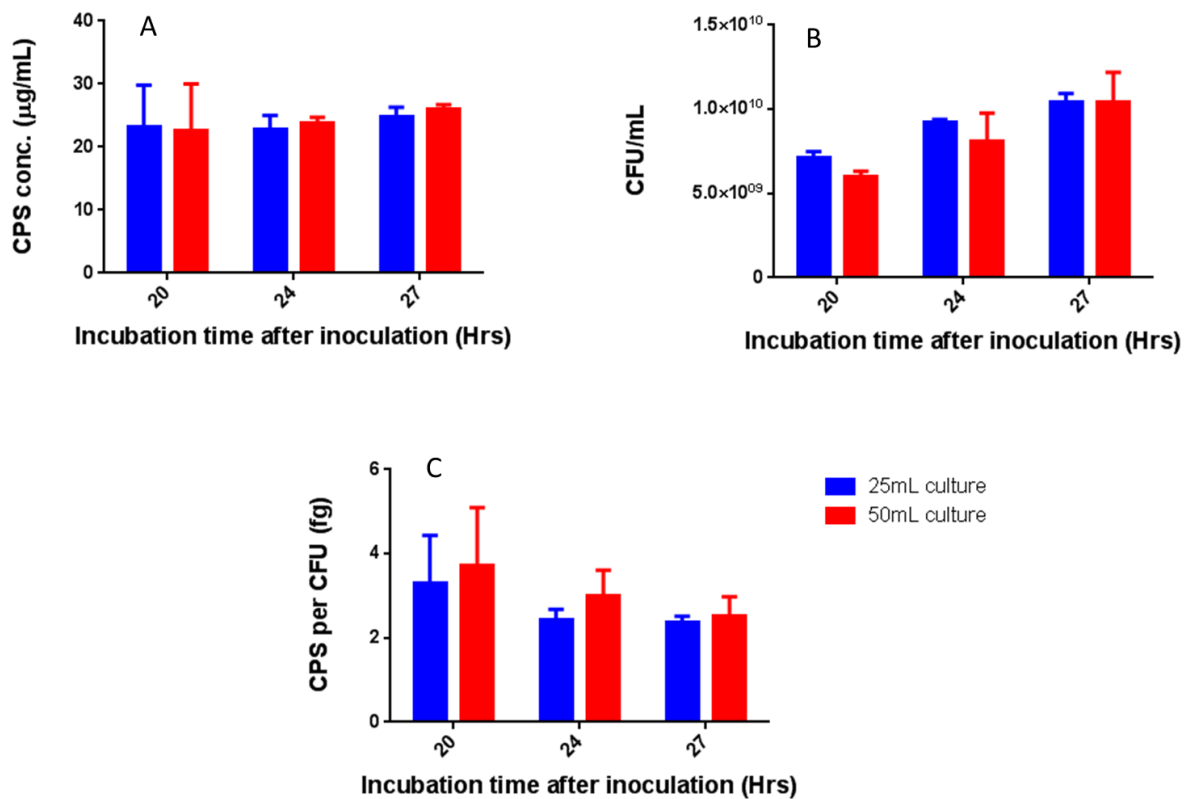


Figure 28 Effect of reducing culture volume on *B. thailandensis* E555 :: *wbil* (Km^r) growth and CPS expression An aliquot of a *B. thailandensis* E555 :: *wbil* (Km^r) starter culture was inoculated into 25 or 50 mL of LB microbiological media in a 250 mL baffled Erlenmeyer flask and culture samples analysed at 20, 24 and 27 hours after inoculation for CPS expression (A), CFU/mL (B), and CPS per CFU (C). Each value represents the mean +SD of three independent experiments.

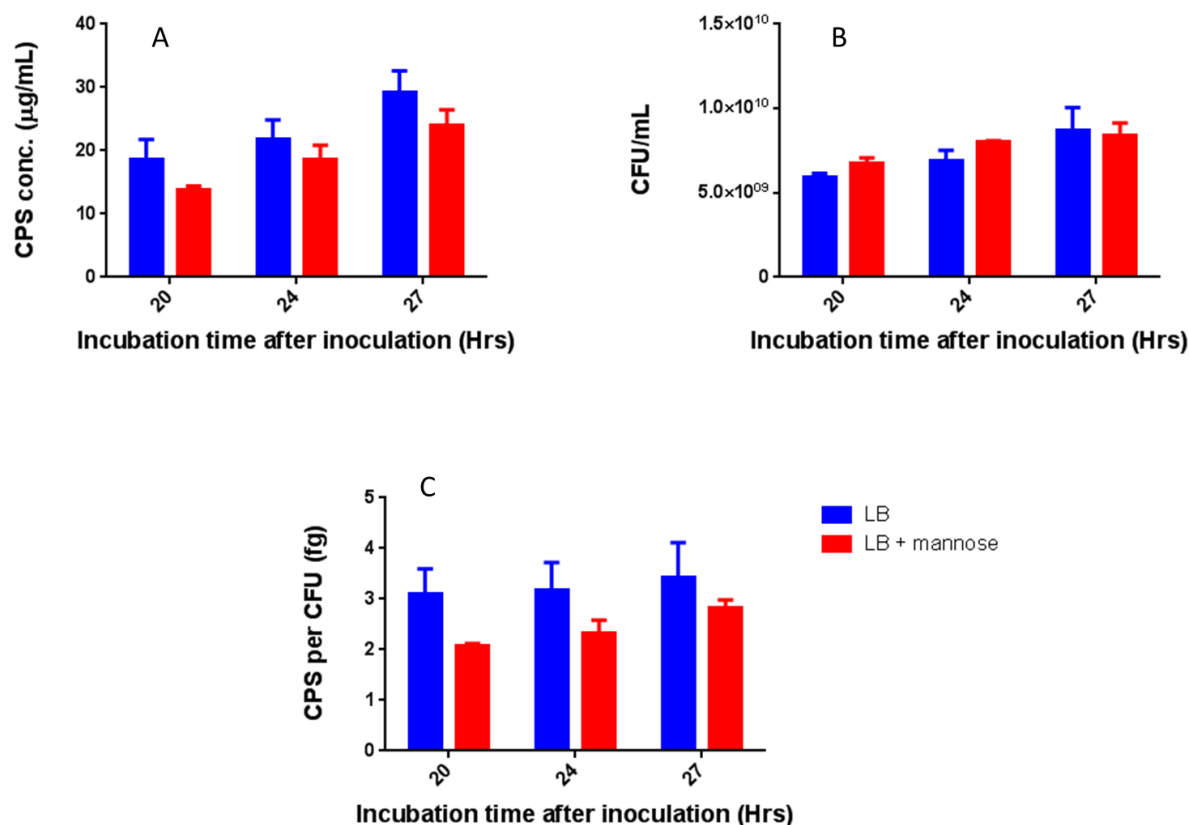


Figure 29 Effect of mannose on *B. thailandensis* E555 :: *wbil* (Km^r) growth and CPS expression. An aliquot of a *B. thailandensis* E555 :: *wbil* (Km^r) starter culture was inoculated into LB microbiological media with and without 2.5 g/L mannose and culture samples analysed at 20, 24 and 27 hours after inoculation for CPS expression (A), CFU/mL (B), and CPS per CFU (C). Each value represents the mean +SD of three independent experiments.

With the assessment of incubation time following inoculation, the use of starter cultures, different microbiological growth media, the use of baffled flasks, altering culture volume and the addition of iron sulfate, the optimisation of CPS culture concentration was completed. An increase in CPS concentration (as determined by ELISA of whole culture samples) was achieved by inoculating enhanced phytone peptone broth with a *B. thailandensis* E555 :: *wbil* (Km^r) starter culture, and culturing for 24-27 hours in baffled flasks (Figure 30).

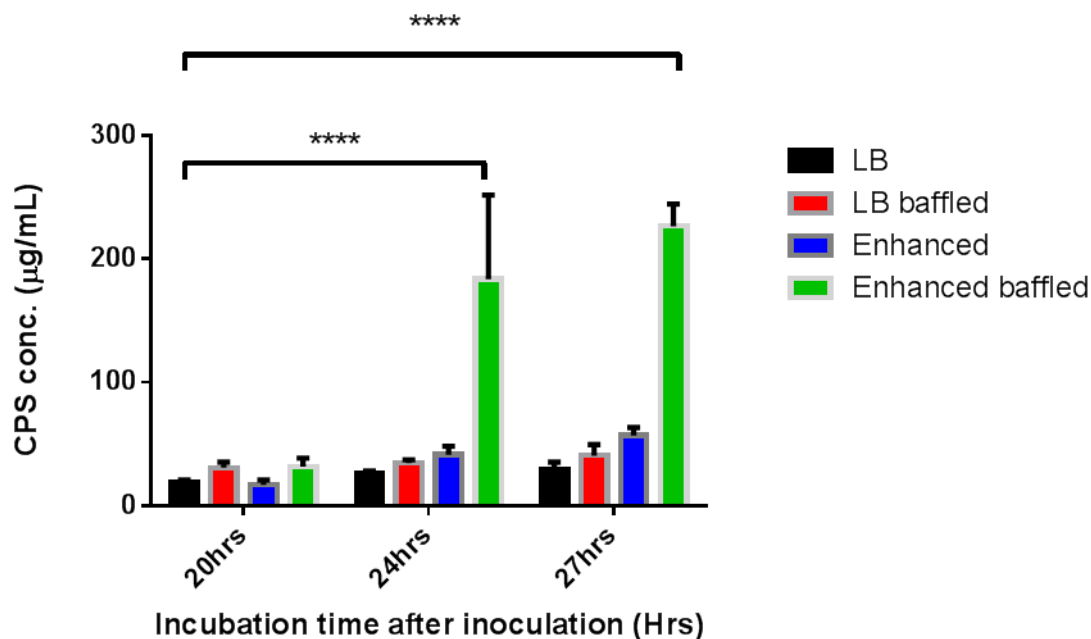


Figure 30 Increase in *B. thailandensis* E555 :: *wbil* (Km^r) CPS expression from the use of starter cultures, enhanced phytone peptone broth, baffled flasks, and a 27 hour incubation period. Each value represents the mean +SD of three independent experiments. **** p≤0.0001 (two-way ANOVA)

To determine yield and purity of CPS with optimised conditions, 5 mL of *B. thailandensis* E555 :: *wbil* (Km^r) starter culture was inoculated into 2 L of enhanced phytone peptone broth, within baffled flasks, and incubated for 27 hours at 37°C, shaking at 180 rpm using the phenol extraction method. Approximately 2 mg of CPS was obtained but purity was decreased according to NMR analysis (Figure 31). As enhanced phytone peptone broth is a rich, complex media, additional purification steps may be required in order to improve purity.

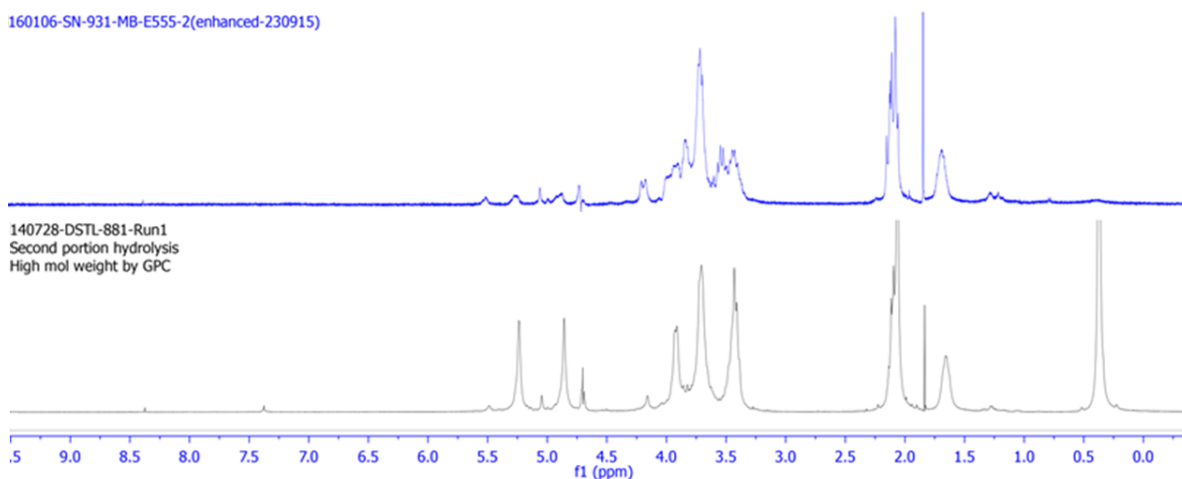


Figure 31 Stacked NMR spectra for CPS obtained from *B. thailandensis* E555 :: *wbil* (Km^r) cultured in enhanced phytone peptone media (Top) and *B. thailandensis* E555 :: *wbil* (Km^r) cultured in LB media (Bottom).

Although results from the optimisation work determined low culture CPS concentration with M9 minimal media, a highly pure product may be obtained as this media is simple and defined. CPS was extracted from 2 L of *B. thailandensis* E555 :: *wbil* (Km^r) cultured in M9 minimal media but the resultant sample was insufficient for NMR analysis (<1 mg) indicating that regardless of purity, CPS yield is simply insufficient with this media.

3.5 CPS expression optimisation – extraction

In order to optimise the modified hot-phenol based CPS extraction procedure, CPS concentration was measured in *B. thailandensis* E555 :: *wbil* (Km^r) LB culture supernatant and pellet fractions to determine the amount of CPS released from the bacterial cell wall (Chapter 2, Method 2.8.1). CPS culture concentration was assessed in the supernatant and pellet fractions of a *B. thailandensis* E555 :: *wbil* (Km^r) culture 27 hours after inoculation with a starter culture. The CPS concentrations are similar in the pellet and supernatant (Figure 32). This indicates that following a 2 L *B. thailandensis* E555 :: *wbil* (Km^r) culture, the supernatant fraction could be utilised with the potential to increase CPS yield. This could possibly alter the extraction process allowing the removal/reduction of phenol (the function of which is to dissolve proteins in the cellular membrane and free the CPS anchored to the cellular membrane for partition in the phenol phase). However, until extraction procedures have been

carried out on the supernatant and the purity of the CPS determined the utility of this approach is unproven.

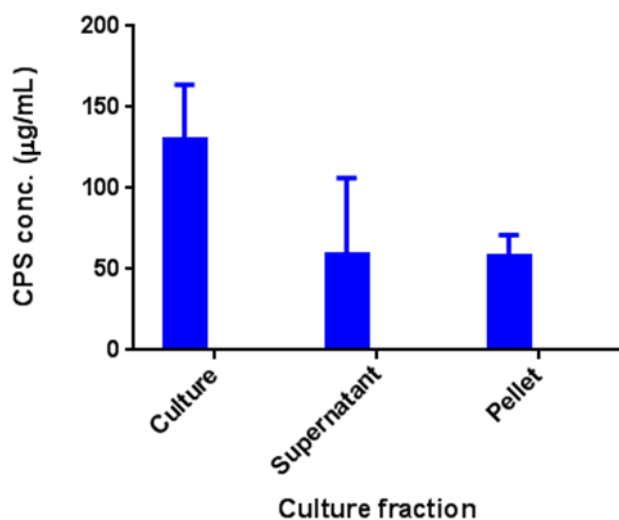


Figure 32 CPS concentration of *B. thailandensis* E555 :: *wbil* (Km^I) culture, supernatant and pellet fractions. An aliquot of a *B. thailandensis* E555 :: *wbil* (Km^I) starter culture was inoculated into LB microbiological media and incubated for 27 hours followed by ELISA analysis of culture, supernatant and pellet fractions. Each value represents the mean +SD of three independent experiments.

It is not possible to determine *B. thailandensis* E555 :: *wbil* (Km^I) culture CPS concentrations by ELISA on the same day after incubating the culture for up to 27 hours after inoculation. Cultures were frozen overnight at -20°C for analysis the following day. To determine the effect on culture CPS concentration, triplicate samples of culture, supernatant and pellet fractions were frozen and then analysed in comparison to live cultures and culture fractions (Chapter 2, Method 2.8.2). The results indicated that freezing overnight does not significantly affect CPS concentration (Figure 33).

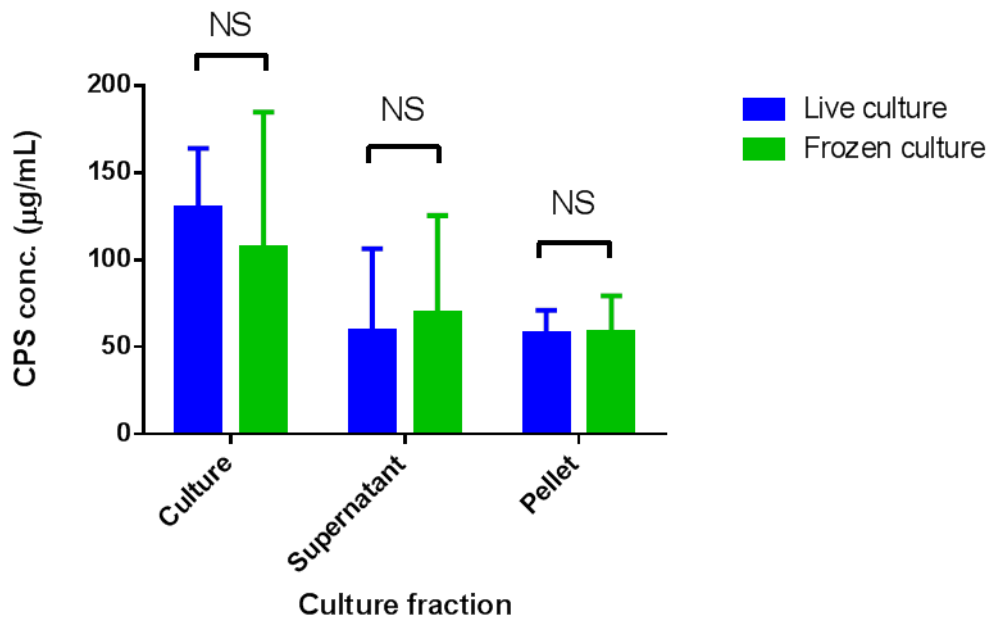


Figure 33 CPS concentration of *B. thailandensis* E555 :: *wbil* (Km^r) culture, supernatant and pellet fractions following overnight storage at -20°C. An aliquot of a *B. thailandensis* E555 :: *wbil* (Km^r) starter culture was inoculated into LB microbiological media and incubated for 27 hours. CPS concentration was determined for fresh culture, supernatant and pellet fractions and samples of the same fractions frozen overnight at -20°C and analysed by ELISA the following day. Each value represents the mean +SD of three independent experiments. NS, $p > 0.05$ (2-way ANOVA)

3.6 *Burkholderia* CPS immunogenic epitope

Work by Marchetti *et al.* (2015) showed that the acetyl group of the CPS molecule is involved in binding to an anti-CPS monoclonal antibody. To expand this work, the binding of four DstI monoclonal antibodies to CPS and deacetylated CPS was investigated.

3.6.1 Antibody recognition to deacetylated CPS

An alternative to native *Burkholderia* CPS as part of a conjugate vaccine is the use of synthetic CPS. The synthesis of CPS is made difficult by the presence of the acetyl groups. The synthesis of deacetylated CPS is less complicated, but the immunogenicity of the resulting structure is unknown. Deacetylated CPS, provided by Prof. Rob Field, was utilised in the CPS ELISA in comparison with native CPS from *B. pseudomallei* 1026b (Chapter 2, Method 2.9.1). No recognition by DSTL189 was observed (Figure 34). DstI have another three

anti-CPS monoclonals; DSTL187, DSTL188 and DSTL190, so an ELISA using these antibodies was performed with deacetylated CPS bound to the plate (Chapter 2, Method 2.9.2). None of these antibodies recognised the deacetylated CPS either (Figure 35).

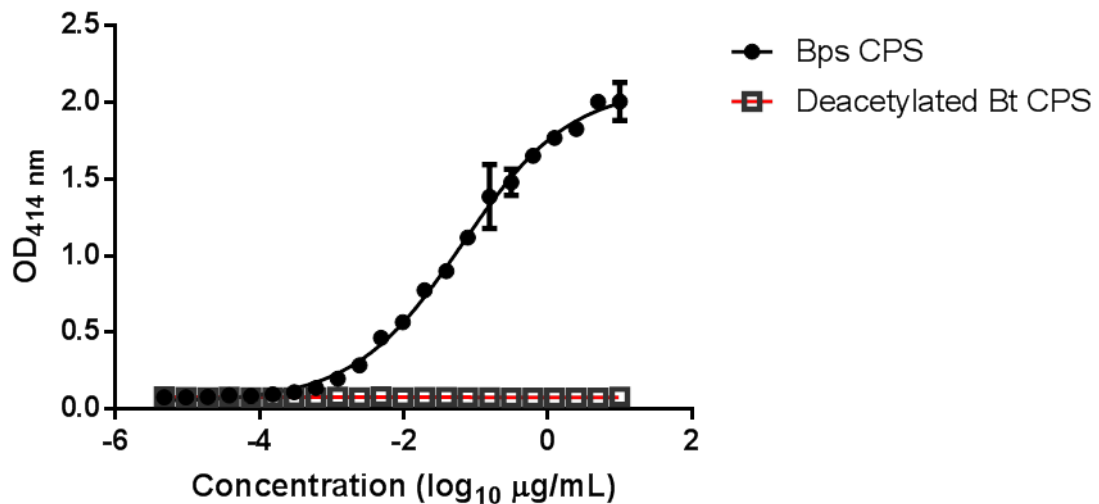


Figure 34 Lack of DSTL189 antibody recognition to deacetylated CPS. Purified *B. pseudomallei* 1026b CPS (Bps CPS) and deacetylated *B. thailandensis* E555 :: *wbil* (Km^r) (Deacetylated Bt CPS) were diluted 1:2 from 10 µg/mL and probed with DSTL189. $p=0.0002$ two-tailed paired t-test. Each value represents the mean +SD of two independent experiments

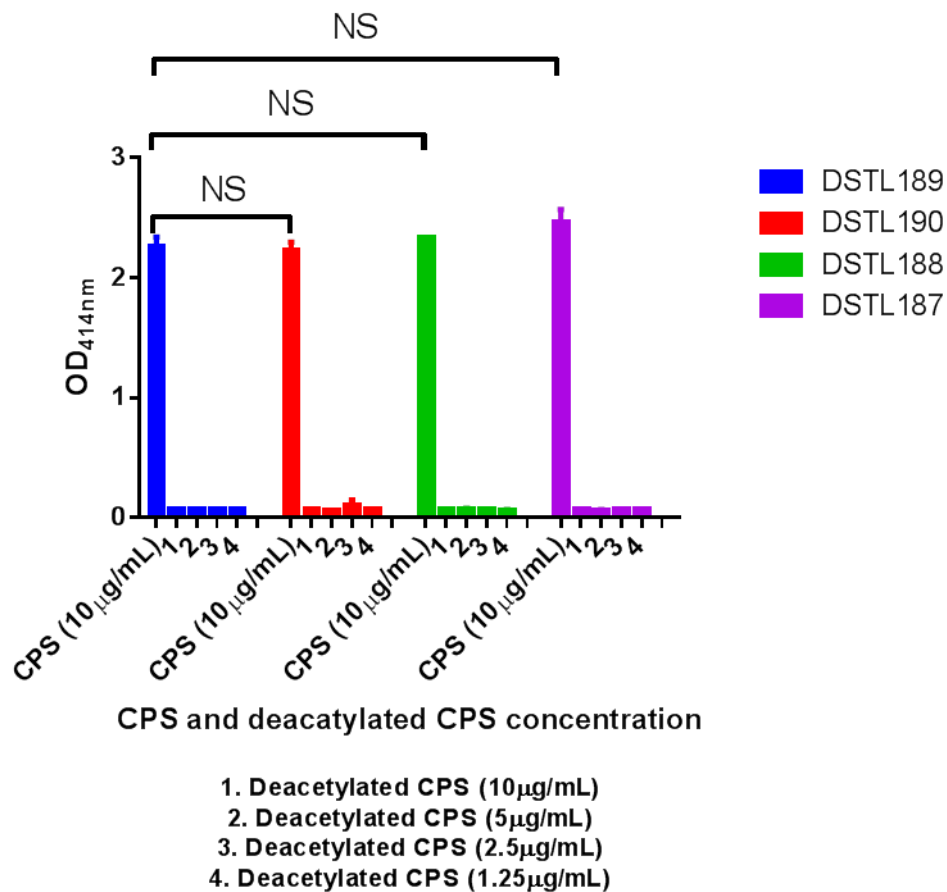


Figure 35 Detection of acetylated and deacetylated *B. thailandensis* E555 :: *wbil* (Km^r) CPS with four anti-CPS monoclonal antibodies. Purified *B. thailandensis* E555 :: *wbil* (Km^r) CPS (at 10 µg/mL) and deacetylated CPS (at 10, 5, 2.5 and 1.25 µg/mL) was bound to an ELISA plate and probed with four anti-CPS monoclonal antibodies (DSTL187,188,189,and 190). (NS, $p > 0.05$, 2 way ANOVA). Each value represents the mean +SD of two independent experiments

3.6.2 Comparison of CPS antibody sequences

No Dstl anti-CPS monoclonal antibody recognised de-acetylated CPS. As CPS recognition was not significantly different between them, the variable regions of the light and heavy chain of each antibody was sequenced (Chapter 2, Method 2.9.3). In brief, RNA from four clones of each antibody cell line was sequenced and the consensus sequence detailed below. As sequence can differ between hybridomas, four clones were sequenced for each antibody cell line.

The antibody nucleotide sequences were translated into amino acid sequences by ExPASy (<http://web.expasy.org/translate/>) and the amino acid sequences are shown in Figure 36. Highlighted framework (FR) and complementarity

determining regions (CDR) were obtained by NCBI blast search (<https://www.ncbi.nlm.nih.gov/igblast/>).

An immunoglobulin blast search (<https://www.ncbi.nlm.nih.gov/igblast/>) of the antibody sequences showed each antibody to have a high degree of homology to the germline sequence of IgHV6-6*01 (DSTL189; 95 %, DSTL187; 95 %, DSTL188; 93 %, DSTL190; 96 %) and IGKV8-28*01 (DSTL189; 93 %, DSTL187; 93 %, DSTL188; 93 %, DSTL190 91 %).

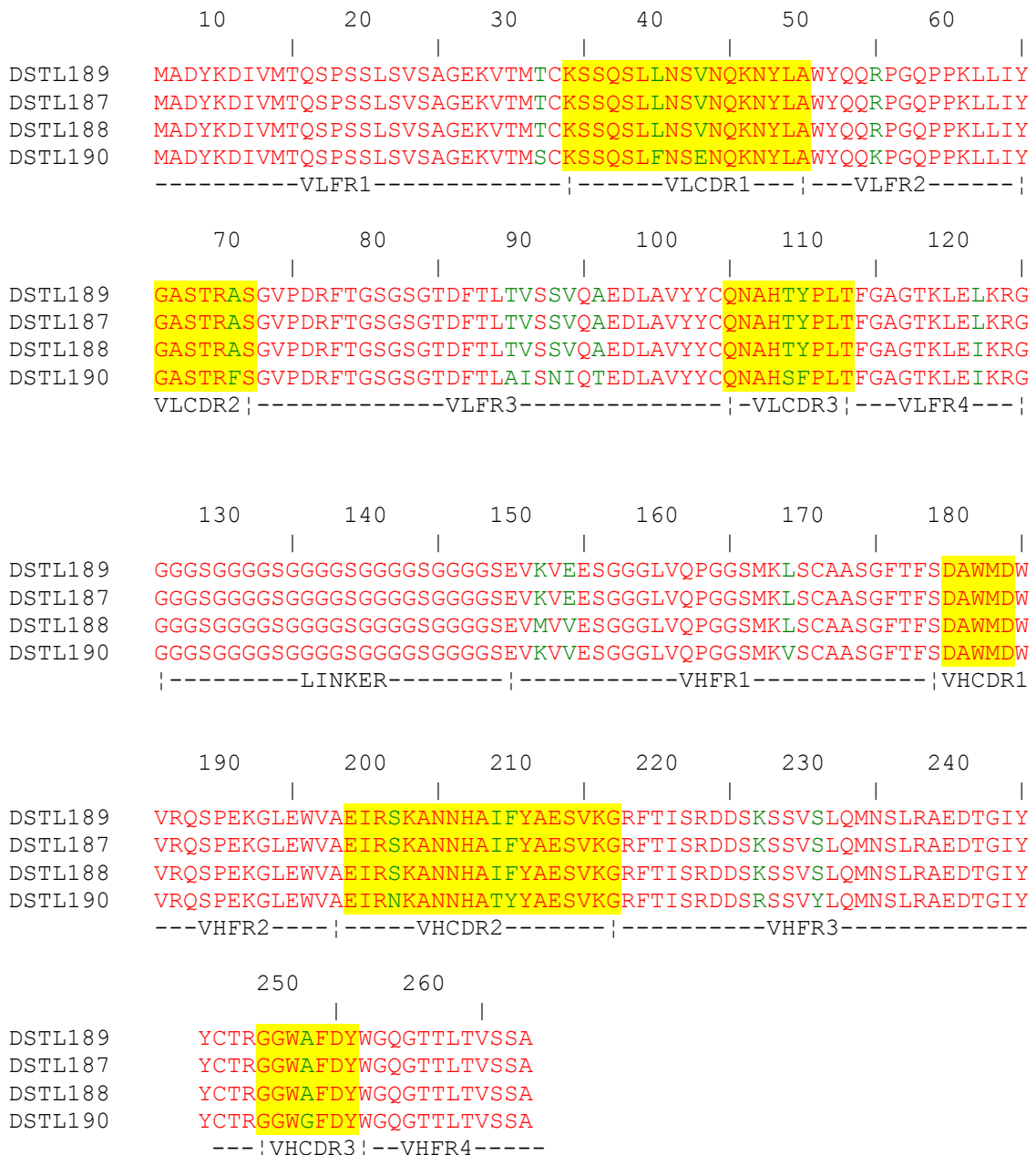


Figure 36 Amino acid sequence of variable light (VL) and heavy (VH) chain framework regions (FR1-4) and complementarity determining regions (CDR1-3) of four Dstl anti-CPS antibodies (DSTL189, DSTL187, DSTL188 and DSTL190). Amino acid differences between the antibodies are highlighted in green. For clarity, CDRs are highlighted in yellow

In the top 5 results of an NCBI blast search of the DSTL189 light chain was a murine antibody to pneumococcal C-polysaccharide backbone with 94 % sequence identity and identity of the CDR regions alone was 88 % (Accession number CAQ76891). A blast search of the *pneumococcal* antibody showed it to be 100 % homologous to the germline sequence of IGKV8-28*01.

Interestingly, within the NCBI blast search results was an anti-*Francisella tularensis* O-antigen antibody (Accession number 4OTX_L) with 89 % full sequence identity to DSTL189 and CDR region homology of 79 %. A BLAST search of the *F. tularensis* antibody showed it to be 100 % homologous to the germline sequence of IGKV8-19*01 and 95 % homologous to IGKV8-28*01. Sequence comparison for both of these antibodies to DSTL189 is shown in Figure 37.

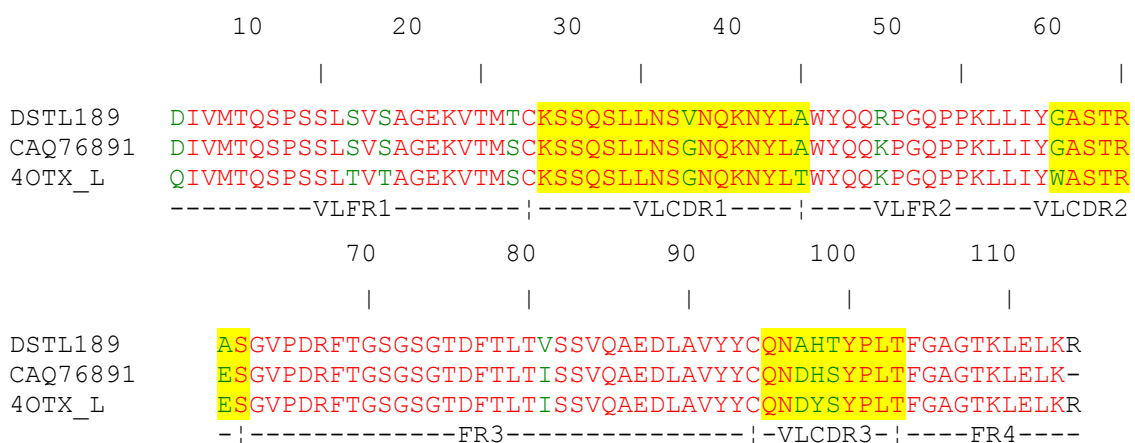


Figure 37 Amino acid sequence of variable light (VL) chain framework regions (VLFR1-4) and complementarity determining regions (VLCDR1-3) of DSTL189; Dstl's anti-CPS antibody, an anti-pneumococcal C-polysaccharide backbone antibody (CAQ76891) and an anti-*F. tularensis* O-antigen antibody (4OTX_L). Amino acid differences between the antibodies are highlighted in green. For clarity, CDRs are highlighted in yellow

In the top 5 results of an NCBI blast search of the DSTL189 heavy chain was an anti-*B. pseudomallei* single-chain variable fragment (scFV) antibody with 89 % full sequence homology (Accession number ACZ65030.1) and CDR region homology of 81 %. A blast search of the *Burkholderia* antibody showed it to be 96 % homologous to the germline sequence of IGHV6-6*01. There was also an entry within the first 10 hits for an antibody to *Shigella flexneri* Y lipopolysaccharide with 86 % homology to DSTL189 (Accession number 1M71

B). A blast search of the *S. flexneri* antibody showed it to be 98 % homologous to the germline sequence of IgHV6-6*02. Interestingly, DSTL189 has also 88 % sequence homology to IgHV6-6*02. Sequence comparison for both of these antibodies to DSTL189 is shown in Figure 38.

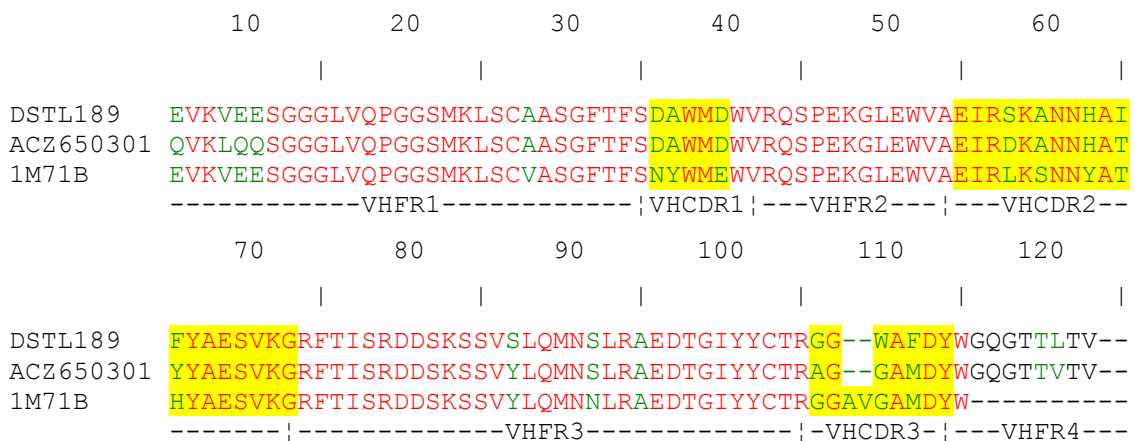


Figure 38 Amino acid sequence of variable heavy (VH) chain framework regions (VHFR1-4) and complementarity determining regions (VHCDR1-3) of DSTL189; Dstl's anti-CPS antibody, an anti-*B. pseudomallei* antibody (ACZ650301) and anti-*S. flexneri* LPS antibody (1M71B). Amino acid differences between the antibodies are highlighted in green. For clarity, CDRs are highlighted in yellow

3.7 Importance of the CPS acetyl group

An animal study performed separately to this work by a Dstl colleague (Andy Scott) showed that deacetylated CPS conjugated to a carrier protein (TetHc) was significantly less efficacious in vaccinated mice to *B. pseudomallei* challenge than a conjugate with acetylated CPS (Figure 39). Analysis of the CPS specific IgG and IgM titres from mouse sera following the third vaccination showed an IgG and IgM response in mice vaccinated with TetHc-CPS (Chapter 2, Method 2.10.1). There was no CPS-specific antibody response in mice vaccinated with deacetylated CPS conjugated to TetHc. Analysis of the deacetylated CPS specific antibody response showed a very low IgG titre in CPS-TetHc vaccinated mice and low titre in deacetylated CPS vaccinated mice. Interestingly, there was no IgM antibody to deacetylated CPS in deAcCPS vaccinated mice (Figure 40). In conjunction with the antibody binding data, this suggests that the acetyl group is crucial in the formation of the CPS immunogenic epitope.

3.8 Discussion

Burkholderia capsular polysaccharide (CPS) is one of the main surface-associated antigens of *B. pseudomallei* and *B. mallei* (Tuanyok *et al.*, 2012). It is a known virulence determinant as *B. pseudomallei* mutants lacking CPS demonstrate a 10^5 -fold increase in the median lethal dose (MLD) in an animal model (Atkins *et al.*, 2002). CPS has also been demonstrated to be a protective antigen in animal models against *B. pseudomallei* challenge (Nelson *et al.*, 2004) and is therefore a good candidate for vaccine development.

B. pseudomallei and *B. mallei* are categorised as Hazard Group 3 organisms by the Advisory Committee on Dangerous Pathogens (ACDP). This means that these agents must be handled in Containment Level 3 laboratories which are specialised facilities with enhanced containment measures. These include maintenance of the workplace at negative air pressure to the environment and high efficiency particulate absorption (HEPA) filtration on extract air. Material must also be handled in a safety cabinet or isolator which is burdensome and time-consuming (ACDP guidance - The management, design and operation of microbiological containment laboratories 2001). Local procedures can also be in place to restrict the volume of agent that can be cultured or techniques that may increase risk of aerosol generation such as freeze-drying. This means that the use of *B. pseudomallei* or *B. mallei* for extraction of CPS is expensive and time-consuming. Whilst this project was funded by DTRA to develop a vaccine for use in a defence setting, cost is an important factor in the development of any product. With the use of a carrier protein as well, this may make a CPS conjugate vaccine prohibitively expensive in a public health setting given the relative wealth of countries endemic for melioidosis (Choh *et al.*, 2013).

The aim of these experiments was to reduce the cost of vaccine production with several objectives. The first was to further the work of Sim *et al.* 2010 where *B. thailandensis* E555 was found to cross-react with a monoclonal antibody raised against *B. pseudomallei* CPS. In this study, CPS was extracted from *B. thailandensis* E555 and comparative NMR analysis with CPS extracted from *B. pseudomallei* 1026b determined the structure of these molecules to be the same. Recognition of these two CPS molecules with a monoclonal antibody that

recognises *B. pseudomallei* CPS (DSTL189) was not significantly different which also suggests a similar secondary structure. These results indicate that *B. thailandensis* E555 could replace *B. pseudomallei* for the extraction of CPS. *B. thailandensis* is considered essentially avirulent and can be handled at lower levels of containment than *B. pseudomallei*. This significantly reduces costs for the production of CPS. In the US, a derivative of the select-agent excluded *B. pseudomallei* strain Bp82, for use at containment level 2, can be used in CPS production (Burtnick *et al.*, 2012) but, as with any mutant, there exists a small chance of reversion to wild-type. The use of a naturally avirulent strain of *Burkholderia* may also make licensing of a potential vaccine easier.

Extraction and purification of CPS was only achieved with the modified hot-phenol extraction method first reported by Perry *et al.* (1995), and further developed by Assoc. Prof. Brett at the University of South Alabama. The modified hot-phenol method required the addition of phenol to live bacterial cultures at a temperature of 80°C. This contrasts to the phenol method initially attempted, which used cultures heat-killed at 80°C for 4 hours and the use of phenol at 60°C. It is considered that the extract obtained from this first phenol method and by ethanol precipitation does contain CPS, as demonstrated by anti-CPS antibody binding by George, 2013, but the purity is not sufficient to identify CPS by NMR.

The yield of CPS obtained in this study from *B. thailandensis* E555 varied from 0.25 to 9 mg per litre of culture and was lower than the 10-15 mg per litre yield recently reported (Burtnick *et al.*, 2012). It is possible that operator inexperience or slight differences in execution of the procedure between laboratories was responsible. In the literature, CPS extraction is from *B. pseudomallei* so it is possible that yield differences may be a result of differences in CPS expression between the two species.

Once the utility of *B. thailandensis* E555 for CPS extraction was established, the focus of this study shifted to maximising the amount of CPS in culture with the aim of increasing CPS yield following purification to again reduce cost. As CPS extraction takes approximately 5 weeks, a way to quickly assess changes in bacterial CPS concentration was required. Initial efforts therefore focussed on

development of a quantitative ELISA. The ELISA developed was acceptable for use with lower and upper limits of quantification defined at 25 and 0.39 ng/mL respectively. The ELISA could also determine CPS concentration of the final vaccine after conjugation to a carrier protein. This is an essential step in production of a conjugate vaccine (WHO TRS 924, 2004) and is currently performed by phenol-sulfuric acid assay (Masuko *et al.*, 2005), a technique used for detection of carbohydrates.

Following development of the ELISA to quantify changes in bacterial CPS culture concentration, efforts to increase CPS concentration focussed on improving *B. thailandensis* E555 growth with the hypothesis that increasing bacterial growth increases CPS expression. Assessment of increased culture aeration by the use of baffled flasks and providing more nutrients through the use of different microbiological growth media were performed first. Both were found to significantly increase culture CPS concentration as did the use of starter cultures to inoculate the larger volumes required (2 L) for CPS extraction and purification. A literature search for other relevant conditions to assess found that iron sulfate increased *B. pseudomallei* growth (Wang-Ngarm *et al.*, 2014). Whilst this finding was replicated, the increase in CFU/mL did not significantly increase CPS concentration. An additional carbon source was also investigated as it has been reported that different sugars modulate exopolysaccharide biosynthesis (Yuksekdag and Aslim 2008, Audy *et al.*, 2010). In this study, mannose was added to LB media, but there were no significant differences in CPS concentration. Through the use of a starter culture, baffled flasks and enhanced phytone peptone broth, culture CPS concentration increased 8 fold over the use of non-baffled flasks without a starter culture with LB media. NMR analysis of CPS extracted from these enhanced conditions showed a decrease in purity over standard conditions. This may result from the use of enhanced phytone peptone broth and may require additional purification steps to be added to the extraction protocol. CPS yield with the enhanced conditions was low, but due to the variable yield experienced from multiple CPS extractions under standard conditions, the extraction following enhanced conditions would need to be repeated. Utilising standard media (LB) with a starter culture and baffled flasks also improved culture CPS concentration.

The aim of improving CPS yield also focussed on optimisation of the CPS extraction method. CPS concentration was measured in the supernatant and pellet fractions after centrifugation of a *B. thailandensis* E555 culture. CPS was measured in similar quantities in both fractions meaning that the supernatant could be utilised for CPS extraction. The current extraction method utilises only the pellet fraction of a *B. thailandensis* E555 culture and requires the addition of phenol to disrupt the cellular membrane to release the CPS and partition the CPS in the phenol phase. Utilisation of the supernatant as well as the pellet would improve CPS yield and utilisation of the supernatant only could reduce the amount of phenol required. Given the toxicity of phenol, the removal or reduction of phenol from the procedure would make waste disposal cheaper and easier. This may also make registration of the vaccine product easier as removal of reagents and by-products should be confirmed (WHO TRS 924, 2004). Until extraction of CPS from supernatant is achieved and yield and purity assessed, however, the utility of supernatant for CPS production cannot be determined.

The lack of anti-CPS antibody binding to deacetylated CPS suggests that the acetyl group forms part of the epitope recognised by these anti-CPS monoclonal antibodies and confirms the work by Marchetti *et al.* 2015. As monoclonal antibodies have been shown to provide protection against *B. pseudomallei* challenge following passive transfer (Jones *et al.*, 2002), this suggested that the acetyl group is important for CPS immunogenicity. This work was furthered by demonstration that the protective efficacy of a deacetylated CPS conjugate vaccine is significantly lower than a native CPS conjugate to *B. pseudomallei* challenge. Together, these data suggest that CPS has a major immunodominant protective antigen and that the acetyl group is either part of the epitope or is involved in its formation. Given that acetyl groups are common across a wide range of molecules, it is likely that the epitope formed is conformational. This observation is also in agreement with several other polysaccharides such as *Neisseria meningitidis* serogroup A CPS (Berry *et al.*, 2002) and *Salmonella typhi* (Szu *et al.*, 1991) where an acetyl group is essential for immunogenicity. Not all acetyl groups are essential for bacterial CPS immunogenicity, however. Examples include the *N. meningitidis* serogroup W135 polysaccharide (Gudlavalleti *et al.*, 2007) and group C meningococcal

CPS, where for the latter the O-acetyl group masks the protective epitope (Fusco *et al.*, 2007). The demonstration of the importance of the acetyl group on *Burkholderia* CPS immunogenicity is important for development of synthetic CPS as it confirms that the acetyl group must be present. This is important as production of the acetylated molecule is more technically demanding and expensive. This conclusion is also supported by analysis of the antibody titres of mice vaccinated with deacetylated CPS, which do not raise antibodies that recognise native CPS. Interestingly, IgG antibody titres were significantly higher to CPS, in CPS conjugate vaccinated mice, than IgG titres to deacetylated CPS in mice vaccinated with a deacetylated CPS conjugate. The reduced IgG titres and lack of IgM antibody generated to deacetylated CPS suggests that deacetylated CPS is significantly less immunogenic than native CPS. While the strict requirement for the acetyl group increases the complexity of synthesising CPS, its use may still be advantageous because as indicated by the World Health Organization (WHO Technical Report Series 784, 1989) the use of synthetic antigens means that no infectious material is present and quality control would be easier as the product would be precisely defined and may be cheaper to produce.

The importance of the acetyl group on immunogenicity is also important for the development of a native CPS conjugate vaccine. The production of shorter CPS chains may be essential for vaccine development as it has been reported that long chains of polysaccharide can affect conjugate vaccine efficacy (Carmenate *et al.*, 2004, Rana *et al.*, 2015). Furthermore, the use of native chain lengths may mean separation of conjugated CPS from unconjugated CPS is difficult, which again affects vaccine efficacy (Rodriguez *et al.*, 1998). A method to generate shorter chain lengths of CPS, in use for *Streptococcus pneumoniae* polysaccharide 6B (Perciani *et al.*, 2013) and *N. meningitidis* serogroup X polysaccharide (Micoli *et al.*, 2013), is acid hydrolysis. However, due to the acid-labile nature of CPS, hydrolysis may lead to a degree of deacetylation and therefore a loss of immunogenicity.

The high sequence homology of the anti-CPS monoclonal antibodies is interesting because it also suggests that the CPS epitope is highly restricted. Further work to determine the influence of amino acid differences between the

antibodies on binding affinity to CPS could be performed by competitive ELISA or surface plasmon resonance. The high sequence homology of the anti-CPS antibodies to germline sequences IGKV8-28*01 and IgHV6-6*01, which is also seen in antibodies that recognise C-pneumococcal polysaccharide backbone and *Francisella tularensis* O-antigen, suggests that antibodies raised against bacterial polysaccharides in mice are derived from a restricted set of germline sequences that do not undergo extensive maturation. This is already suggested for pneumococcal C-polysaccharide (Fernandez-Sanchez *et al.*, 2009) and for light-chain antibody responses in humans to Hib CPS (Adderson *et al.*, 1992).

Chapter 4: Immunogenic *Burkholderia* proteins

4.1 Introduction

A vaccine aims to induce immunity to a particular infection, typically by the generation of a protective-immune response to a vaccine component equal or improved to the immune response elicited from natural infection of the disease-causing organism.

Traditionally, the vaccine component that fulfilled this requirement was the use of live organism (as for smallpox), killed whole organism (as for plague) or protein and polysaccharide subunits (as for Hepatitis B) (Hussein *et al.*, 2015). For melioidosis all of these approaches have been considered (Silva and Dow, 2013, Choh *et al.*, 2013), but recent vaccine approaches have focused on polysaccharide conjugated to a carrier protein (Scott *et al.*, 2014, Garcia-Quintanilla *et al.*, 2014).

It is hypothesised that both humoral and cellular protective immune responses are required for complete protection against *B. pseudomallei* (Healey *et al.*, 2005, Silva and Dow, 2013). The aim of this chapter was to identify immunogenic *Burkholderia* proteins that could be used in a vaccine with CPS in order to provide melioidosis relevant T-cell epitopes. The proteins were used in three ways; chemically conjugated to CPS to form a CPS-*Burkholderia* protein conjugate, co-mixed with a CPS-Virus-like particle conjugate or inserted into the Tandem CoreTM (VLP) construct for expression of the VLP molecule displaying the *Burkholderia* protein with the resultant molecule chemically conjugated to CPS. The protective efficacy of two of these constructs against bacterial challenge is detailed in Chapter 5; Immunogenicity and efficacy of candidate vaccines. Insertion of *Burkholderia* protein into major immunodominant region 1 or 2 of the Tandem CoreTM construct hindered VLP assembly. Several of the proteins were membrane associated which may have hindered VLP assembly due to the presence of hydrophobic transmembrane regions, therefore a second objective of this chapter was to identify extracellular regions of each protein to

aid in the development of truncated proteins by our collaborator for insertion into the Tandem Core™ construct.

The final objective of this chapter was to identify immunogenic T-cell epitopes of *Burkholderia* proteins to distinguish key immunogenic regions to ensure that immunogenicity was not lost following the development of truncated proteins. T-cells recognize a complex formed between a major histocompatibility complex (MHC) molecule and a bound epitope (Sidney *et al.*, 2008). There are two major types of MHC molecule; MHC-I which presents endogenous epitopes degraded by the proteasome and is important in the development of an immune response against intracellular bacteria and viruses and MHC-II which binds peptides generated by antigen proteolysis in endosomal/lysosomal compartments in antigen processing cells (APCs) for processing and presentation to CD4+ T-helper cells (Roche and Cresswell, 2016).

The binding groove of MHC-I molecules typically bind peptides of 9 amino acids whereas the more open groove of MHC-II molecules can bind between 11 to 30 (Meydan *et al.*, 2013). If immunogenic epitopes of protective antigens are identified, they can form the basis of a vaccine as demonstrated for the licensed Human Papillomavirus vaccine (Huber and Tantiwongkosi, 2014). The advantages of this approach would be a vaccine with an improved safety profile as unnecessary components would not be present with the potential to cause side-effects which may make licensure less difficult due to the highly pure and well characterized antigens. They would also be safe to use in immunosuppressed individuals and production of a single component may reduce cost. The disadvantage is that epitope based vaccines can have decreased immunogenicity because of the use of highly pure antigens (Vartak and Suheck, 2016).

In this study, epitopes bound by mouse MHC-I and MHC-II molecules were predicted as this was the animal model the candidate vaccines were tested in. This was carried out for the H2^d (BALB/c) and H2^b haplotypes (C57BL/6). Class I genes are K, D and L whilst class II are I-A and I-E. While this project only proposed the use of BALB/c mice, C57BL/6 mice are an established model of chronic melioidosis and were included for any potential future work. C57BL/6

mice do not have the Class I L and class II I-E genes. If peptide insertion into Tandem Core™ improved vaccine efficacy, further epitope predictions would have to be performed for human leukocyte antigen (HLA) class I and II molecules. HLA is extremely polymorphic comprising several thousand alleles (Hoof *et al.*, 2009) but it has been reported that prediction of eight representatives of the 875 known HLA-DR alleles can cover the genetic background of most humans worldwide (Jawa *et al.*, 2013). The computer programs used for transmembrane and epitope predictions, as well as a summary of their function, are detailed in the supplementary information below.

4.2 Immunogenic *Burkholderia* protein selection

Following a literature review, several *Burkholderia* proteins were identified that could be considered for use in a vaccine (Table 7). Selection criteria for identification of immunogenic *Burkholderia* proteins included evidence of protective immunity in an animal model or evidence of an immuno-stimulatory effect. Also considered was cellular location of the protein with preference given to those on the exterior of the cell so as to be readily available for immune system recognition.

LolC (BPSL2277), PotF (BPSS0467) and OppA (BPSS2141) are *B. pseudomallei* proteins of ATP-binding cassette (ABC) systems which have roles in bacterial survival, virulence and pathogenicity. LolC is a membrane protein associated with the LolCDE ABC system, which is involved in lipoprotein sorting between the inner and outer membranes of Gram-negative bacteria. PotF is a periplasmic binding protein of the PotFGHI system, involved in putrescine import in *E. coli* and OppA, an oligopeptide-binding protein of the Opp system in *E. coli* (Harland *et al.*, 2007b). All three proteins were chosen for inclusion on the basis of work by Harland *et al.* 2007a, which showed that the proteins are recognized by mouse T-cells primed with *B. pseudomallei*. The mice generate IgG2a (Th1 bias) antibody responses and protection in LolC and PotF vaccinated mice was significantly greater than controls to *B. pseudomallei* challenge at 54 x MLD. Tippayawat *et al.* (2009) demonstrated that recovered melioidosis patients had T-cell responses that recognized LolC, PotF and OppA.

The outer membrane protein Omp85 (BPSL2151) was chosen on the basis of work by Su *et al.* in 2010, following identification of the protein by the same group from a *B. pseudomallei* genomic expression library screened with melioidosis patient sera (Su *et al.*, 2008). Mice immunized with Omp85 generated high levels of Omp85 specific IgG titres and had significantly greater protection to *B. pseudomallei* challenge than controls. Omp85 is also highly conserved within *B. pseudomallei* strains and with other *Burkholderia* species (Su *et al.*, 2010).

Hcp2 (BPSS0518) and Hcp6 (BPSL3105) are surface-associated proteins from *B. pseudomallei* type VI secretions systems (T6SSs) which are hypothesized to inject effector proteins directly into the cytosol of eukaryotic and/or bacterial cells (Burtnick *et al.*, 2011). Hcp2 and Hcp6 were included in this study on the basis of work by Burtnick *et al.* (2011) which showed them to be protective antigens in a mouse model against *B. pseudomallei* challenge.

Protein	Comment
LoIC (BPSL2277)	Protective antigen in animal model. Harland <i>et al.</i> 2007a. T-cell response in melioidosis patients. Tippayawat <i>et al.</i> , 2009
PotF (BPSS0467)	Protective antigen in animal model. Harland <i>et al.</i> 2007a. T-cell response in melioidosis patients. Tippayawat <i>et al.</i> , 2009
OppA (BPSS2141)	T-cell response in animal model and melioidosis patients. Harland <i>et al.</i> , 2007a, Tippayawat <i>et al.</i> , 2009
Omp85 (BPSL2151)	Protective antigen in animal model. Su <i>et al.</i> 2010
Hcp2 (BPSS0518)	Protective antigen in animal model. Burtnick <i>et al.</i> 2011
Hcp6 (BPSL3105)	Protective antigen in animal model. Burtnick <i>et al.</i> 2011

Table 7 Identified *Burkholderia* proteins from the literature that could be used as antigens in a *Burkholderia* vaccine

4.3 Expression of Tandem Core™ with peptide inserts

Various constructs were prepared by Mologic with a number of *Burkholderia* peptide sequences inserted in one or both of the major immunodominant regions (MIR) of the tandem core constructs. Although Mologic demonstrated that green fluorescent protein (GFP) could be successfully inserted into the VLP (data not shown), *Burkholderia* proteins could not be inserted without disrupting assembly of the VLP. With LolC protein as an example, transmission electron microscopy (TEM) analysis by Mologic revealed that the tandem core containing the full-length LolC fusion construct had formed heterogeneous, irregularly shaped assemblies. Over time these misfolded VLPs tended to form aggregates and were therefore not suitable for conjugation to CPS (Figure 41).

A summary of Mologic's work expressing Tandem Core™ with peptide inserts is detailed in supplementary data (4.5.1).

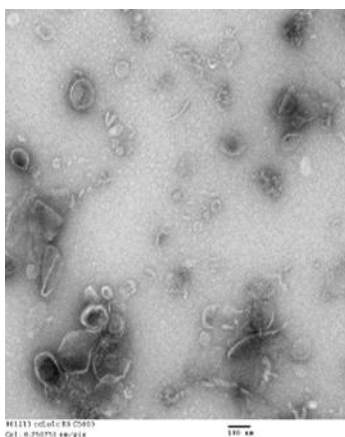


Figure 41 Transmission Electron Microscopy (TEM) analysis of *E. coli* expressed Tandem Core™ VLPs containing LolC fusion protein.

Although insertion of peptide sequences disrupted VLP formation, to determine correct *Burkholderia* protein expression and folding, a VLP-LolC construct expressed from *baculovirus* was tested by ELISA (Chapter 2, Method 2.11.1) utilising sera from mice previously immunised by a Dstl colleague with a LolC expressing DNA vaccine. VLP was used as the negative control and purified LolC as the positive control. The results indicated a high degree of cross-reactivity of mouse sera to the negative control (Figure 42).

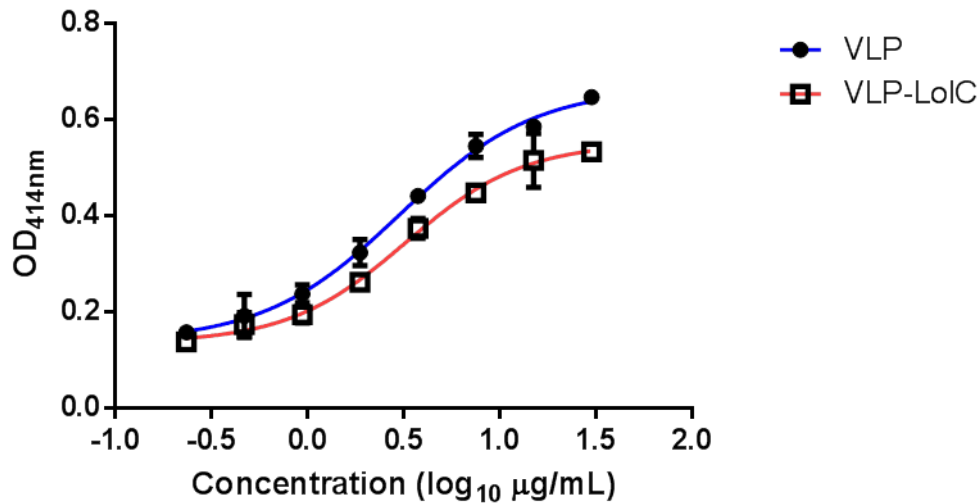


Figure 42 Recognition of purified VLP and VLP-LoIC antigen by ELISA with sera from mice immunised with adenovirus expressing LoIC. A microtiter plate was coated with VLP and VLP-LoIC from 0.2 to 30 µg/mL and probed with sera from mice taken 2 weeks following immunisation with adenovirus expressing LoIC.

The experiment was repeated, but with mouse sera from animals previously immunised by a Dstl colleague (A. Scott) with LoIC expressed from *E. coli*. Cross-reactivity was seen to the negative control VLP, although at a reduced level compared to the previous experiment (Figure 43).

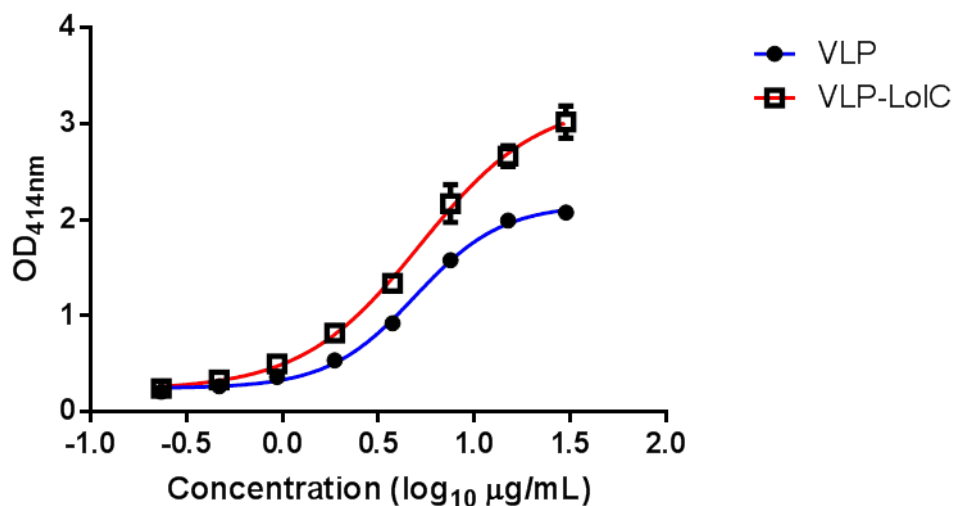


Figure 43 Recognition of purified VLP and VLP-LoIC antigen by ELISA with sera from mice immunised with LoIC. A microtiter plate was coated with VLP and VLP-LoIC from 0.2 to 30 µg/mL and probed with sera from mice taken 2 weeks following immunisation with LoIC.

The experiment was repeated a third time but with sera from mice previously immunised with endotoxin-free LolC expressed from *E. coli*. A small degree of cross-reactivity was seen to the VLP but strong recognition to the VLP-LolC construct was apparent thus confirming the correct folding of the LolC protein by this expression system (Figure 44).

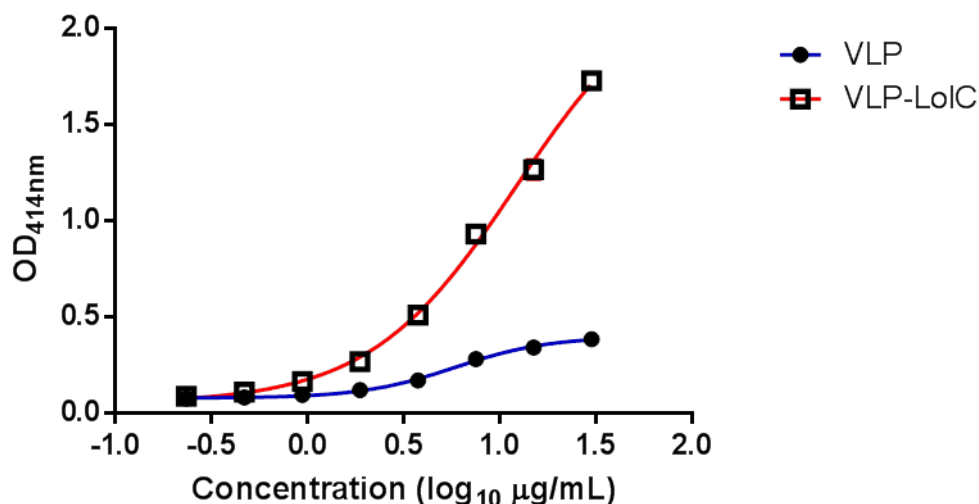


Figure 44 Recognition of purified VLP and VLP-LolC recognition by ELISA with sera from mice immunised with purified LolC. A microtiter plate was coated with VLP and VLP-LolC from 0.2 to 30 µg/mL and probed with sera from mice taken 2 weeks following immunisation with purified LolC.

The cross-reactivity seen to VLP in all three experiments was considered to be a result of virion/host cell component contamination. Although insertion of full-length protein sequences into Tandem Core™ was no longer considered viable, the ELISA developed for this analysis could have been expanded for use with other expression systems.

For LolC and OppA, hydrophilic transmembrane domains within the full protein sequence were considered responsible for hindering VLP assembly so truncated forms of the proteins were produced. For completeness, transmembrane helices predictions were performed with the TMHMM program (<http://www.cbs.dtu.dk/services/TMHMM/>) for all proteins and the predicted major extracellular portion of LolC was constructed into a fusion construct by Mologic.

The purpose of the addition of *Burkholderia* proteins to a CPS conjugate vaccine was to provide T-cell epitopes. To confirm the presence of T-cell epitopes within the truncated form of LolC and OppA, MHC-I and MHC-II epitope predictions were performed. Should the use of truncated proteins also be unsuccessful, a fusion construct of Tandem CoreTM and selected peptide epitopes could also be produced. If this work was to be taken forward, the MHC predictions are available for all selected *Burkholderia* proteins.

For clarity of the process followed, the following membrane domain predictions and MHC predictions are shown for LolC only. Data for the remaining *Burkholderia* proteins is given in the supplementary information 4.5.2 and 4.5.3.

4.3.1 Prediction of *Burkholderia* protein membrane spanning domains

The output of TMHMM for LolC transmembrane helices prediction is given in Figure 45 and overlay of the domain predictions on the amino acid sequence is shown in Figure 46. The first 23 amino acids are located intracellularly, followed by a membrane spanning domain of 23 amino acids. Amino acids 47-273 were predicted to be extracellular but expression of this sequence as a fusion protein with Tandem CoreTM disrupted VLP assembly. TEM analysis by Mologic showed that the VLPs had formed heterogeneous, irregularly shaped assemblies as they had with full length LolC (EM data not shown).

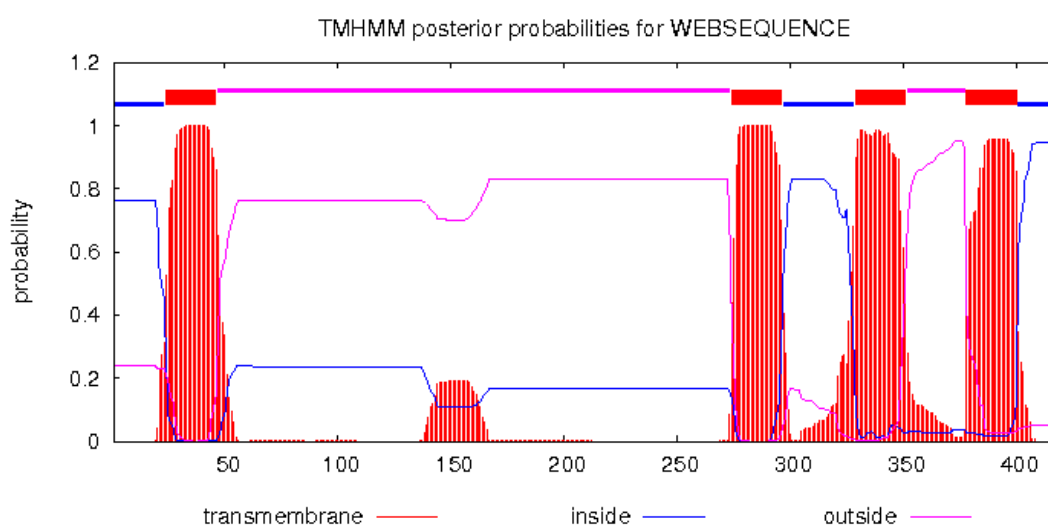


Figure 45 TMHMM calculated probabilities for transmembrane domains within the *Burkholderia* protein LolC [BPSL2277].

LoIC [BPSL2277]

Inside membrane	Membrane spanning domain	Outside membrane
MKLPYEWQIGWRYTRAGKRTTGN	GFISFIALVSMGLGVAALIV	VLSVMNGFQKEVRD
RMLSVLAHVEIFSPGTGMPDWQLTAKEARLNRSVIGAAPYVDAQALLTRQDAVSGVMLRG		
VEPSLEPQVSDIGKDMKAGALTALAPGQFGIVLGNALAGNLGVGVGDKVTLVAPEGTITP		
AGMMPRLKQFTVVGIFESGHYEYDSTLAMIDIQDAQALFRLPAPTGVRLRLTDMQKAPQV		
ARELAHTLSGDLYIRDWTQQNKTWFSAVQIEKR	MMFIILTIIAFAAFNLVSSLVM	TVTN
KQADIAILRTLGAQPGSIMKIFVVOGVT	IGFVGTATGVALGCLIAWSIPWL	IPMIEHAFG
VQFLPPSVYFISELPSE	LVAGDVIKIGVIAFALSALATLY	PSWRGAKVRPAEALRYE

Figure 46 Overlay of TMHMM transmembrane helices prediction onto the amino acid sequence of LoIC. Illustrated are the amino acid sequences predicted to be inside the membrane, spanning the membrane and outside the membrane. The amino acid sequence of the major extracellular portion of the protein, highlighted in red was inserted into Tandem Core™ as a fusion construct.

4.3.2 In-silico *Burkholderia* protein MHC-I and MHC-II epitope predictions

For all proteins, MHC-I predictions for H2-Kd, Dd, Ld and MHC-II predictions I-Ad and I-Ed were performed. For clarity, the output for LoIC only is shown below in Figure 48 to Figure 56. The output for all other *Burkholderia* proteins is given in the supplementary information section 4.5.3. H2-Kd MHC-I predictions can also be performed on the basis of decamer sequence size. This was carried out for each protein sequence (Figure 49).

To increase confidence, sequences were generated from three different programs for each MHC region, with the exception of I-Ed as three different programs were not available. The top 10 highest scoring sequences generated by each program were taken for comparison to the other sequences predicted for that MHC gene. Sequences highlighted in red were predicted by all three programs and sequences highlighted in green were predicted by two of the three programs. These sequences were collated into a single shortlist for each region and then expanded to include the shortlists for each other region to give the total MHC-I or MHC-II predictive output (Figure 52 and Figure 56). An illustration of the procedure used to generate MHC-I predictions is shown in Figure 47, although this was the same procedure used for MHC-II predictions.

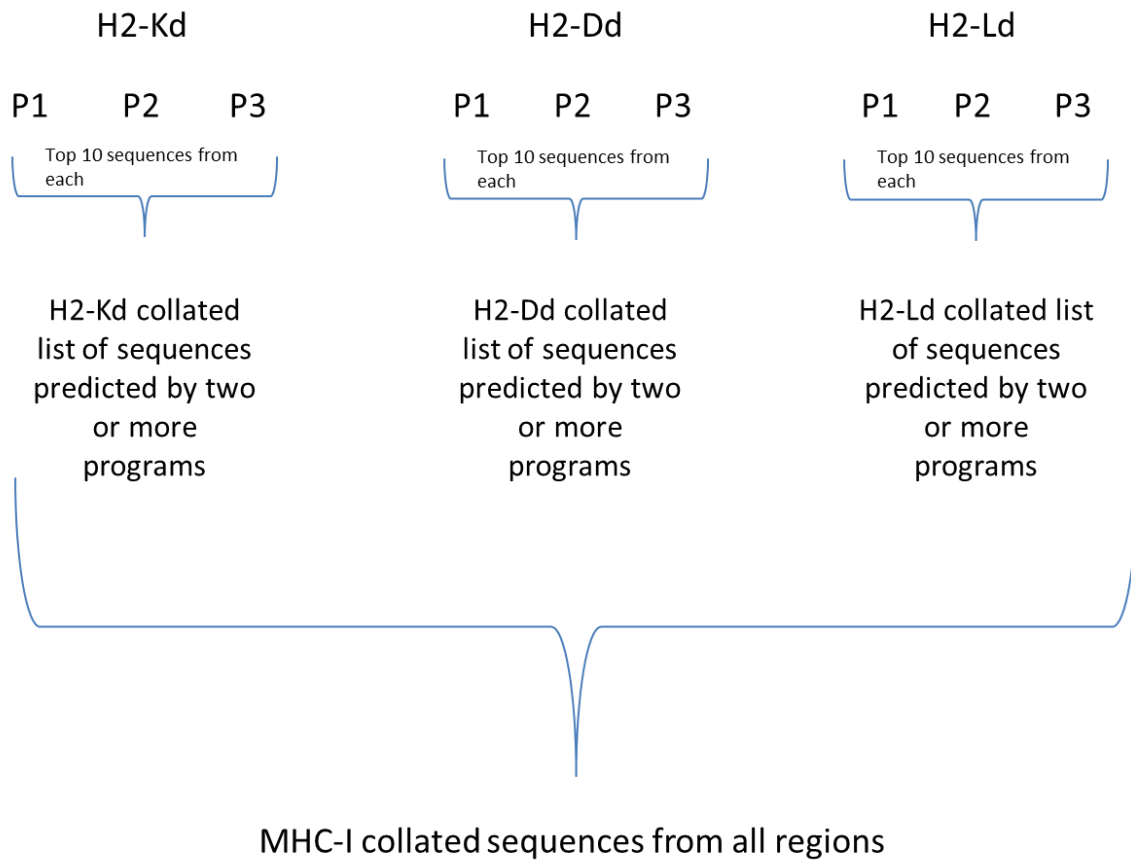


Figure 47 A flow diagram for generation of MHC-I epitope predictions. Three programs (P1-P3) were used to generate epitope predictions for H2-Kd, Dd and Ld with the 10 highest scoring sequences compared within each MHC-I region. Sequences that were predicted by at least two of the programs were collated into a shortlist. Each shortlist was then collated into the final MHC-I predicted epitope sequences

Syfpeithi			
H2-Kd			
Start	End	Sequence NONAMER	% of max score
99	107	PYVDAQALL	65.78%
330	338	GFVGTATGV	65.78%
27	35	SFIALVSML	60.52%
202	210	EYDSTLAMI	60.52%
321	329	IFVVQGVTI	57.89%
37	45	IALGVAALI	55.26%
200	208	HYEYDSTLA	52.63%
376	384	SELVAGDVI	52.63%
219	227	FRLPAPTGV	50%
24	32	GFISFIALV	47.36%

Immuneepitope			
H2-Kd			
Start	End	Sequence NONAMER	Percentile rank
27	35	SFIALVSML	0.1
124	132	SLEPQVSDI	1
18	26	KRTTGNNGFI	1.2
43	51	ALIVVLSVM	1.7
286	294	AAFNLVSSL	1.8
149	157	FGIVLGNAL	1.9
136	144	MKAGALTAL	2.2
332	340	VGATGVAL	2.6
303	311	ADIAILRTL	3.1
388	396	VIAFALSAL	3.1

Propred			
H2-Kd			
Start	End	Sequence	% of Highest on log scale
202	210	EYDSTLAMI	96.09
27	35	SFIALVSML	93.4
275	283	MFIIITLII	91.2
321	329	IFVVQGVTI	89
330	338	GFVGTATGV	76.68
24	32	GFISFIALV	74.48
99	107	PYVDAQALL	74.48
287	295	AFNLVSSLV	68.32
149	157	FGIVLGNAL	57.26
163	171	VGVGDKVTL	57.26

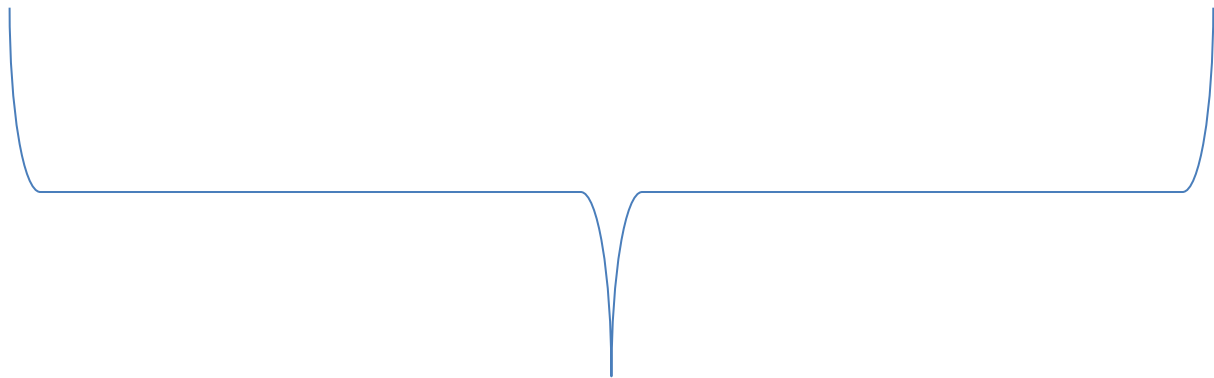
Start	Common sequences	Score		
		Syfpeithi	Immuneepitope	Propred
27	SFIALVSML	60.52	0.1	93.4
330	GFVGTATGV	65.78	-	76.68
99	PYVDAQALL	65.78	-	74.48
202	EYDSTLAMI	60.52	-	96.09
321	IFVVQGVTI	57.89	-	89
24	GFISFIALV	47.36	-	74.48
149	FGIVLGNAL	-	1.9	57.26

Figure 48 The top 10 highest scoring LoIC protein H2-Kd (MHC-I) nonamer epitope predictions from Syfpeithi, Immuneepitope and Propred. Sequences highlighted in red are predicted by all three programs, sequences highlighted in green are predicted by two programs. Sequences highlighted red or green are tabulated to form a shortlist to merge with similar results from the other alleles.

Syfpeithi			
H2-Kd			
Start	End	Sequence DECAMER	% of max score
362	371	QFLPPSVYFI	Not given
369	378	YFISELPSEL	Not given
218	227	LFRLPAPTV	Not given
399	408	LYPSWRGAKV	Not given
390	399	AFALSALATL	Not given
148	157	QFGIVLGNAL	Not given
273	282	RMMFIILTLI	Not given
309	318	RTLGAQPGSI	Not given
116	125	VMLRGVEPSL	Not given
135	144	DMKAGALTAL	Not given

Immuneepitope			
H2-Kd			
Start	End	Sequence DECAMER	Percentile rank
99	108	PVYDAQALLT	0.6
399	408	LYPSWRGAKV	0.7
252	261	LYIRDWTQQN	1.4
368	377	VYFISELPSE	1.5
62	71	MLSVLAHVEI	2
309	318	RTLGAQPGSI	2.1
262	271	KTWFSAVQIE	2.2
169	178	VTLVAPEGTI	2.3
123	132	PSLEPQVSDI	3
205	214	STLAMIDIQD	3.8

NetMHC 3.2			
H2-Kd			
Start	End	Sequence DECAMER	affinity (nM)
85	94	KEARLNRSVI	583
319	328	KIFVVQGVTI	633
389	398	AFALSALATL	1456
368	377	YFISELPSEL	2143
272	281	RMMFIILTLI	4072
11	20	RYTRAGKRTT	4654
147	156	QFGIVLGNAL	5174
199	208	HYEYDSTLAM	5662
134	143	DMKAGALTAL	6834
38	47	LGVAALIVVL	7097



Start	Common sequences	Score		
		Syfpeithi	Immuneepitope	NetMHC 3.2
369	YFISELPSEL	19	1.5	2143
399	LYPSWRGAKV	18	0.7	-
390	AFALSALATL	17	-	1456
148	QFGIVLGNAL	16	-	5174
273	RMMFIILTLI	16	-	4072
309	RTLGAQPGSI	16	2.1	-
135	DMKAGALTAL	1	-	6834

Figure 49 The top 10 highest scoring LoIC protein H2-Kd (MHC-I) decamer epitope predictions from Syfpeithi, Immuneepitope and NetMHC3.2. Sequences highlighted in red are predicted by all three programs, sequences highlighted in green are predicted by two programs. Sequences highlighted red or green are tabulated to form a shortlist to merge with similar results from the other alleles.

NetMHC 3.2			
H2-Dd			
Start	End	Sequence	affinity (nM)
76	84	SMPDWQLTA	275
398	406	LYPSWRGAK	3257
120	128	VEPSLEPQV	3630
96	104	AAPYVDAQA	4275
313	321	QPGSIMKIF	5937
363	371	LPPSVYFIS	6400
181	189	GMMPRLKQF	8958
362	370	FLPPSVYFI	9040
331	339	VGATGVAL	10081
2	10	LPYEWQIGW	10918

Immuneepitope			
H2-Dd			
Start	End	Sequence Octamer	Percentile rank
183	190	MMPRLKQF	0.2
32	39	VSMLGIAL	0.3
389	396	IAFALSAL	0.3
274	281	MMFILTLL	0.7
283	290	IAVAAFNL	0.8
344	351	IAWSIPWL	0.8
367	374	SVYFISEL	0.9
41	48	VAALIVVL	1
363	370	FLPPSVYF	1
347	354	SIPWLIPM	1.4

Propred			
H2-Dd			
Start	End	Sequence	% of Highest on log scale
236	244	KAPQVAREL	31.6
149	157	FGIVLGNAL	29.89
153	161	LGNALAGNL	29.89
23	31	NGFISFIAL	28.17
332	340	VGATGVAL	28.17
347	355	SIPWLIPMI	23.37
363	371	FLPPSVYFI	23.37
21	29	TGNGFISFI	21.66
75	83	TGSMPDWQL	21.66
313	321	AQPGSIMKI	21.66

	Common sequences	Score		
		NetMHC 3.2	Immuneepitope	Propred
363	LPPSVYFIS	6400	0.9	23.37
76	SMPDWQLTA	275	-	21.66
313	QPGSIMKIF	5937	-	21.66
181	GMMPRLKQF	8958	0.2	-
331	VGATGVAL	10081	-	28.17

Figure 50 The top 10 highest scoring LoIC protein H2-Dd (MHC-I) epitope predictions from NetMHC3.2, Immuneepitope and Propred. Sequences highlighted in red are predicted by all three programs, sequences highlighted in green are predicted by two programs. Sequences highlighted red or green are tabulated to form a shortlist to merge with similar results from the other alleles.

Syfpeithi			
H2-Ld			
Start	End	Sequence	% of max score
221	229	LPAPTGVRL	80.64%
145	153	APGQFGIVL	70.96%
223	231	APTGVRLRL	70.96%
98	106	APYVDAQAL	67.74%
179	187	TPAGMMPRL	67.74%
314	322	QPGSIMKIF	67.74%
63	71	LSVLAHVEI	58.06%
366	374	PSVYFISEL	58.06%
26	34	ISFIALVSM	54.83%
346	354	WSIPWLIPM	54.83%

Immuneepitope			
H2-Ld			
Start	End	Sequence	Percentile rank
26	34	ISFIALVSM	0.95
179	187	TPAGMMPRL	1.1
282	290	IIAVAAFNL	1.35
98	106	APYVDAQAL	1.65
145	153	APGQFGIVL	1.65
364	372	LPPSVYFIS	1.65
221	229	LPAPTGVRL	1.75
314	322	QPGSIMKIF	1.95
299	307	TNKQADIAI	2.1
355	363	IEHAFGVQF	2.25

Propred			
H2-Ld			
Start	End	Sequence	% of Highest on log scale
314	322	QPGSIMKIF	87.03
98	106	APYVDAQAL	76.45
145	153	APGQFGIVL	76.45
179	187	TPAGMMPRL	76.45
221	229	LPAPTGVRL	76.45
223	231	APTGVRLRL	76.45
3	11	LPYEWQIGW	62.47
73	81	SPTGSMPDW	62.47
400	408	YPSWRGAKV	62.47
237	245	APQVARELA	58.08

Start	Common sequences	Score		
		Syfpeithi	Immuneepitope	Propred
221	LPAPTGVRL	25	1.75	76.45
145	APGQFGIVL	22	1.65	76.45
98	APYVDAQAL	21	1.65	76.45
179	TPAGMMPRL	21	1.1	76.45
314	QPGSIMKIF	21	1.95	87.03
366	PSVYFISEL	18	1.65	-
26	ISFIALVSM	17	0.95	-

Figure 51 The top 10 highest scoring LoIC protein H2-Ld (MHC-I) nonamer epitope predictions from Syfpeithi, Immuneepitope and Propred. Sequences highlighted in red are predicted by all three programs, sequences highlighted in green are predicted by two programs. Sequences highlighted red or green are tabulated to form a shortlist to merge with similar results from the other alleles.

Start	Sequence	Region
24	GFISFIALV	Kd
26	ISFIALVSM	Ld
27	SFIALVSML	Kd
76	SMPDWQLTA	Dd
98	APYVDAQAL	Ld
99	PYVDAQALL	Kd
135	DMKAGALTAL	Kd
145	APGQFGIVL	Ld
148	QFGIVLGNAL	Kd
149	FGIVLGNAL	Kd
179	TPAGMMPRL	Ld
181	GMMPRLKQF	Dd
202	EYDSTLAMI	Kd
221	LPAPTVRL	Ld
273	RMMFIILTLI	Kd
286	AAFNLVSSL	Kd
309	RTLGAQPGSI	Kd
313	QPGSIMKIF	Dd
314	QPGSIMKIF	Ld
321	IFVVQGVTI	Kd
330	GFVGTATGV	Kd
331	VGATATGVAL	Dd
363	LPPSVYFIS	Dd
366	PSVYFISEL	Ld
369	YFISELPSEL	Kd
390	AFALSALATL	Kd
399	LYPSWRGAKV	Kd

Figure 52 Predicted LoIC MHC-I epitopes collated from shortlists generated for each H2-d allele. Sequences highlighted in red are predicted by all three programs for each allele and sequences highlighted in green by two of the three programs

The data from Figure 52 shows that LoIC MHC-I epitopes for the BALB/c mouse are spread across the whole amino acid sequence. Sequences for multiple MHC-I alleles start at amino acid positions 24-35, 98-107, 145-157, 179-190, 309-323, 330-340 and 363-377 and are highlighted on the amino acid sequence of LoIC which also shows the transmembrane helices predictions (Figure 53).

Inside membrane	Membrane spanning domain	Outside membrane
MKLPYEWQIGWRYTRAGKRTTGN	<u>GFISFIALVSMLGIALGVAALIV</u>	VLSVMNGFQKEVRD
RMLSVLAHVEIFSPTGSMQDWQLTAKEARLNRSVIGAA	<u>APYVDAQALL</u>	TRQDAVSGVMLRG
VEPSLEPQVSDIGKDMKAGALTAL	<u>APGQFGIVLGNAL</u>	AGNLGVGVGDKVTLVAPEGTI <u>TP</u>
<u>AGMMPRLKQF</u>	TVVVGIFESGHYEYDSTLAMIDIQDAQALFRLPAPTGVRLRLTDMQKAPQV	
ARELAHTLSGDLYIRDWTQQNKTWFSAVQIEKR	MMFIILTLLIIAVAAFNLVSSLVM	<u>TVTN</u>
<u>KQADIAILRTLGAQPGSIMKIFV</u>	<u>VQGVTI</u>	<u>IGFVGTATGVAL</u>
<u>VQFLPPSVYFISELPSE</u>	LVAGDVIKIGVIAFALSALATLY	<u>PSWRGAKVRPAEALRYE</u>

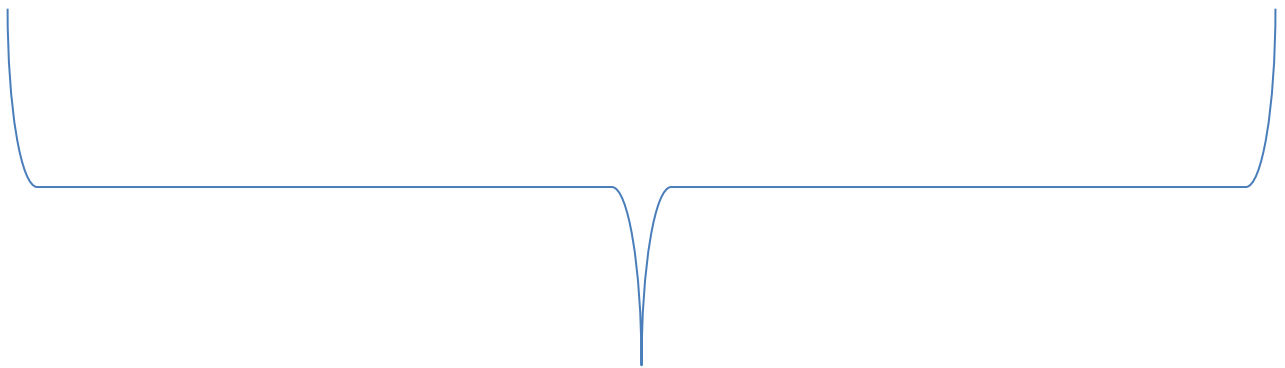
Figure 53 LoIC amino acid sequence highlighting transmembrane helices and MHC-I epitope predictions. Transmembrane helices predictions are highlighted in green, cyan or yellow and MHC-I epitope predictions in bold with underlined text for amino acid positions 24-35, 98-107, 145-157, 179-190, 309-323, 330-340 and 363-377

Figure 54 to Figure 56 show the LoIC MHC-II epitope predictions

Syfpeithi			
I-Ad			
Start	End	Sequence (15-mer)	Score
276	290	FIILTLIIAVAAFNL	30
77	91	SMPDWQLTAKEARLN	29
132	146	IGKDMKAGALTALAP	29
391	405	FALSALATLYPSWRG	28
35	49	LGIALGVAALIVVLS	27
38	52	ALGVAALIVVLSVMN	27
95	109	IGAAPYVDAQALLTR	27
279	293	LTLIIAVAAFNLVSS	27
400	414	YPSWRGAKVRPAEAL	27
24	38	GFISFIALVSMGLIA	26

Immuneepitope			
I-Ad			
Start	End	Sequence (15-mer)	Percentile rank
204	218	DSTLAMIDIQDAQAL	0.2
205	219	STLAMIDIQDAQALF	0.23
203	217	YDSTLAMIDIQDAQA	0.28
202	216	EYDSTLAMIDIQDAQ	0.47
206	220	TLAMIDIQDAQALFR	0.53
207	221	LAMIDIQDAQALFRL	0.53
201	215	YEYDSTLAMIDIQDA	0.57
229	243	LRLTDMQKAPQVARE	0.75
228	242	RLRLTDMQKAPQVAR	0.87
227	241	VRLRLTDMQKAPQVA	0.98

NetMHCII			
I-Ad			
Start	End	Sequence (15-mer)	% rank
133	147	GKDMKAGALTALAPG	0.3
132	146	IGKDMKAGALTALAP	0.3
131	145	DIGKDMKAGALTALA	0.3
130	144	SDIGKDMKAGALTAL	0.4
297	311	TVTNNKQADIAILRTL	0.4
300	314	NKQADIAILRTLGAQ	0.6
299	313	TNKQADIAILRTLGA	0.6
298	312	VTNKQADIAILRTLGA	0.6
226	240	GVRRLTDMQKAPQV	0.6
227	241	VRLRLTDMQKAPQVA	0.7

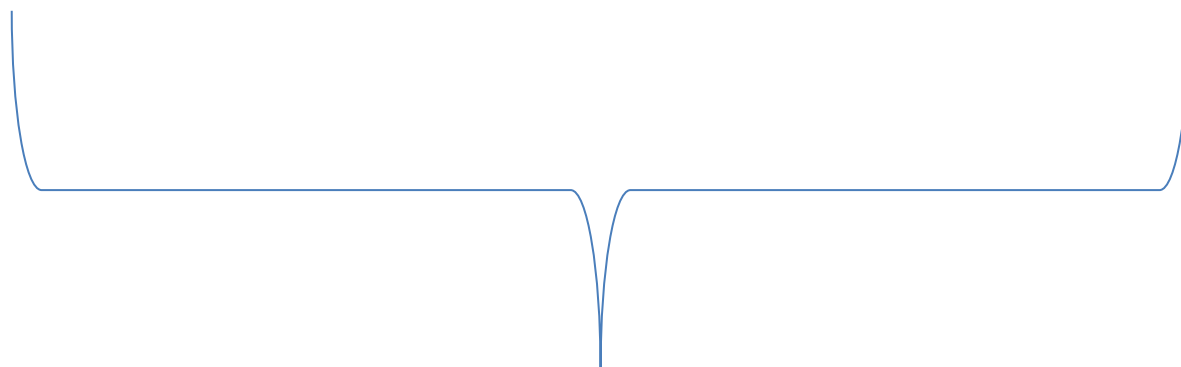


		Score		
	Common sequences	Syfpeithi	Immuneepitope	NetMHCII
132	IGKDMKAGALTALAP	29	-	0.3
229	LRLTDMQKAPQVARE	-	0.75	0.3
228	RLRLTDMQKAPQVAR	-	0.87	0.6
227	VRLRLTDMQKAPQVA	-	0.98	0.7

Figure 54 The top 10 highest scoring LoIC protein H2 I-Ad (MHC-II) epitope predictions from Syfpeithi, Immuneepitope and NetMHCII. Sequences highlighted in green are predicted by two of the three programs and were tabulated to form a shortlist to merge with the shortlist for H2 I-Ed.

Syfpeithi			
I-Ed			
Start	End	Sequence (15-mer)	Score
262	276	KTWFSAVQIEKRMMF	28
8	22	QIGWRYTRAGKRTTG	26
2	16	KLPYEWQIGWRYTRA	20
397	411	ATLYPSWRGAKVRPA	20
4	18	PYEWQIGWRYTRAGK	18
51	65	MNGFQKEVRDRMLSV	18
78	92	MPDWQLTAKEARLNR	18
126	140	EPQVSDIGKDMKAGA	18
261	275	NKTWFSAVQIEKRMM	18
9	23	IGWRYTRAGKRTTGN	16

Immuneepitope			
I-Ed			
Start	End	Sequence (15-mer)	Percentile rank
5	19	YEWQIGWRYTRAGKR	10.04
7	21	WQIGWRYTRAGKRRT	10.53
6	20	EWQIGWRYTRAGKRRT	10.72
8	22	QIGWRYTRAGKRTTG	11.42
4	18	PYEWQIGWRYTRAGK	13.22
396	410	LATLYPSWRGAKVRP	13.97
395	409	ALATLYPSWRGAKVR	14.42
397	411	ATLYPSWRGAKVRPA	15.14
394	408	SALATLYPSWRGAKV	15.98
9	23	IGWRYTRAGKRTTGN	17.01



	Common sequences	Score	
		Syfpeithi	Immuneepitope
8	QIGWRYTRAGKRTTG	26	11.42
397	ATLYPSWRGAKVRPA	20	15.14
4	PYEWQIGWRYTRAGK	18	13.22
9	IGWRYTRAGKRTTGN	16	17.01

Figure 55 The top 10 highest scoring LoIC protein H2 I-Ed (MHC-II) epitope predictions from Syfpeithi and Immuneepitope. There is not another program available for I-Ed predictions. Sequences highlighted in red are predicted by both programs and were tabulated to form a shortlist to merge with the shortlist for H2 I-Ad.

The common sequences predicted for the H2 I-Ad and H2 I-Ed regions are collated into a single table (Figure 56). The common sequences are located mainly in the region located intracellularly as highlighted on the amino acid sequence of LoIC showing the transmembrane helices predictions (Figure 57).

Start	Sequence	Region
4	PYEWQIGWRYTRAGK	Ed
8	QIGWRYTRAGKRTTG	Ed
9	IGWRYTRAGKRTTGN	Ed
132	IGKDMKAGALTALAP	Ad
227	VRLRLTDMQKAPQVA	Ad
228	RLRLTDMQKAPQVAR	Ad
229	LRLTDMQKAPQVARE	Ad
397	ATLYPSWRGAKVRPA	Ed

Figure 56 MHC-II collated LoIC sequences from both alleles of the H2-d region. Sequences highlighted in red are predicted by all three programs for each allele, with the exception of I-Ed, and sequences highlighted in green by two of the three programs

Inside membrane **Membrane spanning domain** **Outside membrane**

MKL**PYEWQIGWRYTRAGKRTTGN**GFISFIALVSMLGIALGVAALIVVLSVMNGFQKEVRD
RMLSVLAHVEIFSPGTGSMQDWQLTAKEARLNRSVIGAAPYVDAQALLTRQDAVSGVMLRG
VEPSLEPQVSD**IGKDMKAGALTALAP**GGFGIVLGNALAGNLGVGVGDKVTLVAPEGTITP
AGMMPRLKQFTVVGIFESGHYEYDSTLAMIDIQDAQALFRLPAPT**G**VRLRLTDMQKAPQV****
ARELAHTLSGDLYIRDWTQQNKTWFSAVQIEKRMMFIILTLIIAFAAFNLVSSLVMTVTN
KQADIAILRTLGAQPGSIMKIFVVQGV**TIGFVGTATGVALGCLIAWSIPWLI**PMIEHAFG
VQFLPPSVYFISELPSE**LVAGDV**IKIGVIAFALSAL**ATLYPSWRGAKVRPAEALRYE**

Figure 57 LoIC amino acid sequence highlighting transmembrane helices and MHC-II epitope predictions. Transmembrane helices predictions are highlighted in green, cyan or yellow and MHC-II epitope predictions in bold with underlined text for amino acid positions 4-23, 132-146, 227-243 and 397-411

From the MHC predictions, the development of a truncated form of LoIC (aa 47 to 273 – the amino acid sequence for the large extracellular loop highlighted in yellow) would contain MHC-I epitopes for the Ld, Kd and Dd allele and the MHC-II epitopes for Ad as shown in Figure 58.

Inside membrane	Membrane spanning domain	Outside membrane
MKLPYEWQIGWRYTRAGKRRTTGN	GFISFIALVSMGLGIALGVAALIV	VLSVMNGFQKEVRD
RMLSVLAHVEIFSPTGSPDPWQLTAKEARLNRSVIGA	<u>APYVDAQALL</u>	TRQDAVSGVMLRG
VEPSLEPQVSD	<u>IGKDMKAGALTALAPGQFGIVLGNAL</u>	AGNLGVGVDKVTLVAPEGTI <u>TP</u>
<u>AGMMPRLKQF</u>	TVVGI FESGHYEYDSTLAMIDIQDAQALFRLPAPTG	<u>VRLRLTDMQKAPQV</u>
<u>ARELAHTLSGDLYIRDWTQQNKTFWSAVQIEKR</u>	MMFIILTLIIAVAAFNLVSSLVMTVTN	
<u>KQADIAILLRTLGAQPGSIMKIFVVQGV</u>	<u>IGFVGTATGVALGCLIAWSIPWLI</u>	<u>IPMIEHAFG</u>
<u>VQFLPPSVYFISELPSE</u>	<u>LVAGDVIKIGVIAFALSALATLY</u>	<u>PSWRGAKVRPAEALRYE</u>

Figure 58 LoIC amino acid sequence highlighting transmembrane helices, MHC-I and MHC-II epitope predictions. Transmembrane helices predictions are highlighted in green, cyan or yellow. MHC-I epitope predictions are in bold with underlined text for amino acid positions 98-107, 145-157 and 179-190 and the MHC-II epitope predictions in bold and underlined text for amino acid positions 132-146 and 227-243

4.4 Discussion

It is hypothesised that a fully efficacious vaccine for melioidosis will need to develop both humoral and cellular protective immune responses (Healey *et al.*, 2005, Silva and Dow, 2013). In this thesis, the protective antibody-generating antigen of the vaccine is CPS, which has already shown to be protective against *B. pseudomallei* challenge (Nelson *et al.*, 2004). The objective of this chapter was to identify *Burkholderia* proteins which provide cellular immunity with melioidosis relevant T-cell epitopes. Selected proteins were mixed as co-antigens in a CPS conjugate vaccine or expressed as fusion proteins on the surface of the Tandem Core™ VLP.

Burkholderia proteins were chosen on the basis that they were proven protective antigens against *B. pseudomallei* challenge or provided an immunostimulatory effect (Harland *et al.*, 2007a, Tippayawat *et al.*, 2009, Su *et al.*, 2010, Burtnick *et al.*, 2011). Preference was given to proteins located extracellularly as they would be amongst the first antigens recognised by cells of the immune system. The proteins chosen for inclusion in this thesis were LoIC, PotF, OppA, Omp85, Hcp2 and Hcp6.

Hepatitis B core antigen (HBcAg) is known to be assembly competent containing fusion peptides within the MIR spike up to approximately 100 amino acids (Pumpens and Grens, 2001) and fusion of two HBcAg open reading

frames to produce the HBcAg dimer as a single polypeptide chain (Tandem Core™) permits insertion of green fluorescent protein (GFP) with VLP assembly (Peyret *et al.*, 2015). Unfortunately, the *Burkholderia* proteins selected in this thesis hindered VLP formation of the Tandem Core™ fusion construct. The reason for this is not known but factors which affect VLP assembly of non-Tandem Core™ HBcAg fusion constructs include molecular size of the protein insert and unfavorable physicochemical characteristics such as hydrophobicity (Pumpens and Grens, 2001). Molecular weight is not the sole predictor of Tandem Core™ VLP assembly as truncated LolC has an estimated molecular weight of 24.6 kDa in comparison to 26.9 kDa for GFP. The main factor is likely to be the differences in amino acid sequence and hydrophobicity. In addition, proximity of the insert N to C termini, which is unknown for these proteins, is instrumental for hepatitis B core assembly as juxtaposed termini fit within the 10 Å distance between the Asp-78 and Ser-81 insert acceptor sites within the core monomer and therefore maintains native VLP structure (Walker *et al.*, 2008). This may explain the failure to insert Hcp2 and Hcp6 as the N and C termini for *Acinetobacter baumannii* Hcp are located on opposite sides of the subunit (Ruiz *et al.*, 2015). Although Tandem Core™ fusion constructs were not assembly competent, it was demonstrated in this thesis that full-length LolC was correctly expressed and so demonstrates the validity of this approach. Further work to identify compliant *Burkholderia* proteins would be beneficial.

The assembly failure of Tandem Core™ fused with full-length LolC or OppA was initially thought to result from high hydrophobicity due to the presence of transmembrane helices. Based on the predictive output of the TMHMM program, Tandem Core™ constructs containing the truncated forms of LolC were produced by Mologic which contained only the main extracellular domain. To determine whether this construct would have removed important immunogenic areas, MHC-I and MHC-II epitope predictions were performed by multiple programs which suggest that areas of potential immunogenicity are spread across the whole amino acid sequence. The main extracellular domain contained predicted epitopes for all H2-d MHC alleles so a truncated LolC protein should not hinder the generation of an immune response although potential immunodominant and protective epitopes in the membrane spanning

and intracellular domains would be lost and the validation of these in-silico predictions to in-vivo immunogenicity was not determined.

Anticipating that truncated LolC as a fusion construct with Tandem Core™ may still impair VLP assembly, MHC predictions were performed for all *Burkholderia* proteins used in this thesis for insertion of short peptide sequences into Tandem Core™. As immunogenicity is influenced by factors that cannot yet be accurately predicted, an in-vitro T-cell test may be required before this option is pursued (Jawa *et al.*, 2013). This could be performed by mouse vaccination and assessment of spleen or peripheral blood mononuclear cell IFN- γ recall response by ELISpot or ELISA (Shete *et al.*, 2011).

MHC epitope prediction is important as experimental identification is costly and time consuming (Wang *et al.*, 2008) and has been reported to reduce downstream in-vitro testing of therapeutic proteins by at least 20-fold (Jawa *et al.*, 2013). Different methods are available to predict MHC peptide binding motifs, each with their own advantages and disadvantages (Sidney *et al.*, 2008) so predictive immunogenicity screening often involves more than one approach which may include in-silico predictions, in-vitro T-cell assays and in-vivo testing in humanised mouse models (Jawa *et al.*, 2013). In this thesis, computational prediction of MHC epitopes provided reassurance that a truncated form of LolC would be immunogenic, but clinical use of *Burkholderia* peptides in a melioidosis vaccine would require that HLA T-cell predicted peptides replace H2-d predicted peptides and further immunogenicity tests to be performed.

4.5 Supplementary information

4.5.1 Expression of Tandem Core™ with peptide inserts

Attempts to insert *Burkholderia* peptide sequences into Tandem Core™ included various derivatives of the amino acid sequence for LolC from full-length to the large extracellular loop in all four VLP expression systems; plant, yeast, insect cell and bacterial.

Tandem Core™ containing either full-length LoIC insert or truncated LoIC containing the major extracellular domain (ExLoIC) were also expressed in *N. benthamiana*. VLPs were not readily seen by negative stain TEM. Figure 59 shows VLPs are present containing the ExLoIC construct but these were not representative of the entire grid where few fields of view contained VLPs.

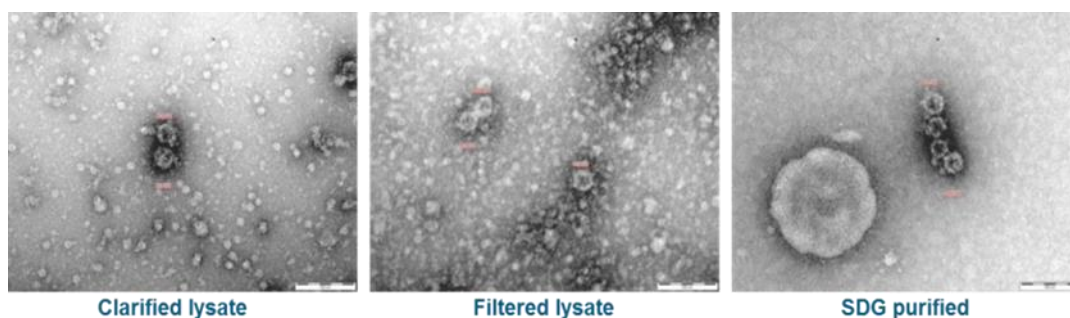


Figure 59 Negative stain TEM images of plant expressed VLP-ExLoIC in clarified lysate, after filtration and sucrose density gradient purification.

LoIC or ExLoIC were also placed in the Tandem Core™ construct and expressed in *P. pastoris*. While high levels of LoIC protein synthesis were demonstrated by dot blot, VLPs were clumped, misassembled and heterologous in size and morphology (data not shown).

4.5.2 Prediction of *Burkholderia* protein membrane spanning domains

The output of TMHMM for PotF transmembrane domain prediction is given in Figure 60. There are no predicted transmembrane domains so only the amino acid sequence is shown in Figure 61. Expression of the PotF fusion construct was successful with as demonstrated by western blot but VLPs were not seen by negative stain TEM (Data not shown).

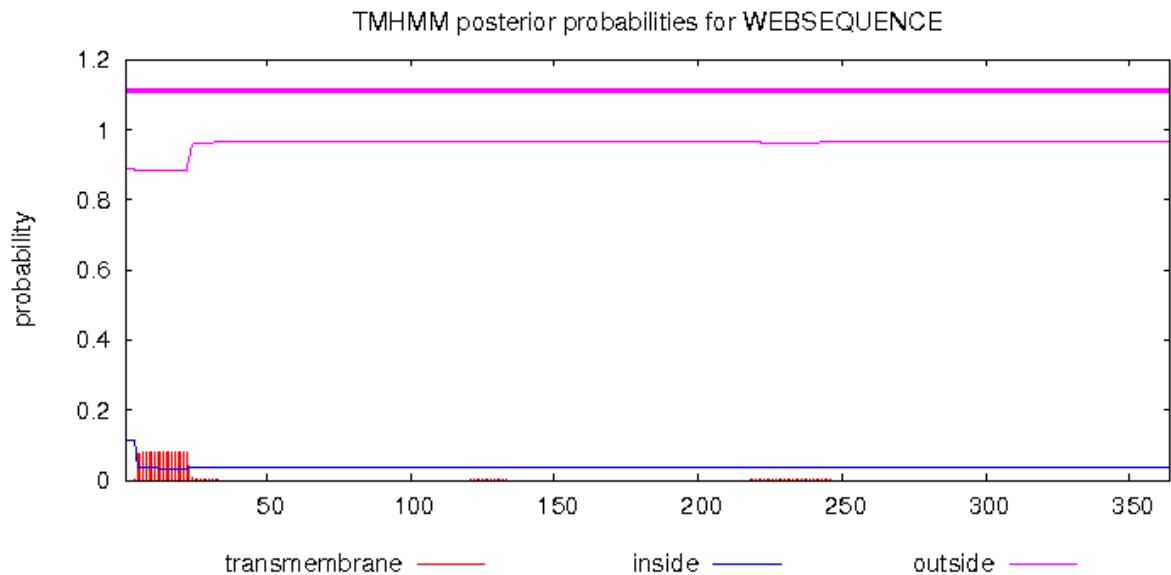


Figure 60 TMHMM calculated probabilities for transmembrane domains within the *Burkholderia* protein PotF [BPSL1555]

PotF [BPSL1555]

```

MKAKVAGRLTALALCAGATVAAAKDTQLNVYNWSDYIAKDTIPNFEKQTGVKVRDNYDSDDTLQAKLLT
GNSGYDIVVPTSNYAGKQIQAGIFTPLDKSKLPNLKYLDAQLMALVAGADPGNKYVVPWAYGTTGLGYNV
DKAQKVLGKVPLDNWDILFKPENLSKPKTCGVSVDLAPDQMF AATLHYIGKDPMSTNPADYQAAMQVLKK
IRPYITQFNSSGYINDMVGGDICFAFGWSDVVI AKHRALEAKKPYKLEYYPKGGAPVWFDVMAIPKDA
KNKDAALQWINYIEDPKVHASITNAVYYPSANAQARKYVRPDVANDPAVYPPPDVVKTLFLLKPLPPEIQ
RLQTRLWTELKSGR

```

Figure 61 Amino acid sequence of PotF. No membrane spanning domains are predicted.

The output of TMHMM for OppA transmembrane domain prediction is given in Figure 62. The first 20 amino acids are predicted to be intracellular, followed by 23 amino acids spanning the membrane and the remainder of the protein located extracellularly (Figure 63). Expression of the OppA fusion construct was successful as demonstrated by western blot but VLPs were not seen by negative stain TEM (Data not shown).

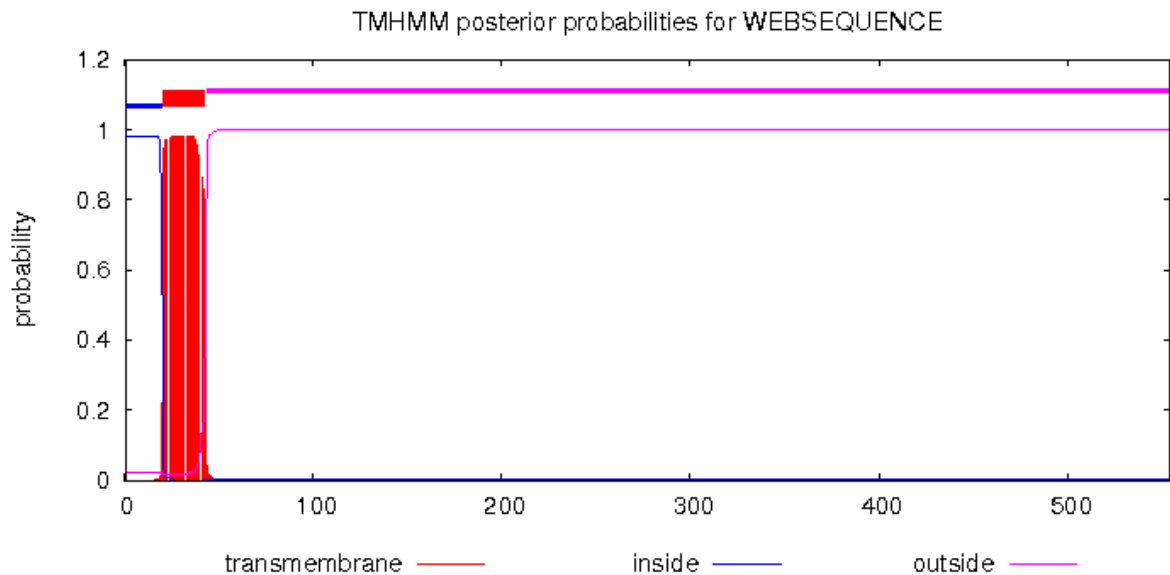


Figure 62 TMHMM calculated probabilities for transmembrane domains within the *Burkholderia* protein OppA [BPSS2141]

OppA [BPSS2141]

Inside membrane	Membrane spanning domain	Outside membrane
MRRALPFRYHYQSHTMKHTH	AFAAVLAALALTIAPSAPAVTVA	SNVTLADQQDLTRQVPAEVESLDPAHI
ESWTGNTIGLDLFEGLARIDASGAVVPGVAQAW	EHKAPDTWIFKLRRDAKWSNGQPVTAADFVYAWQRLA	DPKTGSKYTILVEFVKNASAI IAGKQPPGDLGIRAIDPYTIEVKTEVPVSYFPELTAMAPLTPVNKDAVA
KFGDAWTRPKNIVSNGPYTLVDWQPNNRIVMAKSDKYWNARNVVIRKVTYLP	IENDETALRMYQAGQIDY	TYSI PAGGF'GQISKQFGKELRPGQLATYYYYLKNSDPALDKRVREALAMVLDREILTSKITQAGEVPM
YGLMPKGVKGVQRPFTPDWASWPMARRVDYAKNLLKQAGHGDANPLTFTLTYNTNDLHKKVALFAASEWR	TKLGVTAKLENVEFKVLMKQRHDGKVIARDGWFADYNDAMTFFDLIRCGSSQNTVGYCNPKVDSLVAEA	NQKLDDGARAALLTQAHDLAMNDYPMVPLFQYSADRLVKS YVGGYTLTNYIDMRASQDMYLIKH

Figure 63 Amino acid sequences of OppA highlighting transmembrane helices predictions

The output of TMHMM for Omp85 transmembrane domain prediction is given in Figure 64. There are no predicted transmembrane domains. Due to the lack of success of VLP assembly expressing LolC, PotF or OppA (full protein or truncated extracellular), it was hypothesised that molecular mass may be disrupting VLP assembly. As Omp85 is the largest protein selected (84.9kDa), the decision was taken to exclude Omp85 from the study. The amino acid sequence of Omp85 is below (Figure 65)

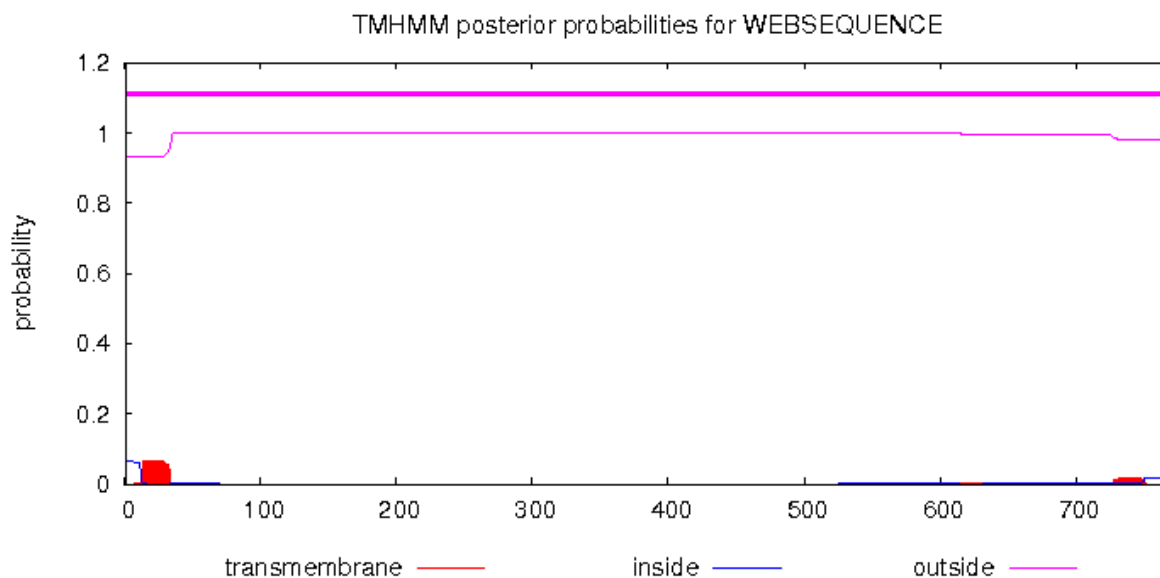


Figure 64 TMHMM calculated probabilities for transmembrane domains within the *Burkholderia* protein Omp85 [BPSL2151]

Omp85 [BPSL2151]

MLFKPHRFVPKTVAAAAALAAHGLAAHATAPFVVQDIKIEGLQRVEAGSVFAYLPIKQGDFTTDDKASEAI
 RALYATGFFNDVRIATQGGVVIVVQVQERPAIASIDFTGIKEFDKDNLNKALKAVGLSQGRYYDKALVDKA
 EQELKRQYLTRGFYAAEVSTTVTPVDANRVSILFAVAEGPSAKIRQINFIGNKAFKTSTLRDEMQLSTPN
 WFSWYTKNDLYSKEKLTGDLENVRSYYLNRGYLEFNIESTQVSI SPDKKDMYLTVALHEGEPYTVSSVKL
 AGNLLDRQAELEKLVKIKPGDRFSAEKLQQTTKAIVDKLGQYGYAFATVNAQPEIDQATHKVGLTLVVDP
 SRRVYVRRINIVGNTRTRDEVVRREMRQLESSWFDSSRLALS KDRVNRRLGYFTDVDVTTVPVEGTNDQVD
 VNVKVAEKPTGAILGAGFSSTDKVVL SAGISQDNVFGSGTSLAVNVNTAKSYRTLTVTQVDPYFTVDGI
 KRITDVFYRTYQPLYYSTNSSFRIITAGGNLKF GIPFSETDTVYFGAGFEQNRLDVSNT PQSYQDYVNE
 FGRVSN TVPLTIGWSRDARDSALIPSRGYFTQANA EYGVPGKIQYYKMDVQGGYYYSFARGFILGLNFQ
 AGYGNIGINPYPIFKNYYAGGIGSVRGYEPSSLGPRD TKTNDPIGGSKMVVGNIELTFPLPGTG YDRTLR
 VFTFLDGGNVWGNAPGGTSTGANGLRYGYIGLAWISP IGP LKLSLGFPLQKHEGDQYQKFQFQIGTAF

Figure 65 Amino acid sequence of Omp85. No membrane spanning domains are predicted.

The output of TMHMM for Hcp2 transmembrane domain prediction is given in Figure 66. There are no predicted transmembrane domains. Expression of the Hcp2 fusion construct was successful with as demonstrated by western blot but VLPs were not seen by negative stain TEM (Data not shown).

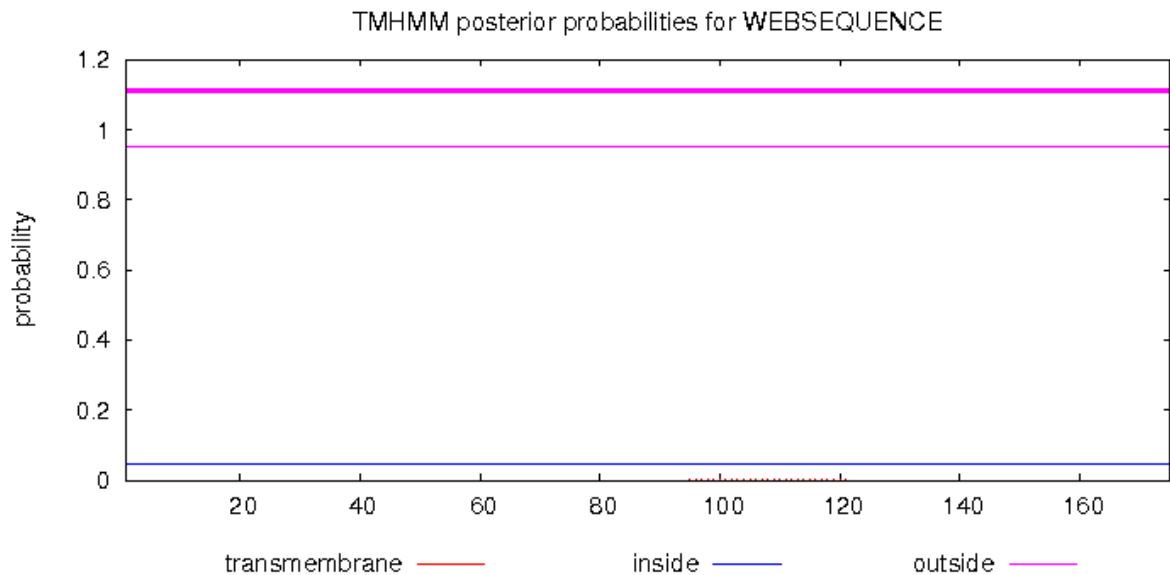


Figure 66 TMHMM calculated probabilities for transmembrane domains within the *Burkholderia* protein Hcp2 [BPSS0518]

Hcp2 [BPSS0518]

MANALVDYFLQIDGVEGESTDQQYPGLIQIQSWQWAEENSGRWGFGSGGGAGKVMKDFEFMVSNKASP
 KLFLMCATGEHIQNAKLICRKSGKGQQEFLTISFASGLVSSFRTLGNMPISQLGHASGEVDGVLPTDQIR
 INFAQIEFEYREQRNDGTMGAVIKAGYDLKQNAP

Figure 67 Amino acid sequence of Hcp2. No membrane spanning domains are predicted.

The output of TMHMM for Hcp6 transmembrane domain prediction is given in Figure 68. There are no predicted transmembrane domains. The amino acid sequence of Hcp6 is shown in Figure 69. Expression of the Hcp6 fusion construct was successful as demonstrated by western blot but VLPs were not seen by negative stain TEM (Data not shown).

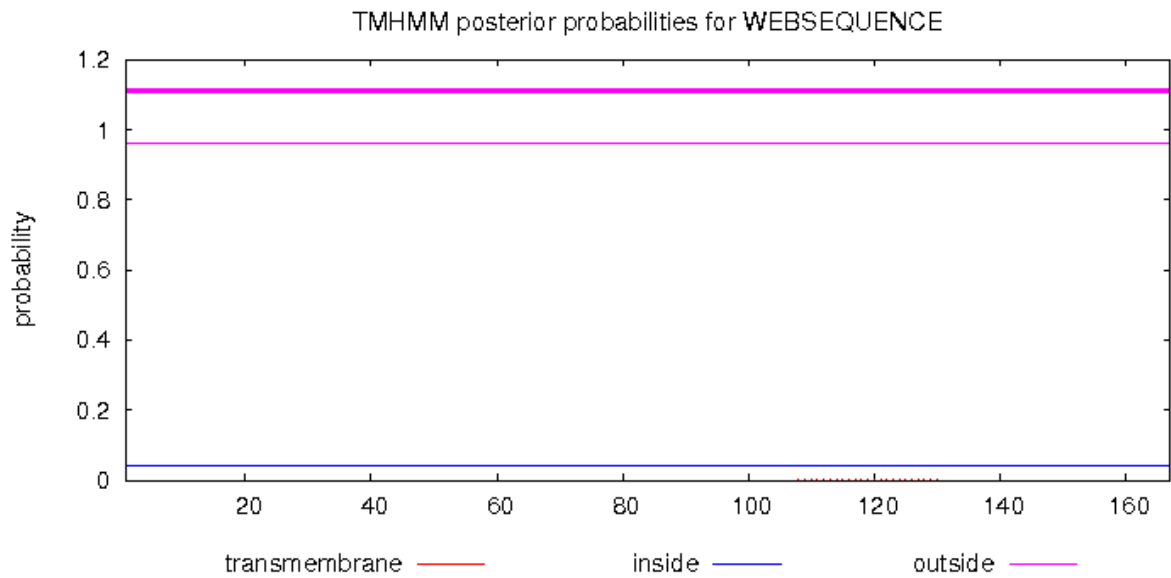


Figure 68 TMHMM calculated probabilities for transmembrane domains within the *Burkholderia* protein Hcp6 [BPSL3105]

Hcp6 [BPSL3105]

MLHMHLLKFGSPAIKGESADKDHEGWIELKSWDHSIVQPRSATASTAGGHTATRCCEHGDMVFTKEIDSSSP
 LLYQHASGGTTFDEVTIDFLRADGEGQRVKYLEIKLKYVVISSIAPSVHTEGLPVETFSLKYAAVQWKQT
 QKIGGNQGGNTQGAWSLTKNDKTYAV

Figure 69 Amino acid sequence of Hcp6. No membrane spanning domains are predicted.

4.5.3 In-silico *Burkholderia* protein MHC-I and MHC-II epitope predictions

Start	Sequence	Region
16	VALAGASAL	Kd
41	WSDYIAKDTI	Dd
91	NYMAKQIQA	Kd
91	NYMAKQIQAG	Kd
101	VYQKLDKSKL	Kd
108	SKLPNLSNL	Kd
113	LSNLDPTLM	Ld
147	NVQAVKKAL	Kd
178	CGVSFLDQAV	Dd
182	SFLDQAVDV	Kd
190	VFAATLQYM	Kd
196	QYMGRNPNST	Kd
206	NPADYQAAF	Ld
209	DYQAAFEVL	Kd
221	RPYITQFNS	Ld
228	NSSGYINDL	Ld
269	FSNPKEGGL	Ld
275	GLLWFDVM	Dd
340	PPEDVLKKM	Ld
351	MRPMPADIL	Dd

Figure 70 MHC-I collated PotF amino acid sequences from all H2-d alleles. Sequences highlighted in red are predicted by all three programs for each allele and sequences highlighted in green by two of the three programs

Start	Sequence	Region
3	VSHLRHAVARAALVA	Ad
5	HLRHAVARAALVALA	Ad
6	HLRHAVARAALVALA	Ad
8	HAVARAALVALAGAS	Ad
10	VARAALVALAGASAL	Ad
17	ALAGASALALPAAHA	Ad
18	LAGASALALPAAHAA	Ad
19	AGASALALPAAHAAG	Ad
20	GASALALPAAHAAGA	Ad
99	AGVYQKLDKSKLPNL	Ed

Figure 71 MHC-II collated PotF sequences from both alleles of the H2-d region. Sequences highlighted in red are predicted by all three programs for each allele, with the exception of I-Ed, and sequences highlighted in green by two of the three programs

Start	Sequence	Region
8	RYHYQSHTM	Kd
21	AFAAVLAAL	Kd
35	PSAPAVTVA	Ld
107	APDTWIFKL	Ld
125	QPVTAADFV	Ld
131	DFVYAWQRL	Kd
147	KYTILVEFV	Kd
153	EFVKNASAI	Kd
178	PYTIEVKTEV	Kd
187	VPVSYFPEL	Ld
190	SYFPELTAM	Kd
190	SYFPELTAMA	Kd
224	NGPYTLVDWQ	Dd
246	KYWNARNVV	Kd
246	KYWNARNVVI	Kd
259	TYLPIENDET	Kd
284	IPAGGFGQI	Ld
311	YYLKNSDPAL	Kd
350	MYGLMPKGV	Kd
366	TPDWASWPM	Ld
372	WPMARRVDY	Ld
477	GVCNPKVDSL	Kd
514	YPMVPLFQY	Ld
519	LFQYSADRL	Kd
530	SYVGGYTLT	Kd
531	VGGYTLNYI	Dd

Figure 72 MHC-I collated OppA amino acid sequences from all H2-d alleles. Sequences highlighted in red are predicted by all three programs for each allele and sequences highlighted in green by two of the three programs

Start	Sequence	Region
17	KHTHFAAVLAALAL	Ad
20	HAFAAVLAALALTIA	Ad
29	THAFAAVLAALALTI	Ad
106	KAPDTWIFKLRRDAK	Ed
110	TWIFKLRRDAKWSNG	Ed
366	TPDWASWPMARRVDY	Ed
405	NDLHKKVALFAASEW	Ad
496	DGARAALLTQAHDLA	Ad

Figure 73 MHC-II collated OppA sequences from both alleles of the H2-d region. Sequences highlighted in red are predicted by all three programs for each allele, with the exception of I-Ed, and sequences highlighted in green by two of the three programs

Start	Sequence	Region
30	PFVVQDIKI	Kd
51	AYLPIKQGD	Kd
51	AYLPIKQGDT	Kd
52	YLPKQDTF	Dd
53	LPIKQGDTF	Ld
73	LYATGFFNDV	Kd
98	RPAIASIDF	Ld
147	QYLTRGFYA	Kd
147	QYLTRGFYAA	Kd
153	FYAAEVSTTV	Kd
179	GPSAKIRQI	Ld
235	SYLNRGYL	Kd
255	SPDKKDMYL	Ld
272	PYTVSSVKL	Kd
276	SSVKLGNL	Ld
321	QYGYAFATV	Kd
348	VDPSRVYVR	Dd
354	VYVRRINIV	Kd
383	WFDSSRLAL	Kd
438	GFSSTDKVV	Kd
455	NVFGSGTSL	Kd
481	VDPYFVDGI	Dd
482	DPYFTVDGI	Ld
488	DGIKRTDVF	Dd
496	VFYRTYQPL	Kd
500	TYQPLYYST	Kd
504	LYSTNSSFR	Kd
505	YYSTNSSFRI	Kd
525	IPFSETDV	Ld
550	TPQSYQDYV	Ld
556	DYVNEFGRV	Kd
596	EYGVPVGKI	Kd
615	YYSFARGFI	Kd
616	YYSFARGFI	Kd
616	YYSFARGFIL	Kd
617	YSFARGFIL	Ld
618	SFARGFILGL	Kd
628	NFQAGYGNGI	Kd
639	NPYPIFKNY	Ld
641	YPIFKNYA	Ld
646	NYYAGGIGSV	Kd
647	YYAGGIGSV	Kd
663	LGPRDKTND	Dd
693	TGYDRLRVF	Dd
697	RTLRFVFTFL	Kd
727	YGYGILAWI	Dd
728	GYGIGLAWI	Kd
736	ISPIGPLKL	Ld
739	IGPLKSLGF	Dd
740	GPLKLSLGF	Ld
757	QYQKFQFQI	Kd

Figure 74 MHC-I collated Omp85 amino acid sequences from all H2-d alleles. Sequences highlighted in red are predicted by all three programs for each allele and sequences highlighted in green by two of the three programs

Start	Sequence	Region
8	FVPKTVAAAALAAHG	Ad
9	VPKTVAAAALAAHGL	Ad
10	PKTVAAAALAAHGLA	Ad
11	KTVAAAALAAHGLAA	Ad
12	TVAAAALAAHGLAAH	Ad
13	VAAAALAAHGLAAHA	Ad
60	TFTDDKASEAIRALY	Ad
61	FTDDKASEAIRALYA	Ad
62	TDDKASEAIRALYAT	Ad
63	DDKASEAIRALYATG	Ad
64	DKASEAIRALYATGF	Ad
65	KASEAIRALYATGFF	Ad
347	VVDPSRRVYVRRINI	Ed
470	AKSYRTLTVTQVDPY	Ad

Figure 75 MHC-II collated Omp85 sequences from both alleles of the H2-d region. Sequences highlighted in red are predicted by all three programs for each allele, with the exception of I-E_d, and sequences highlighted in green by two of the three programs

Start	Sequence	Region
1	MANALVDYF	Ld
2	ANALVDYFL	Ld
7	DYFLQIDGV	Kd
23	QYPGLIQIQ	Kd
24	YPGLIQIQS	Ld
37	EENSGRWGF	Ld
64	VSNKASPKL	Ld
65	SNKASPKLFL	Kd
67	KASPKLFL	Dd
73	FLMCATGEHI	Kd
91	SGKGQQEFL	Dd
91	KSGKGQQEF	Ld
92	SGKGQQEFL	Kd
100	LTISFASGL	Kd
103	SFASGLVSSF	Kd
106	SGLVSSFRTL	Kd
106	GLVSSFRTL	Dd
107	GLVSSFRTL	Kd
110	SSFRTLGNM	Ld
111	SFRTLGNMPI	Kd
113	RTLGNMPISQ	Kd
116	NMPISQLGH	Dd
118	MPISQLGHA	Ld
121	SQLGHASGEV	Kd
126	ASGEVDGVL	Ld
132	VLPTDQIRI	Dd
135	PTDQIRINF	Ld
166	GYDLKQNAPI	Kd

Figure 76 MHC-I collated Hcp2 amino acid sequences from all H2-d alleles. Sequences highlighted in red are predicted by all three programs for each allele and sequences highlighted in green by two of the three programs

Start	Sequence	Region
56	MKDFEFRMVS NKASP	Ed
58	DFEFRMVS NKASPKL	Ad
79	GEHIQNAKLICRKSG	Ed
80	EHIQNAKLICRKSGK	Ed
84	NAKLICRKSGKGQQE	Ed
110	SSFRTLGNMPISQLG	Ad
111	SFRTLGNMPISQLGH	Ad
112	FRTLGNMPISQLGHA	Ad
153	QRNDGTMGAVIKAGY	Ad
155	NDGTMGAVIKAGYDL	Ad

Figure 77 MHC-II collated Hcp2 sequences from both alleles of the H2-d region. Sequences highlighted in red are predicted by all three programs for each allele, with the exception of I-Ed, and sequences highlighted in green by two of the three programs

4.5.4 Programs for transmembrane helices prediction and MHC-I/MHC-II epitope predictions

The software used for prediction of transmembrane domains was TMHMM (<http://www.cbs.dtu.dk/services/TMHMM/>) which is based on a hidden Markov model (HMM) and shown to correctly predict 97-98 % of transmembrane helices (Krogh *et al.*, 2001). The HMM works by defining a set of states corresponding to regions of the protein being modelled which include helix caps, middle of the helix, regions close to the membrane and globular regions. Each state has an associated probability distribution over the 20 amino acids characterising the variability of amino acids in the region it models incorporating hydrophobicity, charge bias and helix lengths. The probability of transition between states is also calculated. Topology is calculated from the states with the highest amino acid and transition probabilities (Sonnhammer *et al.*, 1998, Krogh *et al.*, 2001).

The top 10 highest scoring sequences generated by each program were taken for comparison to the other sequences predicted for that MHC gene. Sequences highlighted in red were predicted by all three programs and sequences highlighted in green were predicted by two of the three programs. These sequences were collated into a single shortlist for each region and then expanded to include the shortlists for each other region to give the total MHC-I

or MHC-II predictive output. These programs were chosen as they are recognised programs for this function and use different methodologies.

For MHC-I predictions, Immunepitope uses the Consensus method consisting of artificial neural networks (ANN), stabilized matrix method (SMM), and CombLib if any corresponding predictor is available for the molecule, otherwise NetMHCpan is used (<http://tools.iedb.org/main/tcell/>).

ProPred is a matrix based method for the prediction of MHC-I binding sites (<http://www.imtech.res.in/raghava/propred1/>). The matrices used were obtained from the BIMAS server (a T-cell epitope prediction server that implements algorithms based on a quantitative matrix-driven method and from the literature. It allows for the simultaneous prediction of MHC binders and proteasome cleavage sites as it has been demonstrated that MHC binders with a cleavage site at the C terminus are likely to be T-cell epitopes (Singh and Raghava 2003).

For the BIMAS method, it is assumed that the amino acids at each position along the sequence contribute with a given binding energy, which when added up yield the overall binding energy of the peptide. This is also the basis of Syfpeithi. These predictions fail to recognize however, where the binding affinity of an amino acid at one position is influenced by amino acids in other positions. Artificial neural networks (ANN) take such correlations into account (Nielsen *et al.*, 2003).

ANN uses a combination of two neural networks using different sequence encoding strategies and input derived from a HMM. One neural network uses a classic orthogonal sparse encoding and another where amino acids are encoded as their Blosom50 scores to the 20 different amino acids. Sparse encoding is where each amino acid is encoded as a 20-digit binary number, with specific series of amino acids corresponding to a certain binding affinity value. Blosom50 is where amino acids are scored for replacement with each of the 20 amino acids based on knowledge of which amino acids are similar and dissimilar to each other (Nielsen *et al.*, 2003).

The SMM method generates quantitative models of the sequence specificity of biological processes which in turn are used to predict these processes. The experimental data used as input consists of same length amino acid sequences associated with a quantitative measurement (Peters and Sette, 2005).

CombLib predicts binding specificity of MHC molecules based on the use of positional scanning combinatorial peptide libraries. The libraries consist of combinatorial mixtures of large numbers of different peptides all sharing a single residue at a certain position. Measuring the binding affinity of each library evaluates the average influence of the shared residue (Sidney *et al.*, 2008).

NetMHCpan uses quantitative peptide MHC binding data consisting of 79,137 unique interactions (Hoof *et al.*, 2009).

For MHC-II predictions, Immunepitope uses the Consensus approach combining NN-align, SMM-align, and CombLib if any corresponding predictor is available otherwise NetMHCIIpan is used (<http://tools.iedb.org/main/tcell/>).

NN-align is a novel artificial neural network based method that allows for simultaneous identification of the MHC II binding core and binding affinity. It encodes peptide flanking residues for amino acid composition and length and deals with data redundancy inherent in peptide data due to multiple examples of identical binding cores (Nielsen and Lund, 2009).

SMM align is also used to simultaneously identify the peptide binding core and predict the binding strength (Nielsen and Lund, 2009).

NetMHCIIpan is a neural network-based algorithm that integrates SMM align with information about the peptide flanking residues (Nielsen and Lund, 2009).

Syfpethi evaluates every amino acid of a peptide and gives a score of 1 if they are only slightly preferred in the respective position while optimal anchor residues are given the value 15. Any value between 1 and 15 is possible as are negative values which are disadvantageous for the peptide's binding capacity at a certain sequence position. The allocation of values is based on the frequency of the respective amino acid in natural ligands, T-cell epitopes, or binding

peptides (<http://www.syfpeithi.de/bin/MHCServer.dll/Info.htm> Rammensee *et al.*, 1999).

NetMHC3.2 predicts the binding of peptides to a number of different MHC-I alleles using ANNs and weight matrices (<http://www.cbs.dtu.dk/services/NetMHC-3.2/> Nielsen *et al.*, 2003).

NetMHCII predicts binding of peptides to HLA-DR, HLA-DQ, HLA-DP and mouse MHC class II alleles using ANNs. The prediction values are given as a percentage rank to a set of 1,000,000 random natural peptides (<http://www.cbs.dtu.dk/services/NetMHCII/> Nielsen and Lund 2009, Nielsen *et al.*, 2007).

Chapter 5: Immunogenicity and efficacy of candidate vaccines

5.1 Introduction

The aim of this chapter was to assess the protective efficacy of CPS chemically conjugated to Crm197, Virus-Like particles (VLP) or a *Burkholderia* protein against an intraperitoneal *B. pseudomallei* challenge in a BALB/c mouse model of melioidosis. CPS for conjugation was extracted from *B. thailandensis* E555 :: *wbil* (Km^r), following inoculation of LB media with a *B. thailandensis* strain E555 :: *wbil* (Km^r) starter culture and incubation for 27 hours at 37°C, shaking at 180 rpm within baffled Erlenmeyer flasks.

Capsular polysaccharide is a known virulence determinant and protective antigen of both *B. pseudomallei* and *B. mallei* (Wikraiphat *et al.*, 2009, Nelson *et al.*, 2004) but polysaccharides generally are T-cell independent antigens and poor inducers of immunological memory (Fernandez *et al.*, 2009). Although some effective vaccines consist of polysaccharide antigen (Jones 2005), it is hypothesised that both a T- and B-cell response is required for a protective *Burkholderia* vaccine (Silva and Dow 2013). In 1931, it was discovered that conjugation of a polysaccharide to a protein augments the immune response to the polysaccharide (Avery and Goebel 1931) which led to development of licensed carbohydrate vaccines for *Haemophilus influenzae* type b and *Streptococcus pneumoniae* where polysaccharide conjugation to a protein carrier invokes T-cell help (Pollabauer *et al.*, 2009, Knuf *et al.*, 2011). It is on this basis that conjugation to a carrier protein is believed necessary for a CPS-based *Burkholderia* vaccine.

Crm197 is a commercially available, non-toxic mutant of *Diphtheria* toxin and is already used in several licensed polysaccharide conjugate vaccines (Knuf *et al.*, 2011). Licensed vaccines containing VLPs are available but with the VLP as the primary antigen such as the hepatitis B virus (HBV) vaccine Engerix[®] which contains purified HBV surface antigen (Kushnir *et al.*, 2012). In this study, the VLP is made of Tandem Core[™] which is a fusion construct of two HBcAg open reading frames to produce HBcAg dimers as a single polypeptide chain (Peyret

et al., 2015). A proposed advantage of Tandem Core™ is insertion of whole proteins within the MIR spike of HBcAg for expression on the surface of assembly competent VLPs. This would allow production of a number of constructs such as a multivalent vaccine containing a VLP expressing a *Burkholderia* protein, chemically conjugated to CPS. VLPs are also highly immunogenic (Kushnir *et al.*, 2012) and may give greater protection against an aerosol challenge than a Crm197 based vaccine which is desirable given the potential exposure of *B. pseudomallei* via the aerosol route which is associated with severe illness and high mortality (Lafontaine *et al.*, 2013).

Throughout this chapter, all VLPs utilised were of heterotandem core. Production of homo-tandem core VLPs was attempted, as the complete absence of contaminating expression-system nucleic acid, through loss of the binding domain, was perceived as an advantage for potential GMP manufacture and licensure. However, stable VLP formation was not achieved with homo-tandem core as a nucleic acid binding domain was found to be essential for assembly.

A further consideration in development of a *Burkholderia* vaccine would be the use of a *Burkholderia* protein as the carrier protein. This would negate potential interference effects from other vaccines that contain Crm197 (Dagan *et al.*, 2010). Use of a *Burkholderia* protein is appropriate if an immunogenic protein, ideally a protective antigen, is found to provide T-cell help for conjugated CPS. This study identified several potential *Burkholderia* protein candidates from the published literature (see Chapter 4; Immunogenic *Burkholderia* proteins) and the protective efficacy of one *Burkholderia* protein-CPS conjugate was determined against intraperitoneal challenge with *B. pseudomallei*.

In addition to testing CPS conjugate vaccines, this study also assessed the protective efficacy of adding the *Burkholderia* proteins LolC, PotF, OppA, and Hcp6 as single co-antigens to a Crm197-CPS conjugate in order to produce a multivalent vaccine.

This work also assessed the protective efficacy of four adjuvants; Alhydrogel®, MF59®, Poly (I:C) with Alum and AS04.

Aluminium compounds have been used as adjuvants for more than 70 years in both human and veterinary vaccines but the most commonly used adjuvants today work by antigen adsorption onto aluminium hydroxide and aluminium phosphate hydrated gels (Lindblad 2004). Alhydrogel® is an aluminium hydroxide wet gel suspension (www.invivogen.com/alhydrogel) and studies have shown that aluminium adjuvants can stimulate Th2 type responses and IL-4 and IL-5 cytokine production but fails to stimulate Th1 responses such as IFN- γ production (Brewer 2006).

Addavax™ is a squalene-based oil-in-water nano-emulsion with a similar formulation to MF59® which is owned by Novartis (www.invivogen.com/addavax). MF59 is licensed in more than 20 countries for use in influenza vaccines (Fluad®) including avian H5N1 (Aflunov®) and H1N1 (Focetria® and Celtura®) influenza. MF59 has shown to be a more potent adjuvant than Alum for the induction of both humoral and cell-mediated responses and enhances the recruitment and activation of antigen presenting cells (APC) and stimulation of cytokines and chemokine production by macrophages and granulocytes (Tritto *et al.*, 2009, O'Hagan *et al.*, 2012).

Polyinosinic-polycytidylic acid (Poly (I:C)) is a synthetic analog of double-stranded RNA and has shown to improve mucosal antigen presentation of HIV antigens by MHC class I molecules. Poly (I:C) activates Toll-like receptor 3 (TLR3) to induce IL-12 and type I IFNs production leading to improved MHC I expression (Liu *et al.*, 2012). It also interacts with the retinoic acid-inducible gene (RIG-I) and melanoma differentiation-associated gene (MDA-5) receptors which are hypothesised to enhance T- and B-cell immunity (Toussi and Massari 2014).

Adjuvant System 04 (AS04) contains the TLR4 agonist monophosphoryl lipid A (MPL) and aluminium salt which promotes cytokine secretion and immune cell activation. It is licensed for use in the HPV vaccine Cervarix™ and Hepatitis B vaccine Fendrix™ and has shown to induce a higher and longer lasting immune response than aluminium salt (Didierlaurent *et al.*, 2009). MPL is a derivative of lipid A from *Salmonella minnesota* R595 and is considerably less toxic than

lipopolysaccharide and promotes a Th1-biased response towards co-administered antigens (Lawson *et al.*, 2011).

The mouse model used in this study is the BALB/c. The proinflammatory cytokine response to *B. pseudomallei* infection and the poor recruitment of macrophages and lymphocytes to clear bacteria mean that BALB/c mice are the established animal model of acute melioidosis (Choh *et al.*, 2013).

Survival following challenge is an important criterion for assessment of vaccine efficacy, but on animal welfare grounds death is not a humane end-point. For all animal studies in this chapter clinical signs were recorded and mice culled upon reaching humane end-points. Although not an exhaustive list, these included pathology involving the eyes or where movement was significantly restricted as common signs of melioidosis in the BALB/c mouse model involve the CNS and include hind limb paralysis and eye protrusion (Morris *et al.*, 2015, Welkos *et al.*, 2015). Analysis of survival data is performed by log-rank Mantel-Cox test. This test compares survival curves giving equal weight to deaths at all time points (Bewick *et al.*, 2004).

In addition to survival and clinical signs, bodyweight was also recorded. Animals which survived until study end were culled and the liver, lung and spleen removed, mashed and plated onto microbiological media for assessment of bacterial load. The liver and spleen are assessed due to the organotropism of *B. pseudomallei* for these tissues (Hoppe *et al.*, 1999) and lung as a measure of systemic spread of the organism.

For clarity, a flow diagram illustrating the animal studies performed in this thesis and a brief justification for them are detailed in Figure 78.

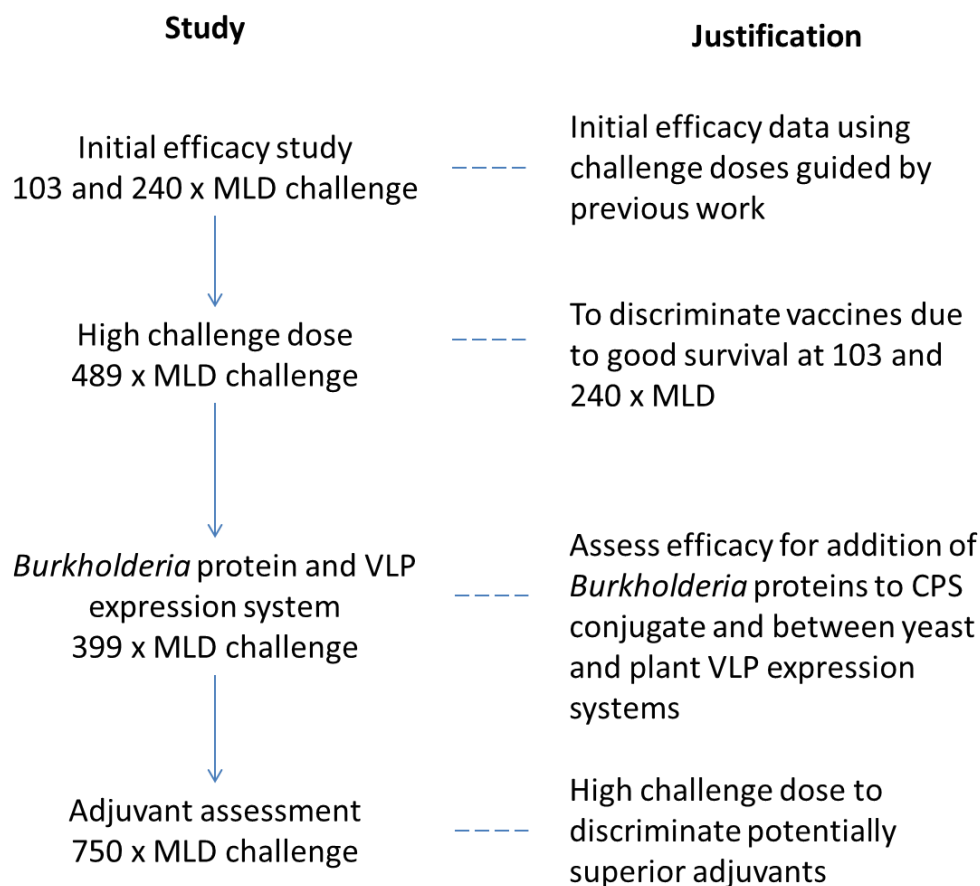


Figure 78 Animal study schedule and justification

5.2 VLP expression systems

VLPs were produced from bacterial (*E. coli*), insect cell (*baculovirus*), plant (*Nicotiana benthamiana*) and yeast (*Pichia pastoris*) expression systems by our collaborators at Mologic and JIC. A summary of these results are given in the supplementary data (5.6.1). Briefly, Tandem Core™ expression by *E. coli* and *baculovirus* was not suitable due to low purity of VLP. The plant and yeast expression systems produced high yields of >80 % pure VLPs which were utilised in challenge experiments. The methods of production are detailed in Chapter 2, Methods 2.12.1 to 2.12.5

5.3 Production and analysis of conjugate vaccines

Chemical conjugation of CPS to carrier protein was achieved by reductive amination. Analysis of the conjugates was performed by phenol sulfuric acid assay (for carbohydrate) and BSA (for protein). All production and analysis was performed by our collaborators at the JIC and methods described in Chapter 2, Method 2.13.1 to 2.13.3.

5.4 Initial vaccine efficacy study of candidates in mice using IP challenge with *B. pseudomallei*

The initial animal challenge experiment was performed to assess efficacy of the conjugate vaccines, especially VLP-CPS since we had no prior experience of this construct. Two different challenge doses of 103 x median lethal dose (MLD) and 240 x MLD were employed which were chosen on the basis of previous work with CPS conjugates (data not shown). BALB/c mice received three immunisations at two-week intervals via the intra-muscular route with the experimental vaccines adjuvantised with Alhydrogel®. Details of vaccine preparation, animal husbandry, immunisation schedule, challenge preparation, statistical analysis and enumeration of bacterial loads are detailed in Chapter 2, method 2.14.1 to 2.14.6. Table 8 details the vaccinations and animal numbers for this study.

Cohort	Vaccine	Number of mice	Adjuvant
A	VLP-CPS (plant)	12	Alum
B	VLP (plant)	12	Alum
C	CPS	12	Alum
D	Crn197-CPS	12	Alum
E	Crn197	12	Alum
F	PBS	12	Alum
G	PBS	12	-

Table 8 Experimental plan for initial efficacy study detailing vaccine candidates, number of mice and adjuvant. For determination of efficacy range for these candidates, six mice from each cohort were challenged with either 103 or 240 x median lethal doses of *B. pseudomallei* K96243 via the intra-peritoneal route and observed for 35 days.

Groups of twelve mice were immunised with either VLP-CPS, VLP, CPS, Crn-197, Crn-197-CPS or PBS, challenged with either 7.66×10^4 CFU (103 x median lethal doses (MLD)) or 1.79×10^5 CFU (240 x MLD) of *B. pseudomallei* K96243 via the intra-peritoneal route (IP) and observed for 35 days in order to determine appropriate challenge doses and group sizes for full efficacy testing in the next study using IP challenge with *B. pseudomallei*. Tail bleeds were also taken to monitor the development of immune responses two weeks after each immunisation. The VLPs were derived from the *N. benthamiana* expression system. Conjugation of CPS to protein is variable between reactions and it is not possible to give exactly the same amount of both protein and polysaccharide to each group. For this reason, each vaccine was formulated on the basis of CPS content to contain 10 µg of CPS per dose. In this study the amount of protein the mice receiving was 2.2 µg of Crn197 or 3.4 µg of VLP per dose.

Survival data from the 103 x MLD challenge is shown in Figure 79A. Highest levels of survival were observed in the VLP-CPS vaccinated group although statistical significance from the Crn197-CPS vaccinated group was not

achieved ($p=0.1385$ log-rank (Mantel-Cox) test). Both conjugate vaccines gave significantly greater protection than CPS alone ($p=0.0003$ log-rank (Mantel-Cox) test).

Survival data from the 240 x MLD challenge is shown in Figure 79B. The highest level of survival was seen in the VLP-CPS vaccinated group although statistical significance from the Crm197-CPS was not achieved ($p=0.0982$ log-rank (Mantel-Cox) test). In this instance, both vaccines did not give significantly greater protection than CPS alone ($p=0.1780$ (log-rank (Mantel-Cox) test). This may be a consequence of a high CPS to protein ratio which may mask the carrier protein from the immune system. For this reason, the amount of CPS per dose would be decreased in the next study to 4 μg per dose.

Survival data from the two challenge doses (103 and 240 MLD) is combined to produce Figure 79C. Highest levels of survival were observed in the VLP-CPS conjugate vaccinated groups and this was significantly higher than the CRM197-CPS conjugate vaccinated group ($p=0.0282$ Log-Rank (Mantel-Cox) test).

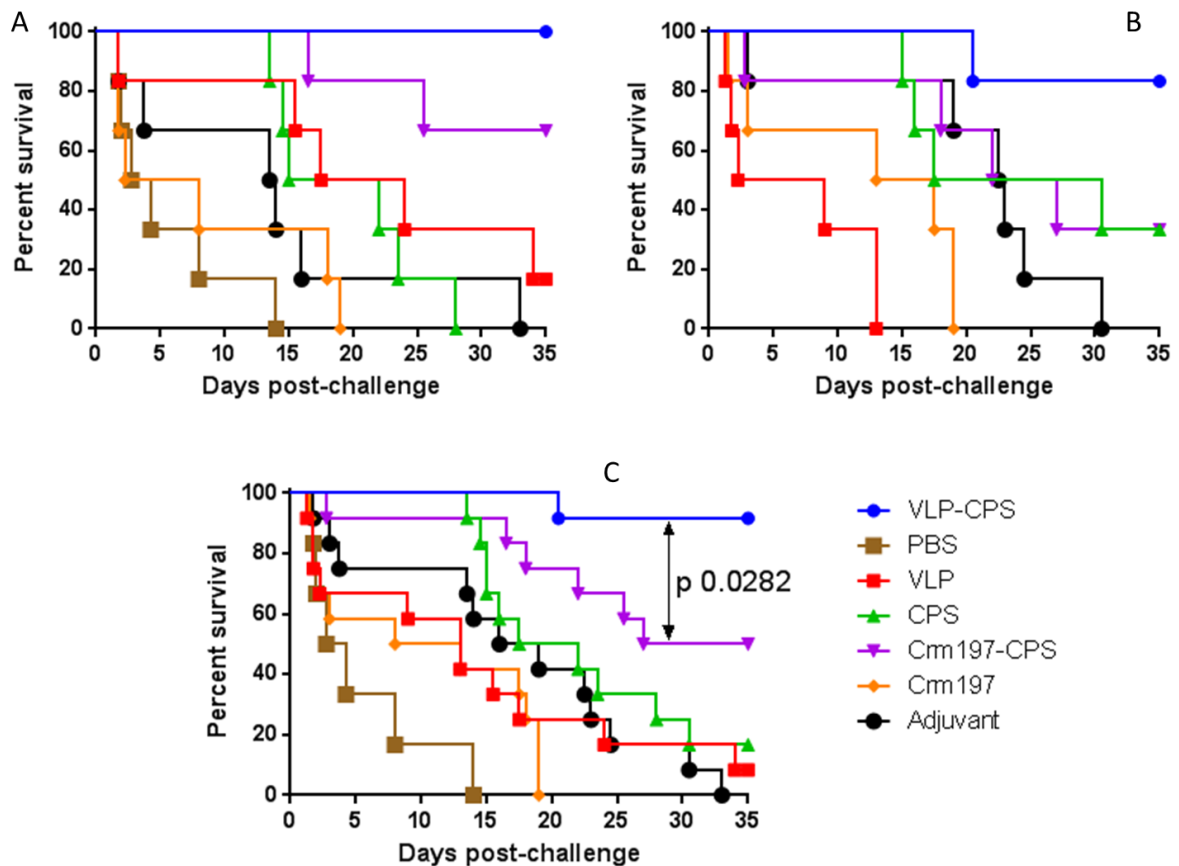


Figure 79 Efficacy of antigens against 103 and 240 x MLD *B. pseudomallei* K96243 challenge. Mice (n = 6 mice per group) were immunized with VLP-CPS and Crm197-CPS conjugate vaccines, formulated with Alum, via the i.m. route on days 0, 14, and 28. Five weeks after the final immunisation, mice were challenged i.p. with 103 x MLD (A) and 240 x MLD (B) of *B. pseudomallei* K96243 and observed for 35 days. Survival curves from both challenge doses were combined into a single curve (C). Significance was determined by the log-rank (Mantel-Cox) test.

ELISA analysis (Chapter 2, Method 2.14.7) of serum obtained from the tail bleed after the third vaccination showed a CPS-specific IgM response from CPS vaccinated mice and isotype switching to IgG from Crm197-CPS and VLP-CPS vaccinated mice (Figure 80). These results were expected as polysaccharide responses are generally IgM biased and the use of a conjugate is to evoke T-cell help leading to development of an IgG response.

Mice vaccinated with Crm197-CPS had significantly greater CPS-specific IgM and IgG titres compared to mice vaccinated with VLP-CPS ($p \leq 0.05$ and $p \leq 0.001$ respectively).

On day 35, surviving animals were culled and the liver, lung and spleen processed for recovery of *B. pseudomallei*. Sterilising immunity was achieved in one mouse that received Crm197-CPS. Several mice that received VLP-CPS had very low levels of bacteria in the spleen with no *B. pseudomallei* detected in liver or lung tissue (Figure 81A, B and C). There was no significant difference in splenic, liver or lung bacterial burden between VLP-CPS and Crm197-CPS vaccinated mice ($p > 0.05$ respectively).

As sterilising immunity was not achieved in the majority of mice, it is likely that these animals had progressed to the chronic stage of infection and would have eventually succumbed to disease. This is illustrated by the loss in bodyweight of these animals over 35 days which in the majority showed no sign of recovery (Figure 82 and Figure 83). The bodyweight data also demonstrates the difference in severity between 103 and 240 x MLD challenge dose with decreases in bodyweight seen at an earlier stage in mice that received 240 x MLD of *B. pseudomallei*.

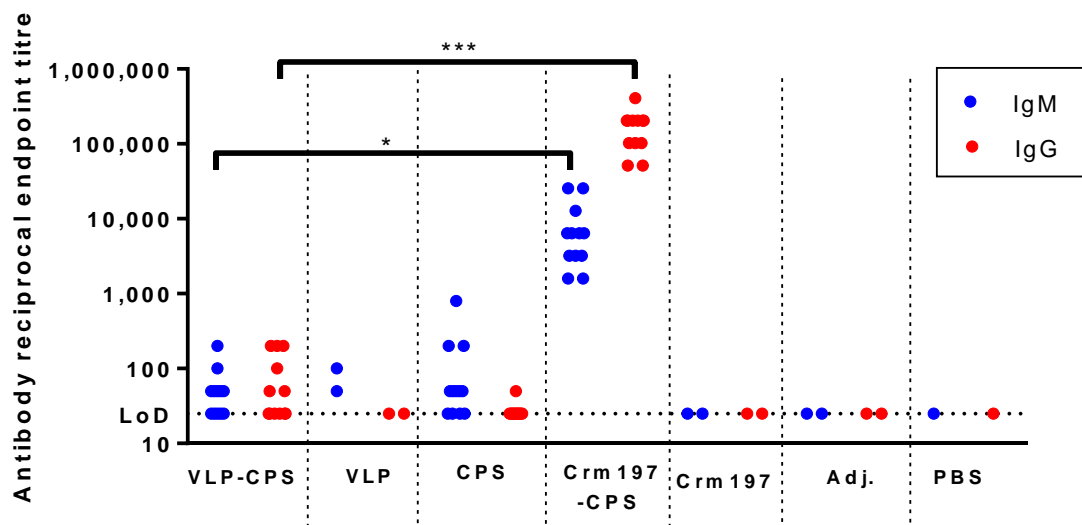


Figure 80 ELISA analysis of the CPS specific IgG and IgM antibody response from mouse sera obtained from the 103 and 240 x MLD challenge study. Mice were immunised on days 0, 14 and 28 via the i.m. route. Sera was obtained from mice 14 days after the final boost, and titres of IgG and IgM specific for CPS were determined by ELISA. Individual symbols represent a single immunised mouse with exception of the VLP, Crm197, adjuvant (Adj.) and PBS controls (n=6). * $p \leq 0.05$, *** $p \leq 0.001$ (1-way ANOVA).

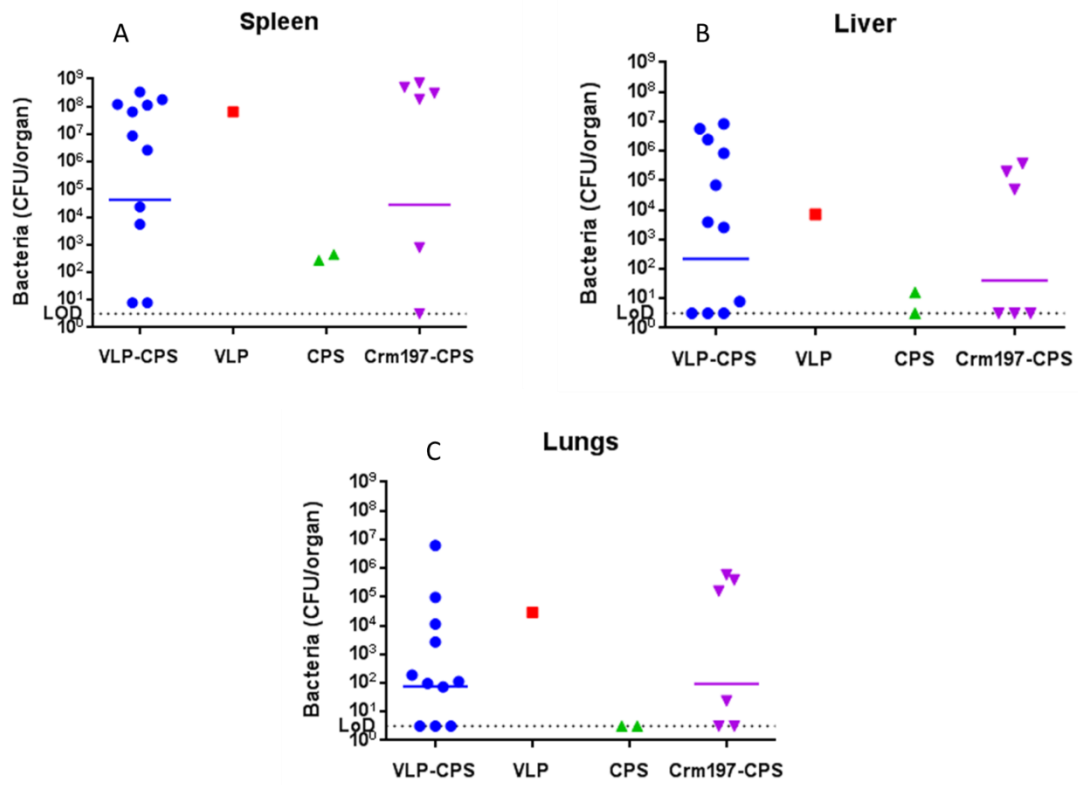


Figure 81 Initial vaccine efficacy study – bacterial burden. 35 days after challenge at either 103 or 240 x MLD *B. pseudomallei* K96243, remaining mice were culled, organs were removed, and bacterial burdens were determined. Individual symbols represent an individual mouse. Horizontal lines indicate geometric means for each group.

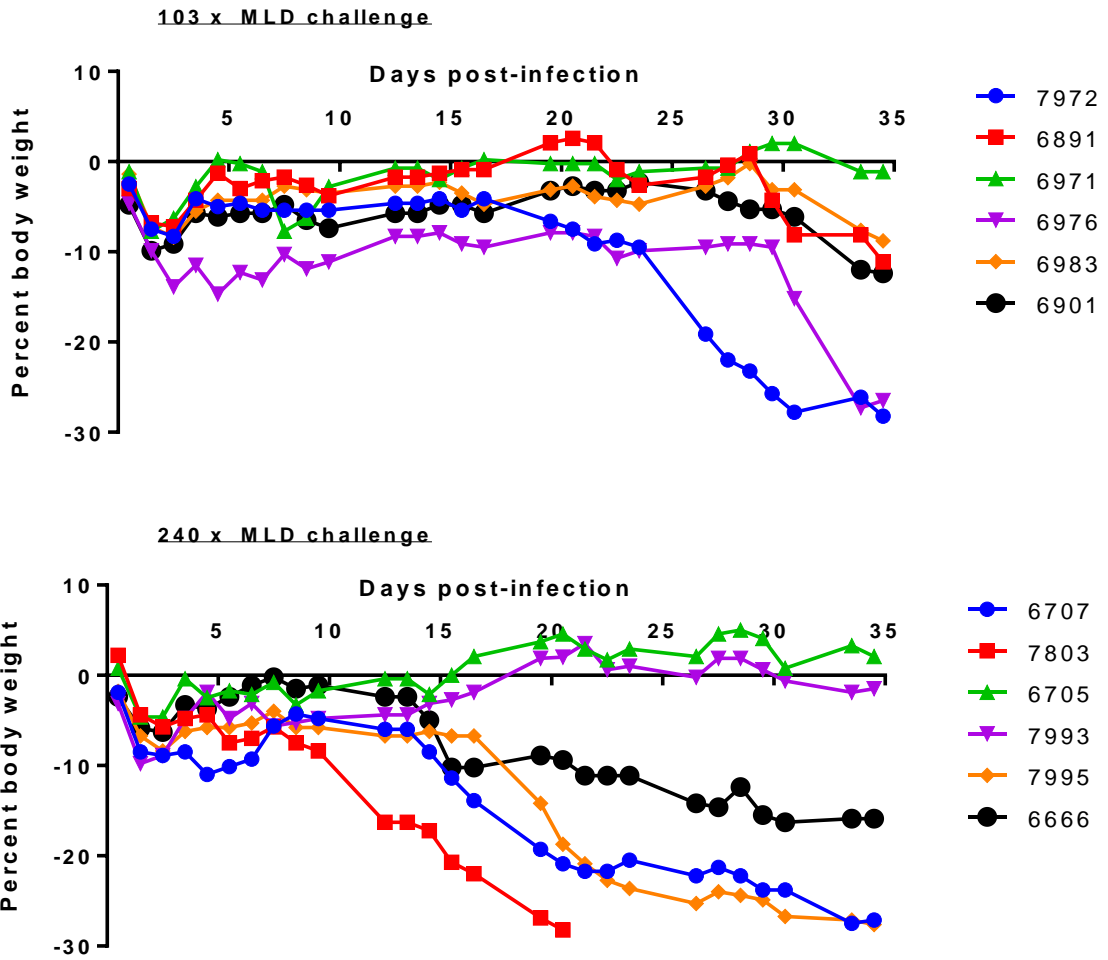


Figure 82 Bodyweight data of VLP-CPS vaccinated groups from the initial efficacy study up to 35 days after challenge with 103 or 240 x MLD of *B. pseudomallei* K96243.

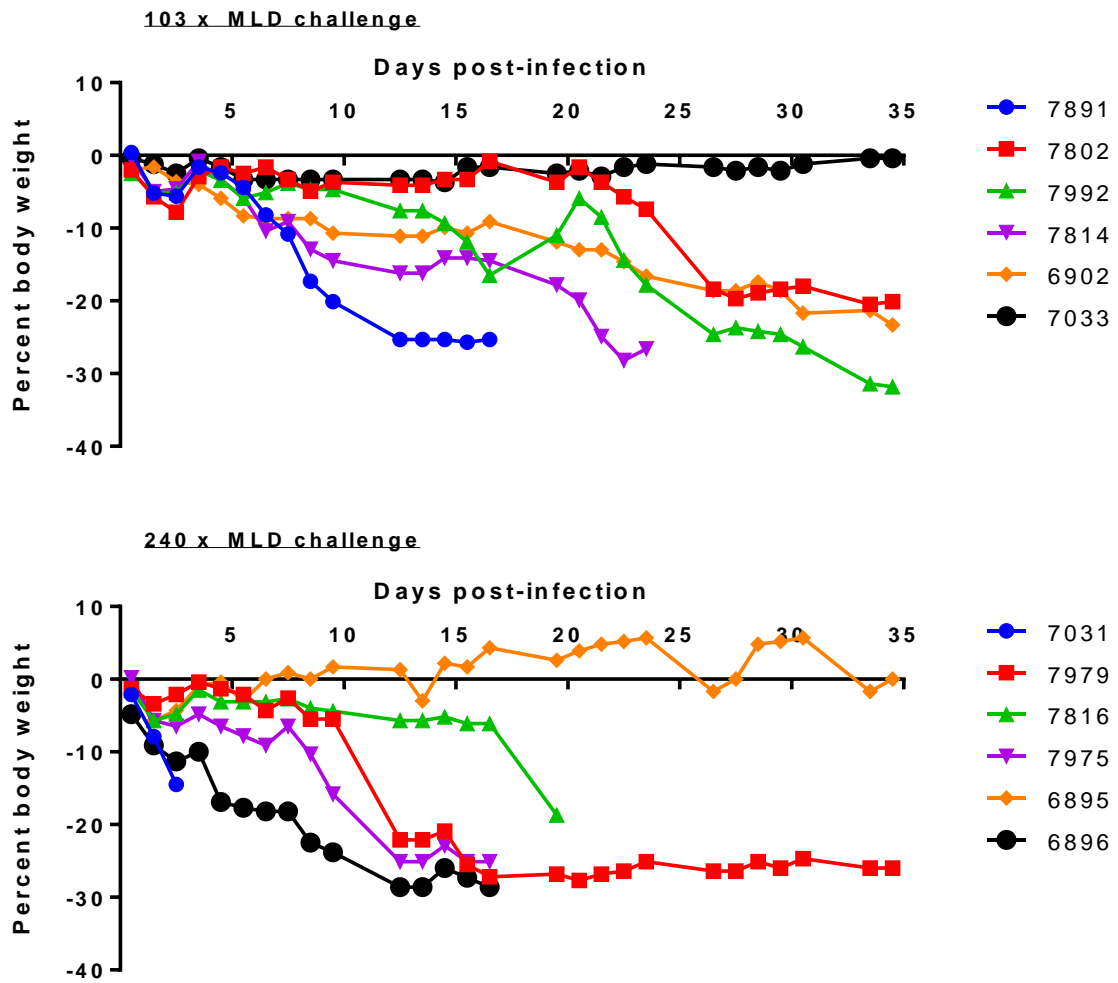


Figure 83 Bodyweight data of Crm197-CPS vaccinated groups from the initial efficacy up to 35 days after challenge with 103 and 240 x MLD of *B. pseudomallei* K96243.

5.4.1 Efficacy testing of conjugates in mice with a high challenge dose of *B. pseudomallei*.

Due to high survival up to day 35 in the initial efficacy study from groups vaccinated with CPS conjugate vaccines, this study utilised a higher challenge dose of 489 x MLD.

195 female BALB/c mice were vaccinated via the intramuscular route according to the groups in Table 9. The aim of this study was to assess protective efficacy of the VLP-CPS and Crm197-CPS conjugate vaccines at a higher challenge dose and to make a preliminary assessment of the protective efficacy of a *Burkholderia* protein conjugated to CPS (LoIC-CPS). A second aim was to assess the impact of VLPs produced from the plant and yeast expression systems.

Cohort	Vaccine	Number of mice	Adjuvant
A	VLP-CPS (plant) + LolC	15	Alum
B	LolC-CPS + VLP (plant)	15	Alum
C	VLP-CPS (plant)	15	Alum
D	LolC-CPS	15	Alum
E	VLP (plant)	15	Alum
F	LolC	15	Alum
G	CPS	15	Alum
H	PBS	15	Alum
I	Crm197-CPS	15	Alum
J	Crm197	15	Alum
K	VLP-CPS (yeast)	15	Alum
L	VLP (yeast)	15	Alum
M	VLP-CPS (yeast) + LolC	15	Alum

Table 9 Experimental plan for full efficacy study detailing vaccine candidates, number of mice and adjuvant. Groups of 15 mice from each cohort were challenged with 489 x median lethal doses of *B. pseudomallei* K96243 via the IP route and observed for 35 days.

Groups of fifteen mice were immunised, challenged with 3.63×10^5 CFU (489 x MLD) of *B. pseudomallei* K96243 via the IP route and observed for 35 days. Tail bleeds were also taken to monitor the development of immune responses two weeks after each immunisation. At formulation, vaccines were diluted for each mouse to receive 4 µg per dose of CPS. Due to variation in CPS conjugation efficiency between the conjugates this resulted in mice receiving 0.51 µg VLP (plant), 5.61 µg VLP (yeast), 1.9 µg Crm197 and 1.3 µg LolC.

For clarity, only the test vaccines are shown in Figures 85 to 88. The controls are shown in Figure 84. At this high challenge dose, as expected, control animal survival is poor with most animals dying in the first few days after challenge.

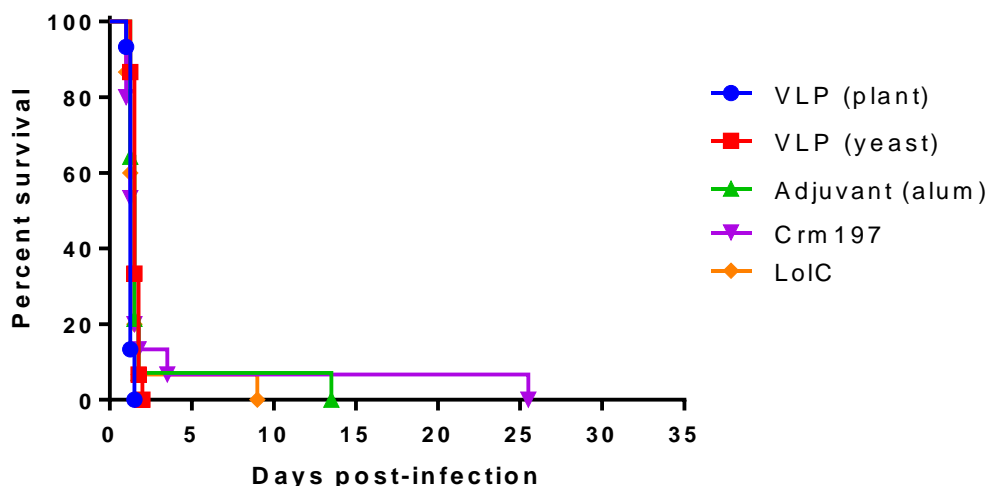


Figure 84 Efficacy of control antigens against 489 x MLD *B. pseudomallei* K96243 challenge. Mice (n = 15 mice per group) were immunized with the control antigens; plant and yeast expressed VLP (VLP plant, VLP yeast), adjuvant, Crm197 and LoIC, formulated with Alum, via the i.m. route on days 0, 14 and 28. Five weeks after the final immunisation, mice were challenged i.p. with 489 x MLD of *B. pseudomallei* K96243.

Protection was greatest in the Crm197-CPS vaccinated group and was significantly higher than mice that received plant expressed VLP conjugated to CPS ($p=0.0185$, Figure 85). Survival in the plant expressed VLP-CPS conjugate groups was significantly greater than from yeast expressed VLPs ($p=0.0301$, Figure 85). The protective efficacy of the VLP-CPS (yeast) was not significantly greater than CPS alone ($p=0.4167$).

The LoIC-CPS conjugate did not offer significantly greater protection than CPS alone ($p=0.5803$, Figure 85).

The protective efficacy of the VLP-CPS (plant) and VLP-CPS (yeast) was not increased with the addition of LoIC ($p=0.4957$ and $p=0.6873$ respectively, (Figure 86). The same was also true for the addition of VLP (plant) to the LoIC-CPS vaccine ($p=0.24$, Figure 87). The addition of LoIC to the yeast VLP conjugate was not carried out.

Although survival from the Crm197-CPS vaccinated groups was significantly greater than mice that received VLP-CPS (plant), and addition of LolC to VLP-CPS (plant) did not significantly increase protection, the protection from VLP-CPS + LolC was not significantly different to the Crm197-CPS vaccine ($p=0.1581$) as shown in Figure 88. Reports in the literature also state improvement in conjugate vaccine efficacy with *Burkholderia* protein co-antigens (Scott *et al.*, 2014).

As with the initial efficacy study, the majority of mice challenged with *B. pseudomallei* lost weight over the course of the study and therefore this is not presented here. Sterilising immunity was not achieved in any animal that survived to the end of the study.

Similar to the previous challenge study, ELISA analysis of serum obtained from the tail bleed after the third vaccination showed a CPS-specific IgM response from CPS vaccinated mice, isotype switching to IgG from Crm197-CPS and VLP-CPS vaccinated mice with significantly greater CPS-specific IgG and IgM titres in the Crm197-CPS vaccinated group ($p\leq 0.05$, Figure 89 and $p\leq 0.0001$ Figure 90).

ELISA analysis of serum obtained from the tail bleed after the third vaccination for LolC-specific IgG and IgM antibody titres (Figure 91 and Figure 92) shows that LolC is highly immunogenic. As protective efficacy of the LolC-CPS vaccine was poor and CPS-specific IgG titres low, these results suggest stimulation of an immune response by the LolC protein that did not promote a protective immune response to the CPS molecule.

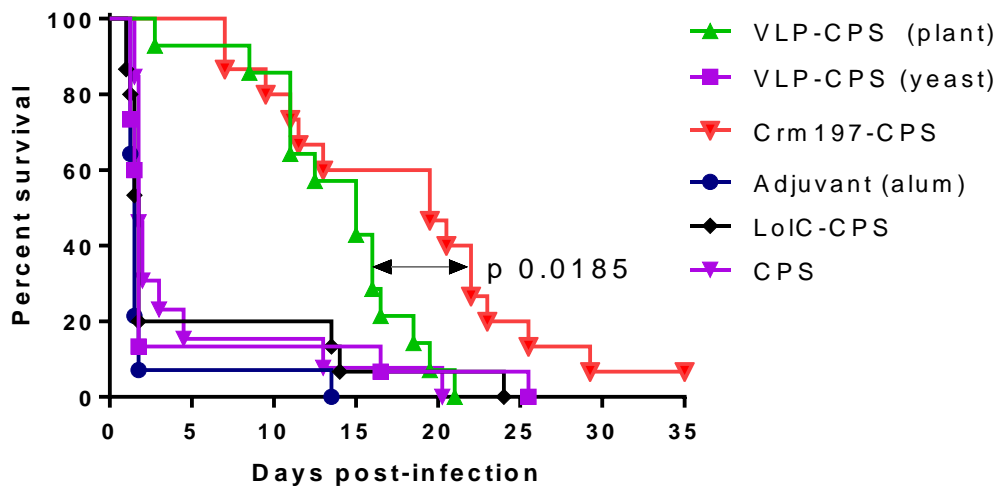


Figure 85 Efficacy of conjugate vaccines against 489 x MLD *B. pseudomallei* K96243 challenge. Mice (n = 15 mice per group) were immunized with Crm197-CPS, LoIC-CPS and VLP-CPS conjugate vaccines, formulated with Alum, via the i.m. route on days 0, 14 and 28. Five weeks after the final immunisation, mice were challenged i.p. with 489 x MLD of *B. pseudomallei* K96243. Significance was determined by the log-rank (Mantel-Cox) test.

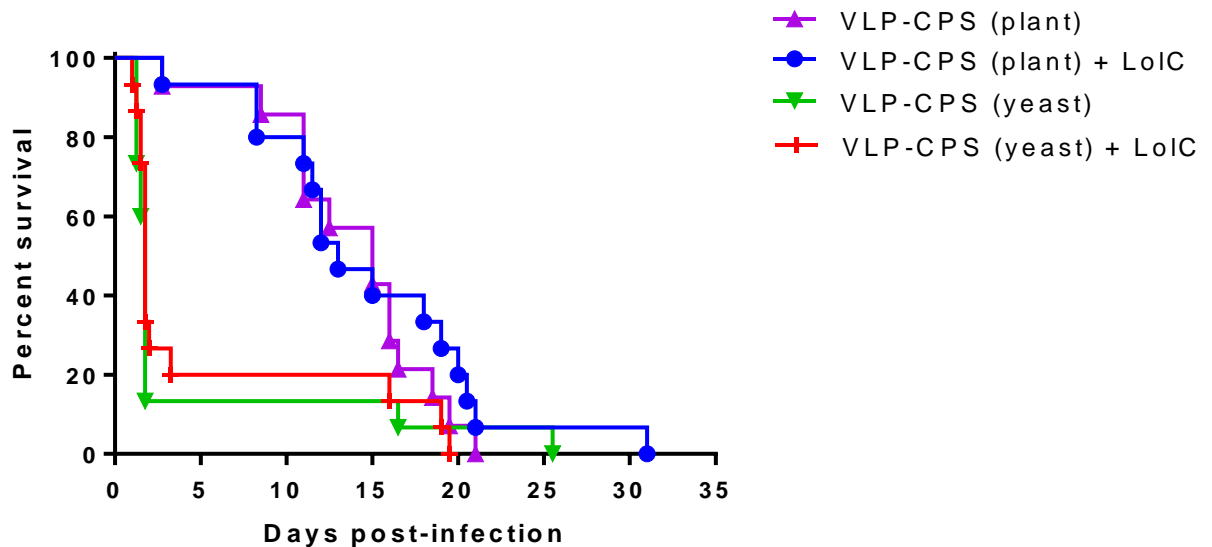


Figure 86 Effect of LoIC on VLP-CPS conjugate efficacy against 489 x MLD *B. pseudomallei* K96243 challenge. Mice (n = 15 mice per group) were immunized with VLP-CPS (plant) and VLP-CPS (yeast) with and without the addition of LoIC, formulated with Alum, via the i.m. route on days 0, 14 and 28. Five weeks after the final immunisation, mice were challenged i.p. with 489 x MLD of *B. pseudomallei* K96243. Significance was determined by the log-rank (Mantel-Cox) test. VLP-CPS plant comparison p=0.4957. VLP-CPS yeast comparison p=0.6873.

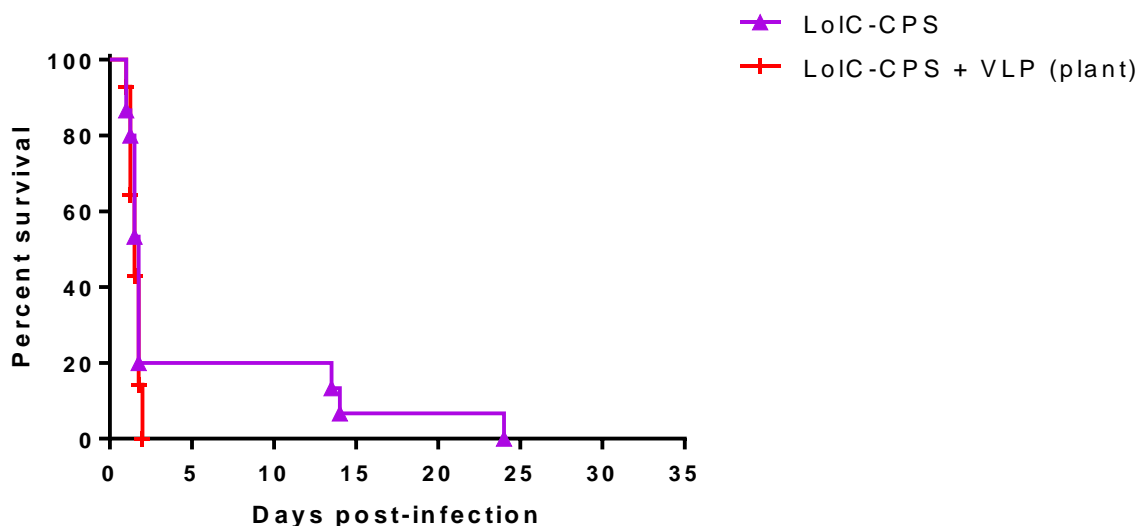


Figure 87 Effect of VLP on LoIC-CPS conjugate efficacy against 489 x MLD *B. pseudomallei* K96243 challenge. Mice (n = 15 mice per group) were immunized with LoIC-CPS and LoIC-CPS with the addition of plant expressed VLP, formulated with Alum, via the i.m. route on days 0, 14 and 28. Five weeks after the final immunisation, mice were challenged i.p. with 489 x MLD of *B. pseudomallei* K96243. Significance was determined by the log-rank (Mantel-Cox) test (p=0.24).

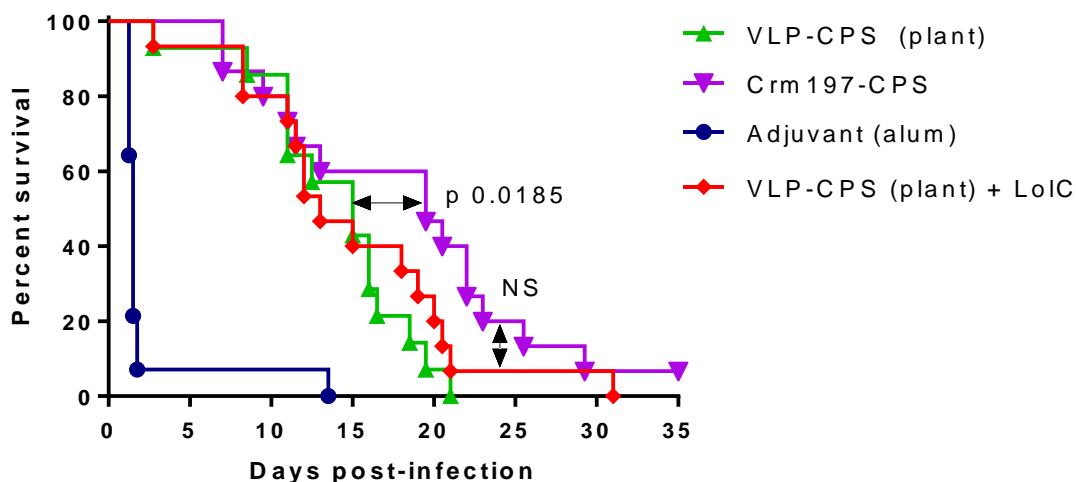


Figure 88 Efficacy comparison of plant purified VLPs conjugated to CPS, with and without addition of LoIC, to Crm197-CPS against 489 x MLD *B. pseudomallei* K96243 challenge. Mice (n = 15 mice per group) were immunized with Crm197-CPS, VLP-CPS (plant) and VLP-CPS (plant) +LoIC, formulated with Alum, via the i.m. route on days 0, 14 and 28. Five weeks after the final immunisation, mice were challenged i.p. with 489 x MLD of *B. pseudomallei* K96243. Significance was determined by the log-rank (Mantel-Cox).

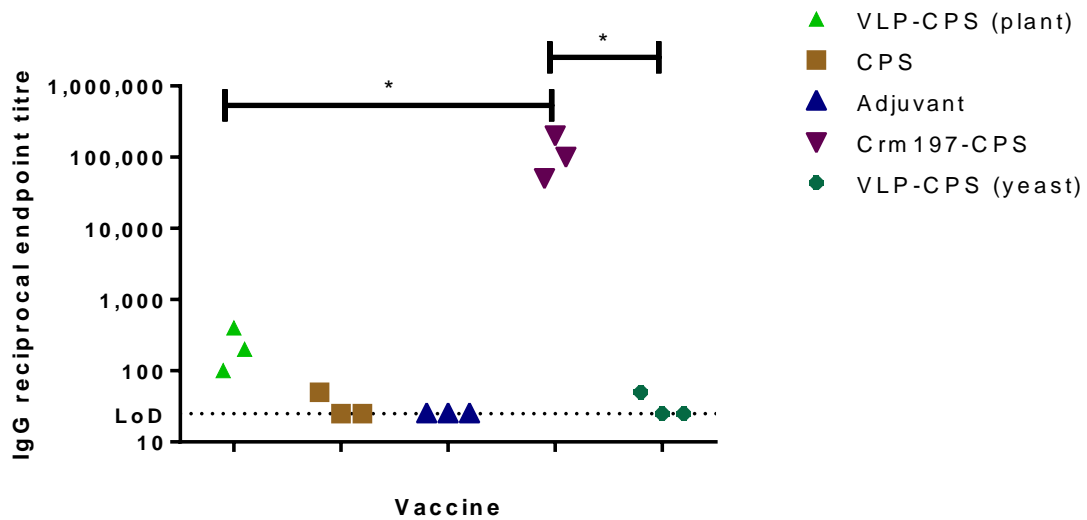


Figure 89 ELISA analysis of the CPS specific IgG antibody response from mouse sera obtained from the 489 x MLD challenge study. Mice were immunised on days 0, 14 and 28 via the i.m. route. Sera was obtained from mice 14 days after the final boost, and titres of IgG specific for CPS were determined by ELISA. Individual symbols represent a cage of 5 mice. * $p \leq 0.05$). LOD = limit of detection

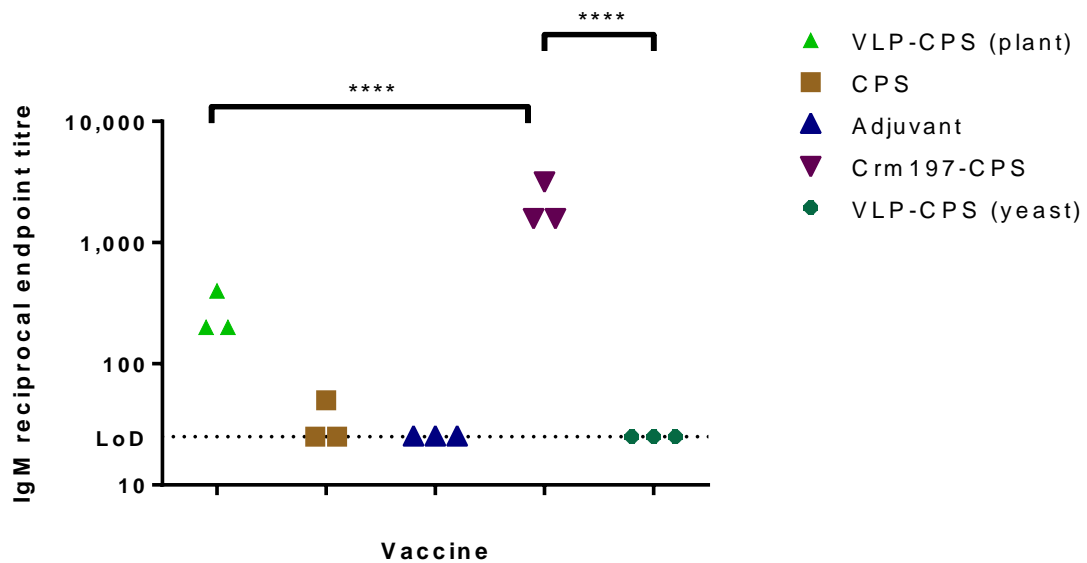


Figure 90 ELISA analysis of the CPS specific IgM antibody response from mouse sera obtained from the 489 x MLD challenge study. Mice were immunised on days 0, 14 and 28 via the i.m. route. Sera was obtained from mice 14 days after the final boost, and titres of IgM specific for CPS were determined by ELISA. Individual symbols represent a cage of 5 mice. **** $p \leq 0.0001$. LOD = limit of detection.

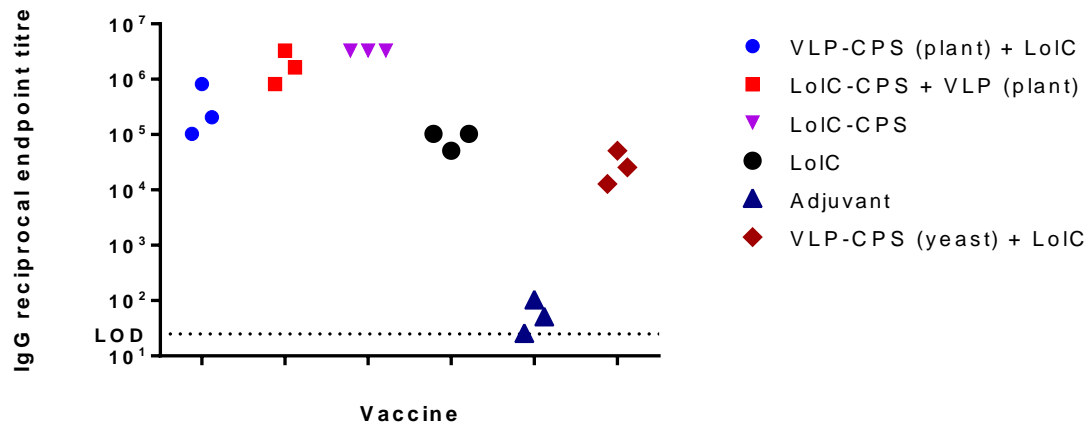


Figure 91 ELISA analysis of the LoIC specific IgG antibody response from mouse sera obtained from the 489 x MLD challenge study. Mice were immunised on days 0, 14 and 28 via the i.m. route. Sera was obtained from mice 14 days after the final boost, and titres of IgG specific for CPS were determined by ELISA. Individual symbols represent a cage of 5 mice. LOD = limit of detection.

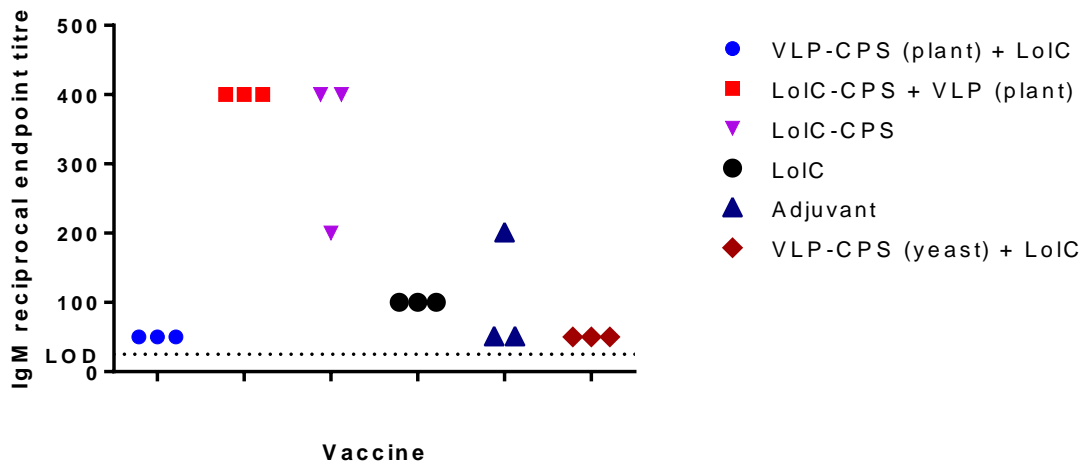


Figure 92 ELISA analysis of the LoIC specific IgM antibody response from mouse sera obtained from the 489 x MLD challenge study. Mice were immunised on days 0, 14 and 28 via the i.m. route. Sera was obtained from mice 14 days after the final boost, and titres of IgM specific for CPS were determined by ELISA. Individual symbols represent a cage of 5 mice. LOD = limit of detection.

Survival data from the pilot and full efficacy studies at 103, 240 and 489 x MLD challenge doses is summarized in Figure 93 for adjuvant, CPS, Crm197-CPS and VLP-CPS (plant). For all vaccine candidates, protective efficacy decreases as the challenge dose is increased. At 103 and 240 x MLD, there is no significant difference in protection between the Crm197-CPS and VLP-CPS

vaccines ($p=0.1385$ and $p=0.0982$ respectively). At 489 x MLD, the protective efficacy of the Crm197-CPS vaccine is significantly greater than from VLP-CPS ($p=0.0185$). When survival data from all challenge doses is combined (Figure 93 - All data), there is no significant difference in protection between the Crm197-CPS and VLP-CPS vaccine ($p=0.5458$).

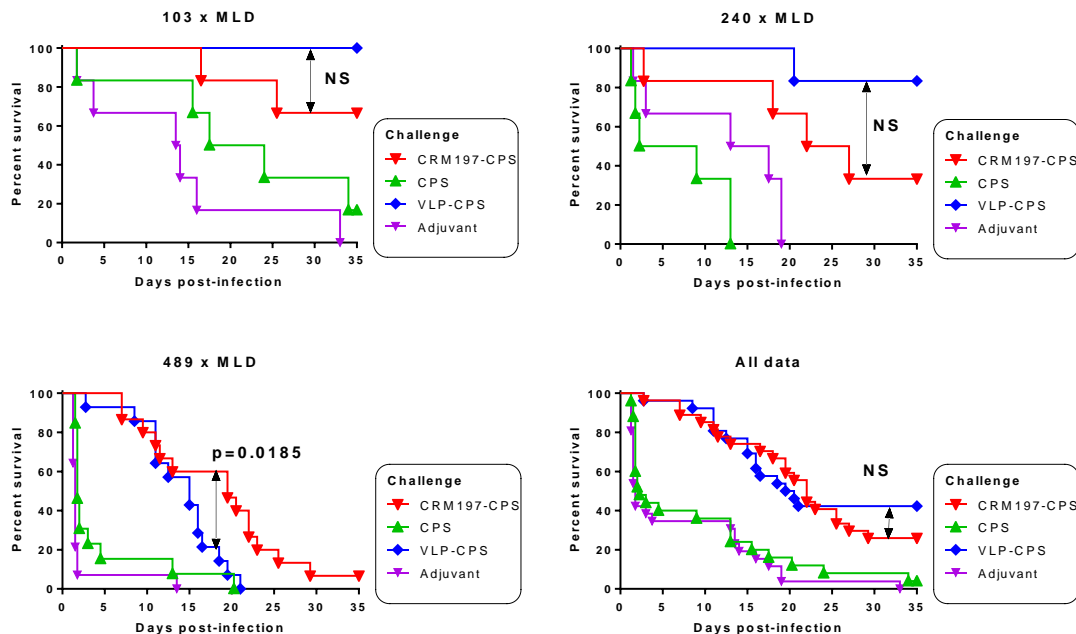


Figure 93 Efficacy comparison of vaccine antigens to 103, 240 and 489 x MLD *B. pseudomallei* K96243 challenge. Mice were immunized with CPS, Crm197-CPS, VLP-CPS, formulated with Alum, and adjuvant (Alum), via the i.m. route on days 0, 14 and 28. Five weeks after the final immunisation, mice were challenged i.p. with 103, 240 or 489 x MLD of *B. pseudomallei* K96243. Significance was determined by the log-rank (Mantel-Cox). 103 and 240 x MLD, $n=6$ per group. 489 x MLD $n=15$ per group

5.4.2 *Burkholderia* protein and VLP expression system efficacy assessment

As the previous studies had shown that protective efficacy between Crm197-CPS and VLP-CPS (plant) is not significantly different ($p=0.5458$), the objective of this study was to determine the protective efficacy of different *Burkholderia* proteins added as co-antigens with a Crm197-CPS conjugate and to compare the plant and yeast expressed VLPs conjugated to CPS. In this study the VLPs both contained the D3K6D3 motif. In the previous studies, only the plant

expressed VLPs contained this motif which may have resulted in the poor protective efficacy of the yeast expressed VLPs.

190 female BALB/c mice were vaccinated via the intramuscular route according to the groups in Table 10 (5-15 mice per group) on three separate occasions, challenged with 2.97×10^5 CFU (399 x MLD) of *B. pseudomallei* K96243 by the IP route and observed for 35 days. The challenge dose was high to improve the chance of observing differences in efficacy between the proteins. These proteins were added to the Crm197-CPS vaccine due to the significantly increased protective efficacy from Crm197-CPS at high challenge doses seen in the previous study.

Cohort	Vaccine	Number of mice	Adjuvant
A	VLP D3K6D3 (plant)	5	Alhydrogel
B	VLP D3K6D3 (yeast)	5	Alhydrogel
C	Crm197	5	Alhydrogel
D	PBS – no challenge	5	Alhydrogel
E	PBS	10	Alhydrogel
F	VLP-CPS D3K6D3 (plant)	15	Alhydrogel
G	VLP-CPS D3K6D3 (yeast)	15	Alhydrogel
H	VLP-CPS D3K6D3 (yeast) + Hcp6	15	Alhydrogel
I	Crm197-CPS	15	Alhydrogel
J	Crm197-CPS + PotF	15	Alhydrogel
K	Crm197-CPS + OppA	15	Alhydrogel
L	Crm197-CPS + Hcp6	15	Alhydrogel
M	Crm197-CPS + LolC	15	Alhydrogel
N	PotF	10	Alhydrogel
O	OppA	10	Alhydrogel
P	Hcp6	10	Alhydrogel
Q	LolC	10	Alhydrogel

Table 10 Experimental plan for assessment of *Burkholderia* protein and VLP expression system efficacy, detailing vaccine candidates, number of mice and adjuvant. Each cohort were challenged with 399 x median lethal doses of *B. pseudomallei* K96243 via the intra-peritoneal route and observed for 35 days.

At formulation, vaccines were diluted for each mouse to receive 5 µg per dose of CPS. Due to variation in CPS conjugation efficiency between the conjugates this resulted in the relevant mice receiving 2 µg VLP (plant), 1 µg VLP (yeast) or 17 µg Crm197. All *Burkholderia* proteins were administered at 5 µg per dose. The addition of *Burkholderia* proteins as co-antigens with the Crm197-CPS conjugate gave no significant difference in protection compared to the Crm197-CPS only vaccinated group ($p=0.7335$, Figure 94). However, Table 11 shows that a Crm197-CPS conjugate containing LolC offers the greatest median survival. For this reason Crm197-CPS conjugate with LolC was used as the basis to assess the protective efficacy of different adjuvants in the next study. The use of *Burkholderia* proteins as vaccines alone gave significantly less protection than the Crm197-CPS vaccinated group ($p\leq 0.0001$, Figure 95). ELISA analysis of serum obtained after the third vaccination for the *Burkholderia* protein-specific IgG response (Figure 96) showed that antibody generated to LolC was significantly lower than for the other proteins, both as the sole vaccine antigen ($p=0.0020$) and added to the Crm197-CPS conjugate ($p=0.0023$). Interestingly, when added as co-antigens to Crm197-CPS, the LolC and Hcp6 specific IgG titres was significantly reduced compared to these proteins as sole antigens ($p=0.0085$ and $p=0.0007$ respectively). The reduction in Hcp6 specific IgG titer was not seen when Hcp6 was added to the VLP-CPS conjugate ($p=0.4950$).

Survival in the Crm197-CPS conjugate vaccinated group was not significantly higher than survival in the plant VLP-CPS conjugate vaccinated group ($p=0.1046$, Figure 97) although mean time to death (MTTD) in the Crm197-CPS group was 26.5 days in comparison to 19.5 days with plant expressed VLP-CPS.

Vaccination with plant expressed VLPs conjugated to CPS resulted in statistically greater protection than yeast expressed VLPs ($p=0.0469$, Figure 98) although due to the concentration of antigen provided, each dose of VLP-CPS (yeast) vaccine contained 9 % alum, not 15 % like the other vaccine candidates. Addition of Hcp6 to yeast expressed VLP-CPS did not significantly increase protection to *B. pseudomallei* challenge ($p=0.11$) but did increase MTTD from 6 days to 19.5 days (Figure 99). There was no statistical difference in the VLP-

specific IgG titres generated by the plant or yeast expressed VLPs conjugated to CPS (p=0.3739, (Figure 100).

ELISA analysis of serum obtained after the third vaccination detected a CPS specific IgG response to CPS in CPS-conjugate vaccinated mice (Figure 101). Significantly higher titers were observed in mice where the vaccine contained Crm197-CPS (p≤0.0001) and the addition of *Burkholderia* protein had no adverse effect on CPS specific titres (p=0.4516).

Due to the large variation in bacterial burden within the liver, lung and spleen in animals surviving to study end, no statistical significance was observed although the geometric mean was lowest in the mice immunised with VLP-CPS (plant) (Figure 102).

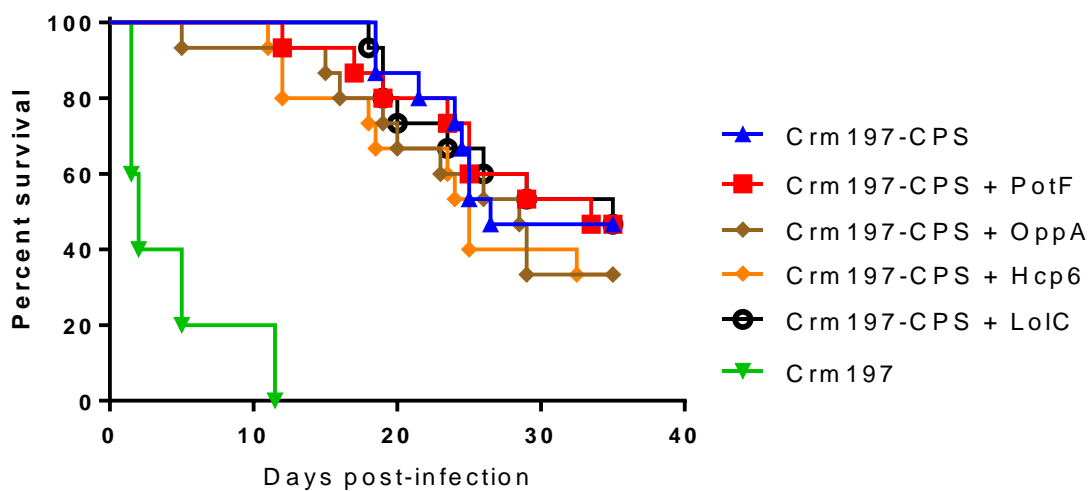


Figure 94 Efficacy comparison of Crm197-CPS conjugate vaccines with and without *Burkholderia* proteins added as co-antigens against 399 x MLD *B. pseudomallei* K96243 challenge. Mice (n = 15 mice per conjugate vaccine group, n = 5 Crm197 control) were immunized with Crm197-CPS, and Crm197-CPS with the addition of PotF, OppA, Hcp6 or LolC, formulated with Alum, via the i.m. route on days 0, 14 and 28. Five weeks after the final immunisation, mice were challenged i.p. with 399 x MLD of *B. pseudomallei* K96243.

Vaccine	Days
Adjuvant	2
Crm197-CPS	26.5
Crm197-CPS + PotF	33.5
Crm197-CPS + OppA	28.5
Crm197-CPS + Hcp6	25
Crm197-CPS + LolC	35

Table 11 Median survival of Crm197-CPS conjugate vaccine co-mixed with the *Burkholderia* proteins PotF, OppA, Hcp6 and LolC.

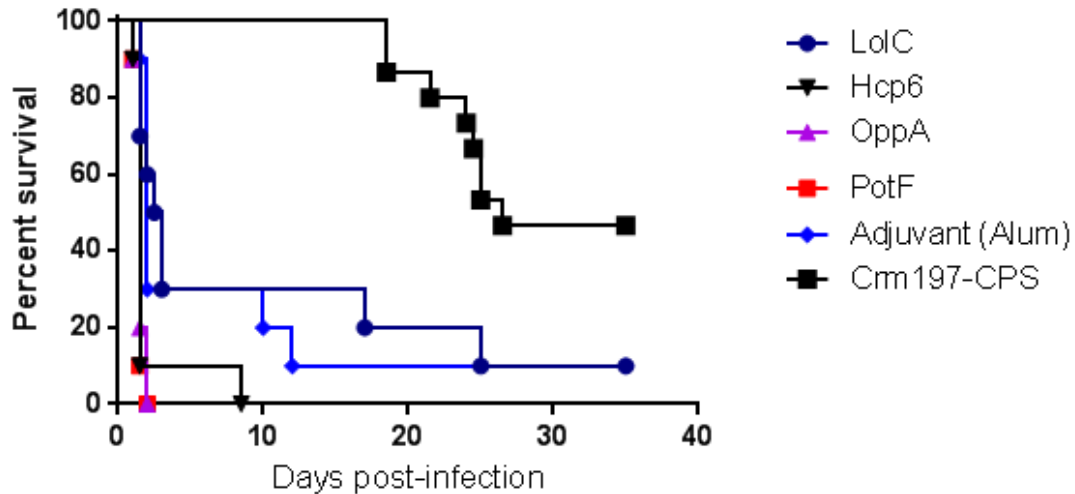


Figure 95 Efficacy comparison of *Burkholderia* protein antigens against 399 x MLD *B. pseudomallei* K96243 challenge. Mice (n = 10 mice per *Burkholderia* protein group, n = 15 for Crm197-CPS, n = 10 for adjuvant control) were immunized with LolC, Hcp6, OppA and PotF, formulated with Alum, via the i.m. route on days 0, 14 and 28. Five weeks after the final immunisation, mice were challenged i.p. with 399 x MLD of *B. pseudomallei* K96243.

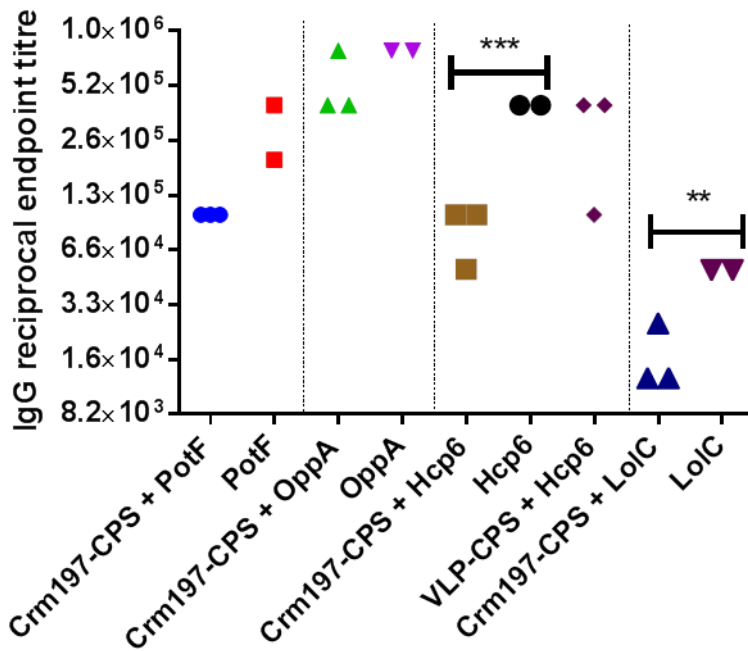


Figure 96 ELISA analysis of the *Burkholderia* protein specific IgG antibody response from mouse sera obtained from the 399 x MLD challenge study. Mice were immunised on days 0, 14 and 28 via the i.m. route. Sera was obtained from mice 14 days after the final boost, and titres of IgM specific for CPS were determined by ELISA. Individual symbols represent a cage of 5 mice. *** p=0.0007, ** p=0.0085).

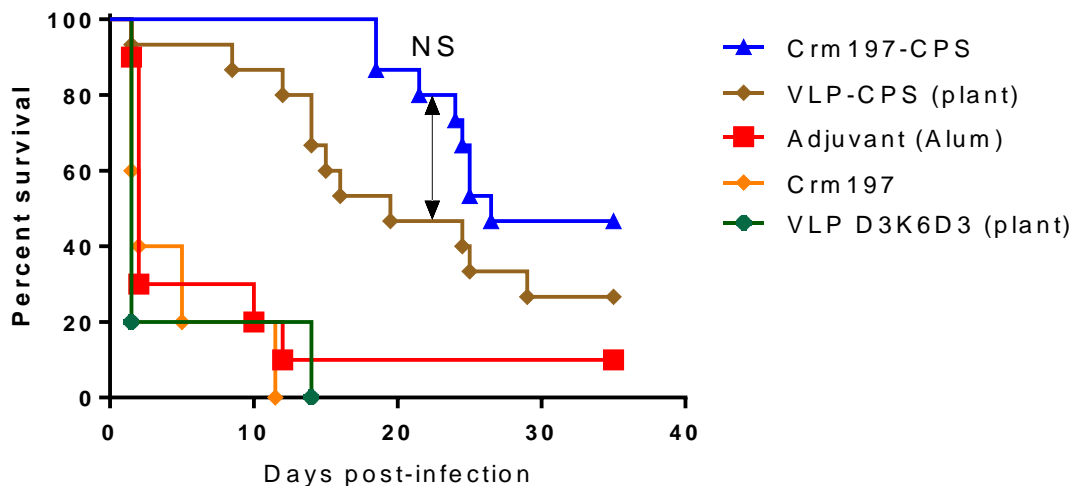


Figure 97 Efficacy comparison of plant-expressed VLPs conjugated to CPS vs Crm197-CPS against 399 x *B. pseudomallei* K96243 challenge. Mice (n = 15 mice per group, n = 10 adjuvant control, n = 5 Crm197, VLP controls) were immunized with antigens formulated with Alum, via the i.m. route on days 0, 14 and 28. Five weeks after the final immunisation, mice were challenged i.p. with 399 x MLD of *B. pseudomallei* K96243. Significance was determined by the log-rank (Mantel-Cox).

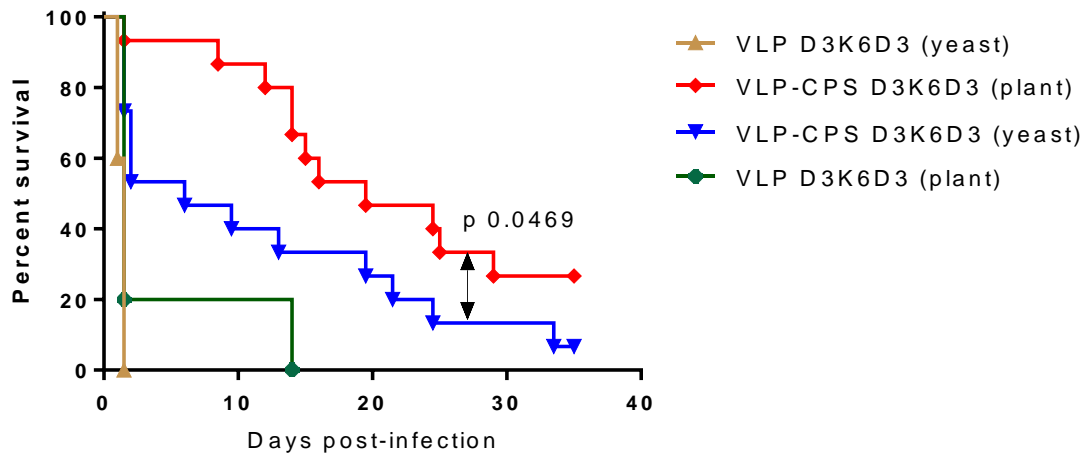


Figure 98 Efficacy comparison of plant-expressed VLPs conjugated to CPS vs yeast expressed VLPs conjugated to CPS against 399 x *B. pseudomallei* K96243 challenge. Mice (n = 15 mice per conjugate vaccine group, n = 5 VLP controls) were immunized with antigens formulated with Alum, via the i.m. route on days 0, 14 and 28. Five weeks after the final immunisation, mice were challenged i.p. with 399 x MLD of *B. pseudomallei* K96243. Significance was determined by the log-rank (Mantel-Cox).

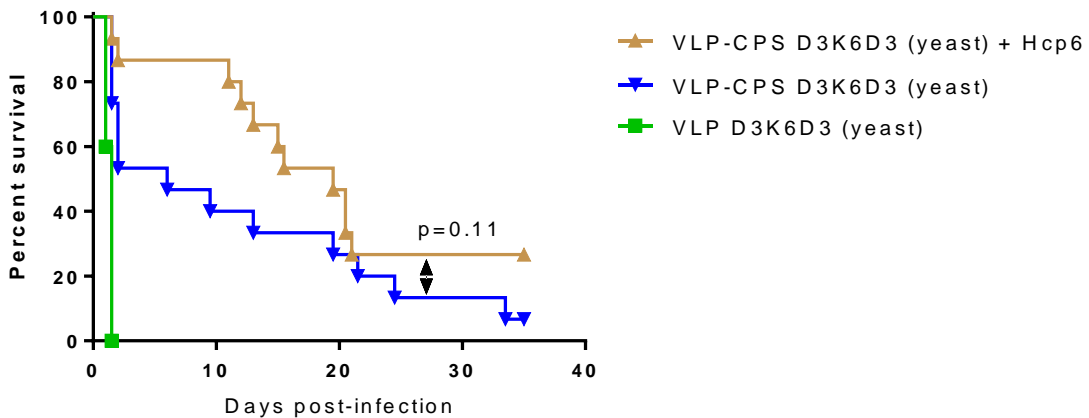


Figure 99 Efficacy comparison of yeast-expressed VLPs conjugated to CPS with and without Hcp6 against 399 x *B. pseudomallei* K96243 challenge. Mice (n = 15 mice per group) were immunized with antigens formulated with Alum, via the i.m. route on days 0, 14 and 28. Five weeks after the final immunisation, mice were challenged i.p. with 399 x MLD of *B. pseudomallei* K96243. Significance was determined by the log-rank (Mantel-Cox).

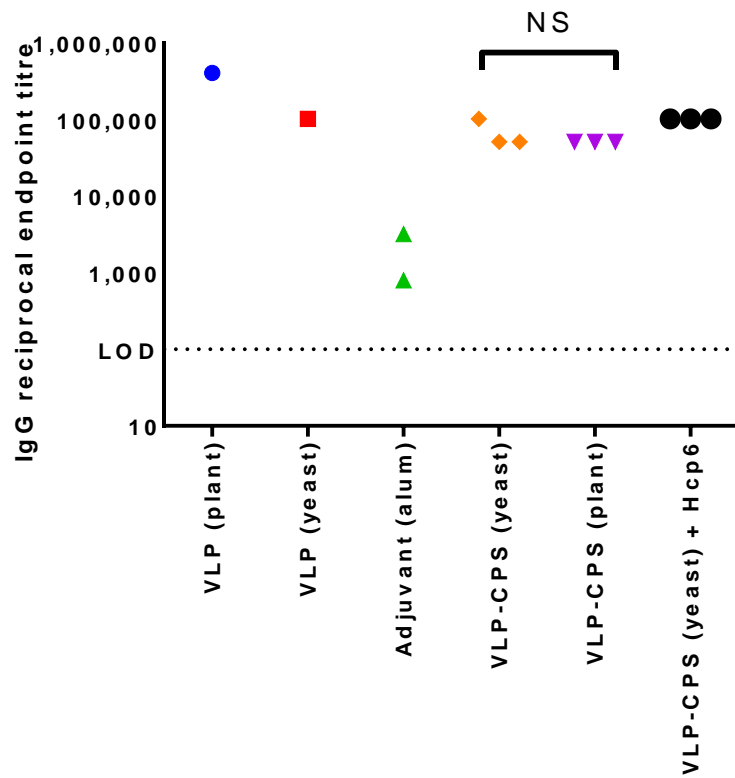


Figure 100 ELISA analysis of the VLP specific IgG antibody response from mouse sera obtained from the 399 x MLD challenge study. Mice were immunised on days 0, 14 and 28 via the i.m. route. Sera was obtained from mice 14 days after the final boost, and titres of IgG specific for VLP were determined by ELISA. Individual symbols represent a cage of 5 mice. NS, no statistical significance (determined by 1-way ANOVA). LOD: limit of detection.

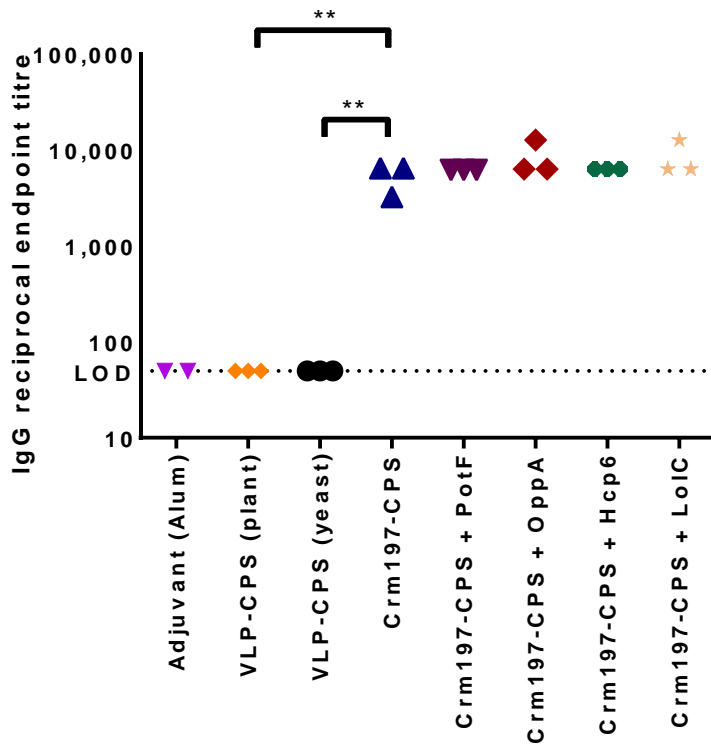


Figure 101 ELISA analysis of the CPS specific IgG antibody response from mouse sera obtained from the 399 x MLD challenge study. Mice were immunised on days 0, 14 and 28 via the i.m. route. Sera was obtained from mice 14 days after the final boost, and titres of IgG specific for CPS were determined by ELISA. Individual symbols represent a cage of 5 mice. ** $p \leq 0.01$ (determined by 1-way ANOVA). LOD: limit of detection

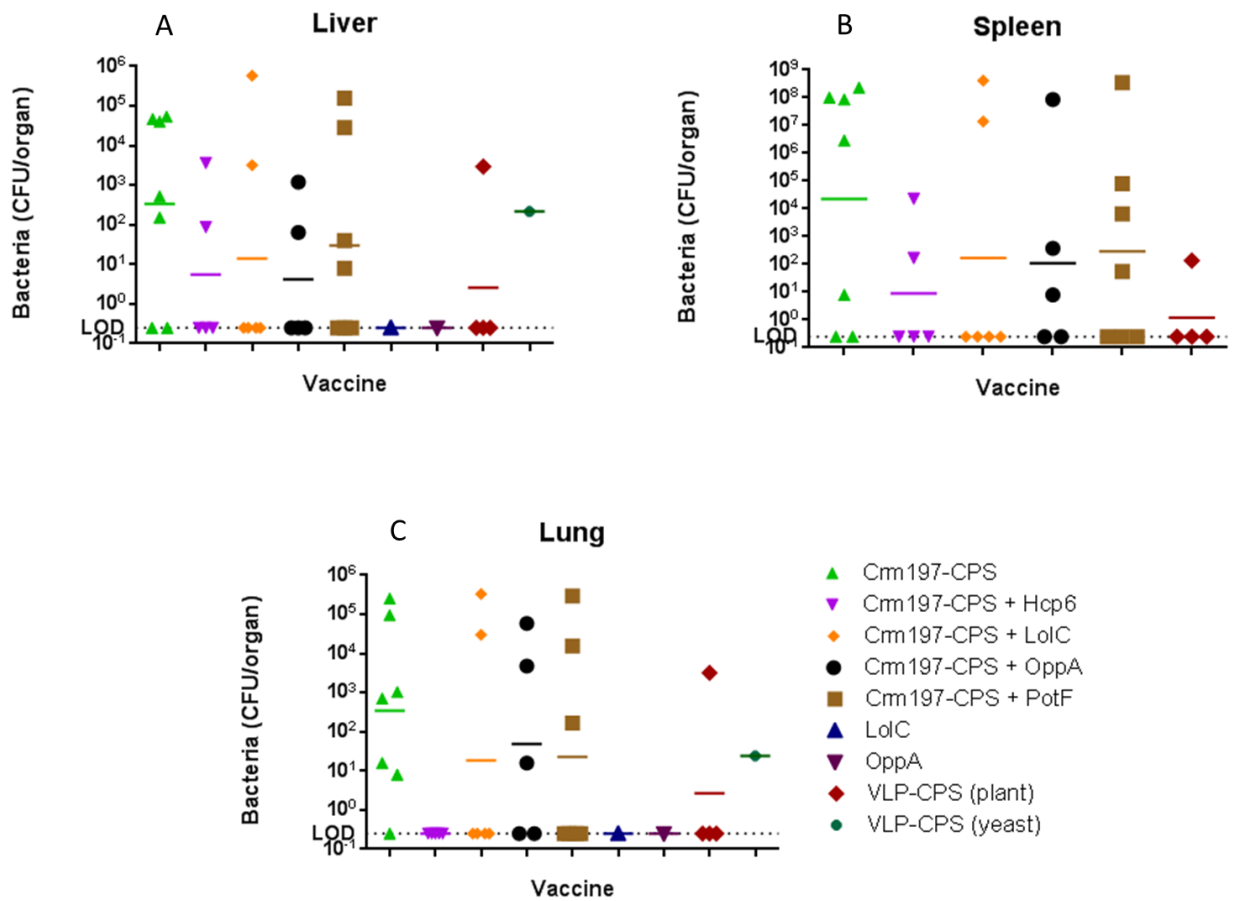


Figure 102 Liver, Spleen and Lung bacterial burden from the 399 x MLD challenge study. 35 days after challenge with 399 x MLD *B. pseudomallei*, remaining mice were culled, organs were removed, and bacterial burdens were determined. Individual symbols represent an individual mouse. Horizontal lines indicate geometric means for each group.

5.4.3 Animal efficacy study – formulation

The primary aim of this study was to directly compare the effect of different adjuvant formulations on the protective efficacy of a conjugate vaccine containing CPS and Crm197.

A secondary aim was to compare the efficacy of Tandem Core™ based VLPs and HBcAg (non-Tandem Core™) VLPs as a platform for a CPS-based conjugate vaccine. As peptide sequences could not successfully be inserted into Tandem Core™ based VLPs, the need for this construct was not apparent. The final aim was to assess the effect of vaccine immunisation route on vaccine efficacy.

205 female BALB/c mice were vaccinated via the intramuscular (IM) or subcutaneous (SC) route according to the groups in Table 12 (15 mice per group) on three separate occasions, challenged with either 3.35×10^5 CFU (450 x MLD) or 5.58×10^5 CFU (750 x MLD) of *B. pseudomallei* K96243 by the IP route and observed for 35 days. A high challenge dose was administered to increase the chances of discriminating between vaccine groups and is based on the preceding studies.

To monitor the development of the immune response, sera were taken at two week intervals after each immunisation by tail bleeds from each mouse for antibody assessment by ELISA. Cell-mediated immunity was also assessed in mice following the vaccination schedule when the mice were culled and splenocyte IFN- γ response assessed (Chapter 2, method 2.14.8).

Vaccine	Number of mice	Adjuvant
Non-vaccinated (750 x MLD)	10	PBS
PBS (750 x MLD) IM	10	Alhydrogel®
Crm197-CPS + LoIC (750 x MLD) IM	20	Alhydrogel®
PBS (750 x MLD) IM	10	Poly(I:C) + Alhydrogel®
Crm197-CPS + LoIC (750 x MLD) IM	20	Poly(I:C) + Alhydrogel®
PBS (750 x MLD) IM	10	AddaVax™
Crm197-CPS + LoIC (750 x MLD) IM	20	AddaVax™
PBS (750 x MLD) 1 st /2 nd IM 3 rd SC	10	AS04
Crm197-CPS + LoIC (750 x MLD) 1 st /2 nd IM 3 rd SC	20	AS04
PBS (750 x MLD) SC	10	Poly(I:C) + Alhydrogel®
Crm197-CPS (750 x MLD) SC	10	Poly(I:C) + Alhydrogel®

Crm197-CPS (750 x MLD) IM	10	Poly(I:C) + Alhydrogel®
Naïve (450 x MLD)	5	PBS
Yeast tandem core VLP- CPS (450 x MLD) IM	15	Alhydrogel®
Yeast monomeric VLP-CPS (450 x MLD) IM	15	Alhydrogel®
Yeast monomeric VLP (450 x MLD) IM	5	Alhydrogel®
Yeast tandem core VLP (450 x MLD) IM	5	Alhydrogel®

Table 12 Experimental plan for Adjuvant selection study detailing vaccine candidates, number of mice, adjuvant and immunisation route. Each cohort were challenged with 450 or 750 x median lethal doses of *B. pseudomallei* K96243 via the IP route and observed for 35 days.

At formulation, vaccines were diluted for each mouse to receive 5 µg per dose of CPS. Due to variation in CPS conjugation efficiency between the conjugates this resulted in mice receiving 0.2 µg VLP (tandem coreTM), 0.3 µg VLP (monomeric) or 7 µg Crm197. *Burkholderia* proteins were administered at 5 µg per dose.

The main focus of the study was to assess the difference in protective efficacy of a Crm197-CPS conjugate with the *Burkholderia* protein LolC added as a co-antigen with four different adjuvants; Alhydrogel®, Poly (I:C), AddaVaxTM or AS04. These groups were immunized by the intramuscular (IM) route. There was no significant difference in protective efficacy between any of the adjuvants

($p=0.3578$, Figure 103) although median survival was greatest in the groups that received Alum and Poly (I:C) with alum (Table 13).

Following vaccine administration however, the development of severe swellings at the injection site in mice that received AS04 resulted in the cull of one mouse following the second vaccination. To avoid further animal loss, the third vaccination for groups that received AS04 was altered to the subcutaneous route.

Analysis of the splenocyte IFN- γ recall response to the Crm197 carrier protein from these mice revealed a statistically significant increase in IFN- γ in those mice vaccinated with the Poly (I:C) + Alhydrogel® adjuvant ($p\leq 0.0001$) compared to mice vaccinated with Alum, indicating that the Poly(I:C) + Alhydrogel® adjuvant offers the greatest enhancement to carrier protein immunogenicity (Figure 104).

This is also confirmed by ELISA analysis of the Crm197 specific IgG response from mouse sera taken after each vaccination. The results indicate that Alhydrogel® vaccinated mice have significantly lower Crm197-specific IgG titres following the third vaccination than mice that received MF59™ ($p\leq 0.01$) or Poly (I:C) + Alhydrogel ($p\leq 0.0001$) (Figure 105).

Following the third vaccination, LolC-specific IgG titres were significantly lower in the Alhydrogel® vaccinated groups ($p=0.0076$). Interestingly, after the second vaccination, IgG antibody titres to LolC were significantly higher in the mice that received AS04 ($p\leq 0.0001$) (Figure 106).

CPS specific IgG and IgM titres were at the limit of detection from the Crm197-CPS conjugates and so are not presented.

To provide a comparison in conjugate protective efficacy between immunisation routes, mice were vaccinated by the intramuscular and subcutaneous routes with Crm197-CPS. No significant difference in protection was observed ($p=0.0902$) (Figure 107).

CPS specific titres from the DstI vaccines given by either route were at the limit of detection for the assay and are not reported.

In this study, the protective efficacy of a VLP-CPS conjugate vaccine made of Tandem Core™ VLPs was compared against a VLP assembled from HBcAg (Conjucore). There was no significant difference in protection between the two vaccines ($p=0.8787$, Figure 108) but the median survival was 3 days from Tandem Core™ vaccinated mice and 11 days from Conjucore.

Figure 109 shows the VLP specific IgG response from mouse sera taken after each vaccination determined by ELISA. The IgG response was significantly higher following the second and third vaccination in those mice that received HBcAg VLPs ($p\leq 0.01$ and $p\leq 0.0001$ respectively). This may result from the difference in VLP concentration that the mice received. For each dose of 5 µg CPS, mice received 0.2 µg of Tandem Core™ VLP or 0.3 µg of HBcAg VLP. This may also account for the relatively low IgG response to VLPs in comparison to previous studies where the amount of VLPs each mouse received was greater than 1 µg.

Neither mouse that received Crm197-CPS + AS04 nor Tandem Core™ VLP-CPS that survived until the end of the study had cleared *B. pseudomallei* infection from the spleen. Both animals had lost approximately 10 % of bodyweight and the continued presence of clinical signs means that both animals would probably have succumbed to infection (data not shown).

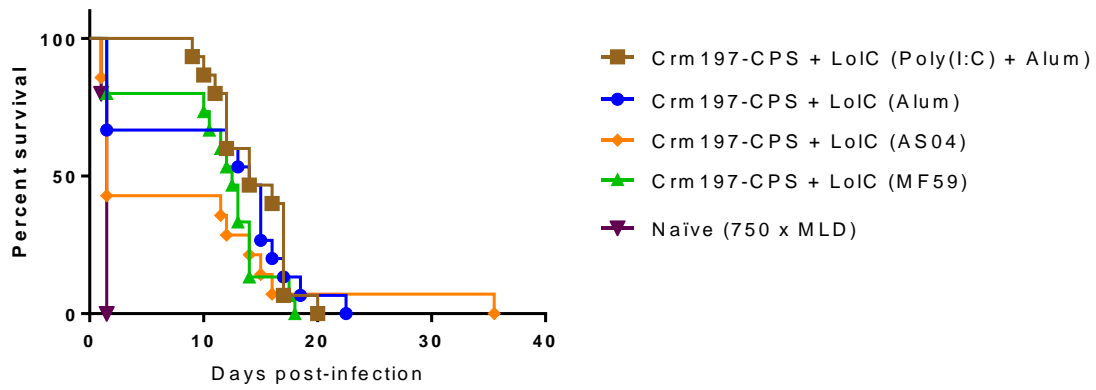


Figure 103 Efficacy comparison of Crm197-CPS conjugate with different adjuvants against a 750 x MLD *B. pseudomallei* K96243 challenge. Mice (n = 15 mice per group) were immunized with Crm197-CPS + LoIC formulated with Alum; MF59; Poly(I:C) + Alum; and AS04 via the i.m. route on days 0, 14 and 28. Five weeks after the final immunisation, mice were challenged i.p. with 750 x MLD of *B. pseudomallei* K96243. Significance was determined by the log-rank (Mantel-Cox).

Adjuvant	Median survival (days)
Alum	14
Poly(I:C) + alum	14
MF59	12.5
AS04	1.5

Table 13 Median survival of mice following vaccination with Crm197-CPS + LoIC adjuvanted with either Alhydrogel®, Poly (I:C) + Alhydrogel®, AddaVax™ or AS04.

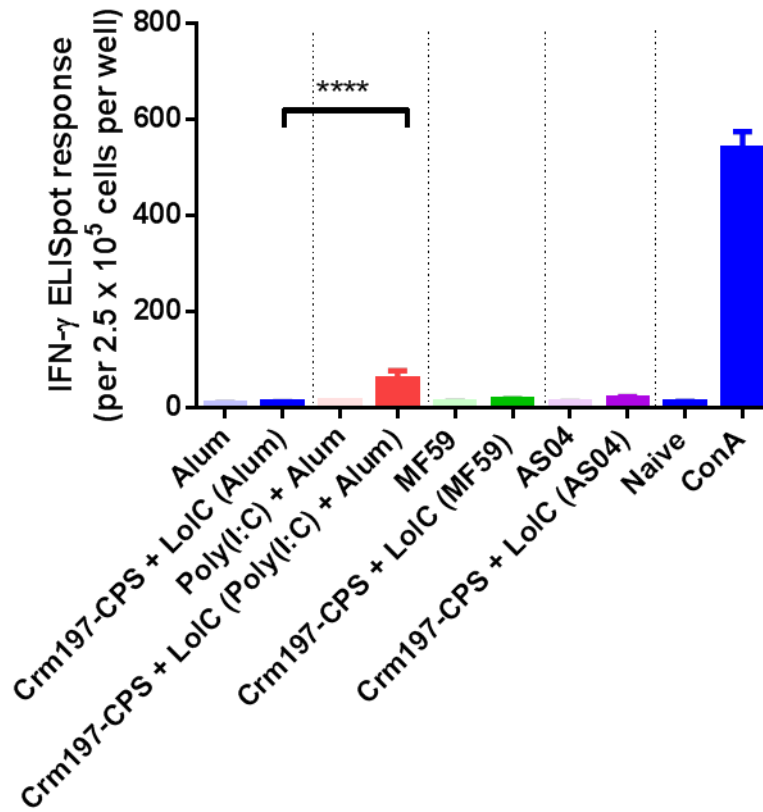


Figure 104 Vaccinated mice splenocyte IFN- γ recall response to Crm197 determined by ELISpot. Mice ($n = 5$ mice per group) were vaccinated on days 0, 14 and 28. Two weeks after the final boost, mice were culled, spleens removed and splenocytes cultured for antigen re-stimulation and measurement of IFN- γ by ELISpot (**** $p \leq 0.0001$).

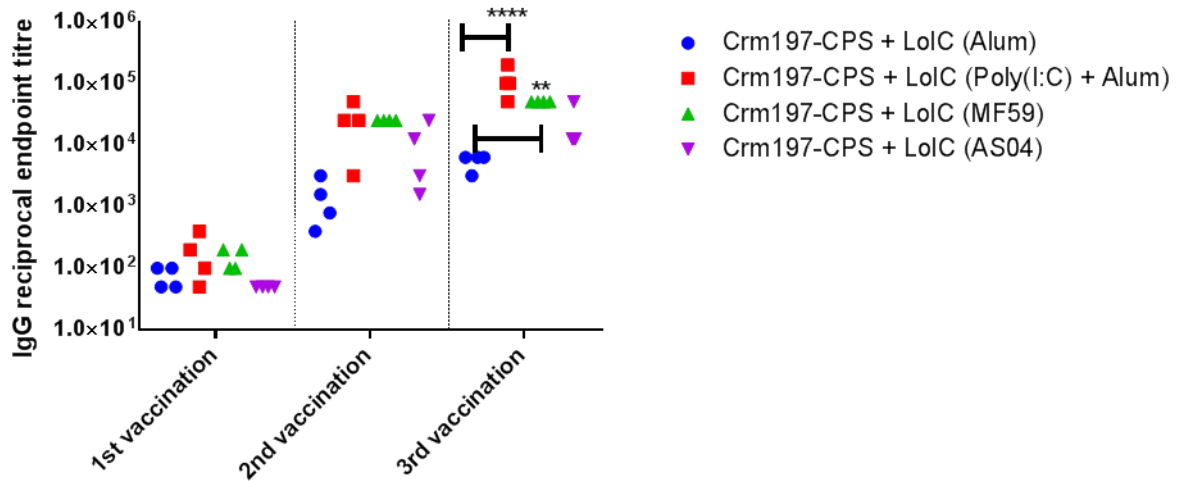


Figure 105 ELISA analysis of the Crm197 specific IgG antibody response from mouse sera obtained after each vaccination from the adjuvant selection study. Mice were immunised on days 0, 14 and 28 via the i.m. route. Sera was obtained from mice 14 days after the final boost, and titres of IgG specific for Crm197 were determined by ELISA. Individual symbols represent a cage of 5 mice. **** $p \leq 0.0001$, ** $p \leq 0.01$).

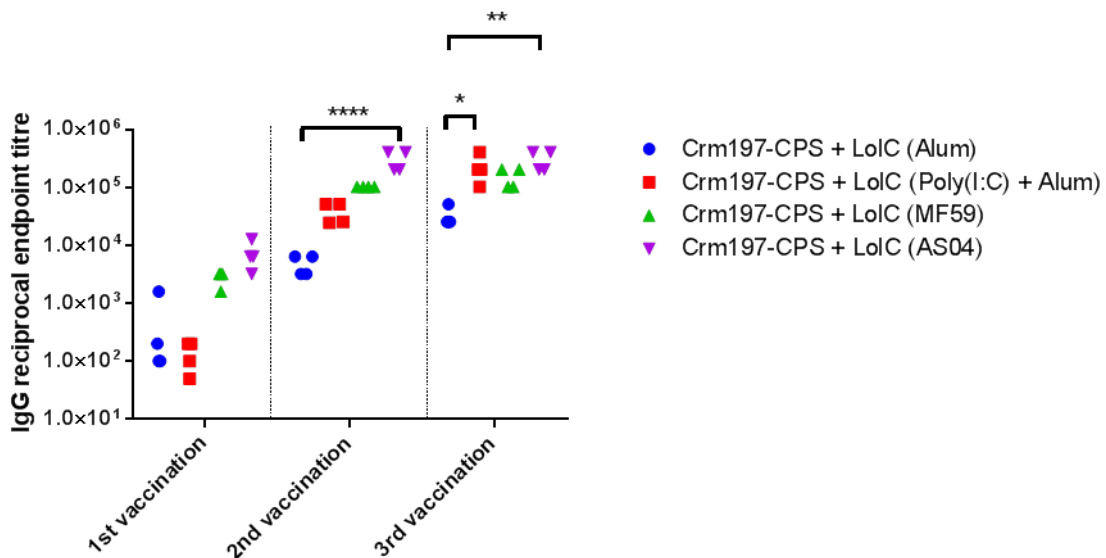


Figure 106 ELISA analysis of the LoIC specific IgG antibody response from mouse sera obtained after each vaccination from the adjuvant selection study. Mice were immunised on days 0, 14 and 28 via the i.m. route. Sera was obtained from mice 14 days after the final boost, and titres of IgG specific for Crm197 were determined by ELISA. Individual symbols represent a cage of 5 mice. **** $p \leq 0.0001$, ** $p \leq 0.01$, * $p \leq 0.05$ (1-way ANOVA).

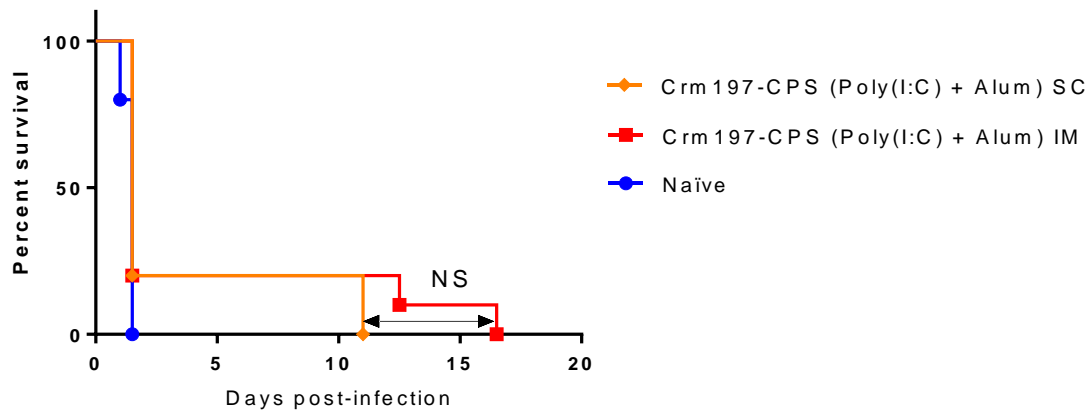


Figure 107 Effect of vaccination route on Crm197-CPS vaccine efficacy against a 750 x MLD *B. pseudomallei* K96243 challenge. Mice (n = 10 mice per group) were immunized with Crm197-CPS + LoIC formulated with Poly(I:C) + Alum via the i.m. and s.c. route on days 0, 14 and 28. Five weeks after the final immunisation, mice were challenged i.p. with 750 x MLD of *B. pseudomallei* K96243. NS, no statistical significance by the log-rank (Mantel-Cox) test.

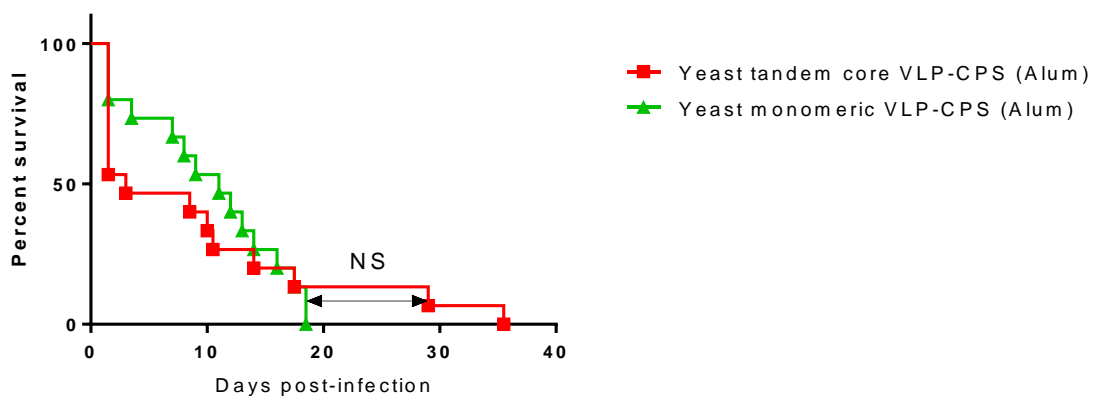


Figure 108 Efficacy comparison of Tandem Core™ and monomeric core VLPs conjugated to CPS against a 450 x MLD *B. pseudomallei* K96243 challenge. Mice (n = 15 mice per group) were immunized with Tandem Core™ VLP-CPS, and monomeric core VLP-CPS, formulated with Alum via the i.m route on days 0, 14 and 28. Five weeks after the final immunisation, mice were challenged i.p. with 450 x MLD of *B. pseudomallei* K96243. NS, no statistical significance by the log-rank (Mantel-Cox) test.

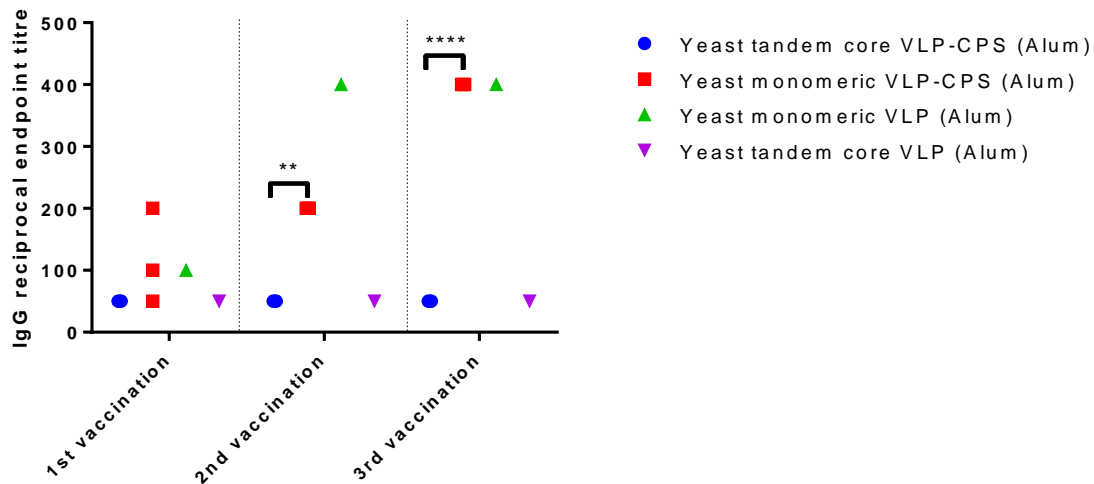


Figure 109 ELISA analysis of the VLP specific IgG antibody response from mouse sera obtained after each vaccination from the adjuvant selection study. Mice were immunised on days 0, 14 and 28 via the i.m. route. Sera was obtained from mice 14 days after the final boost, and titres of IgG specific for VLP were determined by ELISA. Individual symbols represent a cage of 5 mice. ** $p \leq 0.01$, **** $p \leq 0.0001$. (2-way ANOVA).

5.5 Discussion

The aim of this chapter was to assess the protective efficacy of conjugate vaccines in mice against intraperitoneal challenge with *B. pseudomallei* K96243. These candidates included capsular polysaccharide (CPS) conjugated to a non-toxic mutant of diphtheria toxin (Crm197-CPS), virus-like particles (VLP-CPS) and the *Burkholderia* protein LolC (LolC-CPS). The protective efficacy of several *Burkholderia* proteins were also determined as well as their impact on efficacy of a CPS conjugate vaccine when added as co-antigens. The effect of adjuvant selection on Crm197-CPS conjugate vaccine efficacy was also assessed with Alhydrogel®, Poly (I:C) + Alhydrogel®, AddaVax™ and AS04. Finally, the effect of vaccination route, intramuscular or subcutaneous, on vaccine efficacy against bacterial challenge was also determined. These were investigated over four animal studies, each at different challenge doses.

The use of each carrier protein reflects different levels of risk. A commercially available carrier protein such as Crm197 represents the lowest level of risk as

large-scale production of pure material, which can be used in man, is already available. The effectiveness of Crm197 as a carrier protein has also been demonstrated by its use in several licensed vaccines for meningococcal, Hib and pneumococcal disease (Knuf *et al.*, 2011). The use of VLPs was a medium/high risk as their compatibility with *Burkholderia* antigens had not been demonstrated. The use of VLPs for the treatment of bacterial infections is also not well established as the main utility are as vaccine candidates or carrier proteins to viral or parasitic infections (Pumpens and Grens, 2001, Grgacic and Anderson, 2006, Kushnir *et al.*, 2012). Methods for VLP extraction and purification are however available. The use of a *Burkholderia* protein as a carrier is high risk. To the author's knowledge, no one has attempted conjugation of CPS to a *Burkholderia* protein, although *Burkholderia* O-polysaccharide has been successfully conjugated with flagellin from the same species (Brett *et al.*, 1996) and CPS conjugation to bovine serum albumin (Scott *et al.*, 2014). While conjugation of CPS to a *Burkholderia* protein would be relatively straightforward, protective efficacy is completely unknown and is likely to vary with each different protein. Protein expression would also rely on generic methods which are not optimised for *Burkholderia* proteins.

The first animal study was performed in order to determine an initial vaccine efficacy range. The protective efficacy of both VLP-CPS, constructed with VLPs expressed from *N. benthamiana*, and Crm197-CPS were assessed against two *B. pseudomallei* challenge doses of 10³ and 240 x MLD. At both challenge doses the absolute level of survival was greatest in mice that received the VLP-CPS vaccine although statistical significance over Crm197-CPS was not achieved. Combining the data from both challenge doses into a single survival curve resulted in significantly greater protection with VLP-CPS than Crm197-CPS. ELISA analysis of mouse sera taken after the third vaccination showed the presence of CPS-specific IgM antibody titres in mice that received CPS and CPS-specific IgM and IgG antibody titres in the groups that received the conjugate vaccines. This finding was expected as the carrier protein stimulates development of T-cell dependent immunogenicity against the polysaccharide, which includes antibody isotype switching from IgM to IgG (Jones *et al.*, 2005). Interestingly, CPS specific IgG titres were highest in the Crm197-CPS vaccinated groups suggesting that total IgG or IgM antibody titres are not

necessarily indicative of protection at these challenge doses. This is unusual as humoral immunity has been reported as an important mechanism of protection against *B. pseudomallei* infection (Silva and Dow, 2013) and for most other vaccines (Plotkin 2008).

The second animal study determined the protective efficacy of Crm197-CPS, VLP-CPS constructed with VLPs expressed by *P. pastoris* (VLP-CPS (yeast)) and *N. benthamiana* (VLP-CPS (plant)) and LoIC-CPS, at a higher challenge dose of 489 x MLD. The challenge dose was increased due to the high survival from VLP-CPS vaccinated mice in the previous study. At this dose, Crm197-CPS provided significantly greater protection to *B. pseudomallei* challenge in vaccinated mice than VLP-CPS. Efficacy of the VLP-CPS (plant) conjugate mixed with LoIC however, was not significantly different to Crm197-CPS which is in agreement with published data where addition of LoIC to a CPS conjugate vaccine significantly improved survival (Scott *et al.*, 2014).

Crm197-CPS vaccinated mice had greater CPS-specific IgG titres. In conjunction with the previous study, this suggests that antibody titres become important for protection when the challenge dose is high. This is not unexpected as it is known that correlates of protection are often relative to the challenge dose (Plotkin 2008). A LoIC-CPS conjugate gave significantly less protection than either the Crm197-CPS or VLP-CPS (plant) conjugate vaccine. The protective efficacy of LoIC as the primary antigen was also poor as survival in vaccinated mice was not significantly different to mice vaccinated with adjuvant (Alhydrogel®) only. Reported data demonstrating the protective efficacy of LoIC was at a much lower challenge dose of approximately 50 x MLD (Harland *et al.*, 2007) so it is possible that 489 x MLD is too high a challenge for LoIC to provide protection as the primary antigen. High LoIC-specific IgG titres, in groups that received LoIC, demonstrate the difference between an immunogenic and protective antigen. The lack of CPS-specific antibody titres in mice vaccinated with LoIC-CPS suggests LoIC contains immunodominant epitopes which directs the immune response away from CPS. It has been reported that the ideal carrier protein should induce strong immune responses to the conjugated B-cell epitope without inducing a high antibody response to itself (Baraldo *et al.*, 2004, Pobre *et al.*, 2014). The use of other *Burkholderia* proteins may be successful.

The VLP conjugates made from plant expressed VLPs gave significantly better protection in mice to *B. pseudomallei* challenge than conjugates from yeast expressed VLPs. The reason for this is unknown but yeast expressed VLPs contained a double lysine (K1K1) binding motif for conjugation to CPS whereas plant expressed VLPs contained six lysine's flanked on either side by 3 aspartates (D3K6D3). As each lysine could theoretically conjugate CPS, plant expressed VLPs may conjugate more CPS molecules and the flanking aspartate (D3) moieties may have shielded the lysine positive charge leading to efficient VLP assembly. To determine whether the disparity in efficacy was due to these differences in the MIR of the VLPs, a yeast expressed VLP with the D3K6D3 insert was produced and tested in the following study.

The third animal study in this thesis assessed the protective efficacy of *Burkholderia* proteins added as co-antigens with a Crm197-CPS conjugate against *B. pseudomallei* challenge at 399 x MLD. Published data reports that addition of LolC to a CPS conjugate vaccine significantly improved efficacy against *B. pseudomallei* challenge (Scott *et al.*, 2014). This is not unexpected as cellular and humoral immune responses may be required for protection against *B. pseudomallei* challenge (Silva and Dow 2013) therefore addition of a melioidosis relevant protein antigen would be beneficial. Addition of *Burkholderia* proteins as co-antigens in this study gave no significant difference in protection to the Crm197-CPS only vaccinated group, although a Crm197-CPS conjugate containing LolC offers the greatest median survival. The difference between this result and that of Scott *et al.* maybe due to the use of bovine serum albumin (BSA) by Scott as the carrier protein. LolC and Hcp6-specific IgG titres were significantly reduced when added to Crm197-CPS compared to when the protein was administered as the primary antigen, which was also seen for LolC by Scott *et al.* The reduction in *Burkholderia*-specific IgG titres was not seen with the addition of PotF or OppA to Crm197, or Hcp6 to VLP-CPS (yeast). This suggests that within a vaccine, individual antigen immunogenicity affects the immune response to the other components.

The poor protective efficacy of the *Burkholderia* proteins against *B. pseudomallei* challenge is probably a result of the challenge dose used in

this study as LolC and PotF have been shown to be protective at ~50 x MLD (Harland *et al.*, 2007a) and Hcp6 at ~67 x MLD (Burtnick *et al.*, 2011).

An additional objective in this study was to compare plant and yeast expressed VLPs conjugated to CPS. As in the previous study, vaccination with plant expressed VLPs conjugated to CPS resulted in statistically greater protection in mice to *B. pseudomallei* challenge than yeast expressed VLPs. In this study, both VLP constructs contained a D3K6D3 binding motif for chemical conjugation to CPS, thereby discounting this structural difference as the reason for the difference in protection. It is not known why plant expressed VLPs are more efficacious. It is possible that despite the high purity of the VLPs, contaminants specific to the expression system remain and plant-derived contaminants act as an additional adjuvant increasing vaccine efficacy. Alternatively, yeast expression systems have differences in protein glycosylation to mammalian cells whereas plants do not (Mett *et al.*, 2008). As expression of hepatitis B surface antigen for the licensed vaccine Recombivax HB® is expressed in yeast (Kushnir *et al.*, 2012), it is unlikely that this is the reason. In communication with Mologic, it was reported that plant expressed VLPs were more robust than yeast expressed VLPs which may have effect conjugate stability.

Vaccines consisting of pure or recombinant antigens can be less immunogenic than whole-cell alternatives and usually require an adjuvant to increase immunogenicity (Mohan *et al.*, 2013). Aluminium salts are the most widely used human adjuvants and generate a strong Th2 response (Ghimire 2015) which means that Alhydrogel® may not provide full protection against *B. pseudomallei* infection if both humoral and cellular immune responses are required (Silva and Dow, 2013). Therefore, the final animal study assessed the protective efficacy of a Crm197-CPS conjugate vaccine containing LolC with four different adjuvants; Alhydrogel®, Poly (I:C) + Alhydrogel®, AddaVax™ and AS04 in mice against 750 x MLD challenge of *B. pseudomallei*. There was no significant difference in protection between them although median survival was lower in groups that received AS04. The LolC and Crm197 specific IgG antibody response was lower in mice vaccinated with Alhydrogel®, indicating increased T-cell recruitment from the other adjuvants. The IFN- γ response to Crm197, the

classical indicator of a Th1 response, was only significantly improved with Poly (I:C) with Alhydrogel®. AddaVax™ stimulates a mixed Th1 and Th2 response and AS04 Th1 (Hagan *et al.*, 2012, Didierlaurent *et al.*, 2009) so the lack of IFN- γ to Crm197 was unexpected but the immune response to an adjuvant is multifactorial and depends on the antigen and immune status of the host (O'Hagan *et al.*, 2012). It is possible that Crm197 is predominantly processed as a Th2 stimulating antigen or that it is difficult to stimulate cell mediated reactions in BALB/c mice as they are Th2-biased. The suggestion in this thesis that CPS-specific antibody titres are not a good correlate of protection indicates that a Th1 stimulating adjuvant may still improve vaccine efficacy compared to Alhydrogel®, therefore assessment of alternative adjuvants is still justified. It may be appropriate for adjuvant assessment in C57BL/6 mice as they are Th1-biased (Hoppe *et al.*, 1999). The replacement of aluminium based adjuvants may be beneficial as Alhydrogel® cannot be frozen or lyophilised (Sivakumar *et al.*, 2011) which is an important aspect of any military medical countermeasure as it can be difficult to maintain a cold chain.

The inflammatory immune response at the injection site in mice that received AS04 resulted in the cull of one mouse following the second vaccination and a change in administration route from intramuscular to subcutaneous to avoid potential animal loss following the third vaccination. It is possible that this response was deleterious to the protective efficacy of the vaccine. Alternatively, the LolC-specific IgG titres were highest in mice that received AS04, whereas the Crm197-CPS specific IgG titres generated in mice that received this adjuvant were not significantly different to Alum vaccinated mice. This suggests that AS04 has directed the immune response towards LolC, which at this challenge dose is not protective.

Adjuvants also considered include CpG and immune stimulating complexes (ISCOM). CpG is composed of small sequences of cytosine and guanine separated by phosphate and is a TLR9 agonist. It induces strong Th1 responses and has been investigated for use in cancer, HIV and malaria vaccines (Lawson *et al.*, 2011). ISCOM are ring structures containing cholesterol, phosphatidylcholine and saponins. They induce a Th1 and Th2 immune response and have been investigated for use with influenza and cancer

vaccines (Levast *et al.*, 2014). CpG and ISCOM were not included because they are still in the research phase and it will be many years before they can be used in the clinic.

The final animal study also assessed the protective efficacy of a Crm197-CPS conjugate administered by either the subcutaneous or intramuscular route. There were no significant differences in survival or generation of CPS-specific IgG titres. Subcutaneous vaccination with these conjugates is an improvement to animal welfare as localised swelling at the injection site, which was seen in all studies in this thesis, may restrict mobility following intramuscular administration. Muscle fibre distension can also be painful following intramuscular injection (Ward, 2008).

The advantage of the Tandem CoreTM system lies in the ability to manipulate the two antigenic loops of core protein dimers individually and had been selected on the basis that proteins could be expressed in a single MIR on a dimer spike (Peyret *et al.*, 2015). However, since this advantage could not be exploited, the efficacy of monomeric HBcAg VLPs conjugated to CPS was assessed in the final study against 450 x MLD challenge with *B. pseudomallei*. Conjucore, made by our collaborators at Mologic, is a full length HBV core protein that was engineered to introduce 3 lysine residues in the antigenic loop. The insert was charge neutralised by 3 alternate aspartic acid residues (DKDKDK). There was no significant difference in protection between the Tandem CoreTM based VLP conjugated to CPS and monomeric VLP-CPS thereby allowing the use of monomeric based VLPs for future studies.

To summarise, VLP-CPS vaccines had greater efficacy than Crm197-CPS at the lower challenge doses of 103 and 240 x MLD whereas Crm197-CPS had greater efficacy at 399 and 489 x MLD. The significantly lower CPS-specific IgG antibody titres generated by a VLP-CPS conjugate suggests that titre is not indicative of vaccine efficacy at lower challenge levels but may become significant at higher challenge doses. This is unexpected as for nearly all vaccines, prevention of infection correlates with the induction of specific antibodies. For the three of the main bacterial pathogens that cause disease; *H. influenzae* type b, pneumococci, and meningococci, the correlates are

opsonophagocytic or bactericidal antibodies (Plotkin 2010). A possible explanation is that a VLP-CPS conjugate may generate low levels of high-affinity antibody or is efficacious via a different, perhaps cellular mediated, mechanism. This effect is superior at low doses but at high doses bacterial numbers may overwhelm the immune response, and therefore the relatively low antibody titre, or denies the time needed for generation of a cellular response.

The majority of mice surviving up to day 35 on all studies, with all vaccines, displayed continued bodyweight loss and clinical signs over this period. At study end it is possible that these mice had entered the chronic phase of melioidosis infection and would have eventually succumbed to the infection. It could be argued that these vaccine candidates had essentially extended the mean time to death as sterilising immunity was not achieved in the majority of animals. While this may be true, it would be argued that the challenge doses used across these studies were chosen to discriminate the protective efficacy between vaccine candidates only and they are not indicative of challenge doses that a vaccine would be expected to provide full protection against and that despite the high challenge doses, several mice did clear *B. pseudomallei* infection from the liver, lung or spleen. The pathology and clinical signs associated with the IP route of infection in this thesis correlate well with those reported by Welkos *et al.*, (2015). The most common pathological finding included abscess formation in the spleen and splenomegaly. A few animals developed large swellings on the tail. The majority of mice were culled due to immobility, with no movement despite provocation. Some of the mice culled had developed rear limb paralysis. As reported by Welkos *et al.*, (2015), mice usually presented with a limp before progression to paralysis.

An important consideration for production of a conjugate vaccine and comparing protective efficacy is the polysaccharide to carrier protein ratio. Licensed vaccines typically have a 1:1 ratio by weight (Plotkin *et al.*, 2013). Production of a CPS vaccine is made difficult by the unknown chain length of CPS and the difficulty of reliable fragmentation of CPS whilst retaining immunogenicity (Chapter 3; *Burkholderia* capsular polysaccharide). Inefficiencies with carbohydrate coupling to protein by reductive amination also results in different CPS to carrier protein ratios (Gildersleeve *et al.*, 2008). Assessment of the

importance of CPS-protein ratio is difficult with the VLP conjugates due to differences in construct binding motifs and use of different expression systems. For this reason, the effect of CPS-protein ratio on vaccine efficacy across these studies has focussed on the Crm197-CPS conjugates only, without the addition of LolC (Figure 110).

Three of the Crm197-CPS conjugates have polysaccharide to protein ratios in favour of CPS (efficacy assessed at 103, 240 and 489 x MLD challenge doses). For these, the protective efficacy of the conjugate decreases as the challenge dose increases. At a challenge dose of 399 x MLD, the CPS: Crm197 ratio (w/w) was in favour of Crm197. At this challenge dose, the protective efficacy of the vaccine is not significantly different to vaccine efficacy at 240 x MLD, although the CPS-specific IgG titre is significantly lower. As carrier protein is critical for development of a TD response to polysaccharide, it is perhaps not surprising that a greater amount of Crm197 leads to an improved immune response to CPS and protective efficacy against challenge. A greater amount of polysaccharide may lead to greater polysaccharide-specific antibody titres but this is offset by the comparatively reduced T-cell help and reduced antibody affinity or protective functionality.

The MW of CPS is approximately 200 kDa, whilst that of Crm197 is 58.4 kDa, therefore a w/w ratio of 1:3.4 is required to achieve a 1:1 ratio based on molecular weight. This is exactly the ratio for the vaccine assessed against 399 x MLD. This suggests that production of a Crm197-CPS conjugate should aim for antigen equivalency based on molecular weight rather than the amount of each component administered.

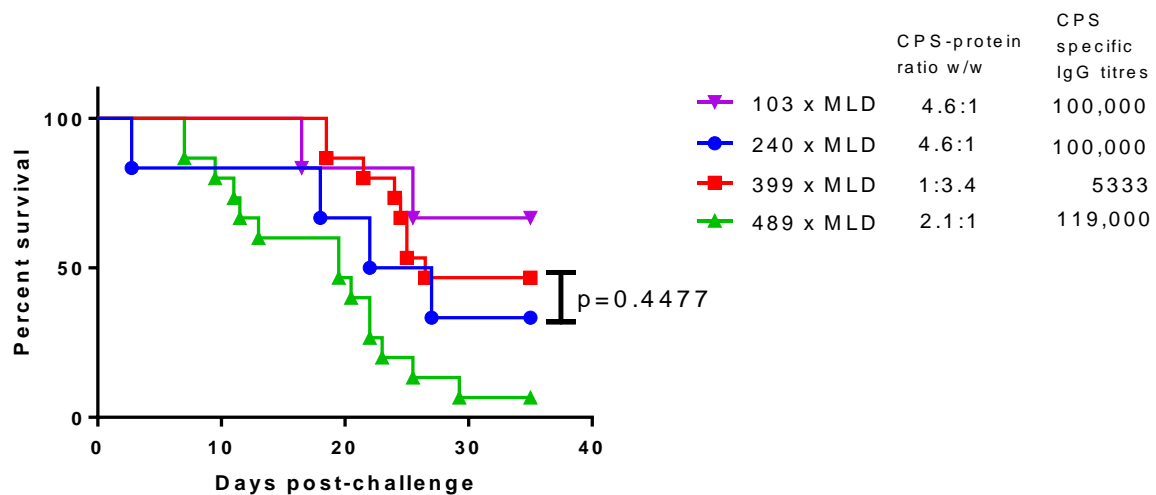


Figure 110 Efficacy of Crm197-CPS conjugate vaccines with different CPS-protein ratios against 103, 240, 399 and 489 x MLD *B. pseudomallei* K96243 challenge. Mice were immunised with Crm197-CPS formulated with Alum, via the i.m. route on days 0, 14 and 28. Five weeks after the final immunisation, mice were challenged i.p. with 103, 240, 399 or 489 x MLD of *B. pseudomallei* K96243. Significance was determined by the log-rank (Mantel-Cox). n = 6 for 103 and 240 x MLD, n = 15 for 399 and 489 x MLD.

With large differences in CPS-protein ratios (w/w) in favour of CPS, the carrier protein may not be displayed efficiently to the immune system and a ratio in favour of the protein may be insufficient to generate a CPS antibody response if the protein is present in excessive amounts. This has been demonstrated in paediatric studies with meningococcal group C (MenC) conjugates where Crm197 amounts greater than 47 µg per dose lowered geometric mean antibody titres to MenC (Lee and Blake 2012).

Analysis of the CPS to VLP ratio on vaccine efficacy is more complex due to changes in binding motif and expression system but Figure 111 suggests that for yeast expressed VLPs conjugated to CPS, the CPS to protein ratio does not make any significant difference to protective efficacy and that an increase in the ratio of CPS does not improve CPS specific IgG antibody titres. The CPS-VLP ratio for nearly all constructs were in favour of CPS with the exception of VLP-CPS (yeast) assessed against 489 x MLD challenge (1:1.4). As the MW of the Tandem CoreTM is approximately 39 kDa and CPS ~200 kDa then the CPS-protein ratio would need to be 1:5.1 to achieve a 1:1 ratio based on molecular

weight. This assumes however, that each Tandem Core™ is conjugated to a CPS molecule which is unknown.

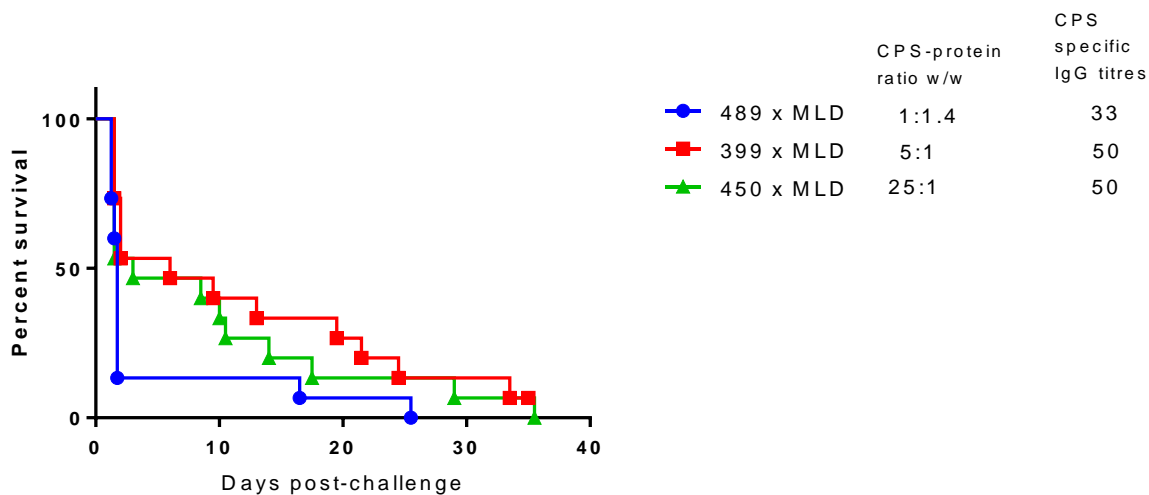


Figure 111 Efficacy of VLP-CPS conjugate vaccines with different CPS-protein ratios against 399, 450 and 489 x MLD *B. pseudomallei* K96243 challenge. Mice (n = 15 mice per group) were immunised with yeast expressed VLPs conjugated to CPS formulated with Alum, via the i.m. route, on days 0, 14 and 28. Five weeks after the final immunisation, mice were challenged i.p. with 399, 450, or 489 x MLD of *B. pseudomallei* K96243. Significance was determined by the log-rank (Mantel-Cox).

Several difficulties remain in the production of a CPS conjugate vaccine. It is reported that free polysaccharide can reduce the effectiveness of a conjugate vaccine (Rodriguez *et al.*, 1998). In licensed vaccines, free polysaccharide is removed by size fractionation although this is made possible by hydrolysis of the polysaccharide to small chain lengths prior to conjugation (Plotkin *et al.*, 2013). As CPS cannot be hydrolysed reproducibly and without potential removal of the acetyl group (Chapter 3; *Burkholderia* capsular polysaccharide), free CPS cannot easily be removed from the conjugate and there is no method available to determine the amount of free or conjugated polysaccharide. This problem is faced by all researchers of Melioidosis vaccines and may reduce the potency of vaccine candidates.

5.6 Supplementary information

5.6.1 VLP expression systems

5.6.1.1 Expression and purification of VLPs in *E.coli*

While high levels of tandem core expression were achieved with the use of *E. coli* (Chapter 2, Method 2.12.1), protein purified by size exclusion chromatography was of approximately 40 % purity (determined by SDS PAGE). Transmission Electron Microscopy (TEM) analysis revealed that the tandem core had formed heterogeneous, irregularly shaped assemblies. Over time these miss-folded VLPs tended to form aggregates with contaminating host protein and were therefore not suitable for conjugation to CPS (Figure 112).

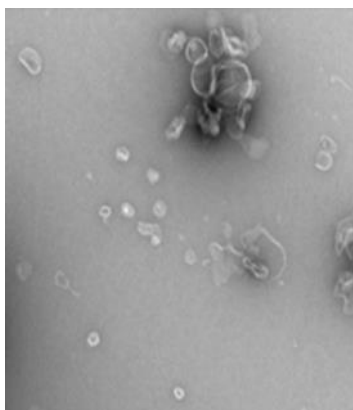


Figure 112 TEM analysis of *E. coli* expressed tandem core VLPs.

5.6.1.2 Expression and purification of VLPs from *baculovirus*

The *baculovirus* expression system is a versatile platform for the production of recombinant proteins requiring multiple post-translational modifications (Liu *et al.*, 2012) and FDA approval for an influenza recombinant product made in *baculovirus* was attained in 2012. A *baculovirus* expression system was investigated and found to be capable of producing the VLPs (Chapter 2, Method 2.12.2). Expression was reasonable but was contaminated with *baculovirus* itself as capsids were clearly visible by electron microscopy (Figure 113).

Purification by CL4B size exclusion chromatography resulted in co-elution of tandem core.

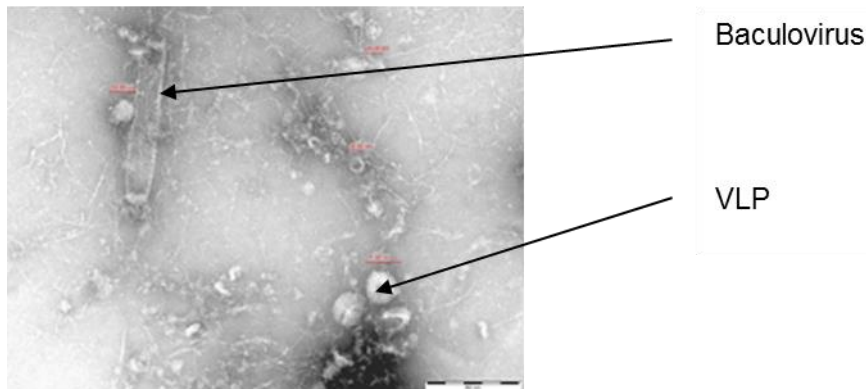


Figure 113 Electron micrograph of VLP from *Baculovirus*

5.6.1.3 Expression of tandem core constructs in *Nicotiana benthamiana*

Plants are considered as a novel, speedy and economical production platform for VLP-based vaccines (Chen and Lai, 2013) and therefore were investigated in this work. Expression in plants was achieved using *Agrobacterium*-mediated transient transformation technology with six *Nicotiana benthamiana* plants producing approximately 3 mg of rVLP containing a K6 insert at 90 % purity (Chapter 2, Method 2.12.3). This material was shown to be highly immunogenic for core protein and from 100 g infiltrated leaves, 20 mg VLP were purified with an estimated purity of > 80 % by SDS PAGE and TEM analysis (Figure 114).

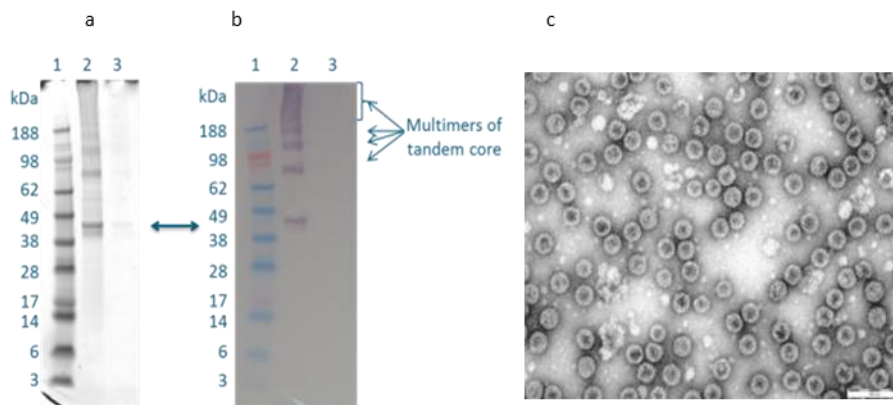


Figure 114 SDS PAGE (a) western blot (b), and negative stain TEM analysis of purified VLP. 1. Protein standards, 2. Purified VLPs (neat), 3 Purified VLPs (1:10 diluted).

5.6.2 Expression of tandem core constructs in *Pichia pastoris*

Transformation of *P. pastoris* with the tandem core construct, codon optimised for expression in *P. pastoris*, followed by selection of high expression clones using zeocin concentrations up to 10 mg / mL resulted in high levels of protein expression. TEM analysis of cell lysates revealed that this construct produced very high yields of symmetrical VLPs with the expected size (34-38 nm) and morphology at an estimated 90 % purity. Immunogold labelling with negative stain TEM confirmed the presence of HBV core (Data not shown).

Chapter 6: Discussion

6.1 Introduction

Burkholderia capsular polysaccharide (CPS) is one of the main surface-associated antigens of *B. pseudomallei* and *B. mallei* (Tuanyok *et al.*, 2012) and is a known virulence determinant demonstrated by the fact that *B. pseudomallei* mutants lacking CPS have a 10^5 -fold increase in the median lethal dose (MLD) in an animal model (Atkins *et al.*, 2002). CPS has also been shown to be a protective antigen in animal models against *B. pseudomallei* challenge (Nelson *et al.*, 2004) and is therefore a good candidate for vaccine development.

The aim of this thesis was to assess the protective efficacy of a capsular polysaccharide protein conjugate vaccine utilising Tandem Core™, (VLPs), Crm197 and the *Burkholderia* protein LolC against *B. pseudomallei* challenge. This work was made up of three main objectives. The first was to investigate a potentially less-expensive source of CPS expressed by *B. thailandensis* E555. This work included optimising purified CPS extraction, and determining the importance of the CPS acetyl moiety to inform synthetic CPS production. The second was to identify *Burkholderia* proteins and the key immunogenic regions that could be used as co-antigens with a CPS-based conjugate vaccine. The final objective was to test the immunogenicity and protective efficacy of developed CPS conjugate vaccines in mice against an intraperitoneal *B. pseudomallei* challenge and assess adjuvant effect on efficacy.

6.2 Summary of results

6.2.1 CPS extraction and optimisation

A primary objective of this thesis was to optimise the extraction of CPS from *Burkholderia* species with a focus on improving yield or lowering cost of production (Chapter 3: *Burkholderia* capsular polysaccharide).

The work carried out in this project furthers the results of Sim *et al.*, (2010) by demonstrating that the CPS expressed by *B. thailandensis* E555 is structurally and immunologically indistinguishable from the CPS expressed by *B. pseudomallei* and *B. mallei*. The Advisory Committee on Dangerous Pathogens (ACDP) categorises *B. pseudomallei* as a Hazard Group 3 organism (approved list of Biological agents, HSE, 2013). This is defined as a biological agent that can cause severe human disease but effective prophylaxis or treatment is available. This means that *B. pseudomallei* has to be handled in containment level 3 (CL3) laboratories, which in the UK means the use of specialised laboratories and manipulation of the organism within a safety cabinet or isolator. This makes work at CL3 burdensome, time-consuming and expensive. Local procedures at Dstl also restrict the volume of bacterial culture that can be grown to 100 mL in a single volume. Given that the method for CPS extraction requires two litres of bacterial culture, this makes the use of *B. pseudomallei* onerous. In addition, the extraction procedure generates up to 40 litres of phenol waste and involves ultracentrifugation, freeze-drying and gel filtration (Perry *et al.*, 1995). All of these would be difficult to perform in a containment level 3 laboratory. *B. thailandensis* is not classified as hazardous by the ACDP and is considered essentially avirulent. CPS extraction from *B. thailandensis* can therefore be performed at lower levels of containment and this is highly advantageous in terms of cost, time and safety.

Extraction of CPS from *B. thailandensis* E555 was initially attempted by ethanol precipitation and phenol extraction, but both methods were unsuccessful. Utilising a modified hot-phenol extraction method used in previous studies (Perry *et al.*, 1995), native *Burkholderia* CPS was successfully extracted. This CPS was used for the development of a reliable and robust ELISA in order to measure CPS concentration. This was an invaluable tool for yield optimisation. Optimisation of purified CPS extraction focussed on improving yield by maximisation of bacterial culture CPS content. I hypothesised that a greater input would translate into a greater output and therefore reduce the cost of purified CPS. Other options considered to decrease cost were reducing the time taken to complete the extraction process by removal of unnecessary steps; and replacing phenol given the toxicity of the chemical and necessity to incinerate phenol-contaminated waste. Whilst these options were worthy of investigation,

maximising yield by increasing culture CPS concentration was considered to have the greatest potential impact.

The results from the CPS optimisation showed that the use of a bacterial starter culture, an extended incubation time, use of baffled flasks and enhanced phytone peptone broth increased CPS culture content 8-fold. However, the translation of this to yield of purified CPS is uncertain. Calculation of CPS was performed on live bacterial cultures so it is not unexpected that a multi-step extraction process, taking approximately 5 weeks to complete, would lead to a variable purified CPS yield. A CPS extract from *B. thailandensis* cultured in enhanced phytone peptone broth resulted in a yield of approximately 9 mg of purified CPS, which has been previously achieved with cultures in LB media. As CPS yield has varied from 0.5 to 18 mg with LB broth, further extractions would have to be performed utilising enhanced phytone peptone broth before a conclusion can be reached as to whether this is reproducibly increasing CPS yield.

Demonstration that CPS is released into the supernatant of a *B. thailandensis* E555 culture offers the opportunity to increase CPS yield as the supernatant is discarded in the current extraction method (Perry *et al.*, 1995). The feasibility of this approach is however unclear. Extraction of CPS from one litre of culture supernatant was attempted, but resulted in a negligible quantity of purified CPS (<1 mg). It is clear that the method for isolating CPS from supernatant will require optimisation to resolve this problem.

6.2.2 CPS immunogenicity

There is potential to lower the production cost of CPS by chemical synthesis of the molecule which is technically challenging due to the presence of an acetyl group on the second carbon. Less challenging would be synthesis of the molecule without this moiety but recent work suggested that the acetyl group is essential for the interaction of the CPS epitope with a monoclonal antibody (Marchetti *et al.*, 2015).

The development of an ELISA assay for CPS quantification also allowed for investigation of the importance of the acetyl group on immunogenicity. A total lack of anti-CPS monoclonal binding affinity was observed over a range of deacetylated CPS concentrations. This result was confirmed with three other anti-CPS monoclonal antibodies at Dstl. The importance of the acetyl group on CPS immunogenicity was confirmed in the animal study by A. Scott at Dstl and CPS-specific antibody analysis in this thesis. Deacetylated CPS was significantly less efficacious against *B. pseudomallei* challenge and sera from mice vaccinated with deacetylated CPS did not recognise CPS (Chapter 3: *Burkholderia* capsular polysaccharide). This result will guide the manufacture of synthetic CPS and development of a purified CPS-based vaccine, when production of known chain-lengths of CPS may be important. If this were achieved by hydrolysis, this might also remove a proportion of acetyl groups.

6.2.2.1 Anti-CPS antibody sequencing

The sequences of described anti-CPS monoclonal antibodies were investigated to determine heterogeneity. The high sequence homology of anti-CPS monoclonal antibodies suggests that the CPS epitope is highly restricted and underlines the importance of the acetyl group. The anti-CPS antibodies show high sequence homology to germline IGKV8-28*01 and IgHV6-6*01 (Chapter 4: Immunogenic *Burkholderia* proteins). This is also seen in antibodies that recognise C-pneumococcal polysaccharide backbone and *F. tularensis* O-antigen. This suggests that antibodies raised against bacterial polysaccharides are derived from a restricted set of germline sequences that do not undergo extensive maturation. This is already suggested for pneumococcal C-polysaccharide (Fernandez-Sanchez *et al.*, 2009) and for light-chain antibody responses in humans to Hib CPS (Adderson *et al.*, 1992).

6.2.3 VLP fusion constructs

An initial aim of this work was to generate a VLP based vaccine by insertion of whole sequences or key immunogenic regions of *Burkholderia* proteins into the Tandem CoreTM construct. However, protein insertion into major

immunodominant region 1 or 2 prevented VLP assembly, but the expressed *Burkholderia* protein LolC retained antibody epitopes which suggests correct folding of LolC had occurred. Whilst the physicochemical properties of the *Burkholderia* proteins may hinder VLP formation, it is possible that insertion of foreign sequences into Hepatitis B core VLPs is restricted. It may be that only small, hydrophilic proteins (e.g. green fluorescent protein) or peptide sequences, as has been demonstrated for influenzae (Tsybalova *et al.*, 2015), can be added to VLPs.

6.2.4 CPS conjugate vaccine efficacy

The primary objective of this project was to compare the protective efficacy of a VLP-CPS conjugate vaccine against CPS conjugated to the commercially available, classic-carrier Crm197. Both VLPs and Crm197 were shown in this thesis to be suitable carrier proteins for conjugation to CPS on the basis of protection against *B. pseudomallei* challenge in an animal model of melioidosis (Chapter 5: Immunogenicity and efficacy of candidate vaccines). The use of the *Burkholderia* protein LolC was not suitable for use as a carrier protein. At lower challenge levels, mice vaccinated with VLP-CPS had greater survival than mice that received Crm197-CPS. As the challenge dose increased, efficacy of the Crm197 conjugate was significantly greater. Interpretation of these results is difficult however due to the different protein to polysaccharide ratios between the conjugate vaccines. For nearly all studies, the protein to polysaccharide ratio for both Crm197-CPS and VLP-CPS was in favour of CPS but the effect of ratio differences is unknown. The addition of *Burkholderia* proteins added to a Crm197-CPS conjugate did not improve survival over Crm197-CPS alone, although this may be due to the high challenge dose employed. The use of modern Th1/Th2 biased adjuvants did not significantly affect vaccine efficacy compared to the traditional alum (Alhydrogel®) adjuvant.

6.3 Challenges encountered in this work

The majority of challenges in this thesis relate to the use of CPS. The extraction of CPS was a challenging process and would have been very difficult to achieve

without a detailed method provided by Assoc. Prof. Brett which is based on the modified hot-phenol method of Perry *et al.*, 1995. Initial attempts to extract CPS, while unsuccessful and were made difficult due to the lack of a method for CPS quantification. NMR analysis, the standard technique for analysis of polysaccharides (Frasch 2009), requires a sample with high purity and is unsuitable for CPS extraction or purification method development. The key marker for any CPS extraction method development however is purity of the final product. As the modified hot-phenol extraction procedure can take up to 5 weeks to complete, the effect on purity of any method alterations to increase yield take a significant time to become apparent as a full extraction will be required to give an unequivocal result.

While sufficient CPS was extracted for this project, the yield from each CPS extraction was lower than the reported 10-15 mg per litre yield in the literature (Burtnick *et al.*, 2012). It is possible that operator inexperience or slight, unknown, procedural differences in the modified hot-phenol extraction method may account for this. In the literature, CPS is extracted from *B. pseudomallei* whereas the use of *B. thailandensis* in this project means that yield differences may result from differences in CPS expression between the two *Burkholderia* species.

The work carried out by our collaborators at Mologic highlights the technical difficulties for expression of foreign proteins in the Tandem Core™ VLP construct. It is hypothesised that the genetic linker between hepatitis B core protein monomers would increase stability and allow for insertion of larger proteins but this was proved not to be the case for *Burkholderia* proteins. Foreign protein insertion into the Tandem Core™ VLP construct has been demonstrated with green fluorescent protein (Peyret *et al.*, 2015) which has a molecular weight of 27 kDa. However, as the proteins selected in this study ranged from 18 to 57 kDa and the VLP core protein is 38 kDa, it may not be surprising that VLP assembly was impaired. In the literature, fusion proteins of hepatitis B core protein, not made of Tandem Core™, have been limited to peptides for influenza (Tsybalova *et al.*, 2015), tuberculosis (Dhanasooraj *et al.*, 2013), anthrax (Yin *et al.*, 2014) and malaria (Gregson *et al.*, 2008). This suggests that insert size is important for competent VLP assembly.

The importance of the acetyl group on CPS immunogenicity and protective efficacy has been demonstrated in this thesis. However, identification of the minimum protective epitope would have directed CPS synthesis to structures less technically challenging to produce. The identification of polysaccharide epitopes is difficult as there are fewer tools in comparison to those available for proteins. For proteins, the methods include X-ray crystallography for visualization of bound antigen and antibody; overlapping peptide scanning where overlapping peptide sequences are tested for antibody recognition; nucleotide mutagenesis with assessment of antibody binding affinity to the target; antigen proteolysis with antibody-bound fragments detected by either mass spectroscopy or western blot; and in-silico predictions which have been performed in this study. By comparison, the tools available for investigation of carbohydrate epitopes are limited to the specialised NMR techniques; saturation-transfer-difference NMR spectroscopy, where ligand binding is determined by subtraction of saturated receptor binding from a reference spectrum without saturation and surface plasmon resonance where binding is detected by changes in refractive index. Diffraction data from fibrillar polysaccharide samples are usually not of a sufficient quality to resolve the crystal structure (Sarkar *et al.*, 2012). Nucleotide mutagenesis can be difficult as although more is now known about the genes that encode polysaccharide biosynthesis and expression, it can be a complex pathway including synthesis of component monosaccharides, activation and coordinated transfer of each sugar to the repeating oligosaccharide and subsequent polymerisation (Guidolin *et al.*, 1994). Hydrolysis of polysaccharide for fragment-antibody recognition is also difficult as hydrolysis can be indiscriminate and may result in the loss of key antigenic moieties as demonstrated in this thesis.

As polysaccharide epitope elucidation is made difficult by the lack of analytical tools, so is the production of CPS conjugate vaccines. The inability to hydrolyse *Burkholderia* CPS to shorter chain lengths, due to the acid-labile nature of CPS, means that CPS chains may tangle to form large complexes which may mask a protein carrier from the immune system following conjugation. In addition, long chains of conjugated CPS may reduce vaccine efficacy as recent reports in the literature suggest that low molecular weight polysaccharide conjugate vaccines

generate an optimal immune response for *H. influenzae* type b (Rana *et al.*, 2015).

All licensed polysaccharide vaccines utilise specific chain-lengths (Plotkin *et al.*, 2013). The large size of native CPS may make separation of unconjugated polysaccharide from the conjugate difficult. This has been shown to reduce vaccine efficacy of a *Streptococcus pneumoniae* vaccine (Rodriguez *et al.*, 1998), and is further compounded by the lack of methodology to determine the amount of free CPS in a conjugate vaccine. The inefficiencies of reductive amination conjugation also mean it is impossible to produce conjugates with a specific carrier protein to CPS ratio. Batch-to-batch variation can therefore make comparison of efficacy difficult. An approach used by other melioidosis vaccine researchers is to measure protein content and assume the rest of the material is conjugated polysaccharide. This does not, however, account for contaminants or unconjugated polysaccharide (Scott *et al.*, 2014).

6.4 Implications for *Burkholderia* vaccine development

Producing CPS from *B. thailandensis* at containment level 2 is less expensive, quicker and safer than the containment level 3 required for *B. pseudomallei*. This should increase the pace of melioidosis vaccine research. The improvement of bacterial CPS content may also increase CPS yield but further work is required to confirm this. CPS extraction from large-scale batch fermentation would require further growth condition optimisation but this work has shown that aeration, a nutrient-rich media and extended incubation time following inoculation all increase bacterial culture CPS content.

The suggestion that CPS is released into the culture supernatant would allow the possible replacement of the phenol extraction process as only the supernatant from a culture would be required. To the knowledge of the author, all other research groups use a phenol-based extraction method to isolate CPS from *Burkholderia* (Burtnick *et al.*, 2012, Heiss *et al.*, 2012, Reckseidler *et al.*, 2005, Masoud *et al.*, 1997, Perry *et al.*, 1995). Approximately 40 litres of liquid phenol waste is produced from two litres of *B. thailandensis* E555 :: *wbil* culture.

Therefore, the replacement of phenol would be advantageous for all future CPS production. Alternatively, CPS extraction from both the supernatant and bacterial pellet could increase CPS yield as opposed to the use of the pellet only. Furthermore, the development of a quantitative ELISA for CPS means that alternative methods of CPS extraction can be quickly assessed rather than having to wait for NMR analysis of the final purified product which may take several weeks.

The demonstration of the importance of the acetyl group for CPS immunogenicity and protective efficacy confirms that although technically challenging, attempts to synthesise CPS must be of the full molecule. However, if the immunodominant epitope was identified, a synthetic polysaccharide epitope/mimitope could be produced. This has been recently proposed following the development of peptide mimitopes of *B. pseudomallei* CPS and LPS (Guo *et al.*, 2016).

The demonstration of protective efficacy of both a VLP-CPS and Crm197-CPS conjugate vaccines, which generate different levels of CPS-specific IgG antibody, suggests that antibody titres are not a good correlate of protection. Analysis of survival and antibody titres generated from a Crm197-CPS vaccine at different polysaccharide to protein ratios, where protection from a CPS-specific IgG titre of 5333 was not significantly different to 100,000, further indicates that antibody titre is not indicative of protection. It is considered that antibody is important for protection against melioidosis infection, as the CPS antigen is protective. However, it is probable that antibody affinity/function is important or that VLP use as a carrier effects a different immune pathway. It is possible that a combination vaccine of VLP and Crm197 would be beneficial. Alternatively, a carrier with an immunodominant T-cell epitope and a carrier with an immunodominant B-cell epitope could be used.

The efficacy data from Crm197-CPS vaccination in the BALB/c mouse suggests that a Crm197 conjugate should have an equivalency of CPS and protein based on molecular weight and not the amount of each antigen added. This is in contradiction to licensed vaccines which utilise a 1:1 polysaccharide to protein ratio based on amount of antigen per dose (Plotkin *et al.*, 2013).

The demonstration that the *Burkholderia* protein LolC was a poor carrier protein for CPS does not mean that the use of a *Burkholderia* protein as a carrier should be abandoned. However, it does show that the immunogenicity of the protein should be considered: highly immunogenic epitopes may direct the immune response away from CPS. When added as co-antigens, immunogenicity of *Burkholderia* proteins may not be a concern. In the case of the Crm197-CPS vaccine, the immunogenicity of the co-antigen did not affect the development of the CPS-specific IgG antibody titres. The failure of *Burkholderia* proteins to increase vaccine efficacy when added as co-antigens suggest that at high challenge doses, melioidosis relevant T-cell epitopes are not protective in the acute animal model of melioidosis. As only a small number of surviving animals were clear of infection in this study, T-cell epitopes with more relevance to infection may be required. Alternatively, the effective treatment for melioidosis may be a combination therapy of vaccine and antibiotics. It would be interesting to see the effect of *Burkholderia* proteins on CPS conjugate vaccine efficacy in the chronic animal model of melioidosis, as the Th1-biased immune response of C57BL/6 mice may change the outcome.

It was demonstrated that there was no significant difference in protective efficacy between VLPs made up of Tandem CoreTM and monomeric hepatitis B core protein. This means that should VLPs prove efficacious against an aerosol challenge of *B. pseudomallei*, monomeric based VLPs can be used in future research. This will lower the cost of development and production as they do not attract costs associated with intellectual property.

6.5 Future work

There are a number of important areas where this work with CPS could be extended. Further study into the factors affecting CPS gene transcription and resultant expression in *B. thailandensis* E555 would be beneficial in order to increase yield. This could be investigated by microarray analysis as performed by Reckseidler-Zenteno *et al.*, (2010) for CPS-III. The use of *B. thailandensis* supernatant for CPS extraction as an alternative or addition to the use of the culture pellet could also be a key area of work. Investigation into the anchor of

CPS to the extracellular membrane could be beneficial: a knockout mutant of the anchor would mean all CPS expressed is shed in the media which may simplify the CPS extraction procedure and remove the need for phenol. A lipid has been suggested as a polysaccharide anchor for *Salmonella enterica*, *Campylobacter jejuni* and *Streptococcus pneumoniae* and could be a place to start (Liston *et al.*, 2016, Corcoran *et al.*, 2006, Cartee *et al.*, 2005). The development of an unmarked O-antigen mutant of *B. thailandensis* E555 will also be advantageous as it removes the requirement for antibiotic in the culture media. This would be particularly beneficial if CPS production moves to large-scale batch fermentation. Optimisation of the current modified hot-phenol method could also be attempted as changes in CPS content could be quickly assessed by the CPS ELISA. This work could start with ELISA analysis of the product at each stage in the extraction procedure to determine where CPS loss occurs which would highlight steps to optimise. Gene knockouts of the CPS gene cluster would also be useful to determine the genes responsible for α 1-3 mannan expression (Heiss *et al.*, 2012). This would allow subsequent mannan extraction in order to elucidate its role in protection and immunogenicity studies.

The VLP and Crm197 conjugates showed similar efficacy against bacterial challenge but generated markedly different CPS-specific antibody titres. This suggests a difference in immune function between the two vaccines. Investigation of this difference could be important for development of a melioidosis vaccine as stimulation of these two pathways by a combination vaccine may provide full protection with sterilising immunity. The work in this thesis suggests that efficacy of a Crm197-CPS conjugate is improved when the vaccine contains similar amounts of protein and polysaccharide based on molecular weight. This is in disagreement with licensed conjugate vaccines, which are produced on weight equivalency (Plotkin *et al.*, 2013). Investigation into the effect of different protein and polysaccharide ratios on melioidosis vaccine efficacy would be a key requirement for future development. This in turn requires a method to be developed for the production of known chain-lengths of CPS, and an ability to effectively separate free polysaccharide from the conjugate. Development of these methods is also critical for further development and licensure of a vaccine as the presence of unconjugated polysaccharide, the removal of which is reliant on the generation of short chain

lengths of CPS, is known to adversely affect vaccine efficacy (Rodriguez *et al.*, 1998).

Assessment of VLP and Crm197 conjugate vaccine efficacy against a *B. pseudomallei* aerosol challenge must be performed before the use of VLPs as a carrier protein for melioidosis is halted. This would be in the chronic mouse model of melioidosis (C57BL/6) as BALB/c's are 10- to 100-fold more susceptible to *B. pseudomallei* infection (Tan *et al.*, 2008) and as aerosol exposure is associated with severe disease this may render the use of BALB/c's ineffective. Additional work could focus on administration of conjugates via the inhalational route rather than the intraperitoneal route. The generation of secretory IgA antibody may improve disease outcome as has been reported for rotavirus infection (Blutt *et al.*, 2012) and respiratory infection of *Mycobacterium bovis* Bacillus Calmette-Guerin (Rodriguez *et al.*, 2005).

A deficiency of the conjugate vaccines used in this thesis is the lack of sterilising immunity in mice that survived to study end. This may be caused by intracellular infection and the lack of effective CD8+ T-cell responses due to the ability of *B. pseudomallei* to escape from the phagosome (Willcocks *et al.*, 2016). All of Dstl's anti-CPS monoclonal antibodies were derived from mouse immunisation with inactivated whole-cell *B. pseudomallei*. This infers that CPS is a major B-cell epitope of the organism. In combination with the strong suggestion that CPS contains one immuno-dominant epitope, the following novel therapy could be investigated: an anti-CPS antibody with opsonophagocytosis effector function conjugated to an antibiotic with an acid-labile linker. In the phagosome, hydrolysis of the conjugate linker would free the antibiotic to clear infection. In combination with a vaccine, this therapy may effectively control *B. pseudomallei* infection.

6.6 Conclusion

The fact that isolates of *B. pseudomallei* and *B. mallei* appear to express only a limited repertoire of capsular polysaccharides (Burtnick *et al.*, 2012) means that the prospect of a vaccine against both melioidosis and glanders utilising -3-)-2-

O-acetyl-6-deoxy- β -D-manno-heptopyranose-(1 is feasible. In this thesis I have also discussed the extraction of CPS from *B. thailandensis* E555 and confirmation of structural and immunological identity to CPS extracted from *B. pseudomallei* with the advantages this confers.

In this thesis I have also shown that a CPS conjugate vaccine is able to protect mice against *B. pseudomallei* challenge at doses potentially higher than would be expected in either a clinical or bio-threat exposure. Both virus-like particles and Crm197 have been shown to be efficacious, although difficulties associated with VLP expression favour the use of Crm197. At this point it would be unwise to abandon VLPs as they have yet to be tested against an aerosol challenge of *B. pseudomallei*. Given the potential for immune interference from licensed Crm197-containing vaccines, the use of VLPs may still be appropriate. It is thought that both a cellular and humoral response is required for protection against *B. pseudomallei* infection. While the addition of *Burkholderia* proteins in this study did not achieve this aim, the mechanism of protection between Crm197 and VLP carrier proteins is different. Investigation of this difference and use of a combination vaccine of either these two components, or components with similar effector responses, could be instrumental to development of an effective melioidosis vaccine.

There is still much to be done to develop a glycoconjugate vaccine for melioidosis. The work in this project has shown the difficulty in utilising CPS as an antigen, as there are far fewer tools available for vaccine development as there are for proteins. A pressing technical need is for the production of known chain-lengths of CPS, an ability to effectively separate conjugated and free polysaccharide and determination of the optimum protein to polysaccharide content. All of these variables are known to affect polysaccharide conjugate vaccine efficacy and need to be controlled for development and eventual licensure.

This thesis has shown that CPS conjugate vaccines can be efficacious against *B. pseudomallei* challenge doses of over half a million bacteria. A correlate of protection and demonstration of efficacy against an aerosol challenge will be crucial next steps.

Chapter 7: Bibliography

- Ada G, Isaacs D. 2003. Carbohydrate-protein conjugate vaccines. *Clinical microbiology and infection : the official publication of the European Society of Clinical Microbiology and Infectious Diseases* 9(2):79-85.
- Adderson EE, Shackelford PG, Insel RA, Quinn A, Wilson PM, Carroll WL. 1992. Immunoglobulin light chain variable region gene sequences for human antibodies to *Haemophilus influenzae* type b capsular polysaccharide are dominated by a limited number of V kappa and V lambda segments and VJ combinations. *The Journal of clinical investigation* 89(3):729-738.
- Alexeyev MF. 1999. The pKNOCK series of broad-host-range mobilizable suicide vectors for gene knockout and targeted DNA insertion into the chromosome of gram-negative bacteria. *BioTechniques* 26(5):824-826, 828.
- Allwood EM, Devenish RJ, Prescott M, Adler B, Boyce JD. 2011. Strategies for Intracellular Survival of *Burkholderia pseudomallei*. *Frontiers in microbiology* 2:170.
- Anderson P, Pichichero ME, Insel RA. 1985. Immunogens consisting of oligosaccharides from the capsule of *Haemophilus influenzae* type b coupled to diphtheria toxoid or the toxin protein CRM197. *The Journal of clinical investigation* 76(1):52-59.
- Apostolico Jde S, Lunardelli VA. 2016. Adjuvants: Classification, Modus Operandi, and Licensing. *Journal of immunology research* 2016:1459394.
- Atkins T, Prior R, Mack K, Russell P, Nelson M, Prior J, Ellis J, Oyston PC, Dougan G, Titball RW. 2002a. Characterisation of an acapsular mutant of *Burkholderia pseudomallei* identified by signature tagged mutagenesis. *Journal of medical microbiology* 51(7):539-547.
- Atkins T, Prior RG, Mack K, Russell P, Nelson M, Oyston PC, Dougan G, Titball RW. 2002b. A mutant of *Burkholderia pseudomallei*, auxotrophic in the branched chain amino acid biosynthetic pathway, is attenuated and protective in a murine model of melioidosis. *Infection and immunity* 70(9):5290-5294.

- Audy J, Labrie S, Roy D, Lapointe G. 2010. Sugar source modulates exopolysaccharide biosynthesis in *Bifidobacterium longum* subsp. *longum* CRC 002. *Microbiology (Reading, England)* 156(Pt 3):653-664.
- Avery OT, Goebel, W. F. 1391. Chemo-immunological studies on conjugated carbohydrate-proteins: V. The immunological specificity of an antigen prepared by combining the capsular polysaccharide of Type III pneumococcus with foreign protein. *Journal of Experimental Medicine* 54:437-447.
- Bachert BA, Choi SJ, Snyder AK, Rio RV, Durney BC, Holland LA, Amemiya K, Welkos SL, Bozue JA, Cote CK and others. 2015. A Unique Set of the *Burkholderia* Collagen-Like Proteins Provides Insight into Pathogenesis, Genome Evolution and Niche Adaptation, and Infection Detection. *PloS one* 10(9):e0137578.
- Baker AL, Ezzahir J, Gardiner C, Shipton W, Warner JM. 2015. Environmental Attributes Influencing the Distribution of *Burkholderia pseudomallei* in Northern Australia. *PloS one* 10(9):e0138953.
- Baker JP. 2008. Mercury, vaccines, and autism: one controversy, three histories. *American journal of public health* 98(2):244-253.
- Balder R, Lipski S, Lazarus JJ, Grose W, Wooten RM, Hogan RJ, Woods DE, Lafontaine ER. 2010. Identification of *Burkholderia mallei* and *Burkholderia pseudomallei* adhesins for human respiratory epithelial cells. *BMC microbiology* 10:250.
- Baraldo K, Mori E, Bartoloni A, Petracca R, Giannozzi A, Norelli F, Rappuoli R, Grandi G, Del Giudice G. 2004. N19 polyepitope as a carrier for enhanced immunogenicity and protective efficacy of meningococcal conjugate vaccines. *Infection and immunity* 72(8):4884-4887.
- Barnes JL, Williams NL, Ketheesan N. 2008. Susceptibility to *Burkholderia pseudomallei* is associated with host immune responses involving tumor necrosis factor receptor-1 (TNFR1) and TNF receptor-2 (TNFR2). *FEMS immunology and medical microbiology* 52(3):379-388.
- Barnes KB, Steward J, Thwaite JE, Lever MS, Davies CH, Armstrong SJ, Laws TR, Roughley N, Harding SV, Atkins TP and others. 2013. Trimethoprim/sulfamethoxazole (co-trimoxazole) prophylaxis is effective against acute murine inhalational melioidosis and glanders. *International journal of antimicrobial agents* 41(6):552-557.

- Barrett AD, Beasley DW. 2009. Development pathway for biodefense vaccines. *Vaccine* 27 Suppl 4:D2-7.
- Baumgartner CK, Malherbe LP. 2011. Antigen-driven T-cell repertoire selection during adaptive immune responses. *Immunology and cell biology* 89(1):54-59.
- Berry DS, Lynn F, Lee CH, Frasch CE, Bash MC. 2002. Effect of O acetylation of *Neisseria meningitidis* serogroup A capsular polysaccharide on development of functional immune responses. *Infection and immunity* 70(7):3707-3713.
- Bewick V, Cheek L, Ball J. 2004. Statistics review 12: survival analysis. *Critical care (London, England)* 8(5):389-394.
- Blutt SE, Miller AD, Salmon SL, Metzger DW, Conner ME. 2012. IgA is important for clearance and critical for protection from rotavirus infection. *Mucosal immunology* 5(6):712-719.
- Bondi SK, Goldberg JB. 2008. Strategies toward vaccines against *Burkholderia mallei* and *Burkholderia pseudomallei*. *Expert review of vaccines* 7(9):1357-1365.
- Breitbach K, Klocke S, Tschernig T, van Rooijen N, Baumann U, Steinmetz I. 2006. Role of inducible nitric oxide synthase and NADPH oxidase in early control of *Burkholderia pseudomallei* infection in mice. *Infection and immunity* 74(11):6300-6309.
- Breitbach K, Kohler J, Steinmetz I. 2008. Induction of protective immunity against *Burkholderia pseudomallei* using attenuated mutants with defects in the intracellular life cycle. *Transactions of the Royal Society of Tropical Medicine and Hygiene* 102 Suppl 1:S89-94.
- Brett PJ, Burtnick MN, Heiss C, Azadi P, DeShazer D, Woods DE, Gherardini FC. 2011. *Burkholderia thailandensis* oacA mutants facilitate the expression of *Burkholderia mallei*-like O polysaccharides. *Infection and immunity* 79(2):961-969.
- Brett PJ, Deshazer D, Woods DE. 1997. Characterization of *Burkholderia pseudomallei* and *Burkholderia pseudomallei*-like strains. *Epidemiology and infection* 118(2):137-148.
- Brett PJ, DeShazer D, Woods DE. 1998. *Burkholderia thailandensis* sp. nov., a *Burkholderia pseudomallei*-like species. *International journal of systematic bacteriology* 48 Pt 1:317-320.

- Brett PJ, Woods DE. 1996. Structural and immunological characterization of *Burkholderia pseudomallei* O-polysaccharide-flagellin protein conjugates. *Infection and immunity* 64(7):2824-2828.
- Breukels MA, Zandvoort A, Rijkers GT, Lodewijk ME, Klok PA, Harms G, Timens W. 2005. Complement dependency of splenic localization of pneumococcal polysaccharide and conjugate vaccines. *Scandinavian journal of immunology* 61(4):322-328.
- Brewer JM. 2006. (How) do aluminium adjuvants work? *Immunology letters* 102(1):10-15.
- Broker M, Costantino P, DeTora L, McIntosh ED, Rappuoli R. 2011. Biochemical and biological characteristics of cross-reacting material 197 CRM197, a non-toxic mutant of diphtheria toxin: use as a conjugation protein in vaccines and other potential clinical applications. *Biologicals : journal of the International Association of Biological Standardization* 39(4):195-204.
- Burkholder WH. 1950. Sour skin, a bacterial rot of onion bulbs. *Phytopathology* 40(115).
- Burtnick MN, Brett PJ, Harding SV, Ngugi SA, Ribot WJ, Chantratita N, Scorpio A, Milne TS, Dean RE, Fritz DL and others. 2011. The cluster 1 type VI secretion system is a major virulence determinant in *Burkholderia pseudomallei*. *Infection and immunity* 79(4):1512-1525.
- Burtnick MN, Heiss C, Roberts RA, Schweizer HP, Azadi P, Brett PJ. 2012. Development of capsular polysaccharide-based glycoconjugates for immunization against melioidosis and glanders. *Frontiers in cellular and infection microbiology* 2:108.
- Carmenate T, Canaan L, Alvarez A, Delgado M, Gonzalez S, Menendez T, Rodes L, Guillen G. 2004. Effect of conjugation methodology on the immunogenicity and protective efficacy of meningococcal group C polysaccharide-P64k protein conjugates. *FEMS immunology and medical microbiology* 40(3):193-199.
- Cartee RT, Forsee WT, Yother J. 2005. Initiation and synthesis of the *Streptococcus pneumoniae* type 3 capsule on a phosphatidylglycerol membrane anchor. *Journal of bacteriology* 187(13):4470-4479.
- Casey WT, Spink N, Cia F, Collins C, Romano M, Berisio R, Bancroft GJ, McClean S. 2016. Identification of an OmpW homologue in *Burkholderia*

- pseudomallei*, a protective vaccine antigen against melioidosis. *Vaccine* 34(23):2616-2621.
- Champion OL, Gourlay LJ, Scott AE, Lassaux P, Conejero L, Perletti L, Hemsley C, Prior J, Bancroft G, Bolognesi M and others. 2016. Immunisation with proteins expressed during chronic murine melioidosis provides enhanced protection against disease. *Vaccine* 34(14):1665-1671.
- Chantratita N, Wuthiekanun V, Boonbumrung K, Tiya-wisutsri R, Vesaratchavest M, Limmathurotsakul D, Chierakul W, Wongratanacheewin S, Pukritiyakamee S, White NJ and others. 2007. Biological relevance of colony morphology and phenotypic switching by *Burkholderia pseudomallei*. *Journal of bacteriology* 189(3):807-817.
- Chen YS, Hsiao YS, Lin HH, Liu Y, Chen YL. 2006. CpG-modified plasmid DNA encoding flagellin improves immunogenicity and provides protection against *Burkholderia pseudomallei* infection in BALB/c mice. *Infection and immunity* 74(3):1699-1705.
- Cheng AC, Currie BJ. 2005. Melioidosis: epidemiology, pathophysiology, and management. *Clinical microbiology reviews* 18(2):383-416.
- Cheng AC, Limmathurotsakul D, Chierakul W, Getchalarat N, Wuthiekanun V, Stephens DP, Day NP, White NJ, Chaowagul W, Currie BJ and others. 2007. A randomized controlled trial of granulocyte colony-stimulating factor for the treatment of severe sepsis due to melioidosis in Thailand. *Clinical infectious diseases : an official publication of the Infectious Diseases Society of America* 45(3):308-314.
- Chitlaru T, Israeli M, Bar-Haim E, Elia U, Rotem S, Ehrlich S, Cohen O, Shafferman A. 2016. Next-Generation *Bacillus anthracis* Live Attenuated Spore Vaccine Based on the htrA(-) (High Temperature Requirement A) Sterne Strain. *Scientific reports* 6:18908.
- Choh LC, Ong GH, Vellasamy KM, Kalaiselvam K, Kang WT, Al-Maleki AR, Mariappan V, Vadivelu J. 2013. *Burkholderia* vaccines: are we moving forward? *Frontiers in cellular and infection microbiology* 3:5.
- Coenye T, Mahenthalingam, E. 2014. *Burkholderia*: From genomes to function. Caister Academic Press:254.

- Coenye T, Vandamme P. 2003. Diversity and significance of *Burkholderia* species occupying diverse ecological niches. *Environmental microbiology* 5(9):719-729.
- Conejero L, Patel N, de Reynal M, Oberdorf S, Prior J, Felgner PL, Titball RW, Salguero FJ, Bancroft GJ. 2011. Low-dose exposure of C57BL/6 mice to *burkholderia pseudomallei* mimics chronic human melioidosis. *The American journal of pathology* 179(1):270-280.
- Conway JF, Cheng N, Zlotnick A, Stahl SJ, Wingfield PT, Belnap DM, Kanngiesser U, Noah M, Steven AC. 1998. Hepatitis B virus capsid: localization of the putative immunodominant loop (residues 78 to 83) on the capsid surface, and implications for the distinction between c and e-antigens. *Journal of molecular biology* 279(5):1111-1121.
- Cooper CA, Mainprize IL, Nickerson NN. 2015. Genetic, Biochemical, and Structural Analyses of Bacterial Surface Polysaccharides. *Advances in experimental medicine and biology* 883:295-315.
- Corcoran AT, Annuk H, Moran AP. 2006. The structure of the lipid anchor of *Campylobacter jejuni* polysaccharide. *FEMS microbiology letters* 257(2):228-235.
- Crowther RA, Kiselev NA, Bottcher B, Berriman JA, Borisova GP, Ose V, Pumpens P. 1994. Three-dimensional structure of hepatitis B virus core particles determined by electron cryomicroscopy. *Cell* 77(6):943-950.
- Cuccui J, Easton A, Chu KK, Bancroft GJ, Oyston PC, Titball RW, Wren BW. 2007. Development of signature-tagged mutagenesis in *Burkholderia pseudomallei* to identify genes important in survival and pathogenesis. *Infection and immunity* 75(3):1186-1195.
- Cuccui J, Milne TS, Harmer N, George AJ, Harding SV, Dean RE, Scott AE, Sarkar-Tyson M, Wren BW, Titball RW and others. 2012. Characterization of the *Burkholderia pseudomallei* K96243 capsular polysaccharide I coding region. *Infection and immunity* 80(3):1209-1221.
- Currie BJ. 2015. Melioidosis: evolving concepts in epidemiology, pathogenesis, and treatment. *Seminars in respiratory and critical care medicine* 36(1):111-125.
- Currie BJ, Fisher DA, Howard DM, Burrow JN, Lo D, Selva-Nayagam S, Anstey NM, Huffam SE, Snelling PL, Marks PJ and others. 2000. Endemic melioidosis in tropical northern Australia: a 10-year prospective study

- and review of the literature. *Clinical infectious diseases : an official publication of the Infectious Diseases Society of America* 31(4):981-986.
- Currie BJ, Kaestli M. 2016. Epidemiology: A global picture of melioidosis. *Nature* 529(7586):290-291.
- Dagan R, Poolman J, Siegrist CA. 2010. Glycoconjugate vaccines and immune interference: A review. *Vaccine* 28(34):5513-5523.
- Daligault HE, Davenport KW, Minogue TD, Bishop-Lilly KA, Broomall SM, Bruce DC, Chain PS, Coyne SR, Frey KG, Gibbons HS and others. 2014. Whole-genome assemblies of 56 *Burkholderia* species. *Genome announcements* 2(6).
- Dance D. 2014. Treatment and prophylaxis of melioidosis. *International journal of antimicrobial agents* 43(4):310-318.
- Deck MB, Sjolín P, Unanue ER, Kihlberg J. 1999. MHC-restricted, glycopeptide-specific T cells show specificity for both carbohydrate and peptide residues. *Journal of immunology (Baltimore, Md : 1950)* 162(8):4740-4744.
- DeShazer D, Brett PJ, Woods DE. 1998. The type II O-antigenic polysaccharide moiety of *Burkholderia pseudomallei* lipopolysaccharide is required for serum resistance and virulence. *Molecular microbiology* 30(5):1081-1100.
- DeShazer D, Waag DM, Fritz DL, Woods DE. 2001. Identification of a *Burkholderia mallei* polysaccharide gene cluster by subtractive hybridization and demonstration that the encoded capsule is an essential virulence determinant. *Microbial pathogenesis* 30(5):253-269.
- Dhanasooraj D, Kumar RA, Mundayoor S. 2013. Vaccine delivery system for tuberculosis based on nano-sized hepatitis B virus core protein particles. *International journal of nanomedicine* 8:835-843.
- Didierlaurent AM, Morel S, Lockman L, Giannini SL, Bisteau M, Carlsen H, Kielland A, Vosters O, Vanderheyde N, Schiavetti F and others. 2009. AS04, an aluminum salt- and TLR4 agonist-based adjuvant system, induces a transient localized innate immune response leading to enhanced adaptive immunity. *Journal of immunology (Baltimore, Md : 1950)* 183(10):6186-6197.
- Druar C, Yu F, Barnes JL, Okinaka RT, Chantratita N, Beg S, Stratilo CW, Olive AJ, Soltés G, Russell ML and others. 2008. Evaluating *Burkholderia*

- pseudomallei* Bip proteins as vaccines and Bip antibodies as detection agents. *FEMS immunology and medical microbiology* 52(1):78-87.
- Easton A, Haque A, Chu K, Lukaszewski R, Bancroft GJ. 2007. A critical role for neutrophils in resistance to experimental infection with *Burkholderia pseudomallei*. *The Journal of infectious diseases* 195(1):99-107.
- Easton A, Haque A, Chu K, Patel N, Lukaszewski RA, Krieg AM, Titball RW, Bancroft GJ. 2011. Combining vaccination and postexposure CpG therapy provides optimal protection against lethal sepsis in a biodefense model of human melioidosis. *The Journal of infectious diseases* 204(4):636-644.
- Eberl L, Vandamme P. 2016. Members of the genus *Burkholderia*: good and bad guys. *F1000Research* 5.
- Essex-Lopresti AE, Boddey JA, Thomas R, Smith MP, Hartley MG, Atkins T, Brown NF, Tsang CH, Peak IR, Hill J and others. 2005. A type IV pilin, Pila, Contributes To Adherence of *Burkholderia pseudomallei* and virulence in vivo. *Infection and immunity* 73(2):1260-1264.
- Fernandez-Sanchez A, Garcia-Ocana M, de los Toyos JR. 2009. Mouse monoclonal antibodies to pneumococcal C-polysaccharide backbone show restricted usage of VH-DH-JH gene segments and share the same kappa chain. *Immunology letters* 123(2):125-131.
- Fiebig T, Freiberger F, Pinto V, Romano MR, Black A, Litschko C, Bethe A, Yashunsky D, Adamo R, Nikolaev A and others. 2014. Molecular cloning and functional characterization of components of the capsule biosynthesis complex of *Neisseria meningitidis* serogroup A: toward in vitro vaccine production. *The Journal of biological chemistry* 289(28):19395-19407.
- Foong YC, Tan M, Bradbury RS. 2014. Melioidosis: a review. *Rural and remote health* 14(4):2763.
- Frasch CE. 2009. Preparation of bacterial polysaccharide-protein conjugates: analytical and manufacturing challenges. *Vaccine* 27(46):6468-6470.
- French CT, Toesca IJ, Wu TH, Teslaa T, Beaty SM, Wong W, Liu M, Schroder I, Chiou PY, Teitell MA and others. 2011. Dissection of the *Burkholderia* intracellular life cycle using a photothermal nanoblade. *Proceedings of the National Academy of Sciences of the United States of America* 108(29):12095-12100.

- Fusco PC, Farley EK, Huang CH, Moore S, Michon F. 2007. Protective meningococcal capsular polysaccharide epitopes and the role of O acetylation. *Clinical and vaccine immunology* : CVI 14(5):577-584.
- Galyov EE, Brett PJ, DeShazer D. 2010. Molecular insights into *Burkholderia pseudomallei* and *Burkholderia mallei* pathogenesis. *Annual review of microbiology* 64:495-517.
- Garcia-Quintanilla F, Iwashkiw JA, Price NL, Stratilo C, Feldman MF. 2014. Production of a recombinant vaccine candidate against *Burkholderia pseudomallei* exploiting the bacterial N-glycosylation machinery. *Frontiers in microbiology* 5:381.
- George A. 2013. Towards the development of a capsular polysaccharide-protein conjugate vaccine to protect against *Burkholderia pseudomallei*. PhD thesis, University of Manchester
- Ghimire TR. 2015. The mechanisms of action of vaccines containing aluminum adjuvants: an in vitro vs in vivo paradigm. *SpringerPlus* 4:181.
- Giannini G, Rappuoli R, Ratti G. 1984. The amino-acid sequence of two non-toxic mutants of diphtheria toxin: CRM45 and CRM197. *Nucleic acids research* 12(10):4063-4069.
- Gildersleeve JC, Oyelaran O, Simpson JT, Allred B. 2008. Improved procedure for direct coupling of carbohydrates to proteins via reductive amination. *Bioconjugate chemistry* 19(7):1485-1490.
- Ginsburg AS, Nahm MH, Khambaty FM, Alderson MR. 2012. Issues and challenges in the development of pneumococcal protein vaccines. *Expert review of vaccines* 11(3):279-285.
- Gong L, Cullinane M, Treerat P, Ramm G, Prescott M, Adler B, Boyce JD, Devenish RJ. 2011. The *Burkholderia pseudomallei* type III secretion system and BopA are required for evasion of LC3-associated phagocytosis. *PloS one* 6(3):e17852.
- Gonzalez-Fernandez A, Faro J, Fernandez C. 2008. Immune responses to polysaccharides: lessons from humans and mice. *Vaccine* 26(3):292-300.
- Goto N, Akama K. 1982. Histopathological studies of reactions in mice injected with aluminum-adsorbed tetanus toxoid. *Microbiology and immunology* 26(12):1121-1132.

- Gourlay LJ, Thomas RJ, Peri C, Conchillo-Sole O, Ferrer-Navarro M, Nithichanon A, Vila J, Daura X, Lertmemongkolchai G, Titball R and others. 2015. From crystal structure to in silico epitope discovery in the *Burkholderia pseudomallei* flagellar hook-associated protein FlgK. *The FEBS journal* 282(7):1319-1333.
- Gregson AL, Oliveira G, Othoro C, Calvo-Calle JM, Thorton GB, Nardin E, Edelman R. 2008. Phase I trial of an alhydrogel adjuvanted hepatitis B core virus-like particle containing epitopes of *Plasmodium falciparum* circumsporozoite protein. *PloS one* 3(2):e1556.
- Grgacic EV, Anderson DA. 2006. Virus-like particles: passport to immune recognition. *Methods (San Diego, Calif)* 40(1):60-65.
- Gudlavalleti SK, Lee CH, Norris SE, Paul-Satyaseela M, Vann WF, Frasch CE. 2007. Comparison of *Neisseria meningitidis* serogroup W135 polysaccharide-tetanus toxoid conjugate vaccines made by periodate activation of O-acetylated, non-O-acetylated and chemically de-O-acetylated polysaccharide. *Vaccine* 25(46):7972-7980.
- Guidolin A, Morona JK, Morona R, Hansman D, Paton JC. 1994. Nucleotide sequence analysis of genes essential for capsular polysaccharide biosynthesis in *Streptococcus pneumoniae* type 19F. *Infection and immunity* 62(12):5384-5396.
- Guo P, Zhang J, Tsai S, Li B, Lo SC. 2016. Developing Peptide Mimotopes of Capsular Polysaccharides and Lipopolysaccharides Protective Antigens of Pathogenic *Burkholderia* Bacteria. *Proceedings of the National Academy of Sciences of the United States of America* 35(3):125-134.
- Hajj Hussein I, Chams N, Chams S, El Sayegh S, Badran R, Raad M, Gerges-Geagea A, Leone A, Jurjus A. 2015. Vaccines Through Centuries: Major Cornerstones of Global Health. *Frontiers in public health* 3:269.
- Hamad MA, Zajdowicz SL, Holmes RK, Voskuil MI. 2009. An allelic exchange system for compliant genetic manipulation of the select agents *Burkholderia pseudomallei* and *Burkholderia mallei*. *Gene* 430(1-2):123-131.
- Haque A, Chu K, Easton A, Stevens MP, Galyov EE, Atkins T, Titball R, Bancroft GJ. 2006. A live experimental vaccine against *Burkholderia pseudomallei* elicits CD4+ T cell-mediated immunity, priming T cells

- specific for 2 type III secretion system proteins. *The Journal of infectious diseases* 194(9):1241-1248.
- Hara Y, Mohamed R, Nathan S. 2009. Immunogenic *Burkholderia pseudomallei* outer membrane proteins as potential candidate vaccine targets. *PloS one* 4(8):e6496.
- Haraga A, West TE, Brittnacher MJ, Skerrett SJ, Miller SI. 2008. *Burkholderia thailandensis* as a model system for the study of the virulence-associated type III secretion system of *Burkholderia pseudomallei*. *Infection and immunity* 76(11):5402-5411.
- Harland DN, Chu K, Haque A, Nelson M, Walker NJ, Sarkar-Tyson M, Atkins TP, Moore B, Brown KA, Bancroft G and others. 2007a. Identification of a LolC homologue in *Burkholderia pseudomallei*, a novel protective antigen for melioidosis. *Infection and immunity* 75(8):4173-4180.
- Harland DN, Dassa E, Titball RW, Brown KA, Atkins HS. 2007b. ATP-binding cassette systems in *Burkholderia pseudomallei* and *Burkholderia mallei*. *BMC genomics* 8:83.
- Hayden HS, Lim R, Brittnacher MJ, Sims EH, Ramage ER, Fong C, Wu Z, Crist E, Chang J, Zhou Y and others. 2012. Evolution of *Burkholderia pseudomallei* in recurrent melioidosis. *PloS one* 7(5):e36507.
- Healey GD, Elvin SJ, Morton M, Williamson ED. 2005. Humoral and cell-mediated adaptive immune responses are required for protection against *Burkholderia pseudomallei* challenge and bacterial clearance postinfection. *Infection and immunity* 73(9):5945-5951.
- Hecht ML, Stallforth P, Silva DV, Adibekian A, Seeberger PH. 2009. Recent advances in carbohydrate-based vaccines. *Current opinion in chemical biology* 13(3):354-359.
- Heiss C, Burtnick MN, Wang Z, Azadi P, Brett PJ. 2012. Structural analysis of capsular polysaccharides expressed by *Burkholderia mallei* and *Burkholderia pseudomallei*. *Carbohydrate research* 349:90-94.
- Hirahara K, Nakayama T. 2016. CD4+ T-cell subsets in inflammatory diseases: beyond the Th1/Th2 paradigm. *International immunology* 28(4):163-171.
- Hodgson KA, Morris JL, Feterl ML, Govan BL, Ketheesan N. 2011. Altered macrophage function is associated with severe *Burkholderia pseudomallei* infection in a murine model of type 2 diabetes. *Microbes and infection / Institut Pasteur* 13(14-15):1177-1184.

- Holden MT, Titball RW, Peacock SJ, Cerdeno-Tarraga AM, Atkins T, Crossman LC, Pitt T, Churcher C, Mungall K, Bentley SD and others. 2004. Genomic plasticity of the causative agent of melioidosis, *Burkholderia pseudomallei*. Proceedings of the National Academy of Sciences of the United States of America 101(39):14240-14245.
- Hoof I, Peters B, Sidney J, Pedersen LE, Sette A, Lund O, Buus S, Nielsen M. 2009. NetMHCpan, a method for MHC class I binding prediction beyond humans. Immunogenetics 61(1):1-13.
- Hopf V, Gohler A, Eske-Pogodda K, Bast A, Steinmetz I, Breitbach K. 2014. BPSS1504, a cluster 1 type VI secretion gene, is involved in intracellular survival and virulence of *Burkholderia pseudomallei*. Infection and immunity 82(5):2006-2015.
- Hoppe I, Brenneke B, Rohde M, Kreft A, Haussler S, Reganzerowski A, Steinmetz I. 1999. Characterization of a murine model of melioidosis: comparison of different strains of mice. Infection and immunity 67(6):2891-2900.
- Horsley A, Jones AM, Lord R. 2016. Antibiotic treatment for *Burkholderia cepacia* complex in people with cystic fibrosis experiencing a pulmonary exacerbation. The Cochrane database of systematic reviews(1):Cd009529.
- Hseu YC, Sung JC, Shieh BS, Chen SC. 2013. *Burkholderia pseudomallei* infection induces the expression of apoptosis-related genes and proteins in mouse macrophages. Journal of microbiology, immunology, and infection = Wei mian yu gan ran za zhi 47(5):394-398.
- Huang Q, Li D, Kang A, An W, Fan B, Ma X, Ma G, Su Z, Hu T. 2013. PEG as a spacer arm markedly increases the immunogenicity of *meningococcal* group Y polysaccharide conjugate vaccine. Journal of controlled release : official journal of the Controlled Release Society 172(1):382-389.
- Huber MA, Tantiwongkosi B. 2014. Oral and oropharyngeal cancer. Genome announcements 98(6):1299-1321.
- Jawa V, Cousens LP, Awwad M, Wakshull E, Kropshofer H, De Groot AS. 2013. T-cell dependent immunogenicity of protein therapeutics: Preclinical assessment and mitigation. Clinical immunology (Orlando, Fla) 149(3):534-555.

- Joiner KA. 1988. Complement evasion by bacteria and parasites. Annual review of microbiology 42:201-230.
- Jones AL, Beveridge TJ, Woods DE. 1996. Intracellular survival of *Burkholderia pseudomallei*. Infection and immunity 64(3):782-790.
- Jones C. 2005. Vaccines based on the cell surface carbohydrates of pathogenic bacteria. Anais da Academia Brasileira de Ciencias 77(2):293-324.
- Jones SM, Ellis JF, Russell P, Griffin KF, Oyston PC. 2002. Passive protection against *Burkholderia pseudomallei* infection in mice by monoclonal antibodies against capsular polysaccharide, lipopolysaccharide or proteins. Journal of medical microbiology 51(12):1055-1062.
- Judy BM, Taylor K, Deeraksa A, Johnston RK, Endsley JJ, Vijayakumar S, Aronson JF, Estes DM, Torres AG. 2012. Prophylactic application of CpG oligonucleotides augments the early host response and confers protection in acute melioidosis. PloS one 7(3):e34176.
- Kaiko GE, Horvat JC, Beagley KW, Hansbro PM. 2008. Immunological decision-making: how does the immune system decide to mount a helper T-cell response? Immunology 123(3):326-338.
- Kawahara K, Dejsirilert S, Ezaki T. 1998. Characterization of three capsular polysaccharides produced by *Burkholderia pseudomallei*. FEMS microbiology letters 169(2):283-287.
- Kespichayawattana W, Rattanachetkul S, Wanun T, Utaisincharoen P, Sirisinha S. 2000. *Burkholderia pseudomallei* induces cell fusion and actin-associated membrane protrusion: a possible mechanism for cell-to-cell spreading. Infection and immunity 68(9):5377-5384.
- Knirel YA, Paramonov NA, Shashkov AS, Kochetkov NK, Yarullin RG, Farber SM, Efremenko VI. 1992. Structure of the polysaccharide chains of *Pseudomonas pseudomallei* lipopolysaccharides. Carbohydrate research 233:185-193.
- Knudsen NP, Olsen A, Buonsanti C, Follmann F, Zhang Y, Coler RN, Fox CB, Meinke A, D'Oro U, Casini D and others. 2016. Different human vaccine adjuvants promote distinct antigen-independent immunological signatures tailored to different pathogens. Scientific reports 6:19570.
- Knuf M, Kowalzik F, Kieninger D. 2011. Comparative effects of carrier proteins on vaccine-induced immune response. Vaccine 29(31):4881-4890.

- Koo GC, Gan YH. 2006. The innate interferon gamma response of BALB/c and C57BL/6 mice to in vitro *Burkholderia pseudomallei* infection. *BMC immunology* 7:19.
- Krogh A, Larsson B, von Heijne G, Sonnhammer EL. 2001. Predicting transmembrane protein topology with a hidden Markov model: application to complete genomes. *Journal of molecular biology* 305(3):567-580.
- Kushnir N, Streatfield SJ, Yusibov V. 2012. Virus-like particles as a highly efficient vaccine platform: diversity of targets and production systems and advances in clinical development. *Vaccine* 31(1):58-83.
- Lafontaine ER, Zimmerman SM, Shaffer TL, Michel F, Gao X, Hogan RJ. 2013. Use of a safe, reproducible, and rapid aerosol delivery method to study infection by *Burkholderia pseudomallei* and *Burkholderia mallei* in mice. *PloS one* 8(10):e76804.
- Lai Z, Schreiber JR. 2009. Antigen processing of glycoconjugate vaccines; the polysaccharide portion of the pneumococcal CRM(197) conjugate vaccine co-localizes with MHC II on the antigen processing cell surface. *Vaccine* 27(24):3137-3144.
- Lau SK, Sridhar S, Ho CC, Chow WN, Lee KC, Lam CW, Yuen KY, Woo PC. 2015. Laboratory diagnosis of melioidosis: past, present and future. *Experimental biology and medicine (Maywood, NJ)* 240(6):742-751.
- Lauw FN, Simpson AJ, Prins JM, Smith MD, Kurimoto M, van Deventer SJ, Speelman P, Chaowagul W, White NJ, van der Poll T. 1999. Elevated plasma concentrations of interferon (IFN)-gamma and the IFN-gamma-inducing cytokines interleukin (IL)-18, IL-12, and IL-15 in severe melioidosis. *The Journal of infectious diseases* 180(6):1878-1885.
- Lawson LB, Norton EB, Clements JD. 2011. Defending the mucosa: adjuvant and carrier formulations for mucosal immunity. *Current opinion in immunology* 23(3):414-420.
- Lazar Adler NR, Govan B, Cullinane M, Harper M, Adler B, Boyce JD. 2009. The molecular and cellular basis of pathogenesis in melioidosis: how does *Burkholderia pseudomallei* cause disease? *FEMS microbiology reviews* 33(6):1079-1099.

- Lee LH, Blake MS. 2012. Effect of increased CRM197 carrier protein dose on meningococcal C bactericidal antibody response. *Clinical and vaccine immunology* : CVI 19(4):551-556.
- Legutki JB, Nelson M, Titball R, Galloway DR, Mateczun A, Baillie LW. 2007. Analysis of peptide mimotopes of *Burkholderia pseudomallei* exopolysaccharide. *Vaccine* 25(45):7796-7805.
- Lentz VM, Manser T. 2001. Cutting edge: germinal centers can be induced in the absence of T cells. *Journal of immunology* (Baltimore, Md : 1950) 167(1):15-20.
- Leonard EG, Canaday DH, Harding CV, Schreiber JR. 2003. Antigen processing of the heptavalent pneumococcal conjugate vaccine carrier protein CRM(197) differs depending on the serotype of the attached polysaccharide. *Infection and immunity* 71(7):4186-4189.
- Levast B, Awate S, Babiuk L, Mutwiri G, Gerdtts V, van Drunen Littel-van den Hurk S. 2014. Vaccine Potentiation by Combination Adjuvants. *Vaccines* 2(2):297-322.
- Limmathurotsakul D, Chaowagul W, Chierakul W, Stepniowska K, Maharjan B, Wuthiekanun V, White NJ, Day NP, Peacock SJ. 2006. Risk factors for recurrent melioidosis in northeast Thailand. *Clinical infectious diseases : an official publication of the Infectious Diseases Society of America* 43(8):979-986.
- Limmathurotsakul D, Golding N, Dance DA, Messina JP, Pigott DM, Moyes CL, Rolim DB, Bertherat E, Day NP, Peacock SJ and others. 2016. Predicted global distribution of *Burkholderia pseudomallei* and burden of melioidosis. *Journal of immunology research* 1(1).
- Lindblad EB. 2004. Aluminium compounds for use in vaccines. *Immunology and cell biology* 82(5):497-505.
- Liston SD, Ovchinnikova OG, Whitfield C. 2016. Unique lipid anchor attaches Vi antigen capsule to the surface of *Salmonella enterica* serovar Typhi. *PNAS* 113(24):6719-6724.
- Liu B, Koo GC, Yap EH, Chua KL, Gan YH. 2002. Model of differential susceptibility to mucosal *Burkholderia pseudomallei* infection. *Infection and immunity* 70(2):504-511.
- Liu J, Guo YM, Hirokawa M, Iwamoto K, Ubukawa K, Michishita Y, Fujishima N, Tagawa H, Takahashi N, Xiao W and others. 2012. A synthetic double-

- stranded RNA, poly I:C, induces a rapid apoptosis of human CD34(+) cells. *Experimental hematology* 40(4):330-341.
- Liu MA. 2011. DNA vaccines: an historical perspective and view to the future. *Immunological reviews* 239(1):62-84.
- Llobet E, Tomas JM, Bengoechea JA. 2008. Capsule polysaccharide is a bacterial decoy for antimicrobial peptides. *Microbiology (Reading, England)* 154(Pt 12):3877-3886.
- Ludwig C, Wagner R. 2007. Virus-like particles-universal molecular toolboxes. *Current opinion in biotechnology* 18(6):537-545.
- Mahla RS, Reddy MC, Prasad DV, Kumar H. 2013. Sweeten PAMPs: Role of Sugar Complexed PAMPs in Innate Immunity and Vaccine Biology. *Frontiers in immunology* 4:248.
- Malito E, Bursulaya B, Chen C, Lo Surdo P, Picchianti M, Balducci E, Biancucci M, Brock A, Berti F, Bottomley MJ and others. 2012. Structural basis for lack of toxicity of the diphtheria toxin mutant CRM197. *Proceedings of the National Academy of Sciences of the United States of America* 109(14):5229-5234.
- Manno G, Dalmastrri C, Tabacchioni S, Vandamme P, Lorini R, Minicucci L, Romano L, Giannattasio A, Chiarini L, Bevivino A. 2004. Epidemiology and clinical course of *Burkholderia cepacia* complex infections, particularly those caused by different *Burkholderia cenocepacia* strains, among patients attending an Italian Cystic Fibrosis Center. *Journal of clinical microbiology* 42(4):1491-1497.
- Marchetti R, Dillon MJ, Burtnick MN, Hubbard MA, Kenfack MT, Bleriot Y, Gauthier C, Brett PJ, AuCoin DP, Lanzetta R and others. 2015. *Burkholderia pseudomallei* Capsular Polysaccharide Recognition by a Monoclonal Antibody Reveals Key Details toward a Biodefense Vaccine and Diagnostics against Melioidosis. *ACS chemical biology* 10(10):2295-2302.
- Masoud H, Ho M, Schollaardt T, Perry MB. 1997. Characterization of the capsular polysaccharide of *Burkholderia (Pseudomonas) pseudomallei* 304b. *Journal of bacteriology* 179(18):5663-5669.
- Masuko T, Minami A, Iwasaki N, Majima T, Nishimura S, Lee YC. 2005. Carbohydrate analysis by a phenol-sulfuric acid method in microplate format. *Analytical biochemistry* 339(1):69-72.

- Medeiros de Souza I, Neto da Silva M, Figueira ES, Leal Mde L, Jessouroun E, Pereira Abrantes Sde M, Brasileiro da Silveira IA. 2013. Single validation of CE method for determining free polysaccharide content in a Brazilian meningococcal C conjugate vaccine. *Electrophoresis* 34(22-23):3221-3226.
- Mett V, Farrance CE, Green BJ, Yusibov V. 2008. Plants as biofactories. *Biologicals : journal of the International Association of Biological Standardization* 36(6):354-358.
- Meydan C, Otu HH, Sezerman OU. 2013. Prediction of peptides binding to MHC class I and II alleles by temporal motif mining. *BMC bioinformatics* 14 Suppl 2:S13.
- Micoli F, Romano MR, Tontini M, Cappelletti E, Gavini M, Proietti D, Rondini S, Swennen E, Santini L, Filippini S and others. 2013. Development of a glycoconjugate vaccine to prevent meningitis in Africa caused by meningococcal serogroup X. *Proceedings of the National Academy of Sciences of the United States of America* 110(47):19077-19082.
- Mohan T, Verma P, Rao DN. 2013. Novel adjuvants & delivery vehicles for vaccines development: a road ahead. *The Indian journal of medical research* 138(5):779-795.
- Moore RA, Reckseidler-Zenteno S, Kim H, Nierman W, Yu Y, Tuanyok A, Warawa J, DeShazer D, Woods DE. 2004. Contribution of gene loss to the pathogenic evolution of *Burkholderia pseudomallei* and *Burkholderia mallei*. *Infection and immunity* 72(7):4172-4187.
- Morris J, Fane A, Rush C, Govan B, Mayo M, Currie BJ, Ketheesan N. 2015. Neurotropic threat characterization of *Burkholderia pseudomallei* strains. *Emerging infectious diseases* 21(1):58-63.
- Muangsoombut V, Suparak S, Pumirat P, Damnin S, Vattanaviboon P, Thongboonkerd V, Korbsrisate S. 2008. Inactivation of *Burkholderia pseudomallei* bsaQ results in decreased invasion efficiency and delayed escape of bacteria from endocytic vesicles. *Archives of microbiology* 190(6):623-631.
- Mulye M, Bechill MP, Grose W, Ferreira VP, Lafontaine ER, Wooten RM. 2014. Delineating the importance of serum opsonins and the bacterial capsule in affecting the uptake and killing of *Burkholderia pseudomallei* by murine

- neutrophils and macrophages. PLoS neglected tropical diseases 8(8):e2988.
- Muthukkumar S, Stein KE. 2004. Immunization with meningococcal polysaccharide-tetanus toxoid conjugate induces polysaccharide-reactive T cells in mice. *Vaccine* 22(9-10):1290-1299.
- Nelson M, Prior JL, Lever MS, Jones HE, Atkins TP, Titball RW. 2004. Evaluation of lipopolysaccharide and capsular polysaccharide as subunit vaccines against experimental melioidosis. *Journal of medical microbiology* 53(Pt 12):1177-1182.
- Ngauy V, Lemeshev Y, Sadkowski L, Crawford G. 2005. Cutaneous melioidosis in a man who was taken as a prisoner of war by the Japanese during World War II. *Journal of clinical microbiology* 43(2):970-972.
- Ngugi SA, Ventura VV, Qazi O, Harding SV, Kitto GB, Estes DM, Dell A, Titball RW, Atkins TP, Brown KA and others. 2010. Lipopolysaccharide from *Burkholderia thailandensis* E264 provides protection in a murine model of melioidosis. *Vaccine* 28(47):7551-7555.
- Nielsen M, Lund O. 2009. NN-align. An artificial neural network-based alignment algorithm for MHC class II peptide binding prediction. *BMC bioinformatics* 10:296.
- Nielsen M, Lundegaard C, Lund O. 2007. Prediction of MHC class II binding affinity using SMM-align, a novel stabilization matrix alignment method. *BMC bioinformatics* 8:238.
- Nielsen M, Lundegaard C, Worning P, Lauemoller SL, Lamberth K, Buus S, Brunak S, Lund O. 2003. Reliable prediction of T-cell epitopes using neural networks with novel sequence representations. *Protein science : a publication of the Protein Society* 12(5):1007-1017.
- Nimtz M, Wray V, Domke T, Brenneke B, Haussler S, Steinmetz I. 1997. Structure of an acidic exopolysaccharide of *Burkholderia pseudomallei*. *European journal of biochemistry / FEBS* 250(2):608-616.
- Nishat S, Andreana PR. 2016. Entirely Carbohydrate-Based Vaccines: An Emerging Field for Specific and Selective Immune Responses. *Vaccines* 4(2).
- Noad R, Roy P. 2003. Virus-like particles as immunogens. *Trends in microbiology* 11(9):438-444.

- Norris MH, Propst KL, Kang Y, Dow SW, Schweizer HP, Hoang TT. 2011. The *Burkholderia pseudomallei* Deltaasd mutant exhibits attenuated intracellular infectivity and imparts protection against acute inhalation melioidosis in mice. *Infection and immunity* 79(10):4010-4018.
- O'Hagan DT, Ott GS, De Gregorio E, Seubert A. 2012. The mechanism of action of MF59 - an innately attractive adjuvant formulation. *Vaccine* 30(29):4341-4348.
- Oliphant CJ, Barlow JL, McKenzie AN. 2011. Insights into the initiation of type 2 immune responses. *Immunology* 134(4):378-385.
- Olive C. 2012. Pattern recognition receptors: sentinels in innate immunity and targets of new vaccine adjuvants. *Expert review of vaccines* 11(2):237-256.
- Organisation WH. 2005. Recommendations for the production and control of pneumococcal conjugate vaccines WHO Technical Report Series No. 927.
- Organization WH. 2004. Recommendations for the production and control of meningococcal group C conjugate vaccines. WHO Technical Report Series No. 924.
- Organization WH. 2011. Recommendations to assure the quality, safety and efficacy of group A meningococcal conjugate vaccines. WHO Technical Report Series 962.
- Parthasarathy N, DeShazer D, England M, Waag DM. 2006. Polysaccharide microarray technology for the detection of *Burkholderia pseudomallei* and *Burkholderia mallei* antibodies. *Diagnostic microbiology and infectious disease* 56(3):329-332.
- Peacock SJ, Limmathurotsakul D, Lubell Y, Koh GC, White LJ, Day NP, Titball RW. 2012. Melioidosis vaccines: a systematic review and appraisal of the potential to exploit biodefense vaccines for public health purposes. *PLoS neglected tropical diseases* 6(1):e1488.
- Peacock SJ, Schweizer HP, Dance DA, Smith TL, Gee JE, Wuthiekanun V, DeShazer D, Steinmetz I, Tan P, Currie BJ. 2008. Management of accidental laboratory exposure to *Burkholderia pseudomallei* and *B. mallei*. *Emerging infectious diseases* 14(7):e2.
- Perciani CT, Barazzone GC, Goulart C, Carvalho E, Cabrera-Crespo J, Goncalves VM, Leite LC, Tanizaki MM. 2013. Conjugation of

- polysaccharide 6B from *Streptococcus pneumoniae* with pneumococcal surface protein A: PspA conformation and its effect on the immune response. *Clinical and vaccine immunology : CVI* 20(6):858-866.
- Perry MB, MacLean LL, Schollaardt T, Bryan LE, Ho M. 1995. Structural characterization of the lipopolysaccharide O antigens of *Burkholderia pseudomallei*. *Infection and immunity* 63(9):3348-3352.
- Peters B, Sette A. 2005. Generating quantitative models describing the sequence specificity of biological processes with the stabilized matrix method. *BMC bioinformatics* 6:132.
- Peyret H, Gehin A, Thuenemann EC, Blond D, El Turabi A, Beales L, Clarke D, Gilbert RJ, Fry EE, Stuart DI and others. 2015. Tandem fusion of hepatitis B core antigen allows assembly of virus-like particles in bacteria and plants with enhanced capacity to accommodate foreign proteins. *PloS one* 10(4):e0120751.
- Pichichero ME. 2013. Protein carriers of conjugate vaccines: characteristics, development, and clinical trials. *Human vaccines & immunotherapeutics* 9(12):2505-2523.
- Pilatz S, Breitbach K, Hein N, Fehlhaber B, Schulze J, Brenneke B, Eberl L, Steinmetz I. 2006. Identification of *Burkholderia pseudomallei* genes required for the intracellular life cycle and in vivo virulence. *Infection and immunity* 74(6):3576-3586.
- Pitman MC, Luck T, Marshall CS, Anstey NM, Ward L, Currie BJ. 2015. Intravenous therapy duration and outcomes in melioidosis: a new treatment paradigm. *PLoS neglected tropical diseases* 9(3):e0003586.
- Plotkin SA. 1999. Vaccination against the major infectious diseases. *Comptes rendus de l'Academie des sciences Serie III, Sciences de la vie* 322(11):943-951.
- Plotkin SA. 2008. Vaccines: correlates of vaccine-induced immunity. *Clinical infectious diseases : an official publication of the Infectious Diseases Society of America* 47(3):401-409.
- Plotkin SA. 2010. Correlates of protection induced by vaccination. *Clinical and vaccine immunology : CVI* 17(7):1055-1065.
- Plotkin SA, Orenstein, W. A., Offit, P. A., . 2013. *Vaccines (Sixth Edition)*. Elsevier Saunders:1550.

- Pobre K, Tashani M, Ridda I, Rashid H, Wong M, Booy R. 2014. Carrier priming or suppression: understanding carrier priming enhancement of anti-polysaccharide antibody response to conjugate vaccines. *Vaccine* 32(13):1423-1430.
- Poland GA, Jacobson RM, Tilburt J, Nichol K. 2009. The social, political, ethical, and economic aspects of biodefense vaccines. *Vaccine* 27 Suppl 4:D23-27.
- Pollabauer EM, Petermann R, Ehrlich HJ. 2009. The influence of carrier protein on the immunogenicity of simultaneously administered conjugate vaccines in infants. *Vaccine* 27(11):1674-1679.
- Pradenas GA, Ross BN, Torres AG. 2016. *Burkholderia cepacia* Complex Vaccines: Where Do We Go from here? *Vaccines* 4(2).
- Pumpens P, Grens E. 2001. HBV core particles as a carrier for B cell/T cell epitopes. *Intervirology* 44(2-3):98-114.
- Pumpuang A, Chantratita N, Wikraiphath C, Saiprom N, Day NP, Peacock SJ, Wuthiekanun V. 2011. Survival of *Burkholderia pseudomallei* in distilled water for 16 years. *Transactions of the Royal Society of Tropical Medicine and Hygiene* 105(10):598-600.
- Purcell AW, van Driel IR, Gleeson PA. 2008. Impact of glycans on T-cell tolerance to glycosylated self-antigens. *Immunology and cell biology* 86(7):574-579.
- Pushko P, Pumpens P, Grens E. 2013. Development of virus-like particle technology from small highly symmetric to large complex virus-like particle structures. *Intervirology* 56(3):141-165.
- Rainbow L, Hart CA, Winstanley C. 2002. Distribution of type III secretion gene clusters in *Burkholderia pseudomallei*, *B. thailandensis* and *B. mallei*. *Journal of medical microbiology* 51(5):374-384.
- Rammensee H, Bachmann J, Emmerich NP, Bachor OA, Stevanovic S. 1999. SYFPEITHI: database for MHC ligands and peptide motifs. *Immunogenetics* 50(3-4):213-219.
- Rana R, Dalal J, Singh D, Kumar N, Hanif S, Joshi N, Chhikara MK. 2015. Development and characterization of *Haemophilus influenzae* type b conjugate vaccine prepared using different polysaccharide chain lengths. *Vaccine* 33(23):2646-2654.

- Reckseidler-Zenteno SL, DeVinney R, Woods DE. 2005. The capsular polysaccharide of *Burkholderia pseudomallei* contributes to survival in serum by reducing complement factor C3b deposition. *Infection and immunity* 73(2):1106-1115.
- Reckseidler-Zenteno SL, Viteri DF, Moore R, Wong E, Tuanyok A, Woods DE. 2010. Characterization of the type III capsular polysaccharide produced by *Burkholderia pseudomallei*. *Journal of medical microbiology* 59(Pt 12):1403-1414.
- Reckseidler SL, DeShazer D, Sokol PA, Woods DE. 2001. Detection of bacterial virulence genes by subtractive hybridization: identification of capsular polysaccharide of *Burkholderia pseudomallei* as a major virulence determinant. *Infection and immunity* 69(1):34-44.
- Redfearn MS, Palleroni NJ, Stanier RY. 1966. A comparative study of *Pseudomonas pseudomallei* and *Bacillus mallei*. *Journal of general microbiology* 43(2):293-313.
- Roche PA, Cresswell P. 2016. Antigen Processing and Presentation Mechanisms in Myeloid Cells. *Microbiology spectrum* 4(3).
- Rodriguez ME, van den Dobbelsteen GP, Oomen LA, de Weers O, van Buren L, Beurret M, Poolman JT, Hoogerhout P. 1998. Immunogenicity of *Streptococcus pneumoniae* type 6B and 14 polysaccharide-tetanus toxoid conjugates and the effect of uncoupled polysaccharide on the antigen-specific immune response. *Vaccine* 16(20):1941-1949.
- Rosenthal KS. 2005a. Vaccines--all things considered. Part I. 2-3 December 2004, San Francisco, CA, USA. *IDrugs : the investigational drugs journal* 8(2):107-109.
- Rosenthal KS. 2005b. Vaccines--all things considered. Part II. 2-3 December 2004, San Francisco, CA, USA. *IDrugs : the investigational drugs journal* 8(2):110-111.
- Rotz LD, Khan AS, Lillibridge SR, Ostroff SM, Hughes JM. 2002. Public health assessment of potential biological terrorism agents. *Emerging infectious diseases* 8(2):225-230.
- Ruiz FM, Santillana E, Spinola-Amilibia M, Torreira E, Culebras E, Romero A. 2015. Correction: Crystal Structure of Hcp from *Acinetobacter baumannii*: A Component of the Type VI Secretion System. *PloS one* 10(8):e0136978.

- Sahoo A, Wali S, Nurieva R. 2016. T helper 2 and T follicular helper cells: Regulation and function of interleukin-4. *Cytokine & growth factor reviews* 30:29-37.
- Salehen N, Stover C. 2008. The role of complement in the success of vaccination with conjugated vs. unconjugated polysaccharide antigen. *Vaccine* 26(4):451-459.
- Sanford JP. 1978. Melioidosis: forgotten but not gone. *Transactions of the American Clinical and Climatological Association* 89:201-205.
- Santanirand P, Harley VS, Dance DA, Drasar BS, Bancroft GJ. 1999. Obligatory role of gamma interferon for host survival in a murine model of infection with *Burkholderia pseudomallei*. *Infection and immunity* 67(7):3593-3600.
- Sarkar-Tyson M, Smither SJ, Harding SV, Atkins TP, Titball RW. 2009. Protective efficacy of heat-inactivated *B. thailandensis*, *B. mallei* or *B. pseudomallei* against experimental melioidosis and glanders. *Vaccine* 27(33):4447-4451.
- Sarovich DS, Ward L, Price EP, Mayo M, Pitman MC, Baird RW, Currie BJ. 2014. Recurrent melioidosis in the Darwin Prospective Melioidosis Study: improving therapies mean that relapse cases are now rare. *Journal of clinical microbiology* 52(2):650-653.
- Scheerlinck JP, Greenwood DL. 2008. Virus-sized vaccine delivery systems. *Drug discovery today* 13(19-20):882-887.
- Schneerson R, Barrera O, Sutton A, Robbins JB. 1980. Preparation, characterization, and immunogenicity of *Haemophilus influenzae* type b polysaccharide-protein conjugates. *The Journal of experimental medicine* 152(2):361-376.
- Schodel F, Moriarty AM, Peterson DL, Zheng JA, Hughes JL, Will H, Leturcq DJ, McGee JS, Milich DR. 1992. The position of heterologous epitopes inserted in hepatitis B virus core particles determines their immunogenicity. *Journal of virology* 66(1):106-114.
- Scott AE, Burtnick MN, Stokes MG, Whelan AO, Williamson ED, Atkins TP, Prior JL, Brett PJ. 2014a. *Burkholderia pseudomallei* capsular polysaccharide conjugates provide protection against acute melioidosis. *Infection and immunity* 82(8):3206-3213.
- Scott AE, Christ WJ, George AJ, Stokes MG, Lohman GJ, Guo Y, Jones M, Titball RW, Atkins TP, Campbell AS and others. 2016. Protection against

- Experimental Melioidosis with a Synthetic manno-Heptopyranose Hexasaccharide Glycoconjugate. *Bioconjugate chemistry* 27(6):1435-1446.
- Scott AE, Laws TR, D'Elia RV, Stokes MG, Nandi T, Williamson ED, Tan P, Prior JL, Atkins TP. 2013. Protection against experimental melioidosis following immunization with live *Burkholderia thailandensis* expressing a manno-heptose capsule. *Clinical and vaccine immunology : CVI* 20(7):1041-1047.
- Scott AE, Ngugi SA, Laws TR, Corser D, Lonsdale CL, D'Elia RV, Titball RW, Williamson ED, Atkins TP, Prior JL. 2014b. Protection against experimental melioidosis following immunisation with a lipopolysaccharide-protein conjugate. *Journal of immunology research* 2014:392170.
- Shete AV, Thakar MR, Tripathy SP, Raut C, Chakrabarti S, Paranjape RS. 2011. T-cell Epitopes Identified by BALB/c Mice Immunized with Vaccinia Expressing HIV-1 Gag lie within immunodominant Regions Recognized by HIV-infected Indian Patients. *Journal of global infectious diseases* 3(3):246-253.
- Shinefield HR. 2010. Overview of the development and current use of CRM(197) conjugate vaccines for pediatric use. *Vaccine* 28(27):4335-4339.
- Sidney J, Assarsson E, Moore C, Ngo S, Pinilla C, Sette A, Peters B. 2008. Quantitative peptide binding motifs for 19 human and mouse MHC class I molecules derived using positional scanning combinatorial peptide libraries. *Immunome research* 4:2.
- Silva EB, Dow SW. 2013. Development of *Burkholderia mallei* and *pseudomallei* vaccines. *Frontiers in cellular and infection microbiology* 3:10.
- Sim BM, Chantratita N, Ooi WF, Nandi T, Tewhey R, Wuthiekanun V, Thaipadungpanit J, Tumapa S, Ariyaratne P, Sung WK and others. 2010. Genomic acquisition of a capsular polysaccharide virulence cluster by non-pathogenic *Burkholderia* isolates. *Genome biology* 11(8):R89.
- Singh H, Raghava GP. 2003. ProPred1: prediction of promiscuous MHC Class-I binding sites. *Bioinformatics (Oxford, England)* 19(8):1009-1014.

- Sirisinha S, Anuntagool N, Intachote P, Wuthiekanun V, Puthucheary SD, Vadivelu J, White NJ. 1998. Antigenic differences between clinical and environmental isolates of *Burkholderia pseudomallei*. *Microbiology and immunology* 42(11):731-737.
- Sivakumar SM, Safhi MM, Kannadasan M, Sukumaran N. 2011. Vaccine adjuvants - Current status and prospects on controlled release adjuvancity. *Saudi pharmaceutical journal : SPJ : the official publication of the Saudi Pharmaceutical Society* 19(4):197-206.
- Sonnhammer EL, von Heijne G, Krogh A. 1998. A hidden Markov model for predicting transmembrane helices in protein sequences. *Proceedings / International Conference on Intelligent Systems for Molecular Biology ; ISMB International Conference on Intelligent Systems for Molecular Biology* 6:175-182.
- Stevens MP, Friebel A, Taylor LA, Wood MW, Brown PJ, Hardt WD, Galyov EE. 2003. A *Burkholderia pseudomallei* type III secreted protein, BopE, facilitates bacterial invasion of epithelial cells and exhibits guanine nucleotide exchange factor activity. *Journal of bacteriology* 185(16):4992-4996.
- Stevens MP, Haque A, Atkins T, Hill J, Wood MW, Easton A, Nelson M, Underwood-Fowler C, Titball RW, Bancroft GJ and others. 2004. Attenuated virulence and protective efficacy of a *Burkholderia pseudomallei* bsa type III secretion mutant in murine models of melioidosis. *Microbiology (Reading, England)* 150(Pt 8):2669-2676.
- Strugnell RZ, F.; Cunningham, A.; Tantawichien, T.;. 2011. Vaccine antigens. *Understanding Modern Vaccines: Perspectives in Vaccinology* 1(1):61-88.
- Su YC, Wan KL, Mohamed R, Nathan S. 2008. A genome level survey of *Burkholderia pseudomallei* immunome expressed during human infection. *Microbes and infection / Institut Pasteur* 10(12-13):1335-1345.
- Su YC, Wan KL, Mohamed R, Nathan S. 2010. Immunization with the recombinant *Burkholderia pseudomallei* outer membrane protein Omp85 induces protective immunity in mice. *Vaccine* 28(31):5005-5011.
- Suarez N, Massaldi H, Franco Fraguas L, Ferreira F. 2008. Improved conjugation and purification strategies for the preparation of protein-

- polysaccharide conjugates. *Journal of chromatography A* 1213(2):169-175.
- Sun GW, Lu J, Pervaiz S, Cao WP, Gan YH. 2005. Caspase-1 dependent macrophage death induced by *Burkholderia pseudomallei*. *Cellular microbiology* 7(10):1447-1458.
- Suwannasaen D, Mahawantung J, Chaowagul W, Limmathurotsakul D, Felgner PL, Davies H, Bancroft GJ, Titball RW, Lertmemongkolchai G. 2011. Human immune responses to *Burkholderia pseudomallei* characterized by protein microarray analysis. *The Journal of infectious diseases* 203(7):1002-1011.
- Szu SC, Li XR, Stone AL, Robbins JB. 1991. Relation between structure and immunologic properties of the Vi capsular polysaccharide. *Infection and immunity* 59(12):4555-4561.
- Tan GY, Liu Y, Sivalingam SP, Sim SH, Wang D, Paucod JC, Gauthier Y, Ooi EE. 2008. *Burkholderia pseudomallei* aerosol infection results in differential inflammatory responses in BALB/c and C57Bl/6 mice. *Journal of medical microbiology* 57(Pt 4):508-515.
- Tippayawat P, Saenwongsa W, Mahawantung J, Suwannasaen D, Chetchotisakd P, Limmathurotsakul D, Peacock SJ, Felgner PL, Atkins HS, Titball RW and others. 2009. Phenotypic and functional characterization of human memory T cell responses to *Burkholderia pseudomallei*. *PLoS neglected tropical diseases* 3(4):e407.
- Titball RW, Russell P, Cuccui J, Easton A, Haque A, Atkins T, Sarkar-Tyson M, Harley V, Wren B, Bancroft GJ. 2008. *Burkholderia pseudomallei*: animal models of infection. *Transactions of the Royal Society of Tropical Medicine and Hygiene* 102 Suppl 1:S111-116.
- Tontini M, Berti F, Romano MR, Proietti D, Zambonelli C, Bottomley MJ, De Gregorio E, Del Giudice G, Rappuoli R, Costantino P and others. 2013. Comparison of CRM197, diphtheria toxoid and tetanus toxoid as protein carriers for meningococcal glycoconjugate vaccines. *Vaccine* 31(42):4827-4833.
- Toussi DN, Massari P. 2014. Immune Adjuvant Effect of Molecularly-defined Toll-Like Receptor Ligands. *Vaccines* 2(2):323-353.
- Tritto E, Mosca F, De Gregorio E. 2009. Mechanism of action of licensed vaccine adjuvants. *Vaccine* 27(25-26):3331-3334.

- Tsybalova LM, Stepanova LA, Kuprianov VV, Blokhina EA, Potapchuk MV, Korotkov AV, Gorshkov AN, Kasyanenko MA, Ravin NV, Kiselev OI. 2015. Development of a candidate influenza vaccine based on virus-like particles displaying influenza M2e peptide into the immunodominant region of hepatitis B core antigen: Broad protective efficacy of particles carrying four copies of M2e. *Vaccine* 33(29):3398-3406.
- Tuanyok A, Stone JK, Mayo M, Kaestli M, Gruendike J, Georgia S, Warrington S, Mullins T, Allender CJ, Wagner DM and others. 2012. The genetic and molecular basis of O-antigenic diversity in *Burkholderia pseudomallei* lipopolysaccharide. *PLoS neglected tropical diseases* 6(1):e1453.
- Ulrich RL, Amemiya K, Waag DM, Roy CJ, DeShazer D. 2005. Aerogenic vaccination with a *Burkholderia mallei* auxotroph protects against aerosol-initiated glanders in mice. *Vaccine* 23(16):1986-1992.
- Van Zandt KE, Greer MT, Gelhaus HC. 2013. Glanders: an overview of infection in humans. *Orphanet journal of rare diseases* 8:131.
- Vartak A, Sucheck SJ. 2016. Recent Advances in Subunit Vaccine Carriers. *Vaccines* 4(2).
- Vellasamy KM, Mariappan V, Shankar EM, Vadivelu J. 2016. *Burkholderia pseudomallei* Differentially Regulates Host Innate Immune Response Genes for Intracellular Survival in Lung Epithelial Cells. *PLoS neglected tropical diseases* 10(7):e0004730.
- Vietheer PT, Boo I, Drummer HE, Netter HJ. 2007. Immunizations with chimeric hepatitis B virus-like particles to induce potential anti-hepatitis C virus neutralizing antibodies. *Antiviral therapy* 12(4):477-487.
- Wagar E. 2016. Bioterrorism and the Role of the Clinical Microbiology Laboratory. *Clinical microbiology reviews* 29(1):175-189.
- Walker A, Skamel C, Vorreiter J, Nassal M. 2008. Internal core protein cleavage leaves the hepatitis B virus capsid intact and enhances its capacity for surface display of heterologous whole chain proteins. *The Journal of biological chemistry* 283(48):33508-33515.
- Wang-Ngarm S, Chareonsudjai S, Chareonsudjai P. 2014. Physicochemical factors affecting the growth of *Burkholderia pseudomallei* in soil microcosm. *The American journal of tropical medicine and hygiene* 90(3):480-485.

- Wang P, Sidney J, Dow C, Mothe B, Sette A, Peters B. 2008. A systematic assessment of MHC class II peptide binding predictions and evaluation of a consensus approach. *PLoS computational biology* 4(4):e1000048.
- Ward JD. 2008a. *A Manual for Laboratory Animal Management*. World Scientific Publishing Co Pte Ltd 5.
- Ward JD. 2008b. *A manual for laboratory animal management*. World Scientific Publishing Co.
- Welkos SL, Klimko CP, Kern SJ, Bearss JJ, Bozue JA, Bernhards RC, Trevino SR, Waag DM, Amemiya K, Worsham PL and others. 2015. Characterization of *Burkholderia pseudomallei* Strains Using a Murine Intraperitoneal Infection Model and In Vitro Macrophage Assays. *PloS one* 10(4):e0124667.
- West TE, Myers ND, Limmathurotsakul D, Liggitt HD, Chantratita N, Peacock SJ, Skerrett SJ. 2010. Pathogenicity of high-dose enteral inoculation of *Burkholderia pseudomallei* to mice. *The American journal of tropical medicine and hygiene* 83(5):1066-1069.
- Whitacre DC, Lee BO, Milich DR. 2009. Use of hepadnavirus core proteins as vaccine platforms. *Expert review of vaccines* 8(11):1565-1573.
- Whitfield C. 2006. Biosynthesis and assembly of capsular polysaccharides in *Escherichia coli*. *Annual review of biochemistry* 75:39-68.
- Whitmore A. 1913. An Account of a Glanders-like Disease occurring in Rangoon. *The Journal of hygiene* 13(1):1-34.31.
- Wiersinga WJ, Currie BJ, Peacock SJ. 2012. Melioidosis. *The New England journal of medicine* 367(11):1035-1044.
- Wiersinga WJ, van der Poll T. 2009. Immunity to *Burkholderia pseudomallei*. *Current opinion in infectious diseases* 22(2):102-108.
- Wikraiphat C, Charoensap J, Utaisincharoen P, Wongratanacheewin S, Taweekhaisupapong S, Woods DE, Bolscher JG, Sirisinha S. 2009. Comparative in vivo and in vitro analyses of putative virulence factors of *Burkholderia pseudomallei* using lipopolysaccharide, capsule and flagellin mutants. *FEMS immunology and medical microbiology* 56(3):253-259.
- Wikraiphat C, Saiprom N, Tandhavanant S, Heiss C, Azadi P, Wongsuvan G, Tuanyok A, Holden MT, Burtnick MN, Brett PJ and others. 2015. Colony morphology variation of *Burkholderia pseudomallei* is associated with

- antigenic variation and O-polysaccharide modification. *Infection and immunity* 83(5):2127-2138.
- Willcocks SJ, Denman CC, Atkins HS, Wren BW. 2016. Intracellular replication of the well-armed pathogen *Burkholderia pseudomallei*. *Current opinion in microbiology* 29:94-103.
- Wolfe DN, Florence W, Bryant P. 2013. Current biodefense vaccine programs and challenges. *Human vaccines & immunotherapeutics* 9(7):1591-1597.
- Wuthiekanun V, Chierakul W, Langa S, Chaowagul W, Panpitpat C, Saipan P, Thoujaikong T, Day NP, Peacock SJ. 2006. Development of antibodies to *Burkholderia pseudomallei* during childhood in melioidosis-endemic northeast Thailand. *The American journal of tropical medicine and hygiene* 74(6):1074-1075.
- Wuthiekanun V, Smith MD, White NJ. 1995. Survival of *Burkholderia pseudomallei* in the absence of nutrients. *Transactions of the Royal Society of Tropical Medicine and Hygiene* 89(5):491.
- Wynne SA, Crowther RA, Leslie AG. 1999. The crystal structure of the human hepatitis B virus capsid. *Molecular cell* 3(6):771-780.
- Yin Y, Zhang S, Cai C, Zhang J, Dong D, Guo Q, Fu L, Xu J, Chen W. 2014. Deletion modification enhances anthrax specific immunity and protective efficacy of a hepatitis B core particle-based anthrax epitope vaccine. *Immunobiology* 219(2):97-103.
- Yu Y, Kim HS, Chua HH, Lin CH, Sim SH, Lin D, Derr A, Engels R, DeShazer D, Birren B and others. 2006. Genomic patterns of pathogen evolution revealed by comparison of *Burkholderia pseudomallei*, the causative agent of melioidosis, to avirulent *Burkholderia thailandensis*. *BMC microbiology* 6:46.
- Zabel F, Kundig TM, Bachmann MF. 2013. Virus-induced humoral immunity: on how B cell responses are initiated. *Current opinion in virology* 3(3):357-362.
- Zandvoort A, Timens W. 2002. The dual function of the splenic marginal zone: essential for initiation of anti-TI-2 responses but also vital in the general first-line defense against blood-borne antigens. *Clinical and experimental immunology* 130(1):4-11.
- Zepp F. 2010. Principles of vaccine design-Lessons from nature. *Vaccine* 28 Suppl 3:C14-24.